

Transcriptional and genomic analyses reveal an analogous mechanism for a Piperidinyl-Benzimidazolone analogue in *Babesia divergens* compared to other apicomplexans.

by

Ingrid Rossouw

Submitted in partial fulfilment of the requirements for the degree

Philosophiae Doctor

In the faculty of Natural and Agricultural Science

Department Genetics

University of Pretoria

Pretoria

2015

Supervisor: Prof. Christine Maritz-Olivier

Co-supervisor: Prof. Lyn-Marie Birkholtz

Declaration

I, Ingrid Rossouw, hereby declare that this dissertation submitted for the degree *Philosophiae Doctor* at the University of Pretoria, is my own work and has not previously been submitted for a degree at this, or any other university.

Ingrid Rossouw

Date

Plagiarism Declaration

Full name: Ingrid Rossouw

Student number: 24075681

Title of work: Transcriptional and genomic analyses reveal an analogous mechanism for a Piperidinyl-Benzimidazolone analogue in *Babesia divergens* compared to other apicomplexans.

Declaration:

1. I understand what plagiarism entails and am aware of the University's policy in this regard.
2. I declare that this **thesis** (eg. essay, report, project, assignment, dissertation, thesis etc.) is my own, original work. Where someone else's work has been used (whether from a printed source, the internet or any other source) due acknowledgement was given and reference was made according to the departmental requirements.
3. I did not make use of another student's previous work and submit it was my own.
4. I did not allow and will not allow anyone to copy my work with the intention of presenting it as his or her own work.

Dedication

I would like to dedicate this work to the memory of my loving mother.

“Be strong and courageous. Do not be terrified; do not be discouraged, for the Lord your God
will be with you wherever you go”

Joshua 1:9

Acknowledgements

I wish to thank the following people and organizations without which my research would not have been possible:

- Prof. Christine Maritz-Olivier my project supervisor for accepting me into her research group, her time, input and guidance.
- Prof. Lyn-Marie Birkholtz, my co-supervisor for her time, helpful advice, input and acceptance into her lab. I greatly appreciate the use of all her equipment and facilities.
- Mr. Nicky Olivier at the AGCT for his excellent bioinformatics assistance and advice.
- My entire research group past and present.
- The entire malaria research group, in particular Ms. Janette Reader, Dr. Dina Coertzen, Dr. Jandeli Niemand and Dr. Bianca Verlinden.
- Mr. Willie van Zyl for his patience, advice, computer skills and friendship.
- Dr. Annel Smit at the flow cytometry unit for her time, input and helpful advice.

- Dr. Stephane Delbecq, Prof. Eric Marechal and Prof. Laurent Brehelin for providing the *Babesia* cultures, drug compound and bioinformatic skills, respectively.
- My dear friends Annette-Christi, Sabine, Bianca, Lorelle, Rudi, Samantha, Luise, Heinrich, Annel and Letitia for their friendship, motivation, lengthy discussions, problem solving abilities, prayers, love and laughter.
- Funding bodies including the National Research Foundation (NRF), Institutional Research Theme (IRT) (Genomics), Embassy of France in South Africa (Campus France) and the University of Pretoria.
- To my family, words fail to describe how much I appreciate your prayers, love, support and encouragement over the course of my tertiary studies and in particular the pinnacle - my PhD. Dad, your friendship, faith and insatiable thirst for knowledge motivated me on a daily basis to put things into perspective and to persevere. I wish to thank my siblings, Nicola, Deon and Lize for their unconditional love, for opening their homes and hearts and allowing me to always be myself. My extended family and support system, Nina, Andre, Hennie, Veronica as well as the joys in my life - all the kids, I appreciate your love and support.
- Lastly to my Lord and Saviour for granting me the opportunity to live my dream, for knowing me better than I know myself and for His unfailing love.

Summary

Human babesiosis is a rapidly emerging, zoonotic, infectious disease causing potentially life-threatening malaria-like symptoms in humans. Disease prevalence has escalated over the past 50 years from a few isolated cases to endemic areas now being recognized. Early disease detection, diagnosis and treatment with effective anti-babesiocidal compounds are vital for both human and animal health. In humans, *Babesia* parasites can be cleared by anti-malarials including atovaquone (with azithromycin) or quinine (plus clindamycin) but highly immune-compromised individuals respond poorly to these treatments. In the past few years, reports of resistance against these combinations have emerged, stressing the need for alternative treatments. Ideally one would prefer one drug compound to be effective against numerous pathogens based on a single, commonly shared target feature within the cells. In the post-genomic era, bioinformatics along with several computational strategies have become invaluable for drug discovery to aid in drug target identification followed by *in vitro* and *in vivo* validation.

The precise progression and duration of the intra-erythrocytic, asexual developmental cycle (IDC) of *Babesia* has not been clarified to date and current understanding is fraught with uncertainties. This study focuses on the application of sensitive cell- biological -and molecular functional genomics tools to describe the IDC of *B. divergens* parasites from immature, mono-nucleated ring forms to bi-nucleated paired piriforms and ultimately multi-nucleated tetrads which was further correlated for the first time to nuclear content increases during intra-erythrocytic development progression. This provides insight into the life cycle that occurs during human infection. This study provides the first temporal evaluation of the functional transcriptome of *B. divergens* parasites.

This study contributes to anti-babesiacid control strategies by evaluating a promising anti-*Plasmodium*, apicoplast specific piperidiny-benzimidazolone analogue (A51B1C1_1) as potential therapeutic with low toxicity, against one of the causative agents of human babesiosis, *B. divergens*. This study set out to describe the global transcriptome of *B. divergens* parasites (under treated conditions) through its IDC as an indicator of the physiological processes involved. By unravelling the *Babesia* transcriptome, key gene expression transcripts were defined and conserved gene expression networks between *P. falciparum* and *B. divergens* parasites treated with the same compound (A51B1C1_1) identified. This study ultimately contributed to the identification of an apicomplexan parasitic response to treatment. Additionally, it established the investigated compounds' mode-of-action.

Table of Contents

Table of Contents	9
Appendixes (provided in electronic format on accompanying CD)	11
List of Tables	12
List of Figures	13
List of Abbreviations	15
Chapter 1	19
Literature Review	19
1.1 Introduction.....	19
1.2 Ticks as vectors of both animal and human disease	20
1.3 The Babesia parasite and pathogenesis of babesiosis	23
1.3.2 Human babesiosis.....	25
1.3.3 Bovine babesiosis	35
1.4 Apicomplexa and the apicoplast	37
1.5 Piperidinyl-benzimidazolone analogues and compound A51B1C1_1 used in this study.....	47
1.6 Hypothesis.....	50
1.7 Aims and Objectives	50
1.8 List of conferences.....	51
1.9 List of research visits	52
1.10 List of awards	52
1.11 Papers from this study.....	53
1.12 References.....	54
Chapter 2	58

Morphological and molecular descriptors of the developmental cycle of *Babesia divergens* parasites in human erythrocytes.....58

2.1	<i>Introduction.....</i>	58
2.2	<i>Materials and Methods.....</i>	62
2.2.1	<i>In vitro cultivation of intra-erythrocytic B. divergens and P. falciparum parasites.....</i>	62
2.2.2	<i>Microscopy.....</i>	63
2.2.3	<i>Flow cytometric analysis using SYBR® Green I fluorescence.....</i>	63
2.2.4	<i>Transcriptome analysis.....</i>	65
2.3	<i>Results.....</i>	68
2.3.1	<i>Flow cytometric analysis using SYBR® Green I fluorescence.....</i>	68
2.3.2	<i>Evaluation of B. divergens in vitro blood stage development.....</i>	70
2.3.3	<i>Nuclear content associated with B. divergens parasites' life cycle compartments.....</i>	72
2.3.4	<i>Temporal evaluation of B. divergens parasites' life cycle progression.....</i>	73
2.3.5	<i>Molecular descriptors characterizing the life cycle of B. divergens parasites.....</i>	75
2.4	<i>Conclusion.....</i>	90
2.5	<i>References.....</i>	92

Chapter 395

Morphological assessment and *in vitro* evaluation of the growth inhibitory effect of a Piperidinyl-Benzimidazolone analogue (A51B1C1_1) against *Babesia divergens*.....95

3.1	<i>Introduction.....</i>	95
3.2	<i>Materials and Methods.....</i>	99
3.2.1	<i>Drug sensitivity and cell viability assays in response to A51B1C1_1 treatment.....</i>	99
3.2.2	<i>Morphological evaluation based on light microscopy.....</i>	101
3.3	<i>Results and Discussion.....</i>	101
3.3.1	<i>Piperidinyl-benzimidazolone analogue (A51B1C1_1) treatment of B. divergens cultures.....</i>	101
3.4	<i>Conclusion.....</i>	108
3.5	<i>References.....</i>	111

Chapter 4 114

***In vitro* evaluation of the growth inhibitory effect of a Piperidinyl-Benzimidazolone analogue (A51B1C1_1) against *Babesia divergens* through comprehensive transcriptome analysis..... 114**

4.1	<i>Introduction.....</i>	114
4.2	<i>Materials and Methods.....</i>	122
4.2.1	<i>Hybridization-based (microarray) transcriptomics.....</i>	122
4.2.2	<i>Comparative transcriptomic evaluation between species in response to A51B1C1_1 treatment</i>	129
4.3	<i>Results and Discussion</i>	130
4.3.1	<i>Hybridization-based (microarray) transcriptomics.....</i>	130
4.3.2	<i>Comparative transcriptome analyses between species</i>	156
4.4	<i>Conclusion</i>	167
4.5	<i>References.....</i>	170

Chapter 5 174

Concluding Discussion 174

5.1	<i>Problem statement.....</i>	174
5.2	<i>Experimental overview and findings</i>	175
5.3	<i>Implications, limitations and future perspectives</i>	177
5.4	<i>References.....</i>	181

Appendixes (provided in electronic format on accompanying CD)

List of Tables

<i>Table 1.1 Distinct differences between the disease-causing pathogens Babesia and Plasmodium. Compiled from (Schuster, 2002).</i>	31
<i>Table 2.1 In vitro cultivation systems of several Babesia species (Compiled from Shuster, 2002).</i>	61
<i>Table 2.2 Biological functions of a subset of transcripts associated with differential abundance in B. divergens parasites upon culture adaptation.</i>	79
<i>Table 3.1 In vitro cultivation systems, screening methods and drug compounds, previously tested against human and animal Babesia species.</i>	97
<i>Table 3.2 Inhibitory properties of the scaffold compound (galvestine-1) and an analogue compound (A51B1C1_1) on apicomplexan parasites and plant cells.</i>	103
<i>Table 4.1 Biological, genomic and metabolic comparisons between three related apicomplexan species (Compiled from Lau, 2009 and Brayton et al., 2007).</i>	116
<i>Table 4.2 RNA yield, cDNA synthesis and labeling efficiency of eight representative samples.</i>	132
<i>Table 4.3 Differential transcript abundance analyses using the LIMMA software package.</i>	138
<i>Table 4.4 Functional annotations of gene transcripts with the highest increase and decrease in abundance according to COG (E-values 1×10^{-4}), together with the number of genes involved in each pathway.</i>	143
<i>Table 4.5 The top five KEGG pathways involved in differential gene expression.</i>	144
<i>Table 4.6 Gene-sets enriched among untreated and treated phenotypes (with highest associated significance levels) observed across all time-points.</i>	147
<i>Table 4.7 Orthologue clustering and functional grouping of transcripts present in P. falciparum and B. divergens data sets post A51B1C1_1 treatment.</i>	159
<i>Table 4.8 Orthologue clustering and functional annotations associated transcripts within the B. divergens and A. thaliana data sets, after A51B1C1_1 and galvestine-1 treatment, respectively.</i>	165

List of Figures

Figure 1.1 Global geographic distributions of human babesiosis and the corresponding ixodid tick vectors (Adapted from (Vannier and Krause, 2012)).	28
Figure 1.2 Diagnostic features of intra-erythrocytic zoonotic Babesia parasites (Adapted from (Gray et al., 2010)).	30
Figure 1.3 Splenic response to Babesia clearance within the host organism (Adapted from Vannier and Krause, 2012).	32
Figure 1.4 The close association between the apicoplast, nucleus and mitochondria of two apicomplexan species <i>B. bovis</i> and <i>P. falciparum</i> (Adapted from Marechal and Cesbron-Delauw, 2001 and Caballero et al., 2012).	39
Figure 1.5 Promising metabolic pathways for novel drug targets in apicomplexan parasites, with specific reference to <i>P. falciparum</i> (Adapted from Botte et al., 2011 and van Dooren and Striepen, 2013).	41
Figure 1.6 Structure and components of membrane glycerolipids in eukaryotic cell (Adapted from Boudiere et al., 2012).	44
Figure 1.7 MGDG synthesis in plant cells (Adapted from Botte et al., 2011).	46
Figure 1.8 Compounds in the selected piperidiny-benzimidazolone analogue library used as scaffolds of <i>Arabidopsis</i> , <i>P. falciparum</i> and <i>T. gondii</i> inhibitors (Adapted from Botte et al., 2011 and Saidani et al., 2014).	48
Figure 2.1 Flow cytometric analyses of intra-erythrocytic <i>B. divergens</i> parasites.	69
Figure 2.2 Morphological discrimination of <i>B. divergens</i> in vitro blood stage development.	71
Figure 2.3 Correlation of nuclear content to IDC compartments (stages) for <i>B. divergens</i> and <i>P. falciparum</i> parasites.	73
Figure 2.4 Temporal evaluation of <i>B. divergens</i> progression over two parasitic life cycles.	75
Figure 2.5 Molecular descriptors characterizing the IDC of <i>B. divergens</i> parasites.	78
Figure 2.6 Biological processes involved in <i>B. divergens</i> parasites' intra-erythrocytic development.	82
Figure 2.7 Model of the intra-erythrocytic developmental cycle of <i>B. divergens</i> parasites.	86
Figure 3.1 Sigmoidal dose-response curve established to calculate the IC_{50} of A51B1C_1 on <i>B. divergens</i> cultures in vitro.	102
Figure 3.2 Morphological evaluation conducted over a 16-hour time period of asynchronous <i>B. divergens</i> cultures treated at $2x IC_{50}$ concentrations of A51B1C1_1.	104
Figure 3.3 Graphical analyses of stage-specificity and life cycle progression of asynchronous <i>B. divergens</i> parasites over a 16-hour period under A51B1C1_1 treated conditions.	106
Figure 3.4 Cell viability assay to determine parasite recrudescence after treatment with compound A51B1C1_1.	108
Figure 4.1 Hybridization-based (microarray) experimental design and layout.	123
Figure 4.2 RNA purity and quality assessment by Experion [®] for use in the microarray experiment.	131
Figure 4.3 Example of the scanned custom designed 8x 15K Agilent arrays.	133
Figure 4.4 Box plots of all M-values (\log_2 ratio) and A-values (intensity) for all 24 arrays, before and after normalization.	135
Figure 4.5 Representative MA-plot before and after data normalization as well as Red-Green (RG) density plots of all three microarray slides before and after normalization.	136
Figure 4.6 GO-annotation and functional grouping of transcripts of increased (up-regulated) and decreased (down-regulated) abundance after treatment.	141

Figure 4.7 Heatmap and correlation plot of the top 50 features associated with each phenotype (untreated or treated) in association with the ranked list of genes. 146

Figure 4.8 Graphical representation (enrichment plots) for the two most significantly enriched gene-sets associated with untreated (transcription; left plot) and treated (cytoskeleton; right plot) phenotypes. 148

Figure 4.9 Major metabolic pathways of *B. divergens* affected by treatment. 150

Figure 4.10 Overview of flow of information in treated *B. divergens* parasites, from DNA to protein. 155

Figure 4.11 Unique and shared orthologue groups between the A51B1C1_1 treated transcriptome data sets from *B. divergens* and *P. falciparum*. 158

Figure 4.12 Unique and shared orthologue groups between the treated transcriptome data sets associated with *B. divergens* and *A. thaliana*. 164

List of Abbreviations

ALA	Aminolevulinic acid
Aminoallyl-dUTP	Aminoallyl deoxyuridine triphosphate
AOS	Allene oxide synthase
Api	Apicoplast
ATP	Adenosine triphosphate
A-value	$A = \frac{1}{2} \log_2 RG$, where R is red and G is green fluorescent signals
B2G	BLAST2GO
BBH	Bi-directional best hit
BLAST	Basic local alignment search tool
cDNA	Complementary deoxyribonucleic acid
COG	Cluster of orthologous genes
Cy 3	Cyanine 3
Cy 5	Cyanine 5
DAG	Diacylglycerol
dCAS	Desktop cDNA annotation software
DEG	Differentially expressed gene
DGDG	Digalactosyldiacylglycerol
dGTP	Deoxyguanosine triphosphate
DMAPP	Dimethylallyl pyrophosphate
DMSO	Dimethyl sulphoxide
DNA	Deoxyribonucleic acid
dNTPs	Deoxynucleoside triphosphates
DOXP	1-deoxy-D-xylose-5-phosphate

DTT	Dithiothreitol
dTTP	Deoxythymidine triphosphate
dUTP	Deoxyuridine triphosphate
EC	Enzyme commission
ePAP	endomembrane PAP's
ER	Endoplasmic reticulum
ES	Enrichment score
EST	Expressed sequence tag
FA	Fatty acid
FE-S	Iron-sulphur
G3P	Glyceraldehyde-3-phosphate
GO	Gene ontology
GSEA	Gene-set enrichment analysis
GTP	Guanosine triphosphate
Hpi	Hours post invasion
IC ₅₀	50% inhibitory concentration
IDC	Intra-erythrocytic developmental cycle
IEM	Inner envelope membrane
IPP	Isopentenyl pyrophosphate
JA	Jasmonic acid
KAAS	KEGG automated annotation server
KEGG	Kyoto encyclopaedia of genes and genomes
LIMMA	Linear model for microarray data analysis
LOWESS	Locally weighted scatterplot smoothing
LOX	Lipoxygenase

MASP	Micro-aerophilus stationary phase
MEP	2C-methyl-D-erythritol-4-phosphate
MFI	Median fluorescence intensity
MGDG	Monogalactosyldiacylglycerol
MHC	Major histocompatibility complex
MIAME	Minimum information about a microarray experiment
Mit-Pla	Mitochondrial and plastid database
mRNA	Messenger ribonucleic acid
MSF	Malaria SYBR-Green I fluorescence
M-value	$M = \log_2$ red/green fluorescence signals
NCBI	National Centre for Biotechnology Information
NES	Normalized enrichment score
NR	Non-redundant
NU	Nucleus
OEM	Outer envelope membrane
OMS	Outermost membrane system
ORF	Open reading frame
PA	Phosphatidic acid
PAP	Phosphatidic acid phosphatase
PBS	Phosphate buffered saline
PC	Phosphatidylcholine
PCR	Polymerase chain reaction
PEP	Phosphoenolpyruvate
Pfam	Protein family sequence
PLC's	Phospholipases C

PLD's	Phospholipases D
pPAP	Plastid phosphatidic acid phosphatase
R ²	Regression coefficient
RNA	Ribonucleic acid
RNA Pol I	RNA polymerase I
RNA Pol II	RNA polymerase II
RNA Pol III	RNA polymerase III
RNase	Ribonucleotidase
RNA-Seq	RNA-Sequencing
RQI	RNA quality indicator
rRNA	Ribosomal ribonucleic acid
SFR-2	Sensitive to freezing -2
SI	Selectivity index
SMART	Simple modular architecture research tool
T	Treated
TAG	Triacylglycerol
TCA-cycle	Tricarboxylic acid cycle
TrioseP	Triose phosphate
tRNA	Transfer ribonucleic acid
UT	Untreated
WHO	World Health Organization

Chapter 1

Literature Review

1.1 Introduction

Some of the most widely distributed, globally recognized and poorly controlled animal and human diseases result from vector-transmitted blood parasites (Brayton *et al.*, 2007). One such phylum, the *Apicomplexa*, contains many important disease-causing pathogens responsible for malaria (*Plasmodium* species), babesiosis (*Babesia* species), toxoplasmosis (*Toxoplasma* species) and cryptosporidiosis (*Cryptosporidium* species) (Vannier and Krause, 2009). Both malaria and babesiosis are transmitted by hematophagous vectors, *Anopheles* mosquitoes and Ixodid ticks, respectively, both of which are prevalent in central and southern African countries (Vannier and Krause, 2009).

Bovine babesiosis is a well-known disease and is regarded as one of the most important arthropod-borne diseases of cattle, with more than half of the world's 1 – 2 billion bovines at risk (Schnittger *et al.*, 2012). In contrast, human babesiosis, which is the topic of this study, is a rapidly emerging zoonotic, infectious disease, causing malaria-like symptoms in humans. It is a tick-borne disease caused by intra-erythrocytic protozoan parasites *Babesia divergens* or *Babesia microti* and is transmitted to humans *via* an ixodid tick vector or blood transfusion from asymptomatic carriers (Hildebrandt *et al.*, 2013). Disease prevalence has escalated over the past 50 years from a few isolated cases to global endemic areas being recognized (Lau, 2009a, Vial and Gorenflot, 2006). Development of new treatment strategies is essential to control this potentially dangerous disease.

This chapter will firstly give an overview of tick vectors and the associated pathogens transmitted. Next, *Babesia* will be discussed with emphasis on the basic biology, epidemiology and treatment in humans and bovines. Finally, an integrative review on apicomplexan species with specific reference to the apicoplast as drug target and the piperidiny-benzimidazolone analogue, compound A51B1C1_1 used as parasitic growth inhibitor in this study.

1.2 Ticks as vectors of both animal and human disease

Ticks are regarded as one of the most successful groups of obligate hematophagous ectoparasites of domestic animals, wildlife and humans (Singh-Behl *et al.*, 2003). They constitute a diverse group of species, distributed among three families; the Argasidae (soft ticks, so called due to their flexible cuticle), Ixodidae (hard ticks, so called due to their sclerotized dorsal plate) and the Nuttalliellidae (represented by a single species) (Horak 2002; Sonenshine, 1991). Approximately 896 tick species have been identified within these 3 families of which some 80% are ixodid ticks (Guglielmone *et al.*, 2010, Horak *et al.*, 2002). Ticks were the first reported arthropod-borne disease vectors and are globally regarded as one of the most important vectors of human disease (surpassed only by mosquitoes) responsible for over 100 000 cases of human disease annually (Jongejan and Uilenberg, 2004). The importance of tick-borne diseases is measured by the levels of morbidity and mortality observed in humans. The global impact of ticks and tick-borne diseases on humans has been observed mostly throughout the temperate regions of the world in the form of tick-borne zoonoses (de la Fuente *et al.*, 2004). The incidence of tick-borne diseases is a growing concern as they are of medical and veterinary importance. For instance, approximately 250 000 cases of lyme borreliosis were reported in North America between 2000 and 2010, with the number of cases reported annually in European countries escalating to 50 000 (http://www.cdc.gov/lyme/stats/chartstables/reportedcases_statelocality.html). Increased global

incidence of ticks and tick-borne diseases may be attributed to changes in human behaviour, environmental changes, changes in land-use, increased levels of travel and trade as well as wildlife migration (Colwell *et al.*, 2011, Filbin *et al.*, 2001).

Ticks are regarded as the most important vectors of disease-causing pathogens in domestic animals and wildlife species, as determined by the loss of animal production and mortality (Jongejan and Uilenberg, 2004). Among livestock, the most important tick transmitted diseases include babesiosis, theileriosis, anaplasmosis and cowdriosis (Dantas-Torres *et al.*, 2012). In sub-Saharan Africa, Asia and South-America, tick-borne diseases are major barriers of productivity as they directly impact the livelihood of farming communities, where malnutrition is rife and the demand for livestock products are high (Ribeiro *et al.*, 2006). A comprehensive summary of ticks, their associated pathogens, host species and geographic distribution affecting both animal and human populations are presented in Appendix 1.1 and Appendix 1.2, respectively.

According to the World Health Organization (WHO), zoonosis is defined as an infection or disease, naturally transmissible between humans and vertebrate animals and *vice versa*. Approximately 200 such diseases have been described, the causative agents of which vary considerably – from bacteria, viruses, endo-parasites and fungi to several unconventional agents such as ticks (<http://www.who.int/zoonoses/en/>). In addition to well established zoonoses, newly emerging zoonoses are continually being discovered. The emergence of a zoonotic disease is a complex process involving several biological interactions and factors such as environmental changes (climate change which may influence the ecology of the vector, animal host and their life cycles), pathogen changes as well as changes in human and animal demographics (Mills *et al.*, 2010). Social and cultural factors contribute to a lesser degree to the emergence of zoonotic diseases <http://www.cdc.gov/climatechange/effects/vectorborne.htm>.

Over the past ten years, approximately 75% of new diseases affecting humans have originated either directly from animals or from animal by-products.

Closer collaborations between medical and veterinary specialists (with specific emphasis on individual health, public health and comparative medicine) will improve surveillance, tracking and managing of zoonoses (Kahn, 2006). In 1983, Smith and Kilbourne, a physician and veterinarian, respectively, confirmed the success of a collaborative effort between two disciplines, when they described the causative agent of Texas cattle fever (*Babesia bigemina*) to be transmitted by a tick vector (as reported by Kahn (Kahn, 2006)).

Tick control refers to treatment that reduces tick load and host exposure within a specific area and point in time (Walker, 2011). Most control and eradication strategies are in place to protect the host species. Current control strategies employed to control tick burdens are predominantly based on the use of chemical acaricides (Dantas-Torres *et al.*, 2012). Acaricide resistance is a major limiting factor in tick control strategies (Willadsen, 2006) and therefore alternative strategies have been proposed such as immunological control (vaccines) (Willadsen, 2008), biological control (plant extracts and fungal species) (Samish *et al.*, 2008), tick resistant cattle breeding programs as well as pasture management and rotational grazing programs (Walker, 2011). Complete eradication of ticks is an unrealistic goal, due to important wildlife species that act as hosts for several economically important tick species known to parasitize several domestic and wildlife species throughout the temperate regions of the world (Jongejan and Uilenberg, 2004).

As the distribution of tick-borne diseases coincides with that of their associated tick vectors, accurate tick control strategies would also alleviate pathogen load (Bock *et al.*, 2004). To maximize tick-borne disease control, a collaborative strategy is ideal as no one technique is invariably effective (Fritz, 2009). The “One Health Approach” is an integrative effort between

medical and veterinary disciplines at local, national and global health levels to ultimately reduce morbidity and mortality rates associated with ticks and tick-borne diseases (Dantas-Torres *et al.*, 2012). The effectiveness of control strategies is improved by rapid detection by clinicians, veterinarians, disease ecologists and epidemiologists. Awareness, management and prevention strategies all contribute to effective tick and tick-borne disease control (Walker, 2011). Prevention is better than cure – this however is not a feasible reality to individuals residing in tick-endemic regions. These individuals require the application of tick-repellents, protective clothing, avoidance to exposure, early detection and removal of ticks as preventative measures (Walker, 2011).

The zoonotic tick-borne disease babesiosis is one of the most important infections affecting both human and animal health systems (Ribeiro *et al.*, 2006) and is therefore of both medical and veterinary importance (McDaniel *et al.*, 2014) and subsequently forms the focus of this study.

1.3 The *Babesia* parasite and pathogenesis of babesiosis

1.3.1 Classification and life cycle of *Babesia* species

Babesia species are classified as apicomplexan parasites of the suborder Piroplasmidea and family Babesiidae, based on their lack of haemozoin, exclusive invasion of erythrocytes and their unique multiplication method by budding (Hunfeld and Brade, 2004). *Babesia* and *Theileria* species are also referred to as piroplasmids, based on their pear-shaped morphological appearance within the hosts' erythrocytes (Schnittger *et al.*, 2012). *Babesia* species differ from other apicomplexans in that they are naturally transmitted by the bite of an infected tick, are restricted to erythrocytes and multiply asexually (Vial and Gorenflot, 2006). Over 100 species have been identified to date, associated with infection of mammalian and some avian species (Hunfeld *et al.*, 2008).

Babesia species classification is based on various factors which include the size and shape of the intra-erythrocytic parasites, the number of merozoites and host-vector specificity (Yabsley and Shock, 2013). The classification based on parasitic size and shape, distinguishes between two groups, the “small” and “large” *Babesias*. The small parasites are 1.0 – 2.5 μm in diameter and include *Babesia gibsoni*, *B. microti* and *Babesia rodhaini* compared to the “large” parasites (2.5 – 5.0 μm in diameter) which include *Babesia bovis*, *Babesia caballi* and *Babesia canis* (Gray *et al.*, 2010, Vannier and Krause, 2012). Traditional morphological classifications are consistent with the phylogenetic classification of *Babesia* species, based on the 18S ribosomal RNA gene sequences (Hunfeld *et al.*, 2008), where phylogeny shows that “large” and “small” *Babesia* species fall into two distinct clusters, with “small” *Babesias* more closely related to *Theileria* species than to “large” *Babesias*. *Babesia divergens* is an exception to this rule as it appears “small” on blood smears (0.4 – 1.5 μm in diameter), but is genetically more closely related to “large” *Babesia* species (Hunfeld *et al.*, 2008).

The life cycle of *Babesia* species is complex and requires both an invertebrate vector and a vertebrate mammalian host. The cycle consists of three stages, namely gamogony, sporogony and merogony (Hunfeld *et al.*, 2008). Gamogony is the sexual stage within the gut of the tick vectors, where formation of gametes takes place, while sporogony is the asexual reproductive stage within the salivary glands of the tick vectors. Merogony refers to the asexual division within the erythrocyte of the vertebrate host (Vial and Gorenflot, 2006). Particularly intriguing is the fact that the precise progression and duration of the intra-erythrocytic, asexual developmental cycle (IDC) of *Babesia* has not been clarified and is fraught with uncertainties. Little attention has been paid to the parasitic sequence of development and descriptions associated with the *in vitro* stages do not share a consensus in literature. Moreover, fundamental biological questions remain unanswered, particularly concerning the molecular

descriptors governing the IDC of *Babesia* parasites, aspects of which will be discussed in detail within Chapter 2.

1.3.2 Human babesiosis

Disease history

Babesiosis is best known as an animal disease, but has recently gained attention as an emerging, global zoonosis. The disease has a global distribution affecting companion animals, domestic animals, livestock, several wildlife species and humans (Vial and Gorenflot, 2006). Natural disease transmission to humans is enhanced by human encroachment on wildlife habitat and travel to endemic areas (Filbin *et al.*, 2001). Alarmingly though, indirect transmission occurs in most instances *via* blood and platelet transfusions of contaminated blood (Oz and Westlund, 2012).

The first historical record of babesiosis may have been the biblical reference in Exodus, which described the plague of murrain (haemoglobinuria) among cattle of the Egyptians and Pharaoh Ramses II (as described by Vial and Gorenflot (Vial and Gorenflot, 2006)). It was however not until 1888 that the parasite was first described in Rumanian cattle, by the Hungarian scientist Victor Babes (as reported by Gray (Gray, 2006)). Five years later in 1893, Smith and Kilbourne discovered the causative agent of Texas cattle fever (known as *B. bigemina*) to be transmitted *via* tick vectors (as reported by Vial and Gorenflot (Vial and Gorenflot, 2006)). Since then, approximately 100 *Babesia* species known to infect companion animals and wildlife species have globally been recognized and described (Krause *et al.*, 2000). In 1908, Wilson and Chowning discovered the first evidence that humans could be affected by *Babesia* parasites (Kjemtrup and Conrad, 2000). In 1957, the first confirmed fatal case of human babesiosis was diagnosed in an asplenic, Yugoslavian farmer as a result of a *B. divergens* infection (Krause *et*

al., 2000). By 1968, several cases of human babesiosis were reported in America. Between 1968 and 1993 the number of human babesiosis cases escalated to approximately 450 (Singh-Behl *et al.*, 2003). In future, reports of human babesiosis will most likely increase, due to an increase in veterinary, medical and public health awareness (Gray *et al.*, 2010).

Disease vector, epidemiology and transmission

The best described *Babesia* pathogens to date are transmitted to their hosts by *Ixodes* species (Marathe *et al.*, 2005). *Ixodes ricinus* is the predominant tick vector of human babesiosis across Europe due to either *B. divergens* or *Babesia venatorum* infections, while *Ixodes scapularis* is the predominant tick vector of *B. microti* infections in North America. Isolated cases of human babesiosis have been reported in Asia, with *Ixodes ovatus* and *B. microti* described as the causative disease vector and pathogen, respectively (Vannier and Krause, 2012).

The *I. ricinus* tick is widely distributed throughout the temperate regions (with moderate to high rainfall) of Europe, Asia and North America (Ruiz-Fons *et al.*, 2012) and is known to feed on a variety of host species, including birds, reptiles, rodents, small and large mammals as well as wild and domestic ungulates (Becker *et al.*, 2009). The global distribution of *I. ricinus* ticks is under constant change and depends on climatic (temperature, rainfall, snow cover) and non-climatic (host animal distribution, habitat structure and connectivity, human activity) factors (Medlock *et al.*, 2013). These factors additionally contribute to the spread of tick-borne diseases by the *I. ricinus* vector. A better understanding of the spread of *I. ricinus* ticks will ultimately contribute to a better understanding of the diseases they transmit. *Ixodes ricinus* ticks are opportunistic and will feed on humans when the need arises, which make them ideal vectors of human tick-borne diseases such as babesiosis, lyme borreliosis, human granulocytic

anaplasmosis, rickettsiosis, tularaemia, tick-borne encephalitis virus, louping ill virus and tribec virus (Medlock *et al.*, 2013).

Since the late 1950's the epidemiology of human babesiosis has changed considerably, from a few isolated global cases, to endemic areas within the United States (southern New England, New York, New Jersey and the northern Midwest). Several sporadic cases have also been reported in South America (Mexico), Europe (Croatia, France, Great Britain, Germany, Ireland, Portugal, Spain, Sweden and Switzerland), Africa (Egypt, Mozambique and South Africa), Asia (Japan, Taiwan), India and South Korea (Hunfeld *et al.*, 2008, Vannier and Krause, 2012) (Figure 1.3). Until recently the public health burden of babesiosis was unknown, the disease however became a nationally notifiable disease in 2011 in the United States (Kavanaugh and Decker, 2012).

The initial geographic distribution of human babesiosis, as a result of a *B. divergens* infection, coincides with *B. divergens* infected cattle populations and *I. ricinus* tick infested regions. In Europe, *B. divergens* is the most common causative agent of human babesiosis (Vannier and Krause, 2009) with over 40 cases reported and diagnosed in asplenic patients with several cases likely unreported or misdiagnosed (Zintl *et al.*, 2003). Three cases of acute human babesiosis due to *B. divergens*-like infection have however recently been reported in asplenic individuals in North America. The rodent associated pathogen *B. microti* is the predominant causative agent of human babesiosis in North America in both spleen-intact and asplenic individuals (Figure 1.1) (Gray *et al.*, 2010).

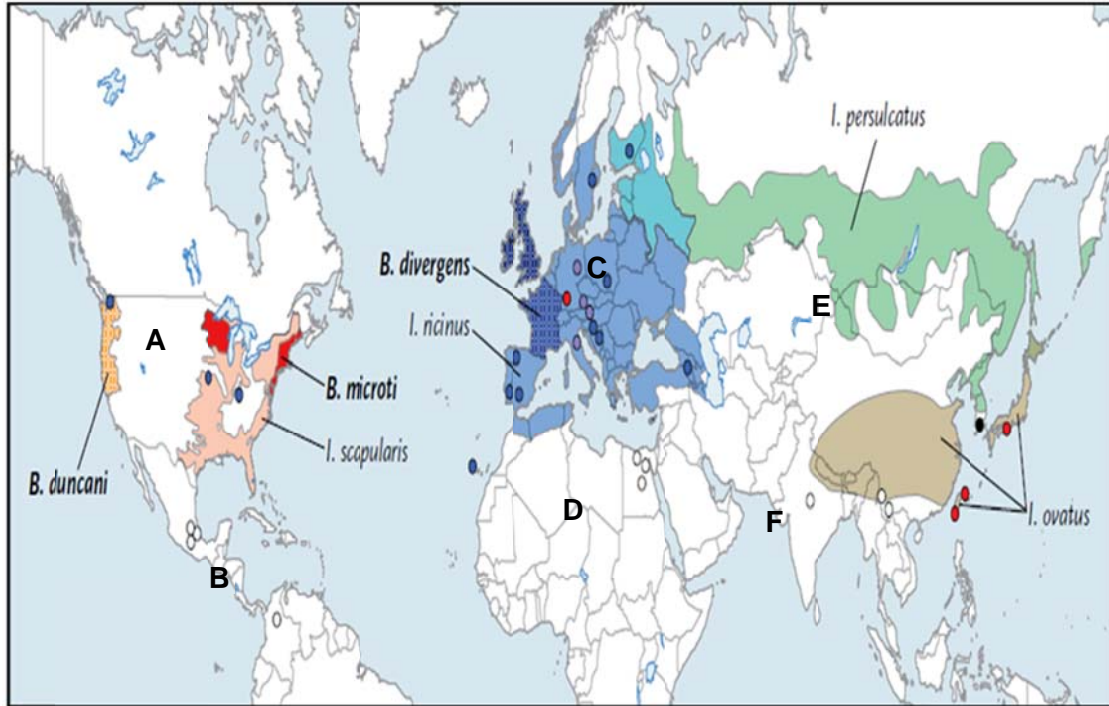


Figure 1.1 Global geographic distributions of human babesiosis and the corresponding ixodid tick vectors (Adapted from (Vannier and Krause, 2012)).

(A) North America: Red shaded areas indicate disease endemic regions due to *B. microti* infections; orange shaded areas indicate sporadic cases of disease due to either *B. duncani* or *B. duncani*-like infections. Blue circles represent reported *B. divergens*-like infections. All infections transmitted via *I. scapularis* ticks. (B) South America: White circles indicate asymptomatic infections reported in Mexico. (C) Europe: Blue circles indicate either *B. divergens* (France, Britain, and Ireland) or *B. venatorum* (Germany, Austria, Italy, Belgium) infections (not shown), transmitted via the *I. ricinus* tick vector. (D) Africa: Disease cases of unknown pathogen and vector have been reported in Egypt (white circles), Mozambique (not shown) and South-Africa (not shown). (E) Asia: Grey shaded areas and red circles indicate *B. microti*-like infections in Taiwan and Japan, transmitted by *Ixodes ovatus* ticks; green shaded areas indicate *B. microti*-like infections of mammals due to *Ixodes persulcatus* tick vectors (*I. persulcatus* not known as vector of human babesiosis); black circle indicates one case of human babesiosis in South Korea due to a *KO1-babesia* strain infection (related to a *Babesia* species isolated in sheep). (F) Uncharacterized *Babesia* species have been known to cause disease in India (white circle).

The status of human babesiosis in South Africa is unclear. Two cases of the disease (initially misdiagnosed) were diagnosed and reported in a 38 year old male and a 16 year old female during the 1990's. Both patients became ill after visiting recognized malaria areas (Bush *et al.*, 1990). Moreover, South Africa contains a highly significant array of ixodid tick vectors exposed to large numbers of immune-compromised individuals (due to high numbers of HIV infections

throughout the country). The number of human babesiosis cases in South Africa is expected to be greatly underestimated and could well be in line with global trends. It is therefore an urgent priority to initiate innovative strategies to diagnose the disease.

Clinical symptoms and diagnosis

Once a host species has been bitten by an infected ixodid tick, the incubation period for the transmitted parasite ranges from five to thirty days (Vial and Gorenflot, 2006). The clinical features of *Babesia* infected patients appear one to three weeks after infection and vary considerably from asymptomatic to life threatening, depending on the particular pathogen and the general health condition of the individual (Hunfeld *et al.*, 2008). Infections are generally regarded as high priority and medical emergencies due to the high morbidity and mortality rates associated with this infection (Vyas *et al.*, 2007). Particularly, immune-compromised or asplenic individuals are regarded as high-risk patients. An array of *Babesia* species is commonly found to infect humans (Appendix 1.2). Although the rodent associated *B. microti* strain is the most common species responsible for human babesiosis, the severity of infection is variable (Vannier and Krause, 2009). Patients infected with *B. microti* may either be asymptomatic or display mild to moderate infection symptoms such as fatigue, fever, headache, nausea, chills and sweats. In more severe cases symptoms may include jaundice, respiratory complications, heart failure, renal failure or splenic rupture (Vannier and Krause, 2009). Infection with the more virulent cattle associated strains *B. divergens* and *B. divergens*-like (WA-1 and MO-1 types) parasites, cause a severe form of disease, resulting in death in more than a third of patients (Vial and Gorenflot, 2006, Schuster, 2002b).

Preliminary diagnosis of human babesiosis can be made from indicative clinical features and should be considered in individuals who either reside in or travel to *Babesia* endemic areas and

experience relatively non-specific viral-like symptoms, or recently received a blood-transfusion (Vannier and Krause, 2009). Disease confirmation can be obtained by additional diagnostic tests such as microscopic identification, polymerase chain reaction (PCR) or serology (Vyas *et al.*, 2007). Definitive laboratory findings depend on the level of infection observed within the host species (Homer *et al.*, 2000). Microscopic disease confirmation relies on the examination of Giemsa-stained thin blood smears and the detection of unique intra-erythrocytic features. The paired piriform is a unique parasitic feature associated with most *Babesia* species (Figure 1.2), except for *B. microti* and *B. microti*-like parasites, where the tetrad and/or maltese cross are regarded as the diagnostic feature of choice. Most zoonotic *Babesia* species are often identified based on the presence of the tetrad (maltese cross) (Figure 1.2) (Gray *et al.*, 2010). If laboratory tests are negative or remain inconclusive and clinical symptoms persist, patient blood-samples can be injected into a laboratory animal (typically hamsters) and monitored to confirm infection (Vannier and Krause, 2012).

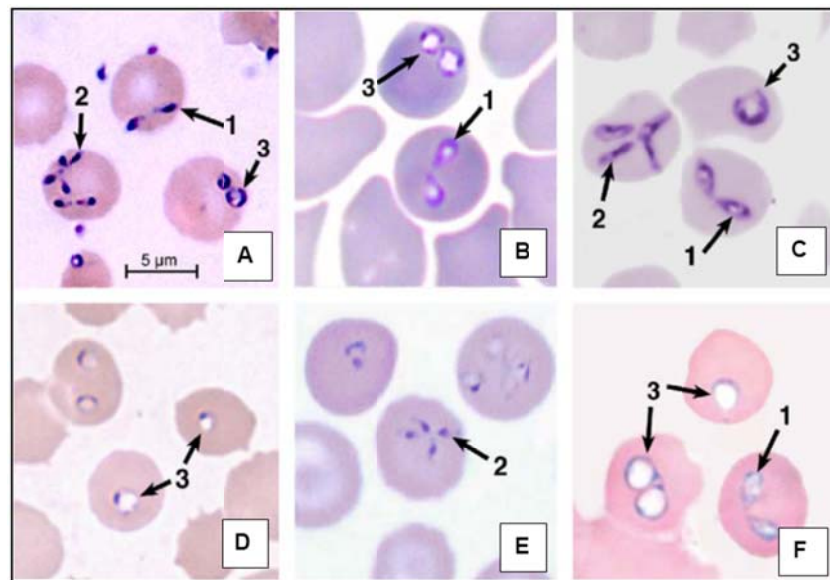


Figure 1.2 Diagnostic features of intra-erythrocytic zoonotic *Babesia* parasites (Adapted from (Gray *et al.*, 2010).

(A) *B. divergens* (B) *B. venatorum* (C) *B. divergens*-like Kentucky isolate (D) *B. microti* (E) *B. duncani* and (F) *Babesia* KO1-strain. Arrows indicate (1) Paired piriforms (2) tetrads/maltese cross and (3) ring forms.

Clinical disease presentation is similar to malaria and also easily confused as *Plasmodium* infection, as *Babesia* ring formations closely resemble those of *Plasmodium falciparum* (Filbin *et al.*, 2001). Misdiagnosis can be eliminated based on careful microscopic examination of thin blood-smears as well as a comprehensive patient travel history (Hunfeld *et al.*, 2008). Specific distinctions between the causative agents of human babesiosis (*Babesia*) and malaria (*Plasmodium*) are summarized in Table 1.1.

Table 1.1 Distinct differences between the disease-causing pathogens *Babesia* and *Plasmodium*. Compiled from (Schuster, 2002)

<i>Babesia</i> species	<i>Plasmodium</i> species
Ixodid tick vectors	Anopheles mosquito vector
Exo-erythrocytic stage absent	Exo-erythrocytic stage present
Divides <i>via</i> binary fission	Divides <i>via</i> shizogony
Develops within the cytoplasm of the hosts' erythrocyte	Develops within the parasitophorous vacuole (PV) of the host
Does not form haemozoin pigment within the infected erythrocyte of host species	Forms haemozoin pigment within the infected erythrocyte of host species

Host resistance, immunity and pathogenesis

Knowledge regarding host resistance against human babesiosis is limited. Most of what is known is based on *in vitro* disease experiments in vertebrate hosts and animal models using *B. bovis*, *B. microti* (Homer *et al.*, 2000) and *B. divergens* (Zintl *et al.*, 2003). It is well known that the spleen plays a pivotal role in the hosts defence strategies, by clearing infected erythrocytes and eliciting a protective immune response (Mebius and Kraal, 2005). Asplenia is therefore a major driver for severe infection (Hunfeld *et al.*, 2008). Individuals at even higher risk of contracting the disease are asplenic, immune-compromised, co-infected with other pathogenic species or individuals older than 50 years of age (Krause *et al.*, 2000) (Figure 1.3).

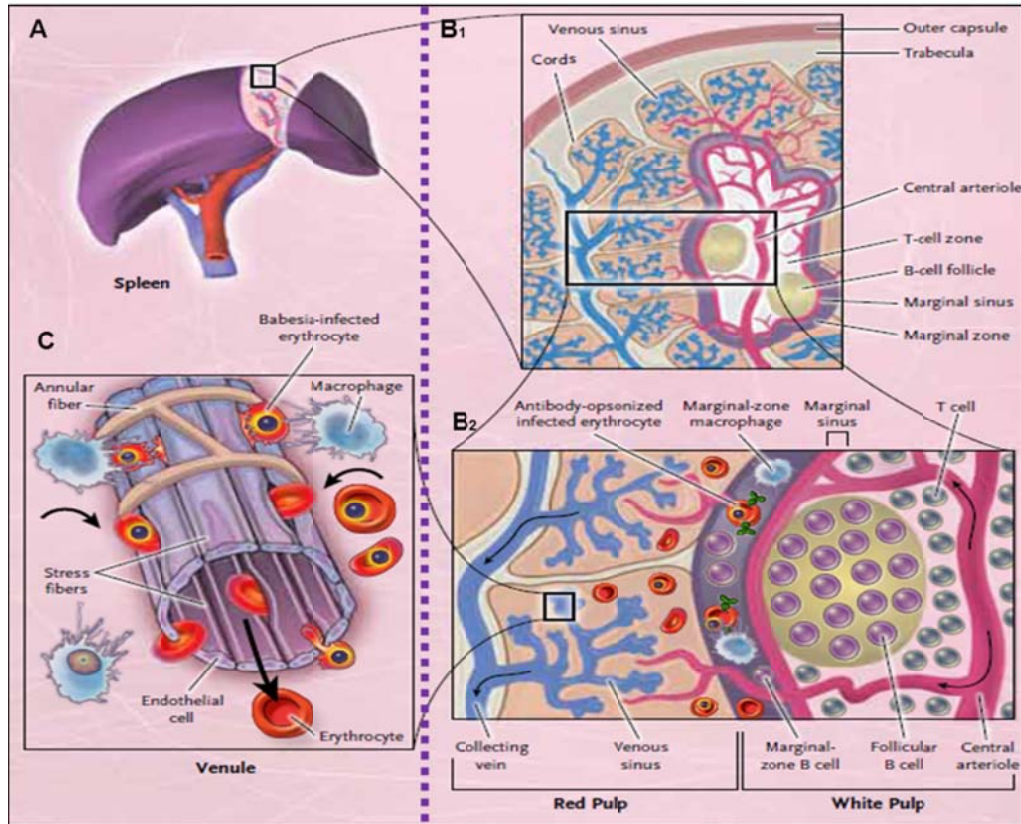


Figure 1.3 Splenic response to *Babesia* clearance within the host organism (Adapted from Vannier and Krause, 2012).

(A) Circulating erythrocytes enter the spleen via the trabecular artery and (B₁) flow into the central arteries and follicular arterioles to eventually reach (B₂) the marginal sinus of the white pulp. Within the marginal zone, dendritic cells and macrophages ingest and destroy *Babesia* infected erythrocytes. The marginal zone associated macrophages do not express major histocompatibility complex (MHC) class II molecules. Pathogen degradation products are released and obtained by the marginal zone associated B-cells. Activated marginal zone B-cells and dendritic cells, move towards the T-cell zone and present antigens to the T-cells within the T-cell zone. These activated T-cells engage B-cells, causing them to activate and differentiate into anti-body secreting cells. Opsonisation of parasitized erythrocytes by antibodies, promote parasite clearance via phagocytosis. Activated B-cells additionally produce interferon- γ which assists in macrophage engulfment of pathogens. Circulating erythrocytes may, however, bypass the white pulp and directly enter the red pulp region of the spleen. Within the splenic chords, infected cells flow (with difficulty) between the reticular fibres and apertures of the endothelium lining and are ultimately ingested by macrophages associated with the chords. (C) The flow and size of cells that reach the venous sinuses collecting vein, are regulated by the contraction and relaxation of the stress and annular fibres.

Cellular immunity appears to be more important than humeral immunity in controlling babesiosis (Vannier and Krause, 2012). Observed within *B. microti* infected mice, CD4+ T-cells produce interferon- γ , known to promote intracellular removal of pathogens by macrophages as well as enhance antibody production by B-cells (Igarashi *et al.*, 1999, Hunfeld *et al.*, 2008). The CD4+ T-cells, therefore, play an important part in combating infection and reducing parasitaemia levels. Depletion of host macrophages increases their susceptibility for contracting disease (Vannier and Krause, 2012). Additionally, within *B. microti* infected mice, those suffering from T-cell receptor deficiencies are readily infected, compared to the less susceptible B-cell deficient mice. B-cells are, therefore, critical for parasite clearance in patients with impaired cellular immunity. Age related decline in cellular immunity offers an explanation to the disease severity observed in older individuals (Vannier *et al.*, 2004, Hunfeld *et al.*, 2008). *Babesia duncani* infected mice displayed an excessive production of pro-inflammatory cytokines (TNF- α and interferon- γ), mostly due to the hosts response to infection and not from the intra-erythrocytic parasite itself (Hunfeld *et al.*, 2008). In mild cases of infection, inflammatory cytokines and adhesion molecules are up-regulated, in contrast to severe cases of infection where excessive cytokine production is observed (Hemmer *et al.*, 2000).

Current treatment strategies for babesiosis

Treatment of human babesiosis depends on the regulatory guidelines of each country and the commercial availability of therapeutics. Successful treatment of the disease depends on the early detection, diagnosis and administration of effective drug compounds (Vial and Gorenflot, 2006). Knowledge on therapeutics applicable to human babesiosis infection is primarily derived from clinical data from *B. microti* and *B. divergens* infected individuals (Hunfeld *et al.*, 2008). Current treatment of human babesiosis is a combination of the anti-malarial compound

atovaquone and the antibiotic azithromycin, administered for seven to ten days. In severe cases, a combination of the anti-malarial drugs clindamycin and quinine is given, but due to the severe adverse side effects (tinnitus, hearing loss and diarrhea) it is less commonly used (Lau, 2009a). During a relapse of the disease, the anti-malarial combination atovaquone-proguanil is used for a minimum of six weeks and at least two weeks after the last positive blood smear (Lau, 2009a). Known anti-malarials such as chloroquine, mefloquine and artemisinin are regarded as ineffective compounds against *Babesia* species (Hunfeld *et al.*, 2008). Literature regarding the emerging resistance of *Babesia* species against azithromycin-atovaquone, clindamycin and quinine, diminazene aceturate, doxycycline and pentamidine, is steadily increasing (Vyas *et al.*, 2007, Wormser *et al.*, 2010), which therefore emphasizes the urgent need to develop new therapeutics and/or improve existing treatment strategies to overcome this emerging disease.

Unfortunately, antibiotic prophylaxis or the use of live attenuated or inactivated vaccines has not been established against zoonotic babesiosis. The use of multiple preventative measures against babesiosis is likely to be most successful which includes personal, residential and community based measures (Hunfeld *et al.*, 2008). Preventative measures range from simple avoidance measures, the use of tick repellents, prompt removal of any tick and public awareness, to more drastic habitat modifications (Vannier and Krause, 2009). Since asplenic and immune-compromised individuals are at higher risk of contracting the disease they should adhere to suggested preventative measures (Vannier and Krause, 2009). Laboratory-based screening programmes of prospective blood-donors from *Babesia* endemic regions may reduce the risk of transfusion transmitted human babesiosis (Hunfeld *et al.*, 2008).

1.3.3 Bovine babesiosis

Bovine babesiosis is an acute, haemolytic tick-borne disease and is regarded as one of the most important tick-borne diseases of cattle (Friedman and Yakubu, 2014). With a global distribution, more than half of the world's cattle population is at risk and economically it is the most important arthropod-borne disease worldwide (Bock *et al.*, 2004). Bovine babesiosis is caused by several species of intra-erythrocytic protozoan parasites of the *Babesia* genus, those most widely represented in current literature include *B. bovis*, *B. bigemina*, *B. divergens* and *Babesia major* (Zintl *et al.*, 2003). Bovine babesiosis is a widely distributed disease, with pathogen distribution determined by their respective tick vectors and host species (Goes *et al.*, 2007).

The beef and dairy cattle industries associated with the tropical and sub-tropical regions of Africa, Asia, Australia and North and South America are at great risk of *B. bovis* and *B. bigemina* infections. These two *Babesia* species are most commonly transmitted by *Rhipicephalus microplus* and *Rhipicephalus annulatus* tick vectors (Zintl *et al.*, 2003, Gohil *et al.*, 2013). In South Africa, *B. bovis* is mostly found in high rainfall areas (KwaZulu Natal, Eastern Cape and eastern parts of Mpumalanga and Limpopo provinces), while *B. bigemina* can be found throughout the country with the exception of extremely dry areas (Regassa *et al.*, 2003). In South American countries such as Brazil, *B. bovis* and *B. bigemina* are the most common pathogens known to infect cattle under natural conditions (Goes *et al.*, 2007). In European countries, *B. divergens* is widespread in the same regions where the tick vector *I. ricinus* is commonly found. Countries such as France, Australia and South Africa, with the highest incidence of bovine babesiosis are generally those with considerable tick populations (Gray, 2006).

The *B. bovis* parasite is unique from other *Babesia* species in that infections may be accompanied by an increase in infected red blood cells within the microvasculature of numerous

organs, which may subsequently develop into severe clinical complications such as cerebral babesiosis, respiratory distress syndrome and multi-organ failure (Gohil *et al.*, 2010, Gohil *et al.*, 2013). The *B. bovis* parasite alters the structure and function of the erythrocytes of the bovine host in which they reside and undergo cyclic replication (Schnittger *et al.*, 2012). For the pathogen to survive within the hosts' erythrocyte, it must maintain the mechanical reliability of the hosts' erythrocyte, attain nutrients, avoid the hosts' immune system and escape destruction by the spleen (Gohil *et al.*, 2013).

Specific symptoms associated with bovine babesiosis include fever, anaemia, weakness, increased heart rate, cessation of rumination, haemoglobinuria, haemolysis, pulmonary oedema as well as changes in the erythrocytes and endothelial cell damage. One of the most critical features of the disease is haemolytic anaemia, which results from the destruction of non-infected erythrocytes (Goes *et al.*, 2007).

Treatment and control strategies for bovine babesiosis remain limited. Current treatment relies mostly on a combination of anti-*Babesia* therapeutics and/or vaccination (Suarez and Noh, 2011). Successful disease control should take into account cattle breed, age, tick distribution, early diagnosis and administration of drug compounds (Mosqueda *et al.*, 2012). The principle chemotherapeutic agent currently applied against bovine babesiosis is the anti-protozoal imidocarb dipropionate, with diminazene aceturate used as alternative. Prolonged treatment may however have a negative impact on meat and dairy products due to the presence of drug residues (Zintl *et al.*, 2003) and resistance against these compounds is a reality (Vial and Gorenflot, 2006). Novel therapeutics with high pathogen specificity and low host toxicity are therefore required (Gohil *et al.*, 2013). Development of vaccines against bovine babesiosis has been hampered by the lack of knowledge as well as the complexity of the disease-causing *Babesia* parasites. Since 1964, live attenuated *B. bovis* vaccines have successfully been produced and applied to cattle in Australia. Several other countries including South Africa,

Brazil, Argentina, Israel and Uruguay also use live attenuated *B. bovis* vaccines as protective measure against bovine babesiosis (de Castro, 1997, Florin-Christensen *et al.*, 2007). Limitations associated with these vaccines include their short-shelf life, expensive to produce as well as contamination with other blood parasites, bacteria or viruses. In addition, several adverse vaccine reactions may appear which hamper vaccine efficiency and may occur in highly susceptible European cattle breeds and high yielding dairy cows (Gohil *et al.*, 2013). Development of alternative compounds against the diseases is of critical importance in the veterinary field (Vial and Gorenflot, 2006).

1.4 Apicomplexa and the apicoplast

Evolutionary origin and structure of the apicoplast

As stated previously, parasites of the phylum *Apicomplexa* are widespread and of considerable medical, veterinary and economic importance. Apicomplexans derive their name from the apical membrane complex which resides in their cellular compartment (van Dooren and Striepen, 2013). Apicomplexan parasites have adapted to a variety of host species, as reflected in their diverse niches and lifestyles which ultimately contribute to variations in their metabolic profiles and genomic compositions (Fleige *et al.*, 2010). The unique evolutionary history of apicomplexans has been shaped by both symbiotic and parasitic events, contributing to their complex architecture (van Dooren and Striepen, 2013). Despite the great diversity of apicomplexan life cycles, *Plasmodium*, *Toxoplasma*, *Theileria* and *Babesia* species, share unique and important sub-cellular characteristics. The apicoplast is one such commonly shared feature and has been most informative in unravelling apicomplexan evolution (Marechal and Cesbron-Delauw, 2001). As the apicoplast was previously identified as the target for the compound evaluated in this study (A51B1C1_1), it will be further discussed.

The apicoplast was first described during the 1990's and recently confirmed as a four-membrane, semi-autonomous plastid-like organelle of cyanobacterial origin, homologous to the chloroplast of plants, without photosynthetic characteristics (McFadden, 2014). It is known that the apicoplast was derived from a secondary endosymbiotic event *via* the engulfment of red algae by apicomplexan parasites (Seeber, 2003). The apicoplast within the apicomplexan lineage varies in shape and size, depending on the different cell cycle stages. It is located at the anterior region of the invading cells and consists of three secretory organelles and a polar ring (Waller and McFadden, 2005). It has a small, circular genome (plastome) and is considered to be the smallest of the plastids (35 kb) encoding 30 - 50 housekeeping genes (Fleige *et al.*, 2010). Most of the apicoplasts' proteome is encoded for in the genome of the nucleus, with proteins being transported to the apicoplast *via* the secretory pathway (Seeber, 2003). Literature regarding the apicoplast associated with *Babesia* species is currently limited and only available for *B. bovis*. The *B. bovis* apicoplast is located adjacent to the nucleus where the close proximity between these two cellular components promotes molecular exchange (Figure 1.4). The circular 33 kb apicoplast genome of the *B. bovis* pathogen encodes 32 putative protein coding genes, a complete set of tRNA genes, small-and-large subunit rRNA's and is more A-T rich (78%) than its nuclear genome (58%) (Brayton *et al.*, 2007, Caballero *et al.*, 2012).

As mentioned, the organelle consists of four membranes. The outer membrane is similar to the phagosomal membrane of the host cell. The second outermost membrane is initiated from the plasma membrane of the engulfed algae cells, with the two inner membranes similar to the inner and outer membranes of the chloroplast (Lim and McFadden, 2010). Only one small, ovoid organelle is found within a cell in close proximity to the mitochondria or nucleus. The membrane system is an on-going topic of debate, but most consider it to have four membranes (Figure 1.5). An exception is *Plasmodium*, with only three membranes (Marechal and Cesbron-Delauw, 2001).

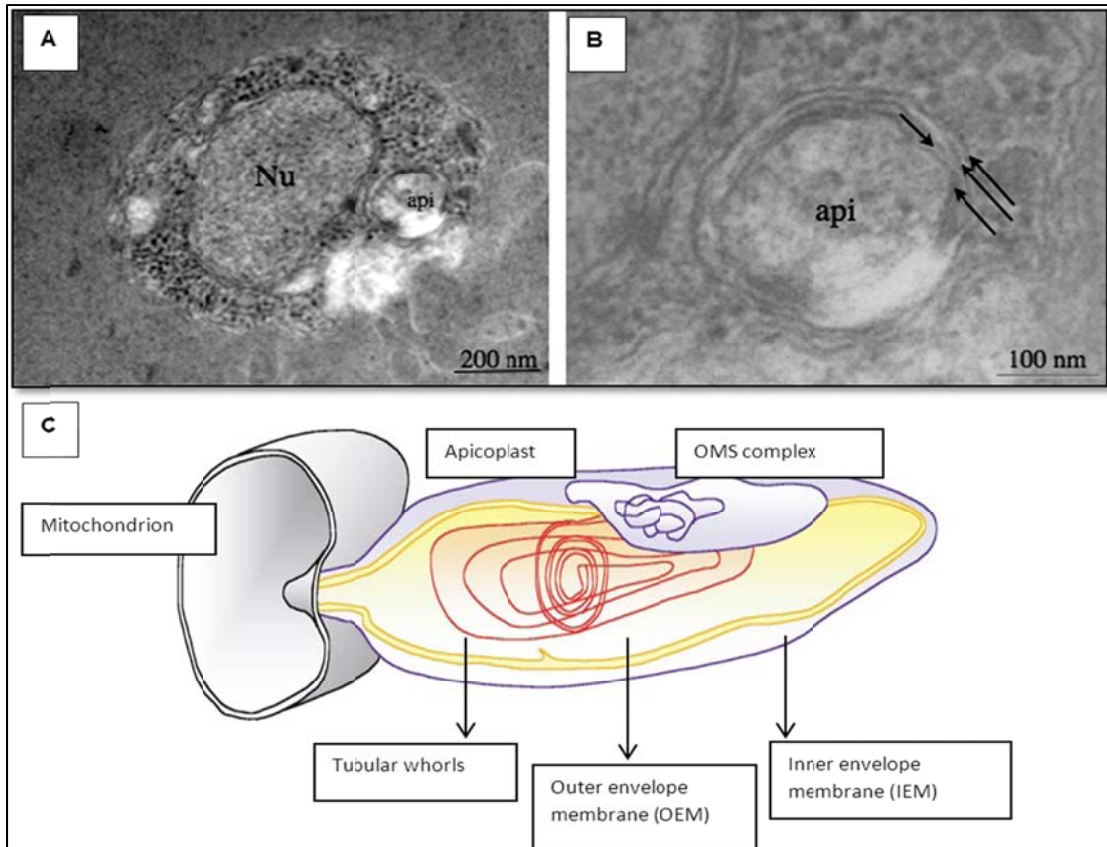


Figure 1.4 The close association between the apicoplast, nucleus and mitochondria of two apicomplexan species *B. bovis* and *P. falciparum* (Adapted from Marechal and Cesbron-Delauw, 2001 and Caballero *et al.*, 2012).

(A) Transmission electron micrograph of the *B. bovis* apicoplast, with specific attention to the nucleus and apicoplast-associated membranes. The close association and adjacent orientation between the nucleus (Nu) and apicoplast (api) of *B. bovis* can be observed. The apical diameter is approximately 200 nm (B) Membranous layer of the *B. bovis* apicoplast indicated by arrows. (C) Putative three-dimensional representation of the *P. falciparum* apicoplast. Tubular whorls, outer envelope membrane (OEM), inner envelope membrane (IEM) and outermost membrane system (OMS) is illustrated.

Function of the apicoplast

The function of the apicoplast has long been debated and still remains poorly understood. What is known is its indispensable nature and importance for the long-term survival and viability of apicomplexan parasites. Identifying the apicoplasts' key function remains a challenge due to its relatively small size and the difficulty to isolate the organelle (Ralph *et al.*, 2004).

The original function of photosynthesis of these plastid-like organelles seems unlikely, as most apicomplexan species are intracellular parasites that live in dark, nutrient rich environments (Marechal and Cesbron-Delauw, 2001). Their function generally ranges from basic metabolic processes (DNA replication, transcription, translation) to more complex catabolic, anabolic and post-translational modification processes. Comparative apicomplexan studies revealed unique differences with regards to apicoplast functionality and confirmed its heterogeneous nature depending on the particular niche and lifestyle the parasite occupies (Fleige *et al.*, 2010). *Plasmodium* species and *Toxoplasma gondii* for example, harbour processes analogous to those present in plant plastids (other than photosynthesis), such as the fatty acid (FA II), haem, isoprenoid, iron-sulphur (Fe-S cluster) and lipoic acid -biosynthesis pathways, most of which are absent in *Theileria* species and *B. bovis* (Marechal and Cesbron-Delauw, 2001, Brayton *et al.*, 2007). Initial genome evaluation studies regarding the *B. bovis* apicoplast failed to identify the presence of protein coding genes involved in the FA II biosynthesis pathway, with the exception of the acyl carrier protein (ACP) coding genes (Caballero *et al.*, 2012). The pathogen may have lost some of the important components as it adapted and evolved into its asexual, intra-erythrocytic conditions (Caballero *et al.*, 2012). In contrast to the FA II biosynthesis pathway, *B. bovis* encodes all the required components for the non-mevalonate, DOXP (1-deoxy-D-xylose-5-phosphate) or MEP (2C-methyl-D-erythritol-4-phosphate) pathways (Caballero *et al.*, 2012). Only two metabolic pathways are consequently shared among all apicomplexans which include the non-mevalonate or DOXP/MEP pathway and the partial iron-sulphur cluster assembly (Fe-S) pathway (Figure 1.5) (Fleige *et al.*, 2010).

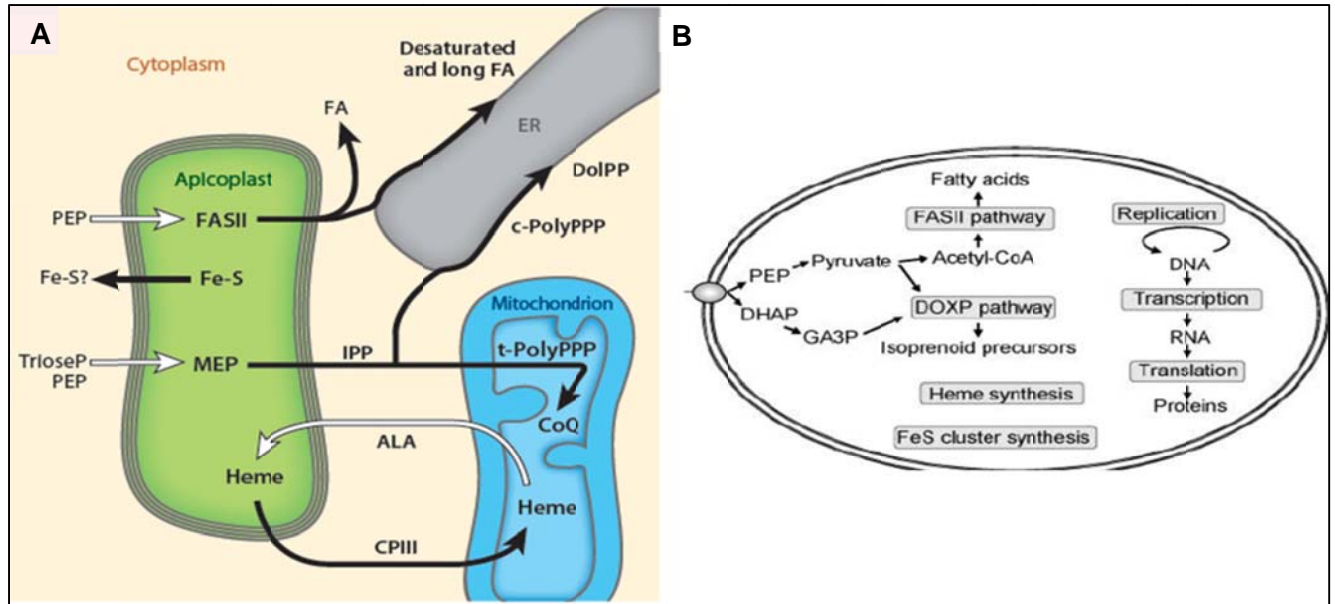


Figure 1.5 Promising metabolic pathways for novel drug targets in apicomplexan parasites, with specific reference to *P. falciparum* (Adapted from Botte *et al.*, 2011 and van Dooren and Striepen, 2013).

(A) The apicoplast, endoplasmic reticulum (ER) and mitochondria involved in metabolic processes for the synthesis of fatty acids (FA II), isoprenoids and iron-sulphur (Fe-S) clusters. The apicoplast imports compounds such as phosphoenolpyruvate (PEP), triose phosphate (TrioseP) and aminolevulinic acid (ALA) to maintain certain housed metabolic pathways. These imported compounds subsequently provide cells with fatty acids (FA), isoprenoids (IPP) and Fe-S clusters. (B) Four metabolic pathways within the apicoplast previously investigated for novel drug targets in *P. falciparum* include the type II fatty acid synthesis, DOXP/MEP, Fe-S cluster synthesis and haem biosynthesis pathways.

The apicoplast as a promising drug target

The discovery of the apicoplast ushered in a new era in therapeutic strategies and anti-apicomplexan drug discovery. Ideally one would prefer one drug compound to be effective and treat numerous apicomplexan parasites based on a single, commonly shared target, such as the apicoplast (Marechal and Cesbron-Delauw, 2001).

The apicoplast is an ideal candidate for parasitocidal drug therapies, not only due to its presence throughout the apicomplexan lineage but also due to the prokaryotic nature of its metabolism as well as its unique metabolic pathways of endosymbiotic origin (Seeber, 2003). Furthermore, the

biosynthetic pathways associated with the apicoplast differ fundamentally from corresponding pathways within their eukaryotic hosts, rendering it a parasite specific target (Brayton *et al.*, 2007). Understanding these apicoplast specific pathways are therefore essential in drug target identification (Foth and McFadden, 2003). An optimal pharmacological treatment targeting the apicoplast should induce a delayed cell death effect, which refers to a lag in parasitic response to the drug and the consequent disruption of the parasites' basic housekeeping processes (Marechal and Cesbron-Delauw, 2001, Aboulaila *et al.*, 2012). The search for apicoplast-specific drug compounds however, appears challenging, as the compound aimed at targeting the organelle have several barriers including the plasma membrane of the parasitized erythrocyte, membrane of the parasitophorous vacuole (for *Plasmodium* species), plasma membrane of the parasite, two membranes of the inner membrane complex and the four membranes of the apicoplast to cross, before reaching the stoma (Botte *et al.*, 2011). In addition, these compounds should have the ability to partition in hydrophilic and lipophilic environments in order to reach their targets, be in a bioavailable form and preferably must be administered orally (Botte *et al.*, 2011).

As previously mentioned, only two metabolic pathways are shared among all apicomplexan parasites, the DOXP/MEP and the Fe-S cluster biosynthesis pathways, which should be further investigated as possible drug targets (Fleige *et al.*, 2010). Isoprenoids are an extensive group of natural compounds that play an integral role in numerous biological systems including cellular respiration, cell signalling, protein modification, tRNA modification and cell membrane maintenance (Hunter, 2011). Two distinct biosynthetic pathways have evolved in nature for the synthesis of isoprenoid precursors (isopentenyl pyrophosphate (IPP) and dimethylallyl pyrophosphate (DMAPP)) and include the mevalonate pathway (MEV) and the non-mevalonate or DOXP/MEP pathways (Hunter, 2011). These two pathways differ substantially with regards to their starting and intermediate products, as well as enzymes involved (Eisenreich *et al.*, 2004).

Most plants, eubacteria, cyanobacteria and apicomplexans follow the DOXP/MEP pathway, whereas eukaryotes, fungi and archaeobacteria mostly follow the MEV pathway. Unlike humans, apicomplexan parasites of *Plasmodium* and *Theileria* species, *B. bovis*, *T. gondii* and *Neospora caninum* synthesize isoprenoids mainly *via* the DOXP/MEP pathway in their apicoplasts (Eisenreich *et al.*, 2004). Enzymes involved in iron-sulphur cluster (Fe-S) biosynthesis pathways are attractive drug targets based on their prokaryotic nature and the fact that they are well conserved among endosymbiotic organelles and eukaryotic pathogens and are essential for cell-viability (Dellibovi-Ragheb *et al.*, 2013). In addition, these clusters have both structural and catalytic functions, form important protein co-factors and are involved in several metabolic processes such as electron-transport reactions, redox-reactions and gene expression regulation (van Dooren and Striepen, 2013).

Throughout the life cycle of apicomplexans, large quantities of glycerolipids are required for membrane compartment synthesis and maintenance (Saidani *et al.*, 2014), a demand which is met by a combination of *de novo* synthesis and scavenging from their host species (Botte *et al.*, 2012). This demand for glycerolipids is illustrated in *Plasmodium* during the asexual, parasitic proliferation stage, where a membrane lipid increase of up to 700% can be expected in infected erythrocytes, compared to uninfected erythrocytes (Dechamps *et al.*, 2010). Based on the importance of glycerolipids in apicomplexan membrane synthesis, the metabolism of glycerolipids may be a potential therapeutic target for novel compounds. The membrane compartments of eukaryotic cells are composed of various polar lipids (*i.e.* glycerolipids), the status of which is influenced by developmental, physiological or environmental factors (Figure 1.6 A). The membrane glycerolipid profile is in a steady-state due to protein activity associated with *de novo* synthesis of lipids, their inter-conversions as well their movement within and between membranes (Boudiere *et al.*, 2012).

Like apicomplexa, plant cells consist of endomembranes, the bulk of which comprise phospholipids (such as phosphatidylcholine (PC)) (Figure 1.6 B). The glycerolipid synthesis within these cells is complex and occurs either within the ER or the plastid of photosynthetic origin, synthesizing phospholipids and monogalactosyl diacylglycerol (MGDG), respectively (Botte *et al.*, 2011). The process is initiated by two major precursors, namely phosphatidic acid (PA) and diacylglycerol (DAG) and can be divided into three major components (i) FA biosynthesis (ii) PA and DAG precursor synthesis and (iii) phospholipid synthesis from PA and DAG precursors (Saidani *et al.*, 2014) (Figure 1.6). Based on the importance of glycerolipids in plant cells, the synthesis and metabolism may be regarded as potential therapeutic targets.

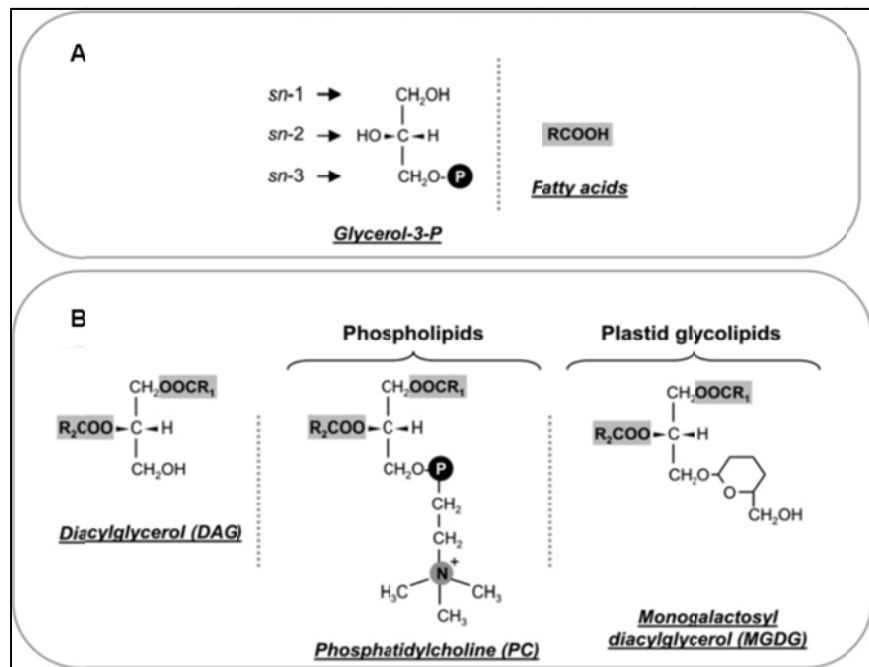


Figure 1.6 Structure and components of membrane glycerolipids in eukaryotic cell (Adapted from Boudiere *et al.*, 2012).

(A) The building blocks of glycerolipids consist of a glycerol-3-phosphate (glycerol-3-P) scaffold, esterified by two fatty acids (RCOOH) at positions *sn*-1 and *sn*-2. (B) The general structure of glycerolipids associated with plant cells consist of three components diacylglycerol (DAG); phospholipids majority which includes phosphatidylcholine (PC) and plastid glycolipids such as monogalactosyl diacylglycerol (MGDG).

Plant cells are characterized by chloroplasts with unique glycerolipid containing membrane systems, which consist of $\pm 80\%$ galactoglycerolipids of which mono- and digalactosyldiacylglycerol (MGDG and DGDG) constitute $\pm 50\%$ and $\pm 30\%$, respectively (Dubots *et al.*, 2010). MGDG and DGDG may differ with regards to the acyl composition at the *sn*-1 and *sn*-2 positions of the glycerol scaffold. Both MGDG and DGDG are synthesized within the two membranes surrounding the chloroplast (*i.e.* envelope) and are essential components for the synthesis and function of photosynthetic membranes (Jouhet *et al.*, 2007). MGDG is synthesized by a galactosyltransferase (MGDG synthase). In *Arabidopsis*, MGDG is encoded for by three genes (*MGDG-1*; *MGDG-2* and *MGDG-3*). Synthesis occurs *via* the galactosylation of DAG from from one of two routes: a neosynthesis in plastids known as the “prokaryotic” pathway and a recycling of extra-plastidial phospholipids referred to as the “eukaryotic” pathway. The “prokaryotic” pathway synthesizes DAG *de novo via* an acyl-ACP:glycerol-3-phosphate O-acyltransferase (ATS1); acyl-ACP:1-acylglycerol-3-phosphate O-acyltransferase (ATS2) and a plastid phosphatidic acid phosphatase (pPAP). The “eukaryotic” pathway synthesizes DAG *via* phospholipases from extra-plastidial phospholipids including phospholipases D (PLD’s); phospholipases C (PLC’s) or endomembrane PAP’s (ePAP’s) (Figure 1.7 A). Both “prokaryotic” and “eukaryotic” synthesized DAG’s can be galactosylated by MGDG synthases *via* the transfer of a β -galactosyl (β -Gal) group from a UDP-donor and further galactosylated *via* the transfer of a α -galactosyl (α -Gal) group from a UDP-donor. The synthesized DGDG group consequently consists of an α -Gal(1-6) β -Gal polar head (Figure 1.7 B₁). Part of the 16- and 18- carbon acyl chains of the synthesized MGDG can be desaturated by FAD5; FAD6 and FAD7/8 to form triacylglycerol (TAG), which can either be released or stored. The synthesized MGDG’s can alternatively be esterified to form Jasmonic acids (JA’s) *via* the lipoxygenase (LOX) and/or allene oxide synthase (AOS) pathways. The *sn*-1 and *sn*-2 positions of MGDG can also be esterified to precursors of JA’s, to form a class of galactolipids known as the arabidosides (Figure 1.7 B₂). Part of the synthesized MGDG chain can alternatively be

catalsed by the *Sensitive to freezing 2* gene (SFR-2) to form DAG and a digalactolipid with a β -Gal(1-6) β -Gal polar head (Figure 1.7 B₃) (Botte *et al.*, 2011, Boudiere *et al.*, 2012).

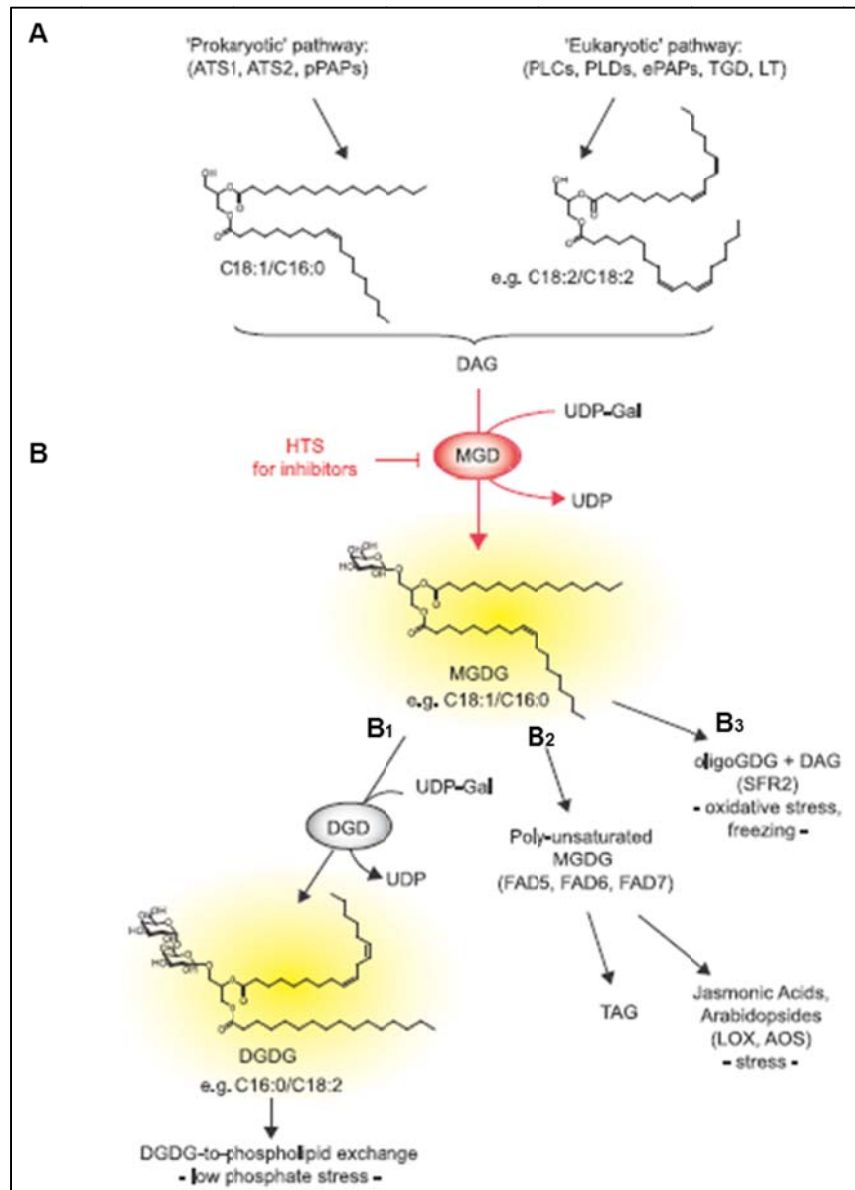


Figure 1.7 MGDG synthesis in plant cells (Adapted from Botte *et al.*, 2011).

(A) MGDG synthesis is catalysed by MGD enzymes (MGD1, MGD2 and MGD3 in *Arabidopsis*). Diacylglycerol (DAG) used for MGDG synthesis originates from the “prokaryotic” (catalysed by ATS1, ATS2, pPAPs) and “eukaryotic” (involving PLCs, PLDs, ePAPs, and the TGD complex) -pathways. (B₁) MGDG is used for DGDG synthesis by the addition of α -Gal and catalysed by DGD enzymes (DGD1 and DGD2 in *Arabidopsis*). (B₂) Acyls esterified at positions *sn*-1 and *sn*-2 of MGDG can be desaturated by FAD5, FAD6 and FAD7/8. Jasmonic acids (JA) are subsequently produced *via* the LOX and/or AOS pathways. The *sn*-1 and *sn*-2 positions of MGDG can be esterified to precursors of JA’s, forming the arabidopsides. (B₃) The addition of β -Gal to MGDG, catalysed by SFR2 gene activity, can also occur.

1.5 Piperidinyl-benzimidazolone analogues and compound A51B1C1_1 used in this study

A set of herbicide-derived compounds were tested by “The Membrane Lipidomics Team” in the Plant Cell Physiology Laboratory (Eric Marechal, Grenoble, France) to identify novel chemical scaffolds as inhibitors of galactolipid metabolism in *Arabidopsis* (Botte *et al.*, 2011) and to explore piperidinyl-benzimidazolone analogues in search of novel compounds inhibiting *P. falciparum* and *T. gondii* proliferation (Saidani *et al.*, 2014).

Several MGDG synthase inhibitors have been described, none of which however, had high activity or selectivity as potential chemical inhibitors of *Arabidopsis* (Boudiere *et al.*, 2012). Based on several genetic and biochemical studies of the multi-gene family of MGDG synthases (*MGDG-1*, *MGDG-2* and *MGDG-3*) in *Arabidopsis*, Botte (2011) reported the first set of specific MGDG inhibitors that allowed a dose-dependent decrease of galactolipids within plants (Botte *et al.*, 2011). High-throughput screening strategies of the above mentioned plant-enzymes were followed to identify small molecules (galvestines) that inhibit the activity of the *Arabidopsis* MGDG synthases (Botte *et al.*, 2011). Approximately 24 000 molecules from the CEREP® diversity-based library were screened, from which only 20 compounds exhibited an inhibitory activity greater than 25%. These 20 compounds, with an additional 40 compounds (of similar chemical structures) were selected from the CEREP® diversity-based library and tested *in vitro* for their inhibitory activity against MGDG-1. Two compounds galvestine-1 and galvestine-2 had a greater than 40% inhibitory activity against MGDG-1 (Figure 1.8 A). Subsequent derivatives were designed based on the galvestine-1 scaffold. *In vitro* and *in vivo* treatment of galvestine-1, galvestine-2 and some of their derivatives revealed inhibition of *Arabidopsis* MGDG synthases, which subsequently reduced the MGDG content.

The study by Botte (2011) showed for the first time that targeting the MGDG synthases could affect cellular lipid homeostasis (Botte *et al.*, 2011). Two compounds, A1B1C1_1 and

A1B1C2_1 (Figure 1.8 B₁) with a general similar scaffold were further selected and 250 piperidiny-benzimidazolone analogues synthesized and tested against the MGDG synthase activity of the *Arabidopsis* chloroplast target. Based on *in vitro* growth inhibitory assays of the 250 analogues, two molecules with improved efficacy were identified as A51B1C1_1 and A21B1C1_1 (Figure 1.8 B) (Botte *et al.*, 2011).

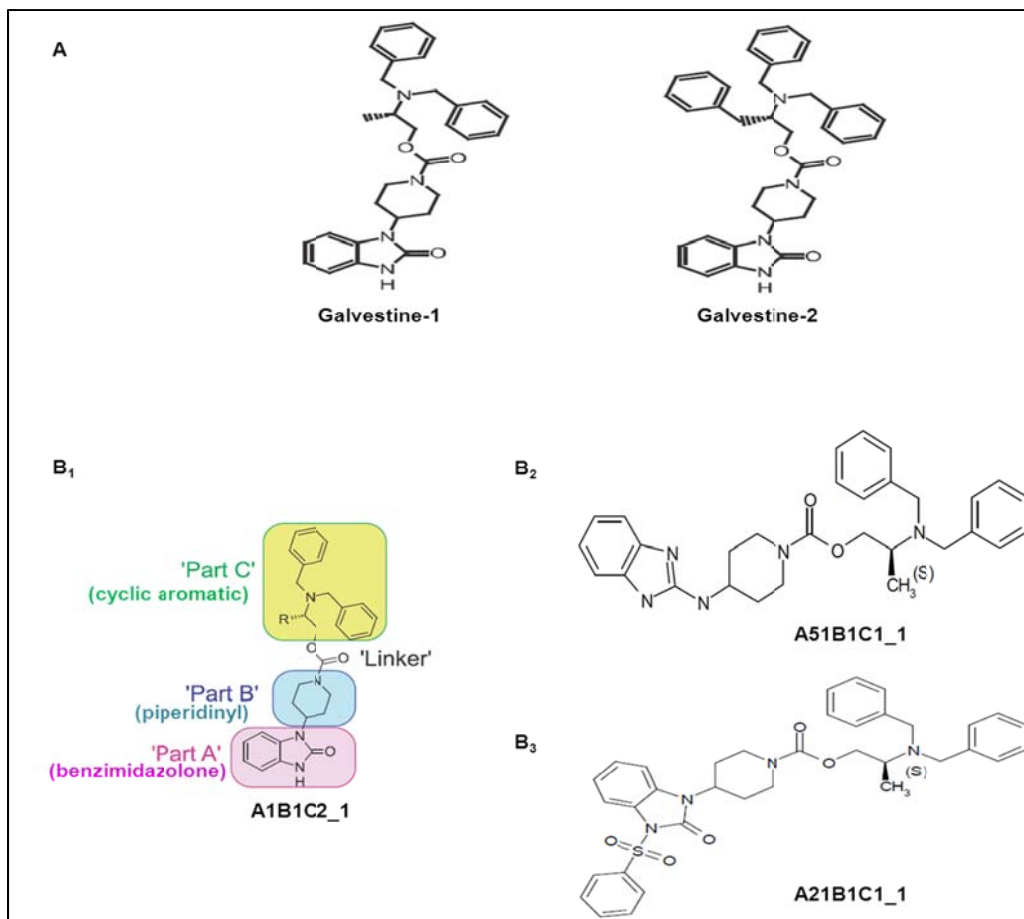


Figure 1.8 Compounds in the selected piperidiny-benzimidazolone analogue library used as scaffolds of *Arabidopsis*, *P. falciparum* and *T. gondii* inhibitors (Adapted from Botte *et al.*, 2011 and Saidani *et al.*, 2014).

(A) Galvestine-1 and galvestine-2 scaffolds obtained after high-throughput screening of compounds to select MGD1 inhibitors from *Arabidopsis*. (B) Effective galvestine-1 analogue inhibitors of MGDG in *Arabidopsis*, *P. falciparum* and *T. gondii*. (B₁) The diversity orientated modular design strategy, based on four regions of the compound's structure subjected to potential chemical variations. Regions include Part A (benzimidazolone end), Part B (piperidiny part), Part C (substituted di/tribezylamino ethoxy end) and the 'linker' initial carboxylate region between part B and part C. (B₂, B₃) Examples of the two most active lead MGDG synthase inhibitors (A51B1C1_1 and A21B1C1_1) identified by Botte (2011) and Saidani (2014).

The study by Saidani (2014) further evaluated piperidinyl-benzimidazolone analogues of galvestine-1 as well as inhibitors of the membrane glycerolipid metabolism acting on PA and DAG, to identify novel therapeutics against *P. falciparum* and *T. gondii* (Saidani *et al.*, 2014). The piperidinyl-benzimidazolone library used was based on the CEREP® diversity-based library (described above) with chemical substitutions at four regions within the structure of the molecules (Botte *et al.*, 2011, Saidani *et al.*, 2014). These regions include Part A (benzimidazolone end), Part B (piperidinyl), Part C (substituted di/tribezylamino ethoxy end) and the 'linker' region between Parts B and C. Following initial synthesis, all compounds within the investigated library were identified by an A#B#C#_# nomenclature (Figure 1.8). *In vitro* and *in vivo* assessment of the two most active compounds (A51B1C1_1 and A21B1C1_1) against *P. falciparum* indicated low toxicities with reduced parasitaemia levels, with no observed curative effect. Further optimization based on the scaffolds of these compounds is required to reach a curative anti-malarial compound acting on membrane glycerolipids (Saidani *et al.*, 2014). Preliminary proteomic analysis, based on a piperidinyl-benzimidazolone analogue further identified 12 major polypeptides and several proteins of unknown function (Saidani *et al.*, 2014). Transcriptome analyses of the most active lead MGDG synthase inhibitors (A51B1C1_1 and A21B1C1_1) identified by Botte (2011) and Saidani (2014) were further evaluated for their anti-malarial properties against *P. falciparum* (Snyman, 2011).

This decade-long, drug-development program (based on MGDG synthase inhibitors) provides support for galactolipid biosynthesis as potential growth inhibitory target in *Arabidopsis* and several apicomplexan species (Boudiere *et al.*, 2012). The absence of this pathway in humans validates the attractive nature of this pathway and strategy for the development of novel anti-malarial compounds. This study subsequently evaluated the anti-babesiocidal activity of one of these active MGDG synthase inhibitors (A51B1C1_1) against the apicomplexan pathogen and known causative agent of human babesiosis, *B. divergens*.

The current technologies and techniques applied in the identification of new anti-babesiocidal drugs rely on *in vitro* and *in vivo* drug screening strategies, new strategies are, however, required to combat babesiosis and elucidate gene functions. The success of transcriptome profiling and functional genomics in *Plasmodium* research have been essential tools in investigating the biology of *Plasmodium* parasites, identifying essential molecules, pathways and gene expression profiles as well as understanding the parasite's response to drug treatment – a much needed activity, given the potential threat of drug resistance (Di Girolamo *et al.*, 2005). We therefore further investigated these functional genomic principles with the goal of accelerating the anti-babesiocidal drug discovery process to identify new, alternative therapeutics against babesiosis.

1.6 Hypothesis

Compounds targeting the galactolipid metabolism will have effective anti-babesiocidal activity against *B. divergens in vitro*.

1.7 Aims and Objectives

The primary aim of this study was to determine the anti-babesiocidal potential of compound A51B1C1_1 against *B. divergens* cultured *in vitro* as well as to determine the parasites' response to treatment using a functional genomics strategy.

Specific objectives included:

- (i) Evaluate the chronology and stage-specificity of intra-erythrocytic development of *B. divergens* parasites (prior to drug assays) by combining advanced cell biological and molecular strategies;

- (ii) Determine the anti-babesicidal potential of a promising piperidinyI-benzimidazolone analogue (A51B1C1_1) previously tested against *P. falciparum* using a functional genomics approach;
- (iii) Perform comparative transcriptome analyses between *B. divergens* and *P. falciparum* pathogens to compare their respective responses to treatment with A51B1C1_1 and subsequently identify unique and/or shared features;
- (iv) Summarize and integrate findings and provide future perspectives in the field of *Babesia* research.

1.8 List of conferences

- South African Genetics and Bioinformatics and Computational Biology Society Conference (Cape Town, South Africa, 2012).

Poster presentation: "A functional evaluation of a promising apicoplast specific compound against *Babesia divergens*"

Authors: I. Rossouw, C. Maritz-Olivier, J. Reader, J. Niemand, N. A. Olivier, E. Marechal, L. M. Birkholtz

- 11th Annual Genetics Postgraduate Symposium (University of Pretoria, South Africa, 2013).

Oral presentation: "A functional evaluation and the transcriptional response to a herbicide-derived compound against the zoonotic *Babesia divergens* parasite"

Authors: I. Rossouw, J. Niemand, A. Smit, N. A. Olivier, C. Maritz-Olivier, L. M. Birkholtz

- Genetics Research Institute (GRI) Symposium (University of Pretoria, South Africa, 2014).

Oral presentation: “Transcriptional response to the herbicide-derived compound A51B1C1_1 in the zoonotic *Babesia divergens* parasite”

Authors: I. Rossouw, J. Niemand, N. A. Olivier, C. Maritz-Olivier, E. Marechal, L. M. Birkholtz

- Joint 8th International Ticks and Tick-borne Pathogens (TTP-8) and 12th Biennial Society for Tropical Veterinary Medicine (STVM) Conference (24-29 August, Cape Town, South Africa, 2014).

Oral presentation: “Transcriptional response to the piperidinyl-benzimidazolone analogue (A51B1C1_1) in the zoonotic *Babesia divergens* parasite”

Authors: I. Rossouw, J. Niemand, R. van Biljon, A. Smit, N. A. Olivier, C. Maritz-Olivier, E. Marechal, L. M. Birkholtz

1.9 List of research visits

- Laboratory of Dr. Laurent Bréhélin (Le Laboratoire d'Informatique, de Robotique et de Microélectronique de Montpellier, LIRMM). Conduct comparative genomic studies between *Babesia divergens*, *Plasmodium falciparum* and *Arabidopsis*.

1.10 List of awards

- National Research Foundation (NRF) Grant Holder Link Bursary (2011 – 2013)
- Embassy of France in South Africa PhD and Protea research grant (Campus France full bursary, 2013)

- National Research Foundation (NRF) Grant Holder Link PhD Extension award (2014)
- IRT (Genomics) Bursary to attend the Joint 8th International Ticks and Tick-borne Pathogens (TTP-8) and 12th Biennial Society for Tropical Veterinary Medicine (STVM) Conference (24-29 August, 2014).

1.11 Papers from this study

- Morphological and molecular descriptors of the intra-erythrocytic development cycle of *Babesia divergens* parasites.
I. Rossouw, C. Maritz-Olivier, J. Niemand, R. van Biljon, A. Smit, N. A. Olivier, L. M. Birkholtz. Department of Genetics & Department of Biochemistry, Centre for Sustainable Malaria Control & Department of Plant Sciences, ACGT Microarray facility, University of Pretoria, Private bag x20, Hatfield, Pretoria, South Africa, 0028. (PLoS Neglected Tropical Diseases)
- Transcriptome evaluation of the effect of potential anti-malarial, herbicide derived piperidinyl-benzimidazolone analogue on *B. divergens*, *P. falciparum* and *A. thaliana*.
I. Rossouw, C. Maritz-Olivier, J. Reader, J. Niemand, N. A. Olivier, E. Marechal, L. M. Birkholtz. Department of Genetics & Department of Biochemistry, Centre for Sustainable Malaria Control & Department of Plant Sciences, ACGT Microarray facility, University of Pretoria, Private bag x20, Hatfield, Pretoria, South Africa, 0028. (Manuscript in preparation)
- Review of past and present *in vitro* cultivation and drug screening strategies applied to zoonotic *Babesia* species.
I. Rossouw and C. Maritz-Olivier Department of Genetics, University of Pretoria, Private bag x20, Hatfield, Pretoria, South Africa, 0028. (Manuscript in preparation)

1.12 References

- ABOULAILA, M., MUNKHJARGAL, T., SIVAKUMAR, T., UENO, A., NAKANO, Y., YOKOYAMA, M., YOSHINARI, T., NAGANO, D., KATAYAMA, K., EL-BAHY, N., YOKOYAMA, N. & IGARASHI, I. 2012. Apicoplast-targeting antibacterials inhibit the growth of Babesia parasites. *Antimicrob Agents Chemother*, 56, 3196-206.
- BECKER, C. A., BOUJU-ALBERT, A., JOUGLIN, M., CHAUVIN, A. & MALANDRIN, L. 2009. Natural transmission of Zoonotic Babesia spp. by Ixodes ricinus ticks. *Emerg Infect Dis*, 15, 320-2.
- BOCK, R., JACKSON, L., DE VOS, A. & JORGENSEN, W. 2004. Babesiosis of cattle. *Parasitology*, 129, S247-S269.
- BOTTE, C. Y., DELIGNY, M., ROCCIA, A., BONNEAU, A. L., SAIDANI, N., HARDRE, H., ACI, S., YAMARYO-BOTTE, Y., JOUHET, J., DUBOTS, E., LOIZEAU, K., BASTIEN, O., BREHELIN, L., JOYARD, J., CINTRAT, J. C., FALCONET, D., BLOCK, M. A., ROUSSEAU, B., LOPEZ, R. & MARECHAL, E. 2011. Chemical inhibitors of monogalactosyldiacylglycerol synthases in Arabidopsis thaliana. *Nat Chem Biol*, 7, 834-42.
- BOTTE, C. Y., DUBAR, F., MCFADDEN, G. I., MARECHAL, E. & BIOT, C. 2012. Plasmodium falciparum apicoplast drugs: targets or off-targets? *Chem Rev*, 112, 1269-83.
- BOUDIERE, L., BOTTE, C. Y., SAIDANI, N., LAJOIE, M., MARION, J., BREHELIN, L., YAMARYO-BOTTE, Y., SATIAT-JEUNEMAITRE, B., BRETON, C., GIRARD-EGROT, A., BASTIEN, O., JOUHET, J., FALCONET, D., BLOCK, M. A. & MARECHAL, E. 2012. Galvestine-1, a novel chemical probe for the study of the glycerolipid homeostasis system in plant cells. *Mol Biosyst*, 8, 2023-35, 2014.
- BRAYTON, K. A., LAU, A. O., HERNDON, D. R., HANNICK, L., KAPPMAYER, L. S., BERENS, S. J., BIDWELL, S. L., BROWN, W. C., CRABTREE, J. & FADROSH, D. 2007. Genome sequence of Babesia bovis and comparative analysis of apicomplexan hemoprotozoa. *PLoS pathogens*, 3, e148.
- BUSH, J. B., ISAACSON, M., MOHAMED, A. S., POTGIETER, F. T. & DE WAAL, D. T. 1990. Human babesiosis--a preliminary report of 2 suspected cases in South Africa. *S Afr Med J*, 78, 699.
- CABALLERO, M. C., PEDRONI, M. J., PALMER, G. H., SUAREZ, C. E., DAVITT, C. & LAU, A. O. 2012. Characterization of acyl carrier protein and LytB in Babesia bovis apicoplast. *Mol Biochem Parasitol*, 181, 125-33.
- COLWELL, D. D., DANTAS-TORRES, F. & OTRANTO, D. 2011. Vector-borne parasitic zoonoses: emerging scenarios and new perspectives. *Veterinary parasitology*, 182, 14-21.
- DANTAS-TORRES, F., CHOMEL, B. B. & OTRANTO, D. 2012. Ticks and tick-borne diseases: a One Health perspective. *Trends in parasitology*, 28, 437-446.
- DE CASTRO, J. J. 1997. Sustainable tick and tickborne disease control in livestock improvement in developing countries. *Vet Parasitol*, 71, 77-97.
- DE LA FUENTE, J., NARANJO, V., RUIZ-FONS, F., VICENTE, J., ESTRADA-PEÑA, A., ALMAZÁN, C., KOCAN, K. M., MARTÍN, M. P. & GORTÁZAR, C. 2004. Prevalence of tick-borne pathogens in ixodid ticks (Acari: Ixodidae) collected from European wild boar (Sus scrofa) and Iberian red deer (Cervus elaphus hispanicus) in central Spain. *European Journal of Wildlife Research*, 50, 187-196.
- DECHAMPS, S., SHASTRI, S., WENGELNIK, K. & VIAL, H. J. 2010. Glycerophospholipid acquisition in Plasmodium - a puzzling assembly of biosynthetic pathways. *Int J Parasitol*, 40, 1347-65.
- DELLIBOVI-RAGHEB, T. A., GISSELBERG, J. E. & PRIGGE, S. T. 2013. Parasites FeS up: iron-sulfur cluster biogenesis in eukaryotic pathogens. *PLoS Pathog*, 9, e1003227.
- DI GIROLAMO, F., RAGGI, C., BULTRINI, E., LANFRANCOTTI, A., SILVESTRINI, F., SARGIACOMO, M., BIRAGO, C., PIZZI, E., ALANO, P. & PONZI, M. 2005. Functional genomics, new tools in malaria research. *Ann Ist Super Sanita*, 41, 469-77.

- DUBOTS, E., AUDRY, M., YAMARYO, Y., BASTIEN, O., OHTA, H., BRETON, C., MARECHAL, E. & BLOCK, M. A. 2010. Activation of the chloroplast monogalactosyldiacylglycerol synthase MGD1 by phosphatidic acid and phosphatidylglycerol. *J Biol Chem*, 285, 6003-11.
- EISENREICH, W., BACHER, A., ARIGONI, D. & ROHDICH, F. 2004. Biosynthesis of isoprenoids via the non-mevalonate pathway. *Cell Mol Life Sci*, 61, 1401-26.
- FILBIN, M. R., MYLONAKIS, E. E., CALLEGARI, L. & LEGOME, E. 2001. Babesiosis. *The Journal of emergency medicine*, 20, 21-24.
- FLEIGE, T., LIMENITAKIS, J. & SOLDATI-FAVRE, D. 2010. Apicoplast: keep it or leave it. *Microbes Infect*, 12, 253-62.
- FOTH, B. J. & MCFADDEN, G. I. 2003. The apicoplast: a plastid in Plasmodium falciparum and other Apicomplexan parasites. *Int Rev Cytol*, 224, 57-110.
- FRIEDMAN, A. & YAKUBU, A. A. 2014. A Bovine Babesiosis model with dispersion. *Bull Math Biol*, 76, 98-135.
- FRITZ, C. L. 2009. Emerging tick-borne diseases. *Veterinary Clinics of North America: Small Animal Practice*, 39, 265-278.
- GOES, T. S., GOES, V. S., RIBEIRO, M. F. & GONTIJO, C. M. 2007. Bovine babesiosis: anti-erythrocyte antibodies purification from the sera of naturally infected cattle. *Vet Immunol Immunopathol*, 116, 215-8.
- GOHIL, S., HERRMANN, S., GUNTHER, S. & COOKE, B. M. 2013. Bovine babesiosis in the 21st century: advances in biology and functional genomics. *Int J Parasitol*, 43, 125-32.
- GOHIL, S., KATS, L. M., STURM, A. & COOKE, B. M. 2010. Recent insights into alteration of red blood cells by Babesia bovis: moovin' forward. *Trends Parasitol*, 26, 591-9.
- GRAY, J., ZINTL, A., HILDEBRANDT, A., HUNFELD, K.-P. & WEISS, L. 2010. Zoonotic babesiosis: overview of the disease and novel aspects of pathogen identity. *Ticks and tick-borne diseases*, 1, 3-10.
- GRAY, J. S. 2006. Identity of the causal agents of human babesiosis in Europe. *Int J Med Microbiol*, 296 Suppl 40, 131-6.
- GUGLIELMONE, A. A., ROBBINS, R. G., APANASKEVICH, D. A., PETNEY, T. N., ESTRADA-PENA, A., HORAK, I. G., SHAO, R. & BARKER, S. C. 2010. The Argasidae, Ixodidae and Nuttalliellidae (Acari: Ixodida) of the world: a list of valid species names.
- HEMMER, R. M., FERRICK, D. A. & CONRAD, P. A. 2000. Role of T cells and cytokines in fatal and resolving experimental babesiosis: protection in TNFRp55^{-/-} mice infected with the human Babesia WA1 parasite. *J Parasitol*, 86, 736-42.
- HILDEBRANDT, A., GRAY, J. & HUNFELD, K.-P. 2013. Human Babesiosis in Europe: what clinicians need to know. *Infection*, 41, 1057-1072.
- HOMER, M. J., AGUILAR-DELFIN, I., TELFORD, S. R., KRAUSE, P. J. & PERSING, D. H. 2000. Babesiosis. *Clinical microbiology reviews*, 13, 451-469.
- HORAK, I. G., CAMICAS, J.-L. & KEIRANS, J. E. 2002. The Argasidae, Ixodidae and Nuttalliellidae (Acari: Ixodida): a world list of valid tick names. *Experimental & applied acarology*, 28, 27-54.
- HUNFELD, K.-P., HILDEBRANDT, A. & GRAY, J. 2008. Babesiosis: recent insights into an ancient disease. *International Journal for Parasitology*, 38, 1219-1237.
- HUNFELD, K. P. & BRADE, V. 2004. Zoonotic Babesia: possibly emerging pathogens to be considered for tick-infested humans in Central Europe. *Int J Med Microbiol*, 293 Suppl 37, 93-103.
- HUNTER, W. N. 2011. Isoprenoid precursor biosynthesis offers potential targets for drug discovery against diseases caused by apicomplexan parasites. *Curr Top Med Chem*, 11, 2048-59.
- IGARASHI, I., SUZUKI, R., WAKI, S., TAGAWA, Y., SENG, S., TUM, S., OMATA, Y., SAITO, A., NAGASAWA, H., IWAKURA, Y., SUZUKI, N., MIKAMI, T. & TOYODA, Y. 1999. Roles of CD4(+) T cells and gamma interferon in protective immunity against Babesia microti infection in mice. *Infect Immun*, 67, 4143-8.

- JONGEJAN, F. & UILENBERG, G. 2004. The global importance of ticks. *Parasitology*, 129, S3-S14.
- JOUHET, J., MARECHAL, E. & BLOCK, M. A. 2007. Glycerolipid transfer for the building of membranes in plant cells. *Prog Lipid Res*, 46, 37-55.
- KAHN, L. H. 2006. Confronting zoonoses, linking human and veterinary medicine. *Emerging infectious diseases*, 12, 556.
- KAVANAUGH, M. J. & DECKER, C. F. 2012. Babesiosis. *Dis Mon*, 58, 355-60.
- KJEMTRUP, A. & CONRAD, P. 2000. Human babesiosis: an emerging tick-borne disease. *International journal for parasitology*, 30, 1323-1337.
- KRAUSE, P. J., LEPORE, T., SIKAND, V. K., GADBAW JR, J., BURKE, G., TELFORD, S. R., BRASSARD, P., PEARL, D., AZLANZADEH, J. & CHRISTIANSON, D. 2000. Atovaquone and azithromycin for the treatment of babesiosis. *New England Journal of Medicine*, 343, 1454-1458.
- LAU, A. 2009. An overview of the Babesia, Plasmodium and Theileria genomes: a comparative perspective. *Molecular and biochemical parasitology*, 164, 1.
- LIM, L. & MCFADDEN, G. I. 2010. The evolution, metabolism and functions of the apicoplast. *Philos Trans R Soc Lond B Biol Sci*, 365, 749-63.
- MARATHE, A., TRIPATHI, J., HANDA, V. & DATE, V. 2005. Human babesiosis--a case report. *Indian J Med Microbiol*, 23, 267-9.
- MARECHAL, E. & CESBRON-DELAUW, M. F. 2001. The apicoplast: a new member of the plastid family. *Trends Plant Sci*, 6, 200-5.
- MCDANIEL, C. J., CARDWELL, D. M., MOELLER, R. B. & GRAY, G. C. 2014. Humans and cattle: a review of bovine zoonoses. *Vector-Borne and Zoonotic Diseases*, 14, 1-19.
- MCFADDEN, G. I. 2014. Apicoplast. *Curr Biol*, 24, R262-3.
- MEBIUS, R. E. & KRAAL, G. 2005. Structure and function of the spleen. *Nat Rev Immunol*, 5, 606-16.
- MEDLOCK, J. M., HANSFORD, K. M., BORMANE, A., DERDAKOVA, M., ESTRADA-PENA, A., GEORGE, J. C., GOLOVLJOVA, I., JAENSON, T. G., JENSEN, J. K., JENSEN, P. M., KAZIMIROVA, M., OTEO, J. A., PAPA, A., PFISTER, K., PLANTARD, O., RANDOLPH, S. E., RIZZOLI, A., SANTOS-SILVA, M. M., SPRONG, H., VIAL, L., HENDRICKX, G., ZELLER, H. & VAN BORTEL, W. 2013. Driving forces for changes in geographical distribution of Ixodes ricinus ticks in Europe. *Parasit Vectors*, 6, 1.
- MILLS, J. N., GAGE, K. L. & KHAN, A. S. 2010. Potential influence of climate change on vector-borne and zoonotic diseases: a review and proposed research plan. *Environ Health Perspect*, 118, 1507-14.
- MOSQUEDA, J., OLVERA-RAMIREZ, A., AGUILAR-TIPACAMÚ, G. & CANTO, G. 2012. Current advances in detection and treatment of babesiosis. *Current medicinal chemistry*, 19, 1504.
- OZ, H. S. & WESTLUND, K. H. 2012. "Human babesiosis": an emerging transfusion dilemma. *Int J Hepatol*, 2012, 431761.
- RALPH, S. A., VAN DOOREN, G. G., WALLER, R. F., CRAWFORD, M. J., FRAUNHOLZ, M. J., FOTH, B. J., TONKIN, C. J., ROOS, D. S. & MCFADDEN, G. I. 2004. Tropical infectious diseases: metabolic maps and functions of the Plasmodium falciparum apicoplast. *Nat Rev Microbiol*, 2, 203-16.
- REGASSA, A., PENZHORN, B. L. & BRYSON, N. R. 2003. Attainment of endemic stability to Babesia bigemina in cattle on a South African ranch where non-intensive tick control was applied. *Vet Parasitol*, 116, 267-74.
- RIBEIRO, J. M., ALARCON-CHAIDEZ, F., FRANCISCHETTI, I. M., MANS, B. J., MATHER, T. N., VALENZUELA, J. G. & WIKEL, S. K. 2006. An annotated catalog of salivary gland transcripts from Ixodes scapularis ticks. *Insect Biochem Mol Biol*, 36, 111-29.
- RUIZ-FONS, F., FERNANDEZ-DE-MERA, I. G., ACEVEDO, P., GORTAZAR, C. & DE LA FUENTE, J. 2012. Factors driving the abundance of ixodes ricinus ticks and the prevalence of zoonotic I. ricinus-borne pathogens in natural foci. *Appl Environ Microbiol*, 78, 2669-76.
- SAIDANI, N., BOTTE, C. Y., DELIGNY, M., BONNEAU, A. L., READER, J., LASSELIN, R., MERER, G., NIEPCERON, A., BROSSIER, F., CINTRAT, J. C., ROUSSEAU, B., BIRKHOLTZ, L. M., CESBRON-

- DELAUW, M. F., DUBREMETZ, J. F., MERCIER, C., VIAL, H., LOPEZ, R. & MARECHAL, E. 2014. Discovery of compounds blocking the proliferation of *Toxoplasma gondii* and *Plasmodium falciparum* in a chemical space based on piperidinyl-benzimidazolone analogs. *Antimicrob Agents Chemother*, 58, 2586-97.
- SAMISH, M., GINSBERG, H. & GLAZER, I. 2008. 20 Anti-tick biological control agents: assessment and future perspectives. *Biology, Disease and Control*, 447.
- SCHNITTGER, L., RODRIGUEZ, A., FLORIN-CHRISTENSEN, M. & MORRISON, D. 2012. Babesia: a world emerging. *Infection, genetics and evolution: journal of molecular epidemiology and evolutionary genetics in infectious diseases*, 12, 1788-1809.
- SCHUSTER, F. L. 2002. Cultivation of Babesia and Babesia-like blood parasites: agents of an emerging zoonotic disease. *Clinical microbiology reviews*, 15, 365-373.
- SEEBER, F. 2003. Biosynthetic pathways of plastid-derived organelles as potential drug targets against parasitic apicomplexa. *Curr Drug Targets Immune Endocr Metabol Disord*, 3, 99-109.
- SINGH-BEHL, D., LA ROSA, S. & TOMECKI, K. 2003. Tick-borne infections. *Dermatologic clinics*, 21, 237.
- SNYMAN, J. 2011. *The effect of herbicides as novel antimalarial drugs on the transcriptome and proteome of Plasmodium falciparum*. *Magister Scientiae*, University of Pretoria.
- SUAREZ, C. E. & NOH, S. 2011. Emerging perspectives in the research of bovine babesiosis and anaplasmosis. *Vet Parasitol*, 180, 109-25.
- VAN DOOREN, G. G. & STRIEPEN, B. 2013. The algal past and parasite present of the apicoplast. *Annu Rev Microbiol*, 67, 271-89.
- VANNIER, E., BORGGRAEFE, I., TELFORD, S. R., 3RD, MENON, S., BRAUNS, T., SPIELMAN, A., GELFAND, J. A. & WORTIS, H. H. 2004. Age-associated decline in resistance to Babesia microti is genetically determined. *J Infect Dis*, 189, 1721-8.
- VANNIER, E. & KRAUSE, P. J. 2009. Update on babesiosis. *Interdisciplinary perspectives on infectious diseases*, 2009.
- VANNIER, E. & KRAUSE, P. J. 2012. Human babesiosis. *New England Journal of Medicine*, 366, 2397-2407.
- VIAL, H. J. & GORENFLOT, A. 2006. Chemotherapy against babesiosis. *Veterinary parasitology*, 138, 147-160.
- VYAS, J. M., TELFORD, S. R. & ROBBINS, G. K. 2007. Treatment of refractory Babesia microti infection with atovaquone-proguanil in an HIV-infected patient: case report. *Clinical infectious diseases*, 45, 1588-1560.
- WALKER, A. R. 2011. Eradication and control of livestock ticks: biological, economic and social perspectives. *Parasitology*, 138, 945-959.
- WALLER, R. F. & MCFADDEN, G. I. 2005. The apicoplast: a review of the derived plastid of apicomplexan parasites. *Curr Issues Mol Biol*, 7, 57-79.
- WILLADSEN, P. 2006. Tick control: thoughts on a research agenda. *Vet Parasitol*, 138, 161-8.
- WILLADSEN, P. 2008. Antigen cocktails: valid hypothesis or unsubstantiated hope? *Trends in parasitology*, 24, 164-167.
- WORMSER, G. P., PRASAD, A., NEUHAUS, E., JOSHI, S., NOWAKOWSKI, J., NELSON, J., MITTLEMAN, A., AGUERO-ROSENFELD, M., TOPAL, J. & KRAUSE, P. J. 2010. Emergence of resistance to azithromycin-atovaquone in immunocompromised patients with Babesia microti infection. *Clinical infectious diseases*, 50, 381-386.
- YABSLEY, M. J. & SHOCK, B. C. 2013. Natural history of Zoonotic Babesia: Role of wildlife reservoirs. *Int J Parasitol Parasites Wildl*, 2, 18-31.
- ZINTL, A., MULCAHY, G., SKERRETT, H. E., TAYLOR, S. M. & GRAY, J. S. 2003. Babesia divergens, a bovine blood parasite of veterinary and zoonotic importance. *Clinical microbiology reviews*, 16, 622-636.

Chapter 2

Morphological and molecular descriptors of the developmental cycle of *Babesia divergens* parasites in human erythrocytes

This work was published in PLoS Neglected Tropical Diseases (2015) as: Morphological and molecular descriptors of the intra-erythrocytic development cycle of *Babesia divergens* parasites.

I. Rossouw, C. Maritz-Olivier, J. Niemand, R. van Biljon, A. Smit, N. A. Olivier, L. M. Birkholtz.
Department of Genetics & Department of Biochemistry, Centre for Sustainable Malaria Control & Department of Plant Sciences, ACGT Microarray facility, University of Pretoria, Private bag x20, Hatfield, Pretoria, South Africa, 0028.

2.1 Introduction

It remains quite surprising that our understanding of the basic biological processes underlying *Babesia* pathophysiology is still poorly understood, even with the recent application of genetic manipulation for transfection of *Babesia* parasites and the sequencing of the *B. bovis* genome (Suarez *et al.*, 2006, Brayton *et al.*, 2007). Particularly intriguing is the fact that the precise progression and duration of the intra-erythrocytic, asexual developmental cycle (IDC) has not been clarified. During its IDC, *Babesia* parasites undergo asexual replication by binary fission (budding) of trophozoites to form 2-4 merozoites (Mackenstedt *et al.*, 1990). Each merozoite is

thought to undergo a single cycle of division and then escape *via* cell lysis to re-infect new erythrocytes (Hunfeld *et al.*, 2008). This establishes a perpetual, asynchronous asexual parasitic growth cycle, which is thought to last approximately 8 hours (Valentin *et al.*, 1991) and encompasses several developmental stages all present at the same point in time within the hosts' bloodstream (Chauvin *et al.*, 2009). At the onset of this study, we however, observed that the description of the IDC and its different stages are fraught with uncertainties: historically different stages were described only based on light microscopy, with little attention paid to their sequence of development. This is reflected in literature, as the various *Babesia* parasitic *in vitro* stages do not share a consensus and display considerable morphological pleiomorphism. Moreover, fundamental biological questions remain unanswered, particularly concerning the molecular descriptors governing the IDC of *Babesia* parasites. An in depth analysis of the IDC of *Babesia* parasites will provide insight into the functions and regulations of several genes, which can provide valuable information in future treatment strategies, including the identification of new chemotherapeutic and vaccine candidates.

Cultivation of *Babesia* parasites

In vitro cultivation systems are important for the evaluation of molecular features and stage differentiation mechanisms of several species (Muller and Hemphill, 2013). Over the past thirty years, several techniques have been established for long-term, continuous *in vitro* cultivation and maintenance systems of several *Plasmodium* (Trager and Jensen, 1976) and *Babesia* species (Gorenflot *et al.*, 1991, Grande *et al.*, 1997, Vayrynen and Tuomi, 1982). These techniques have improved considerably for *Plasmodium* since the original publication by Trager and Jensen, which have led to several advancements in malaria research (Schuster, 2002a). Particular progress has been made with the use of serum replacements (Flores *et al.*, 1997)

and/or substitutes (Cranmer *et al.*, 1997) during the parasites asexual intra-erythrocytic stages. The cost, reproducibility and possible presence of inhibitory immune factors associated with human serum, provoked researchers to investigate these alternatives. The most promising serum-free conditions were achieved by the addition of synthetic, lipid-rich bovine serum, either Albumax (Trager, 1994) or Nutridoma (Lingnau *et al.*, 1993). All human *Plasmodium* species have been maintained *in vitro*, with particular emphasis on *P. falciparum*, with all life stages established in culture (Hollingdale, 1992).

The intra-erythrocytic stages of several *Babesia* species can be maintained with a range of media and sera, depending on the particular species cultivated (Table 2.1) (Schuster, 2002b). A short-term *in vitro* cultivation strategy was originally described for *B. bovis* (Erp *et al.*, 1978). Modifications on this system introduced the micro-aerophilus stationary phase culture system (MASP), which produced higher growth rates and elevated parasitaemia levels over longer time periods. The MASP system was successfully adapted for several *B. bovis* strains and several other *Babesia* species (Pudney and Gray, 1997). The first successful, long-term *in vitro* cultivation method of *B. divergens* in bovine erythrocytes incorporated Media-199, supplemented with 40% bovine serum (Vayrynen and Tuomi, 1982). Modifications of this method allowed for cultivation and maintenance of *B. divergens* parasites in several other species' erythrocytes including human, rat and sheep (Zintl *et al.*, 2003). Further development in *Babesia* culture systems saw a decline in bovine serum concentrations, which was later completely replaced by human serum conditions. Serum-free culture conditions have been applied to several *Babesia* species including *B. divergens*, *B. bovis* and *Babesia bigemina* with varying levels of success (Grande *et al.*, 1997).

Table 2.1 *In vitro* cultivation systems of several *Babesia* species (Compiled from Shuster, 2002).

Species	Medium	Serum type	Serum concentration	References
<i>B. bovis</i>	HEPES-buffered 199 medium	Bovine	40%	(Levy and Ristic, 1980, Igarashi <i>et al.</i> , 1994)
<i>B. bigemina</i>	HEPES-buffered 199 medium	Bovine	40%	(Levy and Ristic, 1980, Igarashi <i>et al.</i> , 1994)
<i>B. divergens</i>	HEPES-buffered RPMI 1640	Human	10%	(Gorenflot <i>et al.</i> , 1991, Grande <i>et al.</i> , 1997)
<i>B. microti</i>	RPMI 1640	Foetal calf	30-40%	(Shikano <i>et al.</i> , 1995)
<i>B. equi</i>	HL-1	Foetal calf	20%	(Holman <i>et al.</i> , 1994)
<i>B. gibsoni</i>	HL-1	Dog	20%	(Zweygarth and Lopez-Rebollar, 2000)
<i>B. caballi</i>	HEPES-buffered HL-1	Serum-free (lipid-rich supplements)	-	(Zweygarth <i>et al.</i> , 1999)
<i>B. odocoilei</i>	TES-buffered medium 199	Deer or bovine	20% or 40%	(Holman <i>et al.</i> , 1988)
<i>Strain WA-1</i>	TES-buffered medium 199	Foetal calf	40%	(Thomford <i>et al.</i> , 1994)

In this study, the *in vitro* IDC of the human pathogen *B. divergens* was comprehensively evaluated by employing various high-content cell biological and molecular strategies as has been previously applied to the more widely studied but related haemoprotozoan malaria parasite, *P. falciparum*. The study particularly focused on *B. divergens* as human pathogen and model organism for *Babesia* since it is amenable to *in vitro* cultivation. This is to our knowledge the first quantitative description and temporal evaluation of intra-erythrocytic *B. divergens* development and enabled clear characterization of the stage-specific development, based on nuclear proliferation in these parasites. The information is novel not just from a biological perspective, but will also be essential in future prioritization of anti-babesiocidal compounds.

2.2 Materials and Methods

2.2.1 *In vitro* cultivation of intra-erythrocytic *B. divergens* and *P. falciparum* parasites

Approval for the importation and cultivation of *B. divergens* was obtained from the South African Department of Agriculture, Forestry and Fisheries. Human blood and sera was collected from volunteer donors and used for cultivation with ethical approval (University of Pretoria EC120821-077 to Prof. L Birkholtz, Department of Biochemistry). All *Babesia in vitro* cultivation was performed in a controlled access P2 facility within the Department of Biochemistry.

The Rouen 1987 strain of *B. divergens* was kindly provided by Dr. Stephane Delbecq (Laboratoire de Biologie Cellulaire et Moleculaire UFR Pharmacie, Montpellier, France). Asynchronous *B. divergens* parasite cultures were maintained in human erythrocytes (type O⁺) suspended in complete culture medium [RPMI-1640 medium supplemented with 25.2 mM HEPES, 22.2 mM D-glucose, 50 mg/l hypoxanthine, 21.4 mM sodium bicarbonate, 48 mg/l gentamycin (Sigma)] further supplemented with 10% human serum (Gorenflot *et al.*, 1991). Cultures were maintained at 37°C in a gaseous environment of 90% N₂, 5% O₂ and 5% CO₂ on a rotary platform (60 rpm) at 5% haematocrit and 10-15% parasitaemia, with daily media replacement. Comparatively, intra-erythrocytic *P. falciparum* (3D7 strain) was maintained at a 5% haematocrit, 2-5% parasitaemia in complete culture medium [RPMI-1640 medium supplemented with 25.2 mM HEPES, 22.2 mM D-glucose, 50 mg/l hypoxanthine, 21.4 mM sodium bicarbonate, 48 mg/l gentamycin (Sigma)] further supplemented with 0.5% Albumax II (Invitrogen) (Trager and Jensen, 1976) in the same gaseous environment under shaking conditions as above.

2.2.2 Microscopy

For both intra-erythrocytic *B. divergens* and *P. falciparum* parasites, Giemsa's Azur Eosin methylene blue (Merck) stained thin smears and light microscopy was used for the daily determination of both the parasitaemia and morphology. Thin blood smears were prepared, air dried, fixed with methanol and stained for 5 minutes prior to examination. The percentage parasitaemia was determined as the number of infected erythrocytes per 100 cells, with a minimum of 1000 erythrocytes counted (Bork *et al.*, 2003). Asynchronous intra-erythrocytic *B. divergens* parasites (5% haematocrit, 10-15% parasitaemia) were examined every two hours over a 16-hour time period using Giemsa-stained smears and light microscopy. The asexual developmental life stages were classified as rings, paired piriform and tetrad and/or multiple infection formations. Fluorescent microscopy (Zeiss Axiovert 200 fluorescent microscope) was also used to examine intra-erythrocytic *B. divergens* parasites using the Axiovision release 4.8.2 software for analyses.

2.2.3 Flow cytometric analysis using SYBR[®] Green I fluorescence

Determining parasitaemia

The parasitaemia of both intra-erythrocytic *B. divergens* and *P. falciparum* parasites was measured using flow cytometry following the staining of nucleic acids with SYBR[®] Green I (Invitrogen). Uninfected erythrocytes (negative control; 5% haematocrit), asynchronous *P. falciparum* samples (positive control; 5% haematocrit, 2% parasitaemia) and asynchronous *B. divergens* samples (5% haematocrit, 12% parasitaemia) were used either unfixed or fixed with 1 ml of 0.025% glutaraldehyde for 45 min and kept at 4°C until use. Glutaraldehyde fixed cells was washed twice with phosphate buffered saline (1x PBS: 137 mM NaCl, 2.7 mM KCl, 1.8 mM KH₂PO₄, 10 mM Na₂HPO₄.7H₂O, pH 7.4) and re-suspended in a final volume of 50 µl PBS.

Plasmodium falciparum parasites were stained at room temperature with 20 µl 1:1000 SYBR® Green I (10 000x SYBR® Green I):PBS solution for 30 minutes in the dark (Verlinden *et al.*, 2011). Glutaraldehyde fixed *B. divergens* cells were stained with various dilutions of SYBR® Green I (10 000x SYBR® Green I):PBS to determine optimal fluorescence. Both unfixed and fixed *B. divergens* parasites were stained with 20 µl 1:100 and 1:1000 SYBR® Green I (10 000x SYBR® Green I):PBS solutions respectively and incubated at 37°C for 30 minutes in the dark.

In all cases, SYBR® Green I fluorescence was measured using the BD FACS Aria I flow cytometer with fluorescence emission collected at an excitation wavelength of 488 nm, 502 nm long-band-pass and 530 nm band-pass emission filter equipped with a 488-nm, 633-nm, 405-nm and 375-nm near UV laser. SYBR® Green I fluorescent dye was detected with the FITC (515-545 nm) band pass filter. The number of events recorded were gated for 10 000 events outside of the erythrocyte's background signal, thereby recording and analysing approximately 10⁴ infected erythrocytes per sample. The gating strategy for quantification of *B. divergens* was plotted on forward (FSC) versus side (SSC) scatter density plots and used to gate and sort cell populations.

Intra-erythrocytic *B. divergens* parasitaemia was calculated based on the number of erythrocytes counted (in relation to the relative fluorescence intensities) and displayed on single parameter histogram plots. Parasitaemia validation was done on all samples with light microscopy using Giemsa-stained smears. Three independent experiments were conducted in triplicate with analysis and compensation of data performed by FlowJo version 9.1 (Tree Star). Statistical data analysis was performed with GraphPad InStat (version 6.04). In all cases, the percentage parasitaemia associated with the x-axis was plotted against the units fluorescence (RFU) associated with the y-axis and subsequently analysed by linear regression to determine the goodness of fit (R²-value).

Determining stage distribution

DNA replication and nuclear division of intra-erythrocytic *B. divergens* parasites were determined using SYBR[®] Green I fluorescence and correlated morphologically to the different developmental stages of the parasite. Intra-erythrocytic *B. divergens* cultures (5% haematocrit, 12% parasitaemia, 50 µl, unfixed) were processed as described above and stained with 20 µl 1:100 SYBR[®] Green I (10 000x SYBR[®] Green I):1xPBS solution and incubated at 37°C for 30 minutes in the dark. Fluorescence was measured as described above. Cell sorting was subsequently set up for a three-way sort of populations P1, P2, P3 and P4 to at least 1 million cells per individual collection tube. Following cell sorting, individual populations were subjected to light microscopy. The content of each collection tube was centrifuged for 10 minutes at 8000xg to obtain a cell pellet which was dissolved in 20 µl 1xPBS solution, placed on a glass slide and examined with light microscopy.

2.2.4 Transcriptome analysis

A custom designed DNA microarray slide was used for gene expression analysis. The base composition probe design strategy and probe selection parameters were selected according to Agilent Technologies eArray 60-mer platform specifications. Available *B. bovis* sequences were downloaded and retrieved from the National Center for Biotechnology Information (NCBI) (<http://www.ncbi.nlm.nih.gov/>) and supplemented with additional published sequence data (Lau, 2009c). Selected probes were randomly distributed across the array using the 8x 15K design format. All arrays were ordered from Agilent Technologies (<https://earray.chem.agilent.com/earray/>).

RNA isolation, DNA microarray hybridizations and quality control

Total RNA was isolated from three biological replicate samples (5% haematocrit, 12% parasitaemia, 10 ml) collected at four time-points (0, 4, 9 and 16 hours) from newly initiated cultures and washed three times with 15 ml 1xPBS solution under RNase-free conditions. TRI-Reagent[®] fractionation was followed by clean-up using the Qiagen RNeasy Protect Mini kit (Qiagen). Contaminating genomic DNA was removed with a DNase I treatment (Qiagen). RNA integrity and quality was subsequently analysed using the Experion[®] automated electrophoresis system (Bio-Rad) at the ACGT Microarray Facility (University of Pretoria).

For gene expression profiling, a reference pool design strategy was followed which consisted of equal RNA quantities (4 µg), prepared from all three biological replicates collected over the 16 hour time period. First-strand cDNA synthesis was performed by incubating 4 µg RNA with 250 pmol oligo(dT₂₅) and 775 pmol random primer 9 for 10 minutes at 70°C, followed by cooling for 10 minutes on ice. Reverse transcription and aminoallyl-dUTP (5-(3-aminoallyl)-2'-deoxyuridine-5' triphosphate) incorporation were performed simultaneously (Bozdech *et al.*, 2003), with minor modifications in reaction time (van Brummelen *et al.*, 2009) using 340 units Superscript[®] III (Invitrogen). Contaminating RNA template was removed by RNA hydrolysis of the cDNA template with 0.5 M EDTA and 1 M NaOH for 15 minutes at 65°C before samples were purified with a NucleoSpin[®] Extract II PCR Clean-up kit (Macherey-Nagel). Purified cDNA samples (1.5 µg) were dried *in vacuo* and resuspended in 2.5 µl RNase-free water. Both Cy3 (reference pool) and Cy5 (samples) fluorescent dyes (GE Healthcare Life Sciences) were dissolved in DMSO and coupled to the cDNA samples at pH 9. Excess (unincorporated) dye was removed using the QIAquick[®] PCR Purification Kit (Qiagen). Overnight hybridization at 65°C (rotation speed of 10), washing and post-processing were performed as described (Bozdech *et al.*, 2003) at the ACGT Microarray Facility (University of Pretoria). Prior to slide scanning with the Axon GenePix 4000B scanner (Molecular Devices) slides were removed, washed and dried by centrifugation.

Microarray data analysis

Axon GenePix Pro 6.0 software (Molecular Devices) measured, recorded and analysed images based on the software's default settings as well as visual inspection of spots (adjusting the grid and flagging of low quality spots). Flagged features were ignored in subsequent analyses and given a zero weight value. Initial data analysis was performed using CLUSTER and TREEVIEW software (Eisen *et al.*, 1998). Data was log transformed, normalized and mean centered prior to hierarchical clustering and subsequently ordered according to expression values (*M*-values) identified over time. Pearson correlation coefficients (*r*) were calculated within the R-statistical environment to identify expression similarities between each of the time points. The linear model for microarray data analysis (LIMMA) within the R-statistical environment (<http://cran.r-project.org/>) was used to simultaneously assess differential expression between several transcripts, collected at different time points. Adaptive background correction (offset = 50) was followed by within-array normalization (global LOWESS) and between-array normalization (Gquantile). Fold change was determined between all transcripts collected at different time-points using the empirical Bayesian statistics and subsequently expressed as *P*-values (corrected for false discovery rate). Transcripts were regarded as differentially expressed if a greater than 1.7 fold change ($0.75 \leq \log_2\text{ratio} \leq -0.75$) in either direction with *P*-value <0.05 were observed. A selected subset of differentially affected transcripts was constructed based on data filtering, fold change and statistical significance ($\log_2\text{FC}$, *P*-values, adjusted *P*-values and *t*-statistics). Functional annotation of transcripts was conducted using the desktop cDNA Annotation System software (dCAS) (Guo *et al.*, 2009). Large-scale BLAST searches were conducted with the gene ontology protein sequence database (GO) and eukaryotic orthologous group database (COG). Functional annotation were obtained based the piroplasmaDB annotations (www.piroplasmaDB.org) and verified by Uniprot (<http://www.uniprot.org/uniprot/>) and BLAST2GO (B2G) (Conesa *et al.*, 2005).

2.3 Results

2.3.1 Flow cytometric analysis using SYBR[®] Green I fluorescence

Flow cytometry (using SYBR[®] Green I fluorescence as nuclear marker) sensitively and accurately discriminated *Babesia* infected from uninfected erythrocytes (Figure 2.1 A). A 1:100 SYBR[®] Green I (10 000x SYBR[®] Green I):PBS solution was able to discriminate uninfected from three separate infected erythrocyte populations with the highest resolution (Figure 2.1 A₂; A₃). However, the use of glutaraldehyde as fixative at both SYBR[®] Green I concentrations, resulted in a marked decrease in resolution compared to the unfixed samples (Figure 2.1 A₄; A₅ and Figure 2.1 C). Asynchronous, unfixed, stained *P. falciparum* was used as positive control as distinct populations have been validated previously using a similar approach (Figure 2.1 A₆) (Grimberg *et al.*, 2008, Izumiyama *et al.*, 2009).

The optimal staining procedure (1:100 SYBR[®] Green I solution with unfixed parasites) was also optimal to accurately determine the percentage infected erythrocytes (parasitaemia) of *B. divergens* cultures (Figure 2.1 B). Even though a 1:100 concentration of the fluorescent dye was more informative with regards to population resolution, parasitaemia could still be accurately detected with a 10-fold dilution of SYBR[®] Green I from 1:100 to 1:1000 (Figure 2.1 B₁; B₂). Fixation of *B. divergens* parasites detrimentally affected the ability to determine parasitaemia accurately by flow cytometry, resulting in a significant 2-fold reduction in reported parasitaemia under these conditions (Figure 2.1 B₄; B₅ and Figure 1 C).

The flow cytometric assay was subsequently verified as alternative method of determining parasitic proliferation compared to light microscopy, by analysing asynchronous *B. divergens* samples in triplicate with both light microscopy and flow cytometry. A strong linear correlation ($R^2 = 0.98$) was observed between the microscopic and flow cytometric analyses (unfixed cells,

1:100 SYBR[®] Green I dilution) based on the parasitaemia obtained either with light microscopy or determined with the BD FACS Aria I flow cytometer (Figure 2.1 D).

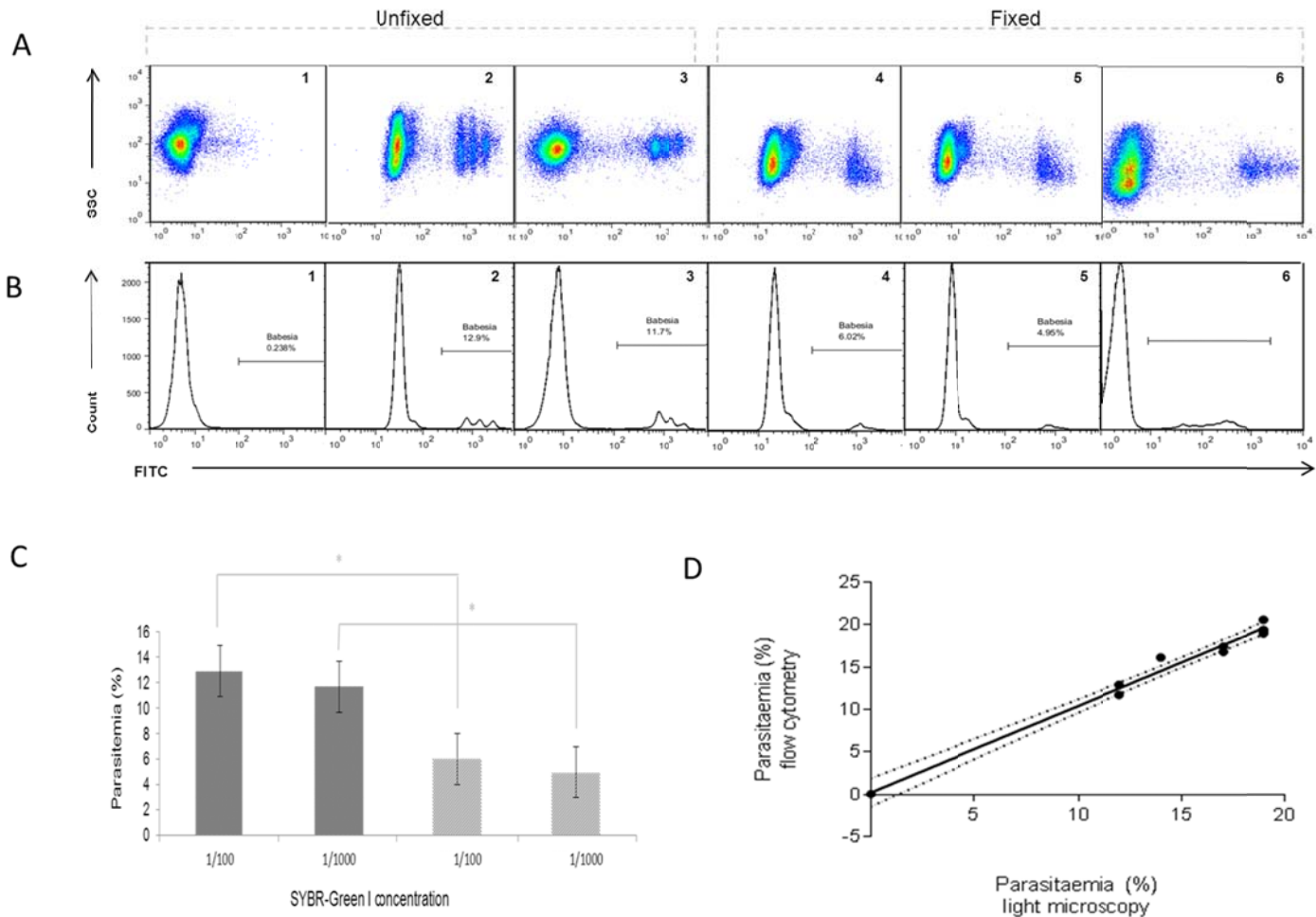


Figure 2.1 Flow cytometric analyses of intra-erythrocytic *B. divergens* parasites.

Uninfected erythrocytes were analysed in parallel to *B. divergens* infected erythrocytes, either fixed (0.025% glutaraldehyde for 45 min) or unfixed. Cells were subsequently stained with either 1:100 and 1:1000 SYBR[®] Green I (30 min, dark, room temperature). (A) Dotplot analysis and (B) histograms of 1) uninfected, unfixed, stained erythrocytes; 2-5) *B. divergens* infected erythrocytes either unfixed (2 & 3) or fixed (4 & 5). In panels 2 and 4 cells were stained with 1:100 SYBR[®] Green I and in panels 3 and 5 with 1:1000 SYBR[®] Green I. Erythrocytes infected with *P. falciparum* parasites were comparatively analysed in panel 6 (glutaraldehyde fixed and stained with 1:1000 SYBR[®] Green I). (C) Effect of SYBR[®] Green I concentrations on parasitaemia determined from both unfixed and fixed *B. divergens* infected erythrocytes. Results are the mean of three independent experiments each performed in triplicate (\pm S.E.). Significance is indicated at $P < 0.001$ (*) (unpaired Student-t test). (D) Linear correlation analysis (R^2 value of 0.98) of *B. divergens* parasitaemia detection between light microscopy and flow cytometry. Data are the mean of three independent experiments each performed in triplicate (\pm S.E.). Confidence levels (95%) indicated by dashed lines.

2.3.2 Evaluation of *B. divergens* *in vitro* blood stage development

Morphological discrimination of life cycle stages

Fluorescent detection of intra-erythrocytic *B. divergens* parasites enabled for the first time further interrogation of the population diversity within unsynchronized *B. divergens* cultures. From the data presented in Figure 2.1, distinct infected erythrocyte populations were observed. We subsequently questioned if these could be correlated to specific parasitic developmental forms by subsequent gating, sorting and isolation of individual cells and cell populations (Figure 2.2 A). By gating for the intra-erythrocytic *B. divergens* populations, three distinct sub-populations could be independently sorted, microscopically evaluated and classified (Gray *et al.*, 2010, Chauvin *et al.*, 2009). The majority (67%) of parasitized erythrocytes from the second population (P2) contained ring formations while the majority associated with the third (58%; P3) and fourth (50%; P4) populations contained paired piriforms and tetrads, respectively (Figure 2.2 A). The various infected populations were not present in equally distributed proportions. Ring forms, paired piriforms and tetrads represented 42%, 32% and 26% of the total infected erythrocytes, respectively. Similarly, the more synchronous development of intra-erythrocytic *P. falciparum* parasites could be evaluated (Figure 2.2 B). Immature ring-stage *P. falciparum* parasites were distinctly visible (mono-nucleated forms, first panel at 0 h and developed through metabolizing trophozoite forms to the multi-nucleated schizonts within 24 h (61% population distribution, Figure 2.2 B). The newly formed daughter merozoites resulting from schizogony (70% population distribution, 36 h) were able to re-infect new erythrocytes, initiating a subsequent development cycle.

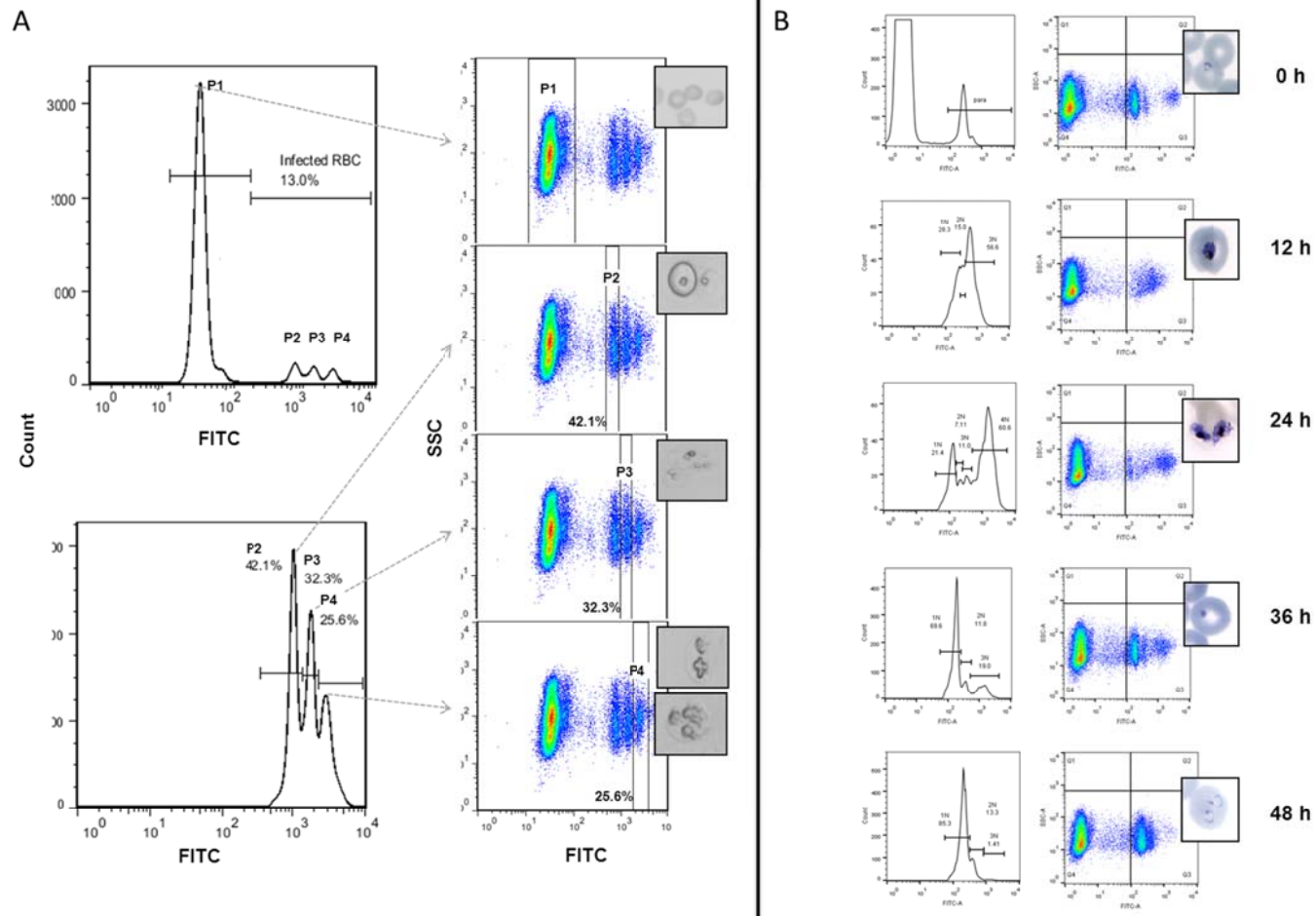


Figure 2.2 Morphological discrimination of *B. divergens* in vitro blood stage development.

(A) Flow cytometric developmental stage differentiation, sorting and isolation of intra-erythrocytic *B. divergens* parasites via SYBR® Green I staining of DNA tracked in the FITC channel. Histogram panels indicate the gated populations as either uninfected (P1) or infected erythrocytes (P2; P3; P3), as well as the percentage infected erythrocytes (parasitaemia). Light microscopy images illustrate the individually sorted and isolated populations as either uninfected (P1) or infected (P2-P3) erythrocytes. Enriched parasite formations include ring (P2), paired piriform (P3) and tetrad and/or multiple infections (P4). (B) Flow cytometric evaluation of intra-erythrocytic *P. falciparum* development over 48 hours. Synchronized *P. falciparum* parasites could be distinguished as either ring forms containing single nuclei, 1N at 0-12 h post invasion, mature trophozoites (2-4N nuclear content) and schizonts (>4N nuclear content) (24 h post invasion) resulting in daughter merozoites (1N nuclear content) re-infecting new erythrocytes at 36-48 hours post invasion.

2.3.3 Nuclear content associated with *B. divergens* parasites' life cycle compartments

The ability to discriminate between distinct populations of intra-erythrocytic life stages of *B. divergens* parasites is highly informative considering that *B. divergens* cultures cannot be synchronized *in vitro* (compared to for instance *P. falciparum* cultures). Since SYBR[®] Green I has shown to be effective as a stoichiometric marker of DNA content in malaria parasites, it can be used to further evaluate the progression of parasite development during the intra-erythrocytic developmental cycle, based on changes in nuclear content (Izumiyama *et al.*, 2009). In Figure 2.3 A, a clear distinction is observed between immature, ring-stage *P. falciparum* parasites (containing a single nucleus with 1N nuclear content) compared to mature, multi-nucleated schizont forms of the parasite where more than 5 distinct nuclei (>5N nuclear content) could be distinguished. Comparatively, fluorescent analysis of the nuclear content of the mixed intra-erythrocytic *B. divergens* parasite cultures revealed a clear correlation between DNA fluorescence and nuclear bodies. Median fluorescence intensities (MFI) increased linearly ($R^2 = 0.96$) between the three observed, infected populations. The MFI values increased from ring to paired piriform populations of *B. divergens* parasites (P2 to P3 increased from 4520 – 5700 units) as well as between paired piriforms to tetrads (P3 and P4 from 5200 – 6400 units). Fluorescent microscopy confirmed the observed morphological findings associated with stage-specific division of each infected population and subsequently indicated nuclear content (Figure 2.3 B). As such, ring stage parasites contained single, clear nuclei (P2). Distinct V-shaped nuclei characterized the bi-nucleated paired piriforms (P3) and the tetrads (P4) were distinguished by at least 3-4 multiple but distinct nuclei. However, the presence of multiple infections of mono-nucleated parasites in both paired piriform and more specifically tetrad populations cannot be ruled out.

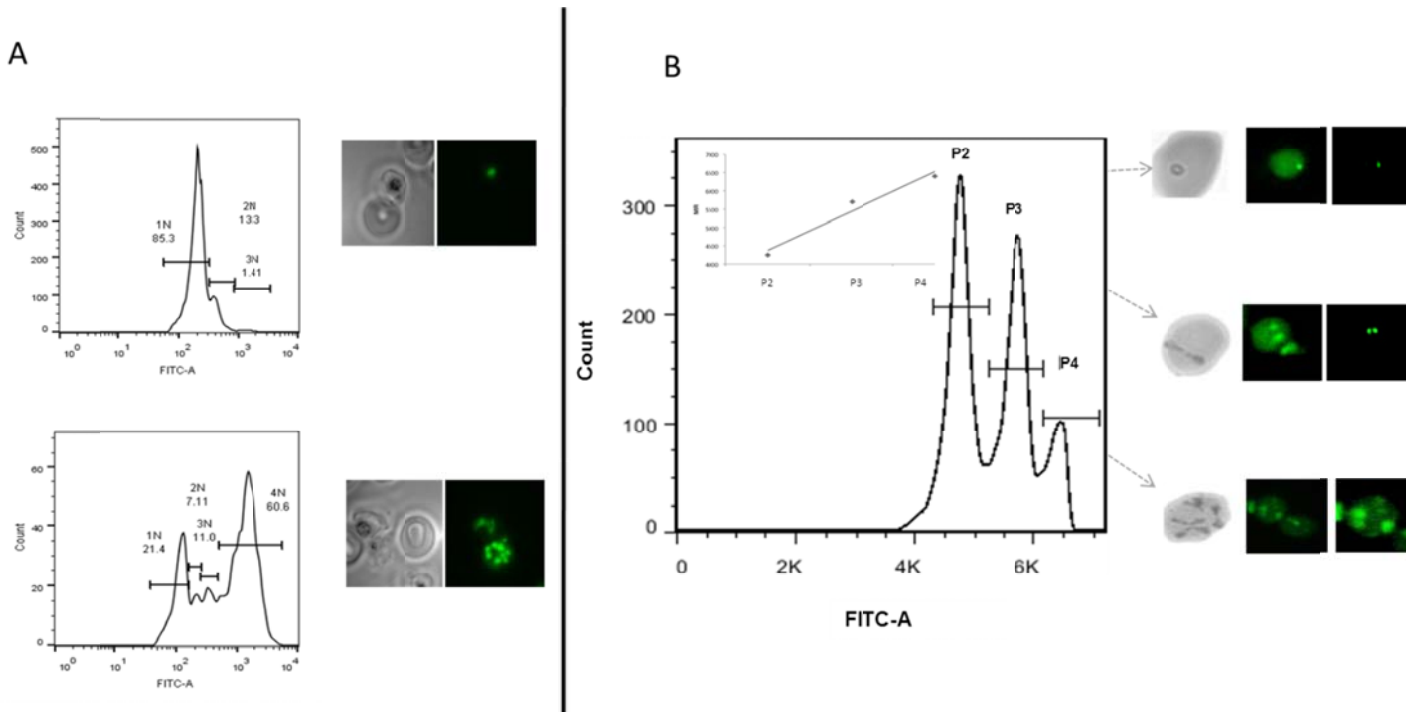


Figure 2.3 Correlation of nuclear content to IDC compartments (stages) for *B. divergens* and *P. falciparum* parasites.

Flow cytometric evaluation of different parasite populations was performed as for Figure 2 and parasite populations additionally analysed with fluorescent microscopy (1:100 SYBR[®] Green I stained, 30 min dark at room temperature and evaluated with green filter). (A) Immature, ring-stage *P. falciparum* parasites containing a single nucleus with 1N DNA content (top) and multi-nucleated schizont forms (at >5 distinct nuclei with >5N DNA content; bottom). (B) *B. divergens* population discrimination based on a linear scale with corresponding median fluorescent intensities (MFI) values. MFI values for each isolated population (indicated by grey arrows) ranged between P2 and P3 (4520 – 5700 units) and between P3 and P4 (5200 – 6400 units) and increased linearly (R^2 value of 0.96) between the three observed, infected populations. Fluorescent microscopy images visualized DNA nuclear content for each infected *B. divergens* erythrocyte population as (P2) single ring formation with a single parasitic nucleus (1N), (P3) paired piriform with two nuclei (2N) and (P4) tetrad and/or multiple infections with two or more nuclei (>2N).

2.3.4 Temporal evaluation of *B. divergens* parasites' life cycle progression

Based on the findings presented here that correlate the linear increase of DNA content to its associated nuclear content and morphological classification, the progression of intra-erythrocytic *B. divergens* parasites in its development from one IDC stage to another could be proposed.

Temporal evaluation of *in vitro* proliferation for each developmental form (ring, paired piriforms, tetrads and/or multiple infections) was performed over a 16-hour period. Parasitaemia steadily increased to 15% over the 16-hour period monitored in the asynchronous culture (Figure 2.4). However, between 4-6 hours of development, the ring formation population doubled (from a 2% to a 4% contribution to parasitaemia, $P < 0.05$, $n = 3$) (Figure 2.4). This was additionally associated with an increase in paired piriforms (2% increase in the contribution to total parasitaemia for paired piriforms). Similar observations were made between 8-10 hours of development, where a significant increase in paired piriforms was again observed (8% to 10%, $P < 0.05$, $n = 3$) (Figure 2.4 A). Overall, the population distribution in the mixed culture remained predominantly paired piriforms ($9.04 \pm 1.03\%$ contribution to total parasitaemia that ranged from 10.3-15.3%) followed by ring formations ($3.33 \pm 0.68\%$ contribution to total parasitaemia) (Figure 2.4). The tetrad (or multiple infection) population is the most stable throughout the temporal evaluation with no significant variation in population size (average $1.08 \pm 0.28\%$ contribution to total parasitaemia maintained throughout).

The increase in ring and piriform populations between 4-6 hours of development additionally contributed to a 3% increase in total parasitaemia (from 10 to 13% total parasitaemia) and again a 2% increase in parasitaemia between 8-10 hours (from 13 to 15% total parasitaemia). This is indicative of life cycle progression through re-infection of erythrocytes (contributing to new rings formed) and parasite developmental maturation (contributing to new paired piriforms). If significant increases in the ring populations are taken as an indicator of merozoite invasions of erythrocytes and initiation of new development cycles, it appears therefore that the *in vitro* development of *B. divergens* is typified by a 4 hour progression window and that, after two parasitic life cycles and under the culture conditions employed, equilibrium could be established and maintained. As such, a multiplication index of 3-fold was subsequently observed for continued *B. divergens in vitro* development.

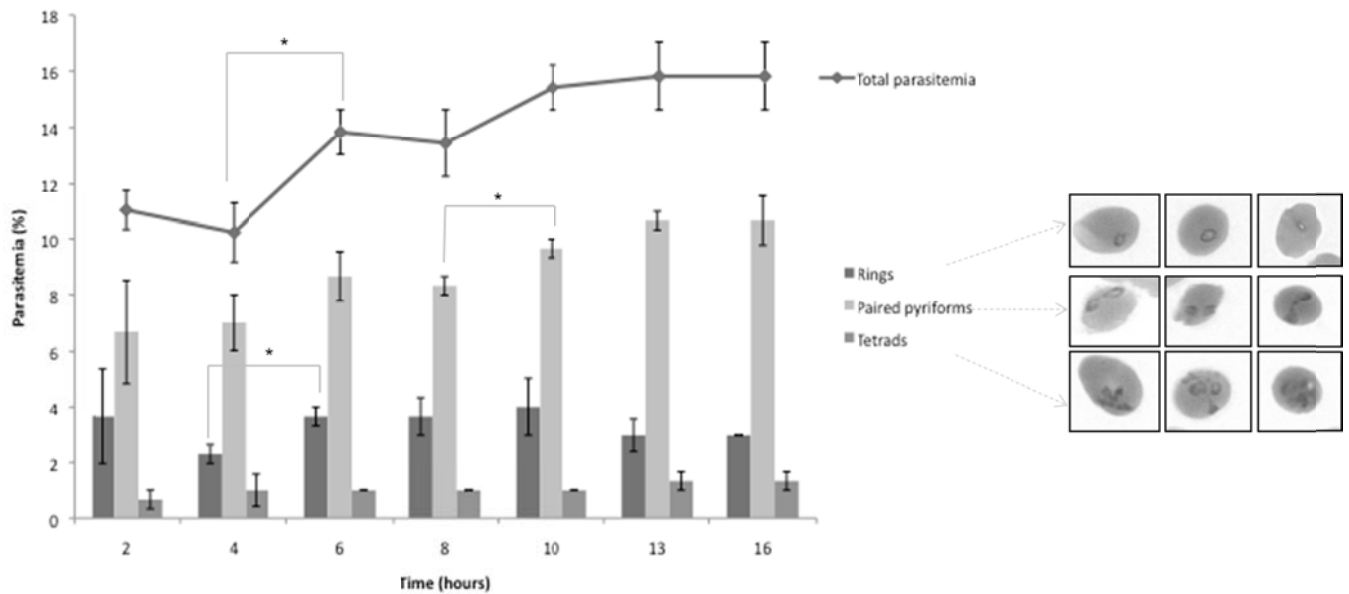


Figure 2.4 Temporal evaluation of *B. divergens* progression over two parasitic life cycles.

An established *B. divergens in vitro* culture was re-inoculated into fresh media (at time 0) and temporal evaluation of the life cycle stage distribution performed every 2 hours over a total 16-hour period. Giemsa stained microscopy was performed and parasite stages classified morphologically as ring, paired pyriforms and tetrads infections according to (Gray *et al.*, 2010). Total parasitaemia is indicated per time point analysed (line graph) and compared to the contribution of each life cycle stage (% of total parasitaemia) at each time point. Results are the mean of three independent experiments, performed in triplicate (\pm S.E.). Significance is indicated at $P < 0.05$ (*) as determined with a unpaired Student-t test.

2.3.5 Molecular descriptors characterizing the life cycle of *B. divergens* parasites

There are currently no data describing the molecular events associated with *B. divergens* intra-erythrocytic development, information that is essential to understanding the nature of stage-specific progression of this parasite's IDC. Since clear contributions of morphologically distinct life cycle compartments were observed to contribute to the IDC progression of *B. divergens* parasites, we set out to describe the global transcriptome of these parasites through its IDC as an indicator of the physiological processes involved. Transcriptome analysis (mRNA abundance determination) was subsequently conducted on asynchronous, newly initiated cultures with a

custom designed DNA microarray containing 15744 target features covering 97% of the *B. bovis* genome (3703 independent ORFs) and using a reference pool design strategy (Figure 2.5).

B. divergens parasites seem to adapt to culturing under unlimited growth conditions (4% increase in parasitaemia, $P < 0.05$, $n = 3$) (Figure 2.5 A). Again, this adaptation was resultant of a significant increase in both ring and paired piriform parasites (from 2.5 to 5% and 4.75 to 7.5%, respectively, $P < 0.05$, $n = 3$); after this the parasite population distribution equilibrated. These observations were further evident from correlation data, indicating that the transcriptome of equilibrated parasites showed the best correlation ($r = 0.19$) between parasites that have been in culture for 9 and 16 hours (C9 vs. C16, Figure 2.5 B). Comparatively, initiate cultures showed complete disconnect from established cultures (C0 vs. C16 anti-correlated at -0.03). This clearly indicates a physiological adaptation event underscored by a predominant transcriptional repression in the initiate culture (931 undefined transcripts, 387 transcripts with increased abundance, compared to 2385 repressed transcripts). Differential expression between the initiate culture and the parasites 4 hours after inoculation resulted in 164 transcripts significantly affected (82 decrease and increase in abundance, respectively) (Appendix 2.1). Of these, only 50 could be annotated using the dCAS annotation system (Guo *et al.*, 2009) based on each transcript's COG classification (E -value cut-off of less than 1×10^{-4}) (Table 2.1). The processes mostly affected include transcription (26%), translation (8%), protein turnover (21%), cellular (30%) and metabolic (11%) processes, and stress defence mechanisms (2%). All activated transcripts may be associated with the changes in parasite population distributions (increases in ring and paired piriforms). Clustering of transcripts based on co-expression profiles indicated the expected similarity in expression profiles across the transcriptome (Figure 2.5 C). Moreover, transcripts in some of these co-expressed clusters additionally showed clear chromosomal synteny (e.g. BBOV_III006240 and BBOV_III007280 on chromosome III; BBOV_IV007380 and

BBOV_IV001730 on chromosome IV) implying transcriptional level regulation for these transcripts.

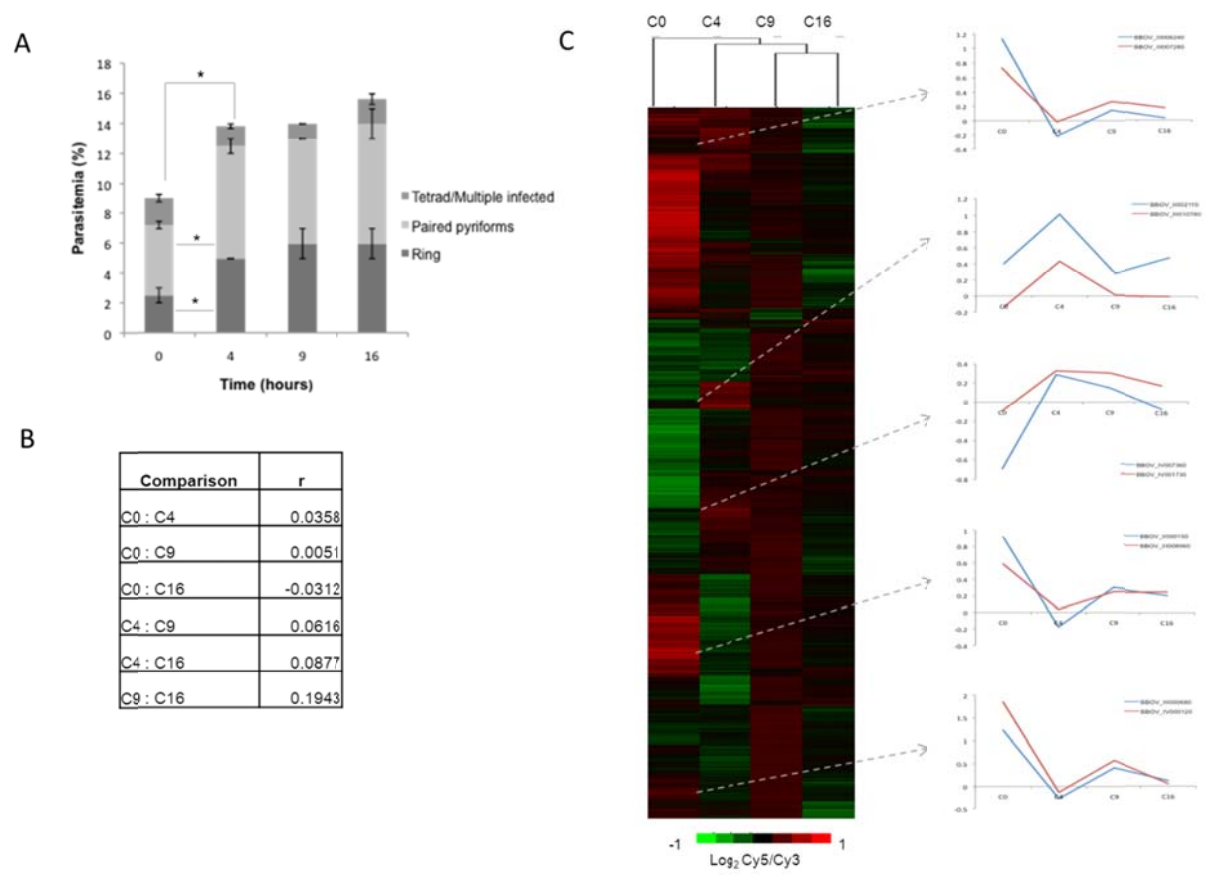


Figure 2.5 Molecular descriptors characterizing the IDC of *B. divergens* parasites.

(A) Morphological evaluation of *B. divergens* life cycle progression from a newly initiated culture over a total of 16 hours, indicating the distribution of life cycle stages to total parasitaemia. (B) Pearson correlations of the mRNA abundance levels of *B. divergens* parasites in an initiate culture compared to parasites that adapted to culture for 4, 9 and 16 hours, respectively. (C) Cy5-labelled cDNA from *B. divergens* parasites across four different times (0, 4, 9, 16 hours post-inoculation) were hybridized to Cy3-labelled cDNA from a reference pool spanning all samples. Transcripts were clustered according to expression values (M-values, $\log_2 \text{Cy5/Cy3}$) of the initiate culture, with the expression profiles of representative genes indicated. On the heat map, scale ($\log_2 \text{Cy5/Cy3}$) is from 1 to -1. Transcripts were classified based on their dCAS annotation and COG classification compared to *B. bovis* homologs.

Table 2.2 Biological functions of a subset of transcripts associated with differential abundance in *B. divergens* parasites upon culture adaptation.

Transcript ID (PiropasmaDB)	Annotation	logFC ^a
Transcription associated		
BBOV_III000190	ATP-dependent RNA helicase	-4.375312774
BBOV_IV001200	ATP-dependent RNA helicase	-2.174634998
BBOV_I000180	CCAAT-binding factor	-1.834245335
BBOV_III004170	Exosomal 3'-5' exoribonuclease complex	1.712442768
BBOV_II002690	Global transcriptional regulator	-2.346777377
BBOV_II005600	mRNA splicing factor	1.590307877
BBOV_IV006920	mRNA splicing factor	2.007870414
BBOV_I002600	RNA polymerase II	2.338999862
BBOV_III000960	RNA polymerase III	-2.020414056
BBOV_III011610	RNA pseudouridylate synthases	2.116373472
BBOV_I004230	Small nuclear ribonucleoprotein (snRNP)	1.121027401
BBOV_III008510	Spliceosomal protein FBP21	-2.346219667
BBOV_IV004470	U4/U6-associated splicing factor PRP4	-1.58664859
BBOV_III005690	Uncharacterized mRNA-associated protein	2.25214499
Translation associated		
BBOV_III000980	60S ribosomal protein L7	1.059907286
BBOV_IV001690	Aspartyl-tRNA synthetase	1.466182198
BBOV_IV006160	Mitochondrial polypeptide chain release factor	-2.421480872
BBOV_IV007450	Mitochondrial/chloroplast ribosomal protein L2	2.098909746
Protein turnover		
BBOV_II002330	20S proteasome, regulatory subunit	1.58165857
BBOV_IV004490	Chaperone-dependent E3 ubiquitin protein ligase	1.097695749
BBOV_II005540	Cysteine protease required for autophagy	-1.679993311
BBOV_III000400	Para-hydroxybenzoate-polyprenyl transferase	1.301434275
BBOV_II007270	Predicted small molecule transporter	1.030631755
BBOV_IV006860	SCF ubiquitin ligase	-4.352294731
BBOV_IV004330	Serine protease	-1.680191261
BBOV_III009930	Ubiquinol cytochrome c reductase	-1.800386366
BBOV_IV001730	Ubiquitin carboxyl-terminal hydrolase	-2.434145021
Cellular process		
BBOV_II004950	Adenylosuccinate synthase	-2.103832513
BBOV_II005700	Ca ²⁺ transporting ATPase	-2.00987223
BBOV_IV008310	Ethanolamine kinase	-2.348186354
BBOV_IV005830	F ₀ F ₁ -type ATP synthase	2.061846648
BBOV_IV010920	GTPase Ran/TC4/GSP1	0.966482698
BBOV_III008970	Membrane coat complex retromer	-3.015783812
BBOV_IV005570	Metallopeptidase	-2.564704469
BBOV_IV003180	Predicted transporter	1.338554072
BBOV_IV000850	Protein containing U1-type Zn-finger	2.078642004

BBOV_I001560	Protein kinase	-1.208185035
BBOV_I001930	Putative arsenite-translocating ATPase	-1.744110089
BBOV_III007370	Serine/threonine protein kinase	-2.604703317
BBOV_III006690	Vesicle coat complex AP-1/AP-2/AP-4	-2.228269371
BBOV_I001880	Vesicle coat complex AP-2	-1.607418322
BBOV_II002960	Vesicle coat complex COPI	-1.541188504
BBOV_IV000740	Vesicle coat complex COPII	1.202748703
Metabolic process		
BBOV_IV000490	Acyl-CoA-binding protein	-2.367008881
BBOV_II006920	Citrate synthase	-2.554668131
BBOV_IV007190	Dihydropyrimidine dehydrogenase	2.002751088
BBOV_III009670	Dihydroorotase	-2.140622832
BBOV_IV001010	Fe-S oxidoreductase	1.445685397
BBOV_IV007210	Succinate dehydrogenase	2.924498163
Stress defense		
BBOV_II006560	Molecular chaperone (DnaJ superfamily)	2.040609594

^a Average fold change

Further temporal evaluation of the *B. divergens* transcriptional landscape during its IDC indicated correlation across the transcriptional landscape (Figure 2.6). However, clear transcriptional activation to a permissive state was observed as the parasites progressed in their life cycle, particularly evident for parasites in culture for at least 9 hours (e.g. in C4, 45% of the transcripts showed increased abundance; this increased to 60% at C9) (Figure 2.6 A). However, after 16 hours in cultivation, the transcriptome seems more unbiased and show a more equal distribution of abundances in transcripts with an inclination towards transcriptional repression. This may be correlated to a slight increase in the paired piriform population in the morphological profiles observed between parasites in culture for 9 or 16 hours. Further comparison of the transcriptomes of the parasite populations indicated the presence of differential expression patterns across the 4-16 hour evaluations. To distinguish only processes associated with IDC progression and minimize adaptation responses as a result of culture initiation (time 0-4 h), transcriptional profiles were evaluated between parasites in culture for 4, 9 and 16 hours, respectively (Figure 2.6 B). Functional annotation of transcripts associated with the alternative

expression patterns identified several transcripts associated with normal biological, cellular and functional pathways throughout the investigated period. This included 11 major functional categories (catalytic activity 16%; energy production and conversion 5%; lipid transport metabolism and synthesis 2%; membrane protein components 6%; mitochondrial components 3%; proteolysis 13%; ribosomal components 17%; transcription and translation 25%; transport 6%, and variant surface antigen expression 9%), which were present across all clusters and time points. However, certain biological processes proved more variable over the temporal evaluation, particularly protein turnover, transcription and translation with increased levels of activity at 9 hours in culture. Comparatively, energy production is, as expected, maintained throughout the temporal evaluation.

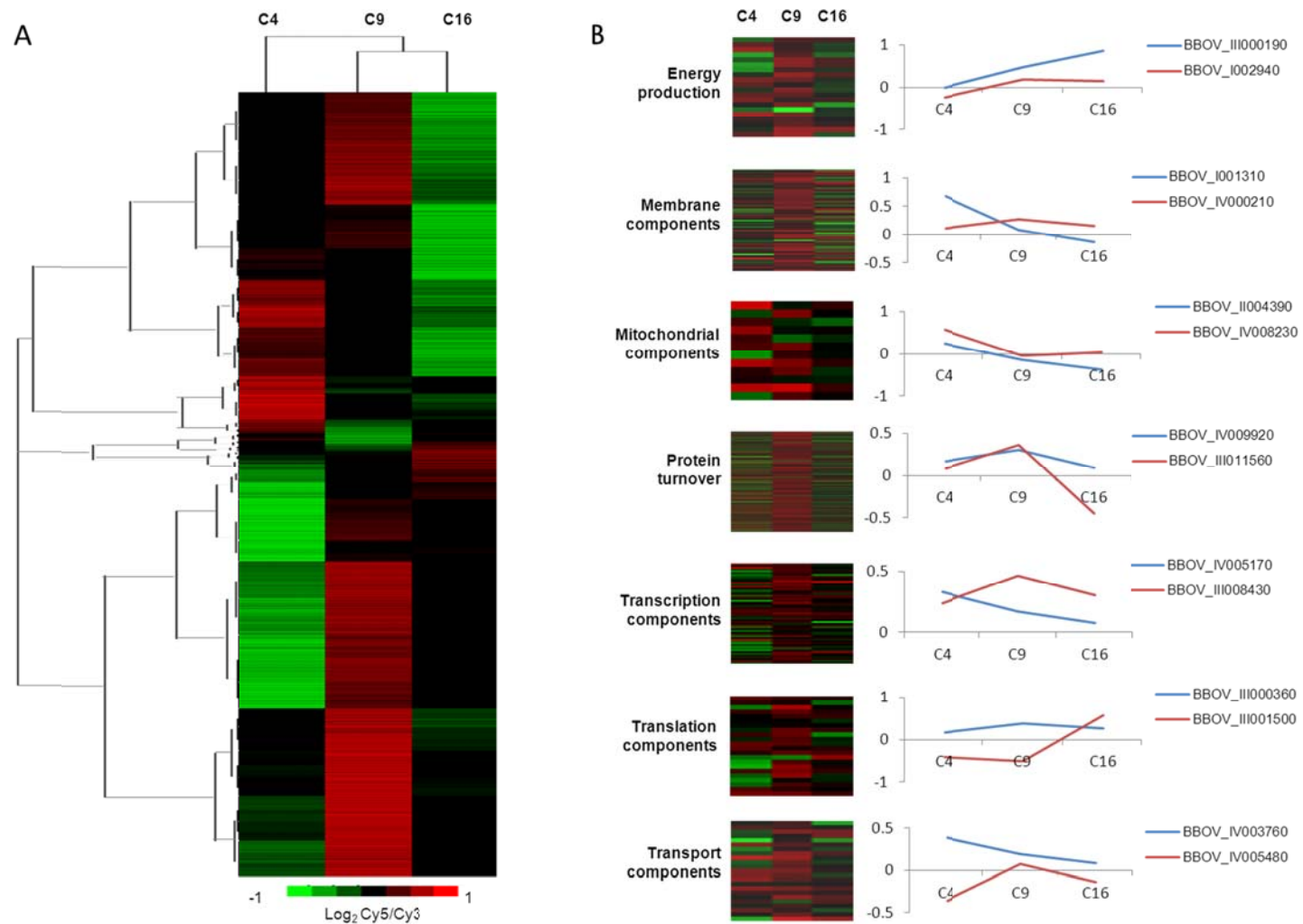


Figure 2.6 Biological processes involved in *B. divergens* parasites' intra-erythrocytic development.

Transcripts from adapted cultures at 4, 9 and 16 hours were analysed based on their *M*-values ($\log_2 \text{Cy5/Cy3}$) and visually inspected to identify an alternative parasitic expression pattern (A). Transcripts were clustered based on their shared expression profiles in the 4-hour culture (C4). Functional classification was performed based on GO-cellular compartment, molecular function and biological process domains (B).

Discussion

Our current understanding of the intra-erythrocytic developmental cycle of *B. divergens* has been clouded by imprecise and conflicting classifications, mostly due to historical analyses relying for the most part only on morphological microscopic observations. For instance, discrepancies in morphological evaluation of different life cycle forms are reported, where trophozoites are sometimes referred to as merozoites (Mackenstedt *et al.*, 1990). Additionally, one of the major challenges with studying the stage-specific development of *B. divergens* intra-erythrocytic development is the inability to synchronize these parasites *in vitro* to a single stage. A well-developed synchronization strategy induced by either sorbitol or mannitol is widely applied in *P. falciparum* research and is mainly associated with changes in membrane permeability and buoyant density of erythrocytes parasitized by this organism (Lambros and Vanderberg, 1979). However, these techniques were evaluated and found to be ineffective against *B. divergens in vitro*, resulting in parasite death within 24 hours (results not shown).

The data obtained by combining advanced cell biological and molecular strategies allow for the first time objective and clear evaluation of the chronology and stage-specificity of intra-erythrocytic development of *B. divergens* parasites. These are sensitive and quantitative and allow various developmental stages to be distinguished. Flow cytometry, light and fluorescent microscopy allowed for the accurate detection of intra-erythrocytic *B. divergens* parasites as well as determination of dynamic proliferation, developmental stage assessment and isolation of asynchronous *B. divergens* parasites, based on morphology as well as nuclear content.

Asynchronous, independent nuclear division occurs during intra-erythrocytic *P. falciparum* development, where daughter merozoites follow a non-geometric expansion and parasitic multiplication consequently deviates from what is expected from equal numbers of binary divisions (Arnot *et al.*, 2011). Similar findings were observed with light microscopy and flow

cytometry for the asynchronous *in vitro* *B. divergens* cultures in this study and enabled the isolation of specific developmental stages over a 16-hour period. The increase in MFI values observed between the three infected populations corresponds to the fluorescent microscopy images, which ultimately indicate an increase in DNA nuclear content from one developmental stage to the next. Based on the DNA measurements, which underlie the morphological findings of the present study, asynchronous *in vitro* *Babesia* dynamics was further evaluated. With primary parasitology classifications in mind, intra-cellular and actively metabolizing parasites are usually classified as trophozoites, which divide asexually (merogony) with the resultant formation of daughter merozoites. Erythrocytes infected with a ring formation, contain a single parasitic nucleus (1N) and erythrocytes infected with either paired piriforms, tetrads or multiple infected erythrocytes, contain two or more nuclei (2N or >2N). These findings correlate nuclear content to a particular isolated cell population (based on morphology); previously unclear for *Babesia* parasites.

Here we define intra-erythrocytic *B. divergens* parasites directly after invasion as mono-nucleated rings (1N nuclear content), which then rapidly progress to metabolically active but still mono-nucleated, haploid trophozoite populations. These forms are only morphologically distinguishable based on anaplasmody in rings compared to the more rounded / ovoid trophozoites and not on differences in nuclear content; further specific classification would require metabolic flux data. With the associated nuclear content information provided in this paper, we were able to indicate the subsequent progression of mono-nucleated ring / trophozoites to bi-nucleated paired piriforms (2N nuclear content) during binary fission in which a single parasite undergoes a single nuclear division event resulting in two daughter merozoites. During this nuclear division event, the nucleus becomes typically V-shaped (as observed with fluorescent microscopy). The formation and origin of multi-nucleated tetrads is less clear. These parasites have undergone two nuclear division cycles and would typically result in the formation

of four daughter merozoites. Binary fission dictates the duplication of nuclear content in a cell, followed by DNA segregation and finally cytokinesis. The formation of tetrads would therefore imply either that (a) a duplicate binary fission event occurred simultaneously from a single ring, visible as the characteristic cross morphology prior to cytokinesis or (b) that a minor proportion of paired piriforms would not undergo cytokinesis after DNA replication but rather undergo a second round of DNA replication, resulting in the tetrad formations with a 4N nuclear content prior to cytokinesis and ultimately to the formation of 4 daughter merozoites. High-resolution real-time microscopy evaluation is needed to address these possibilities. Since tetrad forms are infrequently observed in culture compared to the other morphological forms, tetrad formation is either relatively rare (only 10-25% of the total parasite population) or occurs rapidly (with quick kinetics of cytokinesis) such that these forms are rarely observed. With an optimal multiplication index of 2-3, it does not make a major contribution to *B. divergens* parasite proliferation *in vitro*. All merozoites of *B. divergens* parasites are typically piriform and joined by their pointed ends and also do not fill the complete erythrocyte, as expected of “small babesiae”. The kinetics of invasion (and re-invasion) after initial contact between the parasite and the erythrocyte, proceeds rapidly, between 45 seconds and 10 minutes (Sun *et al.*, 2011).

We therefore hypothesize a parasitic propagation diagram based on the morphological observations, DNA measurements, temporal distribution and transcriptome expression dynamics (Figure 2.7). If an increase in parasitaemia and associated increased ring populations is taken as indicators of new infections, then the significant increase in newly infected erythrocytes (ring formations) observed here during the first 4-6 hours in culture provides indications of the kinetics of the *B. divergens in vitro* IDC merogony. This is markedly quicker than previous reports where the *in vitro* life cycle of *B. divergens* parasites was claimed to last around 8 hours under the culture conditions used in that study (Valentin *et al.*, 1991). However,

the 2 hourly evaluation performed in our study enabled a finer analysis of the IDC progression kinetics that was not probed previously.

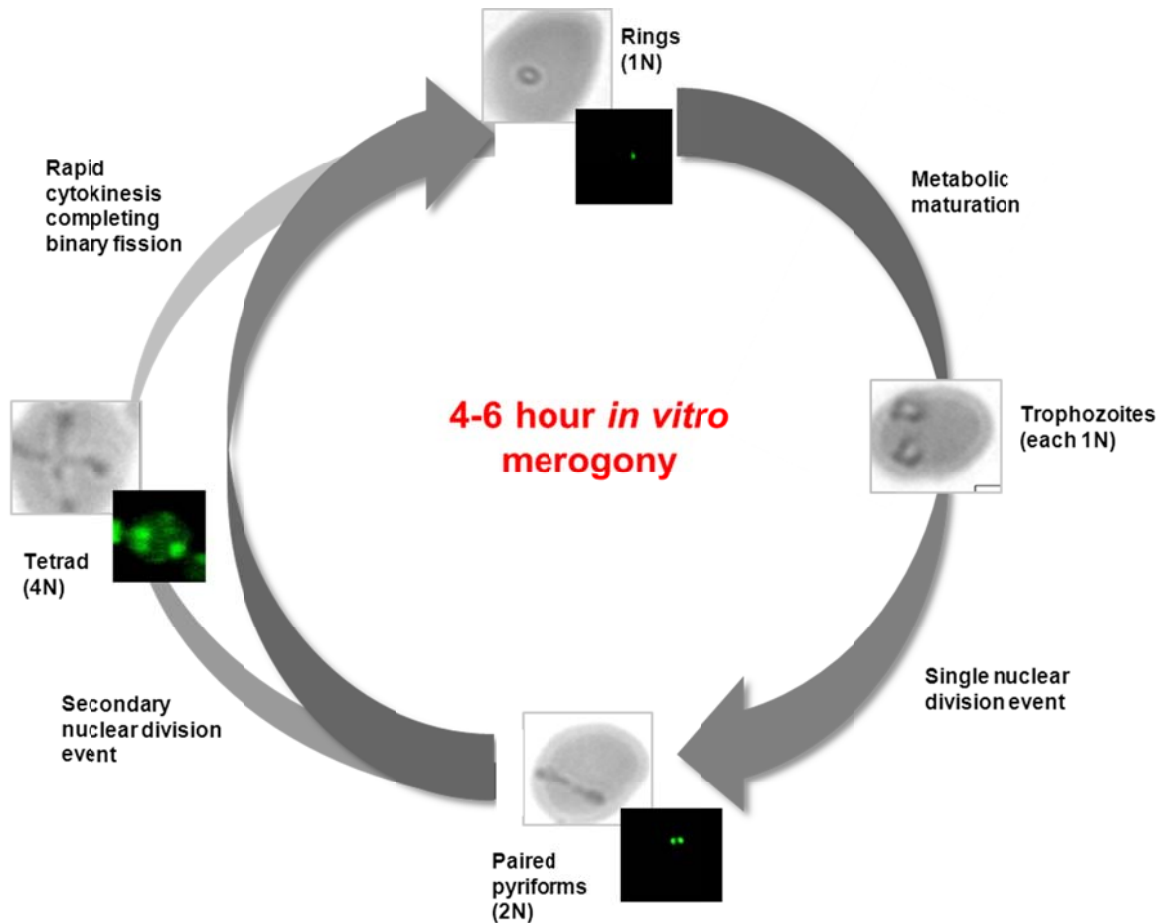


Figure 2.7 Model of the intra-erythrocytic developmental cycle of *B. divergens* parasites.

Merozoites rapidly infect uninfected erythrocytes and develop into anaplasmod ring stage parasites containing a haploid genome (single nuclei content, 1N). Following metabolic maturation in the feeding trophozoite parasites, DNA replication occurs through a single fission event resulting in bi-nucleated (2N) paired pyriforms prior to cytokinesis. A minor proportion will undergo a second fission event resulting in multi-nucleated tetrad forms (4N). Cytosol separation and membrane formation completes the cytokinesis and results in the production of 2-4 daughter merozoites, completing the merogony. In *in vitro* *B. divergens* cultures, the process is completed within 4 hours, resulting in significant increases in new ring parasite populations and concurrent increases in parasitaemia, with a multiplication index of 2-fold.

The asexual *Babesia* parasitic life cycle has only been described within the erythrocytes of their vertebrate hosts and the salivary glands of the tick vector, with limited data currently available concerning the *Babesia* sexual life cycle (Becker *et al.*, 2013). Only two studies have, however, reported on the visualization of intra-erythrocytic gametocytes in *B. divergens* (Mackenstedt *et al.*, 1990, Rudzinska *et al.*, 1976). Our temporal evaluation of *B. divergens* revealed contrasting results to that achieved with the optimized flow cytometry strategy during the interrogation of mixed infected erythrocyte populations. The overall population distribution (associated with temporal evaluation) remained predominantly paired piriforms followed by rings, tetrads and multiple infections. Comparatively, the overall population distribution observed with flow cytometry during the interrogation of mixed infected erythrocyte populations was predominantly ring formations followed by paired piriforms, tetrads and multiple infections. The inability to accurately visualize and characterize gametocytes with light microscopy within mixed *B. divergens* cultures may have contributed these contrasting results. However, we analyzed our transcriptional data set for genes characterizing gametocytes (*i.e.* *bdccp 1*; *bdccp 2* and *bdccp 3*) (Becker *et al.*, 2010), but these were not differentially affected in our data set. This can be interpreted as: 1) we did not observe gametocytes in *B. divergens* cultures *in vitro* (supporting our morphological descriptors characterizing merozoites) or 2) the parasites are not under undue physiological stress, which have been implicated to result in increased gametocytogenesis. The transcriptional response that we do observe therefore mimics typical parasite physiology. Flow cytometry measurements may therefore include ring forms as well as gametocytes, thereby increasing the DNA content. Morphological findings suggest that a trend in parasitic development from one stage to the next can be observed and that all stages reach a plateau in their developmental process.

Transcriptome analyses of the initiate culture revealed an expression pattern for *B. divergens* parasites. The draft *B. divergens* genome (recently deciphered) in combination with the

information presented here, can facilitate future *Babesia* related studies and improve our understanding of the parasites biology, host-parasite interaction as well as improve control and treatment strategies (Cuesta *et al.*, 2014, Jackson *et al.*, 2014). Additionally, the information presented here represents a preliminary catalog for *B. divergens* gene expression during its IDC, measured over time. The differential transcript abundance analysis identified several activated and repressed transcripts associated with parasitic growth and development, which may have contributed to changes in parasite population distributions. The transcriptional analysis was subsequently linked to the morphological findings. The initial stress response (between 0-4 hours) potentially induced by the addition of complete culture media, may have influenced the expression pattern. To minimize the possible stress response effects, an alternative expression pattern was suggested for the hierarchical clustered data set, which ranged between 4-16 hours. Functional annotation of the visualized transcripts and transcriptional response revealed predominantly activated and repressed components associated with transcription, translation, protein turnover, cellular and metabolic response as well as stress defence mechanisms, confirming the observed change in parasite population distributions (increases in ring and paired piriforms). The transcriptome mirrors the *Babesia* genome with glycolysis and components of the TCA cycle, glycerolipid and glycerophospholipid metabolism, pyrimidine and associated nucleotide synthesis, amino acid synthesis and certain components associated to apicoplast metabolism (Brayton *et al.*, 2007). Moreover, almost a tenth of the differential transcriptome is associated with expression of transcripts in the *ves1* family (expressing VESA1). Similar to the malaria parasite, *Babesia* species use antigenic variation to escape detection by the host's immune system (Jackson *et al.*, 2014). The hierarchical clustering employed here indicated that some of these biological processes do however show differential expression (e.g. protein expression and transport). Overall, the transcriptionally permissive state of the *B. divergens* IDC resembles that of the IDC transcriptome of *P. falciparum* parasites (with the exception of silenced virulence genes)

(Bozdech *et al.*, 2003). In the latter, phase-ordering indicated a “just-in-time” transcriptional activation, with transcripts finely associated with highly synchronized specific stages in the IDC. Even through the data presented here for *B. divergens* implies molecular control factors involved in the IDC, fine resolution temporal analysis of this parasite will be confounded as the population is composed of mixed stages, making stage-specific analysis difficult.

More comprehensive identifications of novel compounds against veterinary *Babesia* species have only recently gained attention (Guswanto *et al.*, 2014). However, for screening platforms to identify effective anti-babesiocidal compounds, several lessons may be learnt from highly advanced screening strategies from other thoroughly investigated diseases like malaria. As such, anti-malarial screening strategies have been clearly delineated and require early decision making based on target product and target candidate profiles. Particularly for *in vitro* hit identification, the ability of novel compounds to target specific (or all) stages of malaria parasite development as well as their speed of action is used to classify these *in vitro* specific profiles, thereby enabling their further prioritization (Burrows *et al.*, 2013, Leroy *et al.*, 2014). Similar strategies are required for screening of anti-babesiocidal drugs, as evaluation of the stage-specific nature of compounds would be imperative in understanding its mode-of-action and examine new treatment and dosage strategies.

Current evaluation of growth-inhibiting effects of potential anti-babesiocidal compounds rely on either microscopic examination of Giemsa-stained smears and/or the evaluation of incorporation of isotopes into *in vitro* *Babesia* cultures (Brasseur *et al.*, 1998), with neither of these allowing stage-specific or temporal evaluation of compound action. Light microscopy is time-consuming, subjective, labor intensive and operator dependent with poor quantitative robustness. Although isotopic techniques overcome the latter, this is being replaced by cost effective, reliable and non-radioactive fluorescence-based assays. Apart from the use of such dyes in plate-reader formats (enabling high-throughput screening platforms) (Guswanto *et al.*, 2014) these assays

are usually performed without evaluation of stage-specificity. However, the possibility to combine these dyes with techniques such as flow cytometry will allow for an additional level of characterization that has proved useful to address these caveats. One such example has been the successful application to the stage and temporal evaluation of anti-malarial compounds (Grimberg *et al.*, 2008, Izumiyama *et al.*, 2009). The expansion of our biological knowledge of *B. divergens* parasites' intra-erythrocytic development through the molecular blueprint of its complete transcriptome provided in this paper should enhance future discovery of novel anti-babesiocidal drugs.

2.4 Conclusion

Human babesiosis, especially caused by the cattle derived *B. divergens* parasite, is on the increase, resulting in renewed attentiveness to this potentially life threatening emerging zoonotic disease. The molecular mechanisms underlying the pathophysiology and intra-erythrocytic development of these parasites are poorly understood. This impedes concerted efforts aimed at the discovery of novel anti-babesiocidal agents. By applying sensitive cell biological and molecular functional genomics tools, we describe the intra-erythrocytic development cycle of *B. divergens* parasites from immature, mono-nucleated ring forms to bi-nucleated paired piriforms and ultimately multi-nucleated tetrads that characterizes zoonotic *Babesia* species. This is further correlated for the first time to nuclear content increases during intra-erythrocytic development progression, providing insight into the part of the life cycle that occurs during human infection. High-content temporal evaluation elucidated the contribution of the different stages to life cycle progression. Moreover, molecular descriptors indicate that *B. divergens* parasites employ physiological adaptation to *in vitro* cultivation. Additionally, differential expression is observed as the parasite equilibrates its developmental stages during its life cycle. Together, this information provides the first temporal evaluation of the functional transcriptome

of *B. divergens* parasites; information that could be useful in identifying biological processes essential to parasite survival for future anti-babesiacidal discoveries.

In the following chapter, the information gained here will be used to evaluate the growth inhibitory potential of a promising apicoplast specific piperidinyl-benzimidazolone analogue (A51B1C1_1) as treatment against *B. divergens* parasites *in vitro* (Chapter 3).

2.5 References

- ARNOT, D. E., RONANDER, E. & BENGTSSON, D. C. 2011. The progression of the intra-erythrocytic cell cycle of *Plasmodium falciparum* and the role of the centriolar plaques in asynchronous mitotic division during schizogony. *International journal for parasitology*, 41, 71-80.
- BECKER, C. A., MALANDRIN, L., DEPOIX, D., LARCHER, T., DAVID, P. H., CHAUVIN, A., BISCHOFF, E. & BONNET, S. 2010. Identification of three CCp genes in *Babesia divergens*: novel markers for sexual stages parasites. *Mol Biochem Parasitol*, 174, 36-43.
- BECKER, C. A., MALANDRIN, L., LARCHER, T., CHAUVIN, A., BISCHOFF, E. & BONNET, S. I. 2013. Validation of BdCCp2 as a marker for *Babesia divergens* sexual stages in ticks. *Exp Parasitol*, 133, 51-6.
- BORK, S., YOKOYAMA, N., MATSUO, T., CLAVERIA, F. G., FUJISAKI, K. & IGARASHI, I. 2003. Growth inhibitory effect of triclosan on equine and bovine *Babesia* parasites. *The American journal of tropical medicine and hygiene*, 68, 334-340.
- BOZDECH, Z., LLINÁS, M., PULLIAM, B. L., WONG, E. D., ZHU, J. & DERISI, J. L. 2003. The transcriptome of the intraerythrocytic developmental cycle of *Plasmodium falciparum*. *PLoS biology*, 1, e5.
- BRASSEUR, P., LECOUBLET, S., KAPEL, N., FAVENNEC, L. & BALLEST, J. J. 1998. In Vitro Evaluation of Drug Susceptibilities of *Babesia divergens* Isolates. *Antimicrobial agents and chemotherapy*, 42, 818-820.
- BRAYTON, K. A., LAU, A. O., HERNDON, D. R., HANNICK, L., KAPPMAYER, L. S., BERENS, S. J., BIDWELL, S. L., BROWN, W. C., CRABTREE, J. & FADROSH, D. 2007. Genome sequence of *Babesia bovis* and comparative analysis of apicomplexan hemoprotezoa. *PLoS pathogens*, 3, e148.
- BURROWS, J. N., HOOFT VAN HUIJSDUIJNEN, R., MÖHRLE, J. J., OEUVRAY, C. & WELLS, T. 2013. Designing the next generation of medicines for malaria control and eradication. *Malar J*, 12, 187.
- CHAUVIN, A., MOREAU, E., BONNET, S., PLANTARD, O. & MALANDRIN, L. 2009. *Babesia* and its hosts: adaptation to long-lasting interactions as a way to achieve efficient transmission. *Veterinary research*, 40, 1-18.
- CONESA, A., GÖTZ, S., GARCÍA-GÓMEZ, J. M., TEROL, J., TALÓN, M. & ROBLES, M. 2005. Blast2GO: a universal tool for annotation, visualization and analysis in functional genomics research. *Bioinformatics*, 21, 3674-3676.
- CRANMER, S. L., MAGOWAN, C., LIANG, J., COPPEL, R. L. & COOKE, B. M. 1997. An alternative to serum for cultivation of *Plasmodium falciparum* in vitro. *Trans R Soc Trop Med Hyg*, 91, 363-5.
- CUESTA, I., GONZALEZ, L. M., ESTRADA, K., GRANDE, R., ZABALLOS, A., LOBO, C. A., BARRERA, J., SANCHEZ-FLORES, A. & MONTERO, E. 2014. High-Quality Draft Genome Sequence of *Babesia divergens*, the Etiological Agent of Cattle and Human Babesiosis. *Genome Announc*, 2.
- EISEN, M. B., SPELLMAN, P. T., BROWN, P. O. & BOTSTEIN, D. 1998. Cluster analysis and display of genome-wide expression patterns. *Proceedings of the National Academy of Sciences*, 95, 14863-14868.
- ERP, E. E., GRAVELY, S. M., SMITH, R. D., RISTIC, M., OSORNO, B. M. & CARSON, C. A. 1978. Growth of *Babesia bovis* in bovine erythrocyte cultures. *Am J Trop Med Hyg*, 27, 1061-4.
- FLORES, M. V., BERGER-EISZELE, S. M. & STEWART, T. S. 1997. Long-term cultivation of *Plasmodium falciparum* in media with commercial non-serum supplements. *Parasitol Res*, 83, 734-6.
- GORENFLOT, A., BRASSEUR, P., PRECIGOUT, E., L'HOSTIS, M., MARCHAND, A. & SCHREVEL, J. 1991. Cytological and immunological responses to *Babesia divergens* in different hosts: Ox, gerbil, man. *Parasitology research*, 77, 3-12.
- GRANDE, N., PRECIGOUT, E., ANCELIN, M., MOUBRI, K., CARCY, B., LEMESRE, J., VIAL, H. & GORENFLOT, A. 1997. Continuous in vitro culture of *Babesia divergens* in a serum-free medium. *Parasitology*, 115, 81-89.

- GRAY, J., ZINTL, A., HILDEBRANDT, A., HUNFELD, K.-P. & WEISS, L. 2010. Zoonotic babesiosis: overview of the disease and novel aspects of pathogen identity. *Ticks and tick-borne diseases*, 1, 3-10.
- GRIMBERG, B. T., ERICKSON, J. J., SRAMKOSKI, R. M., JACOBBERGER, J. W. & ZIMMERMAN, P. A. 2008. Monitoring Plasmodium falciparum growth and development by UV flow cytometry using an optimized Hoechst-thiazole orange staining strategy. *Cytometry Part A*, 73, 546-554.
- GUO, Y., RIBEIRO, J. M., ANDERSON, J. M. & BOUR, S. 2009. dCAS: a desktop application for cDNA sequence annotation. *Bioinformatics*, 25, 1195-1196.
- GUSWANTO, A., SIVAKUMAR, T., RIZK, M. A., ELSAYED, S. A. E., YOUSSEF, M. A., ELSAID, E. E. S., YOKOYAMA, N. & IGARASHI, I. 2014. Evaluation of a fluorescence-based method for antibabesial drug screening. *Antimicrobial agents and chemotherapy*, 58, 4713-4717.
- HOLLINGDALE, M. R. 1992. Is culture of the entire plasmodium cycle, in vitro, now a reality? *Parasitol Today*, 8, 223.
- HOLMAN, P. J., CHIEVES, L., FRERICHS, W. M., OLSON, D. & WAGNER, G. G. 1994. Babesia equi erythrocytic stage continuously cultured in an enriched medium. *J Parasitol*, 80, 232-6.
- HOLMAN, P. J., WALDRUP, K. A. & WAGNER, G. G. 1988. In vitro cultivation of a Babesia isolated from a white-tailed deer (Odocoileus virginianus). *J Parasitol*, 74, 111-5.
- HUNFELD, K.-P., HILDEBRANDT, A. & GRAY, J. 2008. Babesiosis: recent insights into an ancient disease. *International Journal for Parasitology*, 38, 1219-1237.
- IGARASHI, S., MINEGISHI, T., NAKAMURA, K., NAKAMURA, M., TANO, M., MIYAMOTO, K. & IBUKI, Y. 1994. Functional expression of recombinant human luteinizing hormone/human chorionadotropin receptor. *Biochem Biophys Res Commun*, 201, 248-56.
- IZUMIYAMA, S., OMURA, M., TAKASAKI, T., OHMAE, H. & ASAHI, H. 2009. Plasmodium falciparum: Development and validation of a measure of intraerythrocytic growth using SYBR Green I in a flow cytometer. *Experimental parasitology*, 121, 144-150.
- JACKSON, A. P., OTTO, T. D., DARBY, A., RAMAPRASAD, A., XIA, D., ECHAIDE, I. E., FARBER, M., GAHLOT, S., GAMBLE, J., GUPTA, D., GUPTA, Y., JACKSON, L., MALANDRIN, L., MALAS, T. B., MOUSSA, E., NAIR, M., REID, A. J., SANDERS, M., SHARMA, J., TRACEY, A., QUAIL, M. A., WEIR, W., WASTLING, J. M., HALL, N., WILLADSEN, P., LINGELBACH, K., SHIELS, B., TAIT, A., BERRIMAN, M., ALLRED, D. R. & PAIN, A. 2014. The evolutionary dynamics of variant antigen genes in Babesia reveal a history of genomic innovation underlying host-parasite interaction. *Nucleic Acids Res*, 42, 7113-31.
- LAMBROS, C. & VANDERBERG, J. P. 1979. Synchronization of Plasmodium falciparum erythrocytic stages in culture. *The Journal of parasitology*, 418-420.
- LAU, A. O. 2009. An overview of the Babesia, Plasmodium and Theileria genomes: A comparative perspective. *Molecular and biochemical parasitology*, 164, 1-8.
- LEROY, D., CAMPO, B., DING, X. C., BURROWS, J. N. & CHERBUIN, S. 2014. Defining the biology component of the drug discovery strategy for malaria eradication. *Trends in parasitology*, 30, 478-490.
- LEVY, M. G. & RISTIC, M. 1980. Babesia bovis: continuous cultivation in a microaerophilous stationary phase culture. *Science*, 207, 1218-20.
- LINGNAU, A., MARGOS, G., MAIER, W. A. & SEITZ, H. M. 1993. Serum-free cultivation of Plasmodium falciparum gametocytes in vitro. *Parasitol Res*, 79, 378-84.
- MACKENSTEDT, U., GAUER, M., MEHLHORN, H., SCHEIN, E. & HAUSCHILD, S. 1990. Sexual cycle of Babesia divergens confirmed by DNA measurements. *Parasitology research*, 76, 199-206.
- MULLER, J. & HEMPHILL, A. 2013. In vitro culture systems for the study of apicomplexan parasites in farm animals. *Int J Parasitol*, 43, 115-24.
- PUDNEY, M. & GRAY, J. S. 1997. Therapeutic efficacy of atovaquone against the bovine intraerythrocytic parasite, Babesia divergens. *J Parasitol*, 83, 307-10.

- RUDZINSKA, M. A., TRAGER, W., LEWENGRUB, S. J. & GUBERT, E. 1976. An electron microscopic study of *Babesia microti* invading erythrocytes. *Cell and tissue research*, 169, 323-334.
- SCHUSTER, F. L. 2002a. Cultivation of *Babesia* and *Babesia*-like blood parasites: agents of an emerging zoonotic disease. *Clin Microbiol Rev*, 15, 365-73.
- SCHUSTER, F. L. 2002b. Cultivation of *Babesia* and *Babesia*-like blood parasites: agents of an emerging zoonotic disease. *Clinical microbiology reviews*, 15, 365-373.
- SHIKANO, S., NAKADA, K., HASHIGUCHI, R., SHIMADA, T. & ONO, K. 1995. A short term in vitro cultivation of *Babesia rodhaini* and *Babesia microti*. *J Vet Med Sci*, 57, 955-7.
- SUAREZ, C. E., NORIMINE, J., LACY, P. & MCELWAIN, T. F. 2006. Characterization and gene expression of *Babesia bovis* elongation factor-1 α . *International journal for parasitology*, 36, 965-973.
- SUN, Y., MOREAU, E., CHAUVIN, A. & MALANDRIN, L. 2011. The invasion process of bovine erythrocyte by *Babesia divergens*: knowledge from an in vitro assay. *Vet Res*, 42, 62.
- THOMFORD, J. W., CONRAD, P. A., TELFORD, S. R., 3RD, MATHIESEN, D., BOWMAN, B. H., SPIELMAN, A., EBERHARD, M. L., HERWALDT, B. L., QUICK, R. E. & PERSING, D. H. 1994. Cultivation and phylogenetic characterization of a newly recognized human pathogenic protozoan. *J Infect Dis*, 169, 1050-6.
- TRAGER, W. 1994. Digestion and indigestion in malaria parasites. *J Clin Invest*, 93, 1353.
- TRAGER, W. & JENSEN, J. B. 1976. Human malaria parasites in continuous culture. *Science*, 193, 673-675.
- VALENTIN, A., RIGOMIER, D., PRÉCIGOUT, É., CARCY, B., GORENFLOT, A. & SCHRÉVEL, J. 1991. Lipid trafficking between high density lipoproteins and *Babesia divergens* infected human erythrocytes. *Biology of the Cell*, 73, 63-70.
- VAN BRUMMELEN, A. C., OLSZEWSKI, K. L., WILINSKI, D., LLINÁS, M., LOUW, A. I. & BIRKHOLTZ, L.-M. 2009. Co-inhibition of *Plasmodium falciparum* S-adenosylmethionine decarboxylase/ornithine decarboxylase reveals perturbation-specific compensatory mechanisms by transcriptome, proteome, and metabolome analyses. *Journal of Biological Chemistry*, 284, 4635-4646.
- VAYRYNEN, R. & TUOMI, J. 1982. Continuous in vitro cultivation of *Babesia divergens*. *Acta Vet Scand*, 23, 471-2.
- VERLINDEN, B. K., NIEMAND, J., SNYMAN, J., SHARMA, S. K., BEATTIE, R. J., WOSTER, P. M. & BIRKHOLTZ, L.-M. 2011. Discovery of novel alkylated (bis) urea and (bis) thiourea polyamine analogues with potent antimalarial activities. *Journal of medicinal chemistry*, 54, 6624-6633.
- ZINTL, A., MULCAHY, G., SKERRETT, H. E., TAYLOR, S. M. & GRAY, J. S. 2003. *Babesia divergens*, a bovine blood parasite of veterinary and zoonotic importance. *Clinical microbiology reviews*, 16, 622-636.
- ZWEYGARTH, E. & LOPEZ-REBOLLAR, L. M. 2000. Continuous in vitro cultivation of *Babesia gibsoni*. *Parasitol Res*, 86, 905-7.
- ZWEYGARTH, E., VAN NIEKERK, C. J. & DE WAAL, D. T. 1999. Continuous in vitro cultivation of *Babesia caballi* in serum-free medium. *Parasitol Res*, 85, 413-6.

Chapter 3

Morphological assessment and *in vitro* evaluation of the growth inhibitory effect of a Piperidinyl-Benzimidazolone analogue (A51B1C1_1) against *Babesia divergens*

3.1 Introduction

The search for new, effective, fast-acting drug compounds, drug combinations as well as chemotherapeutic targets is an on-going process. Moreover, such compounds should have low toxicity and high specificity characteristics to be useful toward decreasing morbidity and mortality levels associated with *Babesia* infection. Several compounds have successfully been identified and used as anti-babesiocidal therapeutics, others have, however, been characterized as ineffective and toxic with severe side-effects (Becker, 2011). The emergence of resistance of *Babesia* species against current treatment strategies is steadily increasing, emphasizing the need to develop new therapeutics and/or improve existing treatment strategies (Vyas *et al.*, 2007, Wormser *et al.*, 2010).

Two well-established, reliable and economically viable models have been established to investigate drug efficacy against the causative agents of animal and human babesiosis (i) *in vitro* cultivation systems with associated observations of decreased parasitaemias and (ii) *in vivo* mouse model proving efficacy regarding increased survival rates and decreased parasite load. The *in vitro* culture system represents an important first step for the potential application of anti-babesiocidal compounds to be tested *in vivo*. Most of the current treatment strategies applied against animal and human babesiosis were developed prior to the genomics era and

were based on *in vitro* cultivation systems, including the MASP system; Giemsa staining and light microscopy as well as the incorporation of radioactive precursors (Mosqueda *et al.*, 2012, Brasseur *et al.*, 1998). Based on the advancement of *Babesia in vitro* cultivation systems, approaches have subsequently been applied to evaluate and visually quantify asynchronous *Babesia* cultures in response to drug pressure. Given that light microscopy is time-consuming, subjective, labor intensive and inter-operator dependent, an alternative fluorescence based strategy, based on the malaria SYBR-Green I- fluorescence based assay (MSF) (Smilkstein *et al.*, 2004, Bennett *et al.*, 2004) was recently developed to screen anti-babesiocidal compounds *in vitro* against *B. bovis* (Guswanto *et al.*, 2014).

Based on these treatment strategies and the particular screening methods applied, compounds with anti-babesiocidal activities have been identified with varying degrees of efficacy against several *Babesia* species, offering alternative treatment options (Table 3.1). These compounds were designed to directly target parasitic enzymes and/or pathways; disrupt parasitic invasion of host erythrocytes or intervene with parasitic metabolism (Becker, 2011). As an example, triclosan, fosmidomycin and terpene-nerolidol compounds, targeted apicoplast specific pathways (fatty-acid biosynthesis and isoprenoid biosynthesis). Simvastatin and lovastatin inhibited 3-hydroxy-3-methylglutaryl coenzyme A reductase, associated with the isoprenoid pathway in *B. divergens* parasites. The novel diamidines and novel bizthiazolium drug T16, interfered with *B. divergens* transcription and the phosphatidylcholine pathway, respectively (Table 3.1).

Table 3.1 *In vitro* cultivation systems, screening methods and drug compounds, previously tested against human and animal *Babesia* species.

Species	Cultivation technique	Growth-inhibitory assay	Drug compounds	Reference
<i>In vitro</i> drug screening methods for compounds directed against human <i>Babesia</i> species				
<i>B. divergens</i>	<i>In vitro</i> cultivation system	Incorporation of radioactive precursor	Novel diamidines	(Nehrbass-Stuedli <i>et al.</i> , 2011)
			Novel Bizthiazolium drug T16	(Richier <i>et al.</i> , 2006)
			Lovastatin, Simvastatin	(Grellier <i>et al.</i> , 1994)
			Mefloquin, Quinine, Chloroquine, Clindamycin, Pentamidine, Imidocarb	(Brasseur <i>et al.</i> , 1998)
			Atovaquone	(Pudney and Gray, 1997)
<i>In vitro</i> drug screening methods for compounds directed against animal <i>Babesia</i> species				
<i>B. bovis</i>	Micro-aerophilus stationary phase (MASP) system	Giemsa staining and light microscopy	Fosmidomycin	(Sivakumar <i>et al.</i> , 2008)
			Triclosan	(Bork <i>et al.</i> , 2003)
			Cytochalasin B, β -glucogallin	(Derbyshire <i>et al.</i> , 2008)
			(-)Epigallocatechin-3-gallate	(Aboulaila <i>et al.</i> , 2010c)
			Terpene-nerolidol	(AbouLaila <i>et al.</i> , 2010b)
			DFMO, MFMO	(Jasmer and Goff, 1989)
			Heparin	(Bork <i>et al.</i> , 2004)
			Staurosporine	(Bork <i>et al.</i> , 2006)
			Epoxomycin	(Aboulaila <i>et al.</i> , 2010a)
			Apicidin	(Aboulaila <i>et al.</i> , 2009)
			Pepstatin A, Mefloquin	(Munkhjargal <i>et al.</i> , 2012)
			Farsenyl pyrophosphate	(Ueno <i>et al.</i> , 2013)
			Fusidic acid	(Salama <i>et al.</i> , 2013)
			Ciprofloxacin, Thiostrepton, Rifampin, Clindamycin	(Aboulaila <i>et al.</i> , 2012)
			<i>B. bigemina</i>	Micro-aerophilus stationary phase (MASP) system
(-)Epigallocatechin-3-gallate	(Aboulaila <i>et al.</i> , 2010c)			
Terpene-nerolidol	(AbouLaila <i>et al.</i> , 2010b)			
Heparin	(Bork <i>et al.</i> , 2004)			
Apicidin	(Aboulaila <i>et al.</i> , 2009)			
Pepstatin A, Mefloquin	(Munkhjargal <i>et al.</i> , 2012)			
Fusidic acid	(Salama <i>et al.</i> , 2013)			
Ciprofloxacin, Thiostrepton, Rifampin, Clindamycin	(Aboulaila <i>et al.</i> , 2012)			
<i>B. caballi</i>	Micro-aerophilus stationary phase (MASP) system	Giemsa staining and light microscopy	Artesunate, pyrimethamine,	(Nagai <i>et al.</i> , 2003)
			Terpene-nerolidol	(AbouLaila <i>et al.</i> , 2010b)
			Heparin	(Bork <i>et al.</i> , 2004)
			Epoxomycin	(Aboulaila <i>et al.</i> , 2010a)

			Pepstatin A, Mefloquin	(Munkhjargal <i>et al.</i> , 2012)
			Fusidic acid	(Salama <i>et al.</i> , 2013)
			Ciprofloxacin, Thiostrepton, Rifampin, Clindamycin	(Aboulaila <i>et al.</i> , 2012)
<i>B. equi</i>	Micro-aerophilus stationary phase (MASP) system	Giemsa staining and light microscopy	Artesunate, pyrimethamine, Pamaquin	(Nagai <i>et al.</i> , 2003)
			Heparin	(Bork <i>et al.</i> , 2004)
			Epoxomycin	(Aboulaila <i>et al.</i> , 2010a)

As discussed in Chapter 1, several studies have been conducted to identify novel chemical scaffolds as inhibitors of galactolipid metabolism in *Arabidopsis* (Botte *et al.*, 2011) and to explore piperidinyl-benzimidazolone analogues as potential inhibitors of *P. falciparum* and *T. gondii* proliferation (Saidani *et al.*, 2014). Based on the CEREP[®] diversity-based library, 20 compounds exhibited an inhibitory activity greater than 25% against these organisms. These 20 compounds, with an additional 40 compounds (of similar chemical structures) were subsequently evaluated for their inhibitory activity against MGDG-1. Two compounds galvestine-1 and galvestine-2 had a greater than 40% inhibitory activity against MGDG-1. Subsequent derivatives were designed based on the galvestine-1 scaffold. *In vitro* and *in vivo* treatment of galvestine-1, galvestine-2 and some of their derivatives revealed inhibition of *Arabidopsis* MGDG synthases, which subsequently reduced the MGDG content. The two molecules with the highest efficacies were identified as A51B1C1_1 and A21B1C1_1. Preliminary proteomic analysis, based on these analogues further identified 12 major polypeptides and several proteins of unknown function (Saidani *et al.*, 2014). *In vitro* and *in vivo* assessment of the two most active compounds (A51B1C1_1 and A21B1C1_1) against *P. falciparum* indicated low toxicities with reduced parasitaemia levels. Transcriptome analyses of these compounds were further evaluated for their anti-malarial properties against *P. falciparum*, which confirmed their success as potential anti-malarials, targeting the galactolipid and glycerophospholipid metabolisms of the parasite (Snyman, 2011). The success of this study

prompted our subsequent evaluation of compound A51B1C1_1 for its anti-babesiicidal activity against *B. divergens*.

3.2 Materials and Methods

Chapter 2 provided a brief description of the materials and methods used for the *in vitro* cultivation of intra-erythrocytic *B. divergens* parasites. This chapter is an extension thereof and provides a more comprehensive description of the materials and methods applied to *in vitro* cultivation of *B. divergens*, together with the drug sensitivity and cell viability assays in response to A51B1C1_1 treatment.

3.2.1 Drug sensitivity and cell viability assays in response to A51B1C1_1 treatment

Asynchronous *B. divergens* parasite cultures were maintained *in vitro* in human erythrocytes (type O⁺) under the same gaseous environment and shaking conditions as described in Chapter 2. Parasitic proliferation assays were adapted and performed as described by Bork (Bork *et al.*, 2003). The A51B1C1_1 compound was dissolved in dimethylsulfoxide (DMSO) to a concentration of 10 mM (final concentration of DMSO, 0.5%). The non-toxic effect of DMSO as drug solvent on parasites and host cells were based on findings observed by Bork (2003), where a final DMSO concentration of 0.5% did not influence *B. bovis* proliferation or result in any morphological changes (Bork *et al.*, 2003).

Serial dilutions of the A51B1C1_1 compound in complete culture medium (RPMI-1640 medium supplemented with 25.2 mM HEPES, 22.2 mM D-glucose, 50 mg/l hypoxanthine, 21.4 mM sodium bicarbonate, 48 mg/l gentamycin) further supplemented with 10% human serum (Gorenflot *et al.*, 1991) were plated out in technical triplicates within 96-well plates

(concentrations ranging between 37 nM and 3650 μ M) for three independent biological replicates. Infected erythrocytes (asynchronous cultures) were diluted with uninfected erythrocytes to obtain a 1% parasitaemia and 5% haematocrit. Of this solution, 100 μ l was dispensed in all 96-wells, together with 200 μ l complete culture media containing the compound serial dilutions, in triplicate. Positive controls for parasite proliferation consisted of wells devoid of the compound, while negative controls contained phosphate buffered saline (1x PBS: 137 mM NaCl, 2.7 mM KCl, 1.8 mM KH_2PO_4 , 10 mM $\text{Na}_2\text{HPO}_4 \cdot 7\text{H}_2\text{O}$, pH 7.4) only. Plates were covered and placed in a sterile gas-chamber, sealed and flushed with a hypoxic gas mixture (90% N_2 , 5% O_2 and 5% CO_2) for 5 minutes and incubated at 37°C for a four day period. During the four day incubation period, the overlaid/spent culture media was replaced daily with 200 μ l fresh complete culture media (containing the specific drug concentrations). Additionally, microscopic evaluation of parasite proliferation with light microscopy and Giemsa-stained smears, were conducted daily. The percentage parasitaemia was calculated based on the number of infected erythrocytes among 100 erythrocytes and a total of 1000 cells were counted in each instance (Bork *et al.*, 2003). The concentration at which parasite proliferation was inhibited by 50% (IC_{50}) was calculated based on parasitaemia levels recorded on day three within the *in vitro* cultivation system (Bork *et al.*, 2004) by interpolation after non-linear 4-parameter curve fitting, using SigmaPlot version 11.0.

To further examine parasitic viability and recrudescence after drug withdrawal, cell viability tests were performed as described (Bork *et al.*, 2003, Aboulaila *et al.*, 2012). Briefly, after four (cultures with an initial 1% parasitaemia, 5% haematocrit) days of A51B1C1_1 treatment, 14 μ l parasite-free human erythrocytes was added to 6 μ l of a previously treated culture in 200 μ l of fresh, complete RPMI-1640 culture medium, devoid of chemical supplementation. Plates were subsequently incubated for five days with daily culture medium replacement and light microscopy evaluation using Giemsa-stained smears, to determine parasite recrudescence and

viability. GraphPad InStat (version 6.04) statistical software was used for the statistical analysis of the *in vitro* experiments by independent Student's *t*-tests. Values were considered to be significantly different at $P < 0.05$.

3.2.2 Morphological evaluation based on light microscopy

The health of *B. divergens* and *P. falciparum* cultures as well as parasitaemia and morphology was monitored daily by means of light microscopy and Giemsa-stained smears. Asynchronous intra-erythrocytic *B. divergens* parasites untreated and treated (10-15% parasitaemia, 5% haematocrit) were examined every hour over the 16-hour investigation period using Giemsa-stained smears and microscopy to evaluate parasite morphology. The asexual developmental life stages were classified as described in Chapter 2.

3.3 Results and Discussion

3.3.1 Piperidinyl-benzimidazolone analogue (A51B1C1_1) treatment of *B. divergens* cultures

Drug sensitivity assay and cell viability evaluation using light microscopy

Sigmoidal dose-response curves were established to determine the concentration at which 50% inhibition of parasite proliferation (IC_{50}) occurred due to treatment of *in vitro* *B. divergens* cultures with the promising A51B1C1_1 compound. The IC_{50} was determined as 500 ± 4.77 nM, on the third day of incubation (72 hours) using Giemsa-stained light microscopy detection of

parasitaemia (Figure 3.1). Concentrations ranging between 3650 μM and 222.5 nM suppressed parasite propagation.

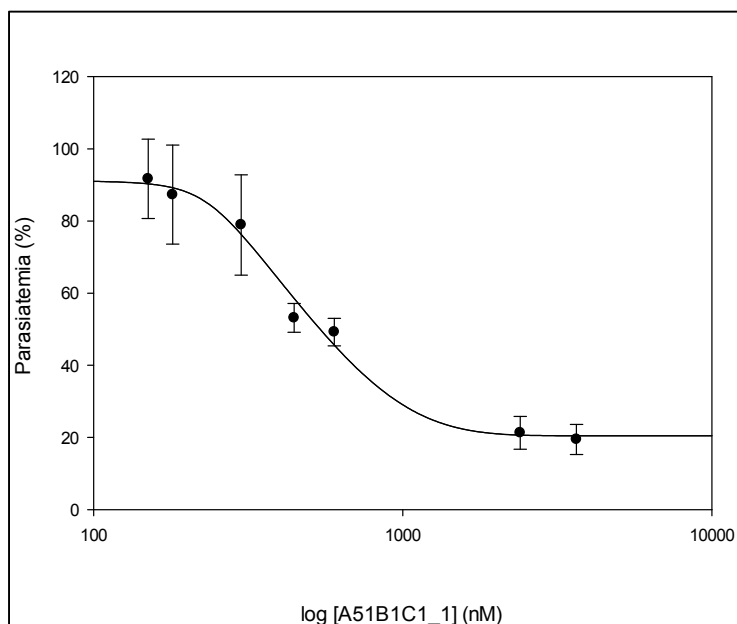


Figure 3.1 Sigmoidal dose-response curve established to calculate the IC_{50} of A51B1C1_1 on *B. divergens* cultures *in vitro*.

Parasitaemia was determined with Giemsa-stained smears and microscopy. The IC_{50} value was determined after three days of drug pressure using a non-linear 4-parameter curve fitting strategy. Statistical data analysis was performed with GraphPad InStat (version 6.04). Data is representative of 3 independent biological experiments, each performed in triplicate (\pm S.E.).

Comparison of the IC_{50} obtained for A51B1C1_1 with the parent compound galvestine-1 indicated that this scaffold had inhibitory properties against *P. falciparum*, *T. gondii* and *A. thaliana* (Table 3.2). Derivatives/analogues of the scaffold compound inhibited *P. falciparum* (A51B1C1_1 and A21B1C1_1) and *T. gondii* (A1B1C3_2 and A7B1C1_1) *in vitro* proliferation, with IC_{50} values in the 100-200 nM range (Saidani *et al.*, 2014). The inhibitory effects of these compounds therefore, had varying efficacies against these parasites, with compound A51B1C1_1 found to act more specifically against *P. falciparum* (IC_{50} 180 nM) and was found to be less potent against *T. gondii* (value not specified) (Saidani *et al.*, 2014). The dosage of the apicoplast targeting compound A51B1C1_1 that proved effective against *B. divergens* in this

study (500 ± 4.77 nM) was in a similar range to that observed for *P. falciparum* (447 ± 16 nM) (Snyman, 2011) (Table 3.2). This similar IC_{50} / dosage range confirms the potency of A51B1C1_1 as potential, anti-apicomplexan therapeutic. Additionally, the IC_{50} values observed for *B. divergens* treated with A51B1C1_1 were found to be in a similar range to other previously tested apicoplast specific compounds (fosmidomycin [$0.88 \mu\text{g/ml}$] and triclosan [$100 \mu\text{g/ml}$]) against *in vitro* cultured *B. bovis* parasites (Sivakumar *et al.*, 2008, Bork *et al.*, 2003).

Table 3.2 Inhibitory properties of the scaffold compound (galvestine-1) and an analogue compound (A51B1C1_1) on apicomplexan parasites and plant cells.

Organism / Plant cell	IC_{50} scaffold compound (Galvestine-1)	IC_{50} A51B1C1_1	References
<i>B. divergens</i> (Rouen 1987 strain)	*ND	500 ± 4.77 nM	This study
<i>P. falciparum</i> (chloroquine sensitive, 3D7 strain)	*ND	447 ± 16 nM	(Snyman, 2011)
<i>P. falciparum</i> (chloroquine sensitive, 3D7 strain)	$1.45 \mu\text{M}$	180 nM	(Saidani <i>et al.</i> , 2014)
<i>T. gondii</i> (RH and RH-B1 strains)	$4.8 \mu\text{M}$	*ND	(Saidani <i>et al.</i> , 2014)
<i>A. thaliana</i>	$10 \mu\text{M}$	*ND	(Boudiere <i>et al.</i> , 2012, Botte <i>et al.</i> , 2011)

* ND refers to non-defined value

Morphological evaluation of untreated and A51B1C1_1 treated *B. divergens* parasites

The morphological data provides essential information regarding the compound's effect on parasitic proliferation and development. Based on light microscopic observations of changes associated with the host cell shape, size and colour; treatment of intra-erythrocytic *B. divergens* parasites affected the morphology of parasites (Figure 3.2). Treatment of *P. falciparum* cultures with A51B1C1_1 at $2x IC_{50}$ (447 ± 16 nM) resulted in noticeable changes in morphology, 48 hours post invasion (hpi), with clear stress characteristics visible (pyknotic parasites) (Snyman,

2011). Comparatively, *B. divergens* samples were collected from asynchronous A51B1C1_1 treated (at $2 \times IC_{50}$ 500 ± 4.77 nM) cultures with morphological changes and visible signs of stress (pyknotic and degenerate parasites) observed at 4, 9 and 16 hours post treatment, as indicated by arrows (Figure 3.2). The morphological changes could not be ascribed to a particular life cycle stage. Comparatively, the morphology of untreated parasites appeared to be intact throughout the 16-hour period. Similar parasite morphologies have been shown between A51B1C1_1 treated *B. divergens* and *P. falciparum* cultures (Snyman, 2011).

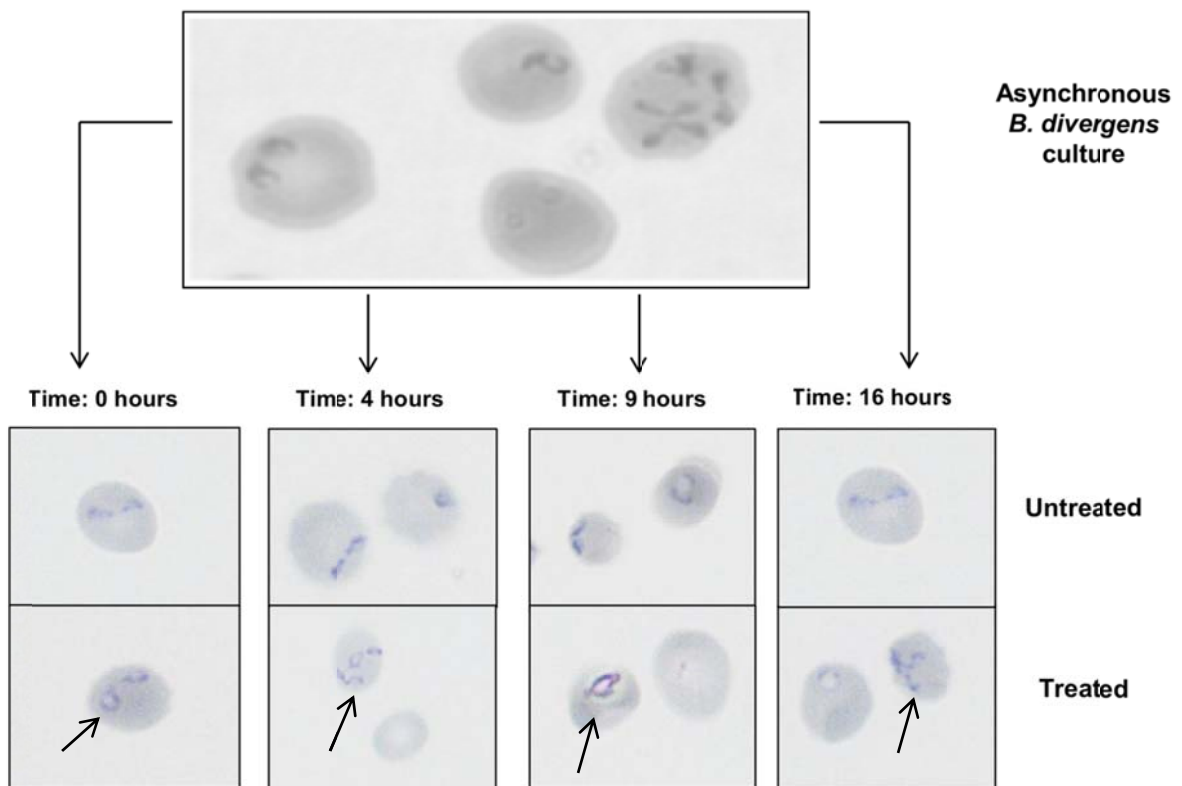


Figure 3.2 Morphological evaluation conducted over a 16-hour time period of asynchronous *B. divergens* cultures treated at $2 \times IC_{50}$ concentrations of A51B1C1_1.

Untreated cultures showed various intact parasitic formations present throughout the parasite's life cycle, with no visible signs of stress. The A51B1C1_1 treated cultures showed both intact and stressed/degenerate parasites from 4-16 hours post treatment.

Stage-specificity and life cycle progression of *B. divergens in vitro* post A51B1C1_1 treatment

The inability to synchronize *B. divergens in vitro* to a single stage complicates the stage-specific evaluation of A51B1C1_1 treated parasites. However, based on our morphological classification of the asexual developmental life stages of *B. divergens* (Chapter 2) and light microscopy analysis of treated and untreated parasites over the 16-hour period, certain conclusions with regards to stage-specificity were made. This time period was selected to link the morphological data associated with the treated cultures to the untreated cultures as described in Chapter 2.

Quantitative morphological evaluation and *in vitro* proliferation for the various developmental forms of *B. divergens* (10-15% parasitaemia, 5% haematocrit) under A51B1C1_1 treated ($2\times IC_{50}$) conditions was performed over a 16-hour period and revealed a significant increase in paired piriform formations (from 12 to 18%, $P<0.05$, $n=3$) between 9-16 hours of development (Figure 3.3 A). This increase in paired piriforms contributed to the significant increase ($P<0.05$, $n=3$) in total parasitaemia to $\pm 22\%$, as monitored in the asynchronous culture (Figure 3.3 A). No significant increase in either ring or tetrad/multiple infected formations were, however, observed throughout the investigated period (Figure 3.3 A). Compared to the untreated culture, which exhibited a significant increase ($P<0.05$, $n=3$) in ring and paired piriform formations between 0-4 hours of development and contributed to the significant increase ($P<0.05$, $n=3$) in total parasitaemia between 0-4 hours of development (Figure 3.3 B). The overall population distribution in the treated, mixed culture resembled that of the untreated culture (as described in Chapter 2), with paired piriforms predominantly contributing to the total parasitaemia followed by ring and tetrad (or multiple infections) formations and was subsequently maintained throughout the investigated period. In this study, A51B1C1_1 treated ($2\times IC_{50}$) conditions induced a parasitic response within the first two developmental life cycles, as no significant increase in total parasitaemia was observed during this time.

In contrast to our present results using *B. divergens* parasites, other studies which were carried out with compound A51B1C1_1 against the *in vitro* proliferation of *P. falciparum* had a different outcome. A51B1C1_1 treated *P. falciparum* growth rate decreased after 36-42 hpi, after which parasites continued to proliferate at this reduced rate. After 48 hpi, parasites showed clear stress characteristics and remained in this state throughout the life cycle, consequently inhibiting re-invasion of erythrocytes as well as ring formation (Snyman, 2011). In a different study, A51B1C1_1 treatment affected *P. falciparum* proliferation within the first growth cycle (*i.e.* 24 hours) (Saidani *et al.*, 2014).

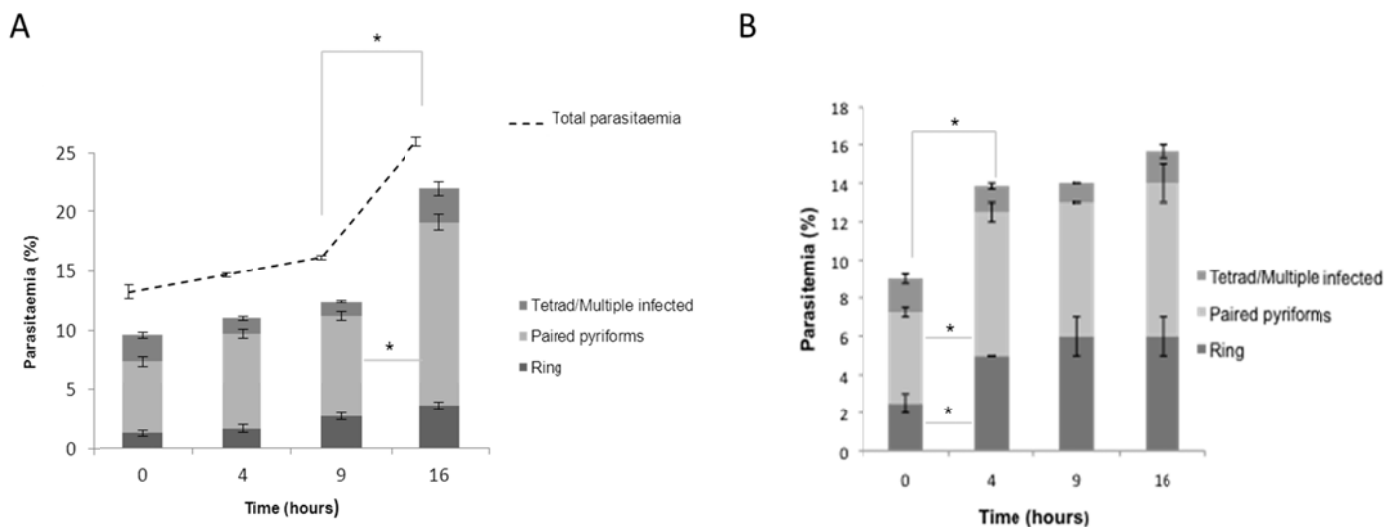


Figure 3.3 Graphical analyses of stage-specificity and life cycle progression of asynchronous *B. divergens* parasites over a 16-hour period under A51B1C1_1 treated conditions.

(A) Morphological and temporal evaluation of the life cycle stage distribution of treated ($2x IC_{50}$) parasites performed at 0, 4, 9 and 16 hours. Parasite stages were classified morphologically as rings, paired pyriforms and tetrads/multiple infected, based on light microscopy and Giemsa-stained slides. Total parasitaemia of treated cultures is indicated per time-point analyzed (dotted line graph). Results are the mean of three independent experiments, performed in triplicate (\pm S.E.). Significance is indicated at $P < 0.05$ (*) as determined with an unpaired Student-t test. (B) Morphological evaluation of untreated *B. divergens* life cycle progression from a newly initiated culture over a total of 16-hours, indicating the distribution of life cycle stages to total parasitaemia (as presented in Chapter 2).

Reversibility assay

In this study we found compound A51B1C1_1 to affect the *in vitro* asexual growth of *B. divergens* (IC₅₀ of 500 ± 4.77 nM). From the sigmoidal dose-response curve data, it appeared as though 20% of parasites are non-proliferating and remain in culture after three days of therapeutic pressure, suggesting a cytostatic drug effect (Figure 3.1). This was confirmed by the subsequent viability results whereby *B. divergens* (1% parasitaemia, 5% haematocrit) parasite recrudescence was monitored (after three days of drug treatment at 2x IC₅₀) in subcultures for 5 days in the absence of A51B1C1_1 and showed a gradual increase in parasite re-growth after compound removal (Figure 3.4). A significant difference ($P < 0.01$, $n = 3$) between treated parasites (day 1 vs. day 5) in the absence of A51B1C1_1 was also observed. The compound therefore failed to completely clear parasites from the *B. divergens* culture and damage caused by treatment was reversible and not an irreversible cytotoxic drug response. The morphology study between treated and untreated parasites revealed an abnormal morphology of treated parasites, confirming damage caused by A51B1C1_1 treatment (Figure 3.2).

Previously reported *in vitro* and *in vivo* trials based on these piperidiny-benzimidazolone analogues as potential anti-malarials refined the compounds' structures and ultimately improved their effect against membrane glycerolipids, which subsequently improved current knowledge regarding the cellular mode-of-action of one of these analogues (A51B1C1_1) against *P. falciparum* (Saidani *et al.*, 2014). In contrast to our findings, these previous analyses showed that the inhibition of *P. falciparum* by A51B1C1_1 (at IC₅₀ of 180 nM) was irreversible after a 12 hour incubation period (Saidani *et al.*, 2014). Since targets of the compound may be shared between the parasites and their human host cells, the *in vitro* selectivity index (SI) based on toxicity against K-562 human cells was previously determined for compound A51B1C1_1 against *P. falciparum*. Results revealed that the pharmacological activity of A51B1C1_1 may be ascribed to a species-specific cytotoxic response within the *Apicomplexa* phylum (Saidani *et al.*,

2014). These results were linked to the current study and suggest that *B. divergens* response to A51B1C1_1 treatment may also be species-specific, as damage caused by treatment was reversible and not an irreversible cytotoxic drug response. Compound A51B1C1_1 further limited *in vivo* proliferation of *P. falciparum* within BALB/c mice, which delayed parasite proliferation, however, no curative effect was observed. The compound additionally had no toxic effect on the mice (Saidani *et al.*, 2014). In order to improve compound A51B1C1_1 as potential anti-babesiicidal, such *in vivo* studies within BALB/c mice are needed to assess treated *B. divergens* proliferation.

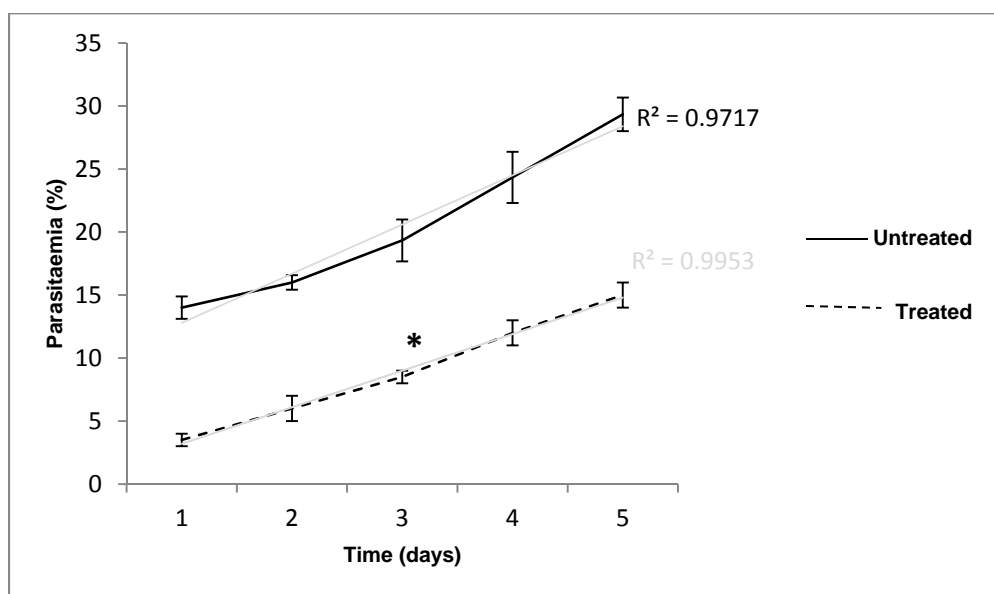


Figure 3.4 Cell viability assay to determine parasite recrudescence after treatment with compound A51B1C1_1.

Parasite recrudescence was monitored (after three days of drug treatment) at $2x$ IC_{50} concentration, with light microscopy in subcultures for 5 days in the absence of A51B1C1_1 to evaluate parasite viability. Parasite proliferation increased linearly for both untreated ($R^2=0.97$) and treated ($R^2=0.99$) *in vitro* *B. divergens* cultures. Significance between treated parasites (day 1 vs. day 5) is indicated at $P<0.01$ (*) as determined with an unpaired Student-t test. Data analysis was based on three independent experiments conducted in triplicate, subsequent to treatment for a five day period, \pm S.E.

3.4 Conclusion

Both malaria and human babesiosis have a wide host range, with immune-compromised individuals highly at risk of contracting the disease. An effective drug compound should

ultimately decrease the morbidity and mortality levels associated with infection. In this chapter we aimed to contribute and improve anti-babesiacid control strategies by evaluating a promising anti-*Plasmodium*, apicoplast specific piperidiny-benzimidazolone analogue (A51B1C1_1) as potential therapeutic against one of the causative agents of human babesiosis, *B. divergens*.

Results demonstrated the efficacy of compound A51B1C1_1 as potential anti-babesiacid, as an IC_{50} of 500 ± 4.77 nM was found to be within a similar range to that achieved for *P. falciparum*. The compound however, only suppressed *B. divergens* propagation and failed to completely clear parasites from the culture as a gradual increase in parasitic recrudescence after treatment was observed in the absence of A51B1C1_1 exposure. It therefore appeared as though the compound induced parasitic stress and subsequently had a static effect on *B. divergens* parasites *in vitro*. Additional studies on the development of *B. divergens* resistance to the compound and the evaluation of the chemotherapeutic effect of A51B1C1_1 *in vivo* are needed to formulate any further conclusions. Our results indicate that the promising anti-*Plasmodium*, apicoplast specific piperidiny-benzimidazolone analogue (A51B1C1_1) can be regarded as a promising anti-babesiacid agent with low toxicity.

Although light microscopy is widely used in *Babesia* research to determine parasitaemia, several disadvantages (including time-consuming, subjective, labor intensive and inter-operator dependent) are associated with this technique. Cost effective, reliable, non-radioactive, fluorescence-based assays have recently been established as *in vitro* methods for evaluating parasitaemia and drug efficacy in both *P. falciparum* (Smilkstein *et al.*, 2004, Bennett *et al.*, 2004) and *B. bovis* (Guswanto *et al.*, 2014). The principles of these assays relies on a nucleic acid stain (*i.e.* SYBR-Green I) and its ability to differentiate between uninfected and infected erythrocytes as well as host erythrocytes which are predominantly devoid of nuclear content, in contrast to the intra-erythrocytic parasite. The incorporation of SYBR-Green I and the

fluorescence plate reader assay should be explored in future *B. divergens* studies, to re-evaluate the inhibitory effect of compound A51B1C1_1 in order to establish a more accurate and reliable IC_{50} . This may additionally allow researchers the opportunity to evaluate alternative treatment strategies, compounds and dosages against one of the causative agents of human babesiosis in more detail.

In conclusion, differences were observed between untreated and A51B1C1_1 treated *B. divergens* parasites especially with regards to parasite proliferation and normal life cycle progression. Further investigation related to the transcriptomic response of A51B1C1_1 treated *B. divergens* parasites will be discussed in Chapter 4.

3.5 References

- ABOULAILA, M., MUNKHJARGAL, T., SIVAKUMAR, T., UENO, A., NAKANO, Y., YOKOYAMA, M., YOSHINARI, T., NAGANO, D., KATAYAMA, K., EL-BAHY, N., YOKOYAMA, N. & IGARASHI, I. 2012. Apicoplast-targeting antibacterials inhibit the growth of Babesia parasites. *Antimicrob Agents Chemother*, 56, 3196-206.
- ABOULAILA, M., NAKAMURA, K., GOVIND, Y., YOKOYAMA, N. & IGARASHI, I. 2010a. Evaluation of the in vitro growth-inhibitory effect of epoxomicin on Babesia parasites. *Vet Parasitol*, 167, 19-27.
- ABOULAILA, M., SIVAKUMAR, T., YOKOYAMA, N. & IGARASHI, I. 2010b. Inhibitory effect of terpene nerolidol on the growth of Babesia parasites. *Parasitol Int*, 59, 278-82.
- ABOULAILA, M., YOKOYAMA, N. & IGARASHI, I. 2010c. Inhibitory effects of (-)-epigallocatechin-3-gallate from green tea on the growth of Babesia parasites. *Parasitology*, 137, 785-91.
- BECKER, K. 2011. *Apicomplexan Parasites. Molecular approaches toward targeted drug development*, Wiley-Blackwell.
- BENNETT, T. N., PAGUIO, M., GLIGORIJEVIC, B., SEUDIEU, C., KOSAR, A. D., DAVIDSON, E. & ROEPE, P. D. 2004. Novel, rapid, and inexpensive cell-based quantification of antimalarial drug efficacy. *Antimicrobial agents and chemotherapy*, 48, 1807-1810.
- BORK, S., DAS, S., OKUBO, K., YOKOYAMA, N. & IGARASHI, I. 2006. Effects of protein kinase inhibitors on the in vitro growth of Babesia bovis. *Parasitology*, 132, 775-9.
- BORK, S., YOKOYAMA, N., IKEHARA, Y., KUMAR, S., SUGIMOTO, C. & IGARASHI, I. 2004. Growth-inhibitory effect of heparin on Babesia parasites. *Antimicrobial agents and chemotherapy*, 48, 236-241.
- BORK, S., YOKOYAMA, N., MATSUO, T., CLAVERIA, F. G., FUJISAKI, K. & IGARASHI, I. 2003. Growth inhibitory effect of triclosan on equine and bovine Babesia parasites. *The American journal of tropical medicine and hygiene*, 68, 334-340.
- BOTTE, C. Y., DELIGNY, M., ROCCIA, A., BONNEAU, A. L., SAIDANI, N., HARDRE, H., ACI, S., YAMARYO-BOTTE, Y., JOUHET, J., DUBOTS, E., LOIZEAU, K., BASTIEN, O., BREHELIN, L., JOYARD, J., CINTRAT, J. C., FALCONET, D., BLOCK, M. A., ROUSSEAU, B., LOPEZ, R. & MARECHAL, E. 2011. Chemical inhibitors of monogalactosyldiacylglycerol synthases in Arabidopsis thaliana. *Nat Chem Biol*, 7, 834-42.
- BOUDIERE, L., BOTTE, C. Y., SAIDANI, N., LAJOIE, M., MARION, J., BREHELIN, L., YAMARYO-BOTTE, Y., SATIAT-JEUNEMAITRE, B., BRETON, C., GIRARD-EGROT, A., BASTIEN, O., JOUHET, J., FALCONET, D., BLOCK, M. A. & MARECHAL, E. 2012. Galvestine-1, a novel chemical probe for the study of the glycerolipid homeostasis system in plant cells. *Mol Biosyst*, 8, 2023-35, 2014.
- BRASSEUR, P., LECOUBLET, S., KAPEL, N., FAVENNEC, L. & BALLEET, J. J. 1998. In Vitro Evaluation of Drug Susceptibilities of Babesia divergens Isolates. *Antimicrobial agents and chemotherapy*, 42, 818-820.
- DERBYSHIRE, E. T., FRANSSSEN, F. J., DE VRIES, E., MORIN, C., WOODROW, C. J., KRISHNA, S. & STAINES, H. M. 2008. Identification, expression and characterisation of a Babesia bovis hexose transporter. *Mol Biochem Parasitol*, 161, 124-9.
- GORENFLOT, A., BRASSEUR, P., PRECIGOUT, E., L'HOSTIS, M., MARCHAND, A. & SCHREVEL, J. 1991. Cytological and immunological responses to Babesia divergens in different hosts: Ox, gerbil, man. *Parasitology research*, 77, 3-12.
- GRELLIER, P., VALENTIN, A., MILLERIOUX, V., SCHREVEL, J. & RIGOMIER, D. 1994. 3-Hydroxy-3-methylglutaryl coenzyme A reductase inhibitors lovastatin and simvastatin inhibit in vitro development of Plasmodium falciparum and Babesia divergens in human erythrocytes. *Antimicrob Agents Chemother*, 38, 1144-8.

- GUSWANTO, A., SIVAKUMAR, T., RIZK, M. A., ELSAYED, S. A. E., YOUSSEF, M. A., ELSAID, E. E. S., YOKOYAMA, N. & IGARASHI, I. 2014. Evaluation of a fluorescence-based method for antibabesial drug screening. *Antimicrobial agents and chemotherapy*, 58, 4713-4717.
- JASMER, D. P. & GOFF, W. L. 1989. In vitro killing of *Babesia bovis* by the ornithine analog alpha-monofluoromethyldehydroornithine methyl ester. *J Protozool*, 36, 493-7.
- MOSQUEDA, J., OLVERA-RAMIREZ, A., AGUILAR-TIPACAMÚ, G. & CANTO, G. 2012. Current advances in detection and treatment of babesiosis. *Current medicinal chemistry*, 19, 1504.
- MUNKHJARGAL, T., ABOULAILA, M., TERKAWI, M. A., SIVAKUMAR, T., ICHIKAWA, M., DAVAASUREN, B., NYAMJARGAL, T., YOKOYAMA, N. & IGARASHI, I. 2012. Inhibitory effects of pepstatin A and mefloquine on the growth of *Babesia* parasites. *The American journal of tropical medicine and hygiene*, 87, 681-688.
- NAGAI, A., YOKOYAMA, N., MATSUO, T., BORK, S., HIRATA, H., XUAN, X., ZHU, Y., CLAVERIA, F. G., FUJISAKI, K. & IGARASHI, I. 2003. Growth-inhibitory effects of artesunate, pyrimethamine, and pamaquine against *Babesia equi* and *Babesia caballi* in in vitro cultures. *Antimicrob Agents Chemother*, 47, 800-3.
- NEHRBASS-STUEDLI, A., BOYKIN, D., TIDWELL, R. R. & BRUN, R. 2011. Novel diamidines with activity against *Babesia divergens* in vitro and *Babesia microti* in vivo. *Antimicrob Agents Chemother*, 55, 3439-45.
- PUDNEY, M. & GRAY, J. S. 1997. Therapeutic efficacy of atovaquone against the bovine intraerythrocytic parasite, *Babesia divergens*. *J Parasitol*, 83, 307-10.
- RICHER, E., BIAGINI, G. A., WEIN, S., BOUDOU, F., BRAY, P. G., WARD, S. A., PRECIGOUT, E., CALAS, M., DUBREMETZ, J. F. & VIAL, H. J. 2006. Potent antihematozoan activity of novel bithiazolium drug T16: evidence for inhibition of phosphatidylcholine metabolism in erythrocytes infected with *Babesia* and *Plasmodium* spp. *Antimicrob Agents Chemother*, 50, 3381-8.
- SAIDANI, N., BOTTE, C. Y., DELIGNY, M., BONNEAU, A. L., READER, J., LASSELIN, R., MERER, G., NIEPCERON, A., BROSSIER, F., CINTRAT, J. C., ROUSSEAU, B., BIRKHOLTZ, L. M., CESBRON-DELAUW, M. F., DUBREMETZ, J. F., MERCIER, C., VIAL, H., LOPEZ, R. & MARECHAL, E. 2014. Discovery of compounds blocking the proliferation of *Toxoplasma gondii* and *Plasmodium falciparum* in a chemical space based on piperidinyl-benzimidazolone analogs. *Antimicrob Agents Chemother*, 58, 2586-97.
- SALAMA, A. A., ABOULAILA, M., MOUSSA, A. A., NAYEL, M. A., EL-SIFY, A., TERKAWI, M. A., HASSAN, H. Y., YOKOYAMA, N. & IGARASHI, I. 2013. Evaluation of in vitro and in vivo inhibitory effects of fusidic acid on *Babesia* and *Theileria* parasites. *Vet Parasitol*, 191, 1-10.
- SIVAKUMAR, T., ABOULAILA, M., KHUKHUU, A., ISEKI, H., ALHASSAN, A., YOKOYAMA, N., IGARASHI, I., 横山直明 & 五十嵐郁男 2008. In vitro inhibitory effect of fosmidomycin on the asexual growth of *Babesia bovis* and *Babesia bigemina*.
- SMILKSTEIN, M., SRIWILAIJAROEN, N., KELLY, J. X., WILAIRAT, P. & RISCOE, M. 2004. Simple and inexpensive fluorescence-based technique for high-throughput antimalarial drug screening. *Antimicrobial Agents and Chemotherapy*, 48, 1803-1806.
- SNYMAN, J. 2011. *The effect of herbicides as novel antimalarial drugs on the transcriptome and proteome of Plasmodium falciparum*. *Magister Scientiae*, University of Pretoria.
- UENO, A., TERKAWI, M. A., YOKOYAMA, M., CAO, S., ABOGE, G., ABOULAILA, M., NISHIKAWA, Y., XUAN, X., YOKOYAMA, N. & IGARASHI, I. 2013. Farsenyl pyrophosphate synthase is a potential molecular drug target of risedronate in *Babesia bovis*. *Parasitol Int*, 62, 189-92.
- VYAS, J. M., TELFORD, S. R. & ROBBINS, G. K. 2007. Treatment of refractory *Babesia microti* infection with atovaquone-proguanil in an HIV-infected patient: case report. *Clinical infectious diseases*, 45, 1588-1560.

WORMSER, G. P., PRASAD, A., NEUHAUS, E., JOSHI, S., NOWAKOWSKI, J., NELSON, J., MITTLEMAN, A., AGUERO-ROSENFELD, M., TOPAL, J. & KRAUSE, P. J. 2010. Emergence of resistance to azithromycin-atovaquone in immunocompromised patients with Babesia microti infection. *Clinical infectious diseases*, 50, 381-386.

Chapter 4

***In vitro* evaluation of the growth inhibitory effect of a Piperidinyl-Benzimidazolone analogue (A51B1C1_1) against *Babesia divergens* through comprehensive transcriptome analysis**

4.1 Introduction

Genomic research on the disease-causing *Babesia* pathogens has recently escalated and generated information that can assist in the identification and optimization of future drug therapies (Brayton *et al.*, 2007). The unraveling of the *Babesia* genome in conjunction with functional genomic tools, can contribute to the development and investigation of anti-babesiocidal control strategies. Based on the growth-inhibitory results achieved in Chapter 3, we further applied functional genomics to evaluate the parasitic response to the apicomplast specific compound A51B1C1_1 as treatment against *B. divergens*.

Functional genomics refers to the development and application of several high-throughput technologies (such as transcriptomics and proteomics) and resources to improve global (genome-wide and system-wide) experimental approaches for gene and gene product identification, function and profiling assessment (Hieter and Boguski, 1997). These technologies associated with the *-omics* era have become constitutive elements of modern biology and provide the potential to evaluate a vast amount of data and should be integrated for improved results (Vemuri and Aristidou, 2005). Functional genomics is founded on certain principles associated with physiological and pharmacological sciences and has become an indispensable

tool in drug target identification and understanding the mode-of-action of several novel compounds (Ohlstein *et al.*, 2000).

Current functional genomic studies related to apicomplexan species incorporates high-throughput tools and a combination of genomic, transcriptomic, proteomic and bioinformatic data sets to elucidate information regarding gene function. Publically available databases such as PiroplasmaDB (<http://www.piroplasmadb.org/piro/>), PlasmoDB (<http://www.plasmodb.org/plasmo/>) and ToxoDB (<http://www.toxodb.org/toxo/>) provide extensive information with regards to genomics, transcriptomics and proteomics of several apicomplexan species. These databases are, however, limited and not yet fully available for *Babesia* species (Gohil *et al.*, 2013).

Genome sequencing of apicomplexan parasites is an ongoing process. As mentioned, the phylum includes several pathogenic species (*Plasmodium*, *Babesia*, *Theileria*, *Toxoplasma* and *Cryptosporidium*) responsible for human and animal diseases (Lau, 2009a). Based on the available data, comparisons between these species with regards to their life cycles, genome structures and metabolisms has previously been described and is summarized in Table 4.1 (Lau, 2009a, Brayton *et al.*, 2007).

According to their associated life cycles, *Plasmodium* and *Theileria* exit their vectors and enter their mammalian hosts where they undergo pre-erythrocytic hepatocyte and lymphocyte stages, while *Babesia* sporozoites directly invade host erythrocytes. Once inside the hosts' erythrocytes, *Babesia* and *Theileria* parasites are found in the cytoplasm of the cell, while *Plasmodium* can be found in the cells parasitophorous vacuole (Lau, 2009a).

Table 4.1 Biological, genomic and metabolic comparisons between three related apicomplexan species (Compiled from Lau, 2009 and Brayton *et al.*, 2007)

	<i>Plasmodium species</i>	<i>Babesia species</i>	<i>Theileria species</i>
Life cycle			
Vector	Anopheles mosquito vector.		Ixodid tick vector
Host invasion	Pre-erythrocytic hepatocyte and lymphocytes	Sporozoites directly invade host erythrocytes	Pre-erythrocytic hepatocyte and lymphocytes
Intra-erythrocytic stage	Yes		
Location in cell	Present in parasitophorous vacuole	Present in cell cytoplasm	
Genome characteristics			
Size (Mbp)	28.8 – 30	8.2	
Nr. Chromosomes	14	4	
Total GC composition (%)	19.4	41.8	34.1
Apicoplast genome size (kbp)	35	33	39.5
Mitochondrial genome size (kbp)	6 linear		
Percent coding region (%)	52.6	70.2	68.4
Metabolic pathways present			
Shared	Glycolysis		
	TCA-cycle (mitochondria)		
	DOXP/MEP pathway (apicoplast)		
	Isoprenoid biosynthesis (apicoplast)		
	Nucleotide inter-conversion		
	Pentose phosphate pathway		
	Glycerophospholipid metabolism		
	Glycerolipid metabolism		
	Pyrimidine biosynthesis		
		Purine salvage pathway	-
	Folate biosynthesis	-	Folate biosynthesis
Unique	Shikimate biosynthesis pathway	-	-
	Type II fatty-acid (FA II) biosynthesis pathway	-	-
	Haem biosynthesis pathway	-	-
	Amino acid metabolism	-	-
	Haem metabolism	-	-
Metabolic pathways absent			
Shared	Polyamine biosynthesis		
	Urea cycle		
	Gluconeogenesis		
	Purine biosynthesis (<i>de novo</i>)		
	-	Shikimate biosynthesis pathway	
	-	Type II fatty-acid (FA II) biosynthesis pathway	
	-	Haem biosynthesis pathway	
	-	Amino acid metabolism	
-	Haem metabolism		

* The dash (-) indicates absent metabolic pathway

Comparative genomic studies and the identification of conserved sequences is vital to understand evolutionary histories, biochemical functions and to facilitate the quality of genome annotations (Li *et al.*, 2003). Comparative analyses between related apicomplexan members have escalated as advances in large-scale, rapid sequencing technologies increased (Lau *et al.*, 2009). Comparative studies between *P. falciparum*, *B. bovis* and *T. parva* revealed both shared and divergent features (Brayton *et al.*, 2007). Despite several chromosomal rearrangements, structural similarities between *B. bovis* and *T. parva* can be observed. Several shared clinical and pathological features have been identified between *B. bovis* and *P. falciparum*, despite their major structural differences (Brayton *et al.*, 2007). Knowledge gained from these comparisons may improve existing disease treatment strategies and can provide additional insight into species biology, phylogenetic diversity, evolution, genetic diversity, parasitic epidemiology and pathogenicity (Beck *et al.*, 2013). Comparative studies between these pathogens are therefore important in developing novel control strategies through vaccine candidate and drug target identification (Lau, 2009b). Defining the biological differences between related *Babesia* and *Plasmodium* species provides an opportunity to evaluate the underlying mechanisms associated with host specificity, pathogenesis and the zoonotic potential of these parasites, under chemically treated conditions.

The concepts of orthology and paralogy originated from the molecular systematics field and have since been applied to species classifications as well as functional and comparative genomics. Orthology detection is especially important for accurate functional annotation and facilitation of comparative and evolutionary genomics (Chen *et al.*, 2007). It is important to keep in mind that orthologue genes share a common ancestor, but are present in different species, due to a speciation event (DeBarry and Kissinger, 2011), which contributes to the valuable nature of orthologues for gene identification, annotation and comparative analyses. Grouping (clustering) of orthologue genes is an important concept in comparative genomics, as it provides

a framework for the investigation of several genomes, highlighting either the divergence or conservation of genes and their corresponding functions (Li *et al.*, 2003). Comparative studies between organisms may identify either ‘core’ (orthologue in all the investigated species), ‘multi-copy’ (genes with at least two copies within a single genome) or ‘species-specific’ (no orthologue between species) orthologous genes (DeBarry and Kissinger, 2011). The OrthoMCL database (<http://www.orthomcl.org/orthomcl/>) was used in this study as it provides a centralized hub for orthology predictions between species and is constantly updated and expanded as new genome sequence data becomes available (Chen *et al.*, 2005, Altenhoff *et al.*, 2013).

Transcriptomics is the quantitative analysis of the expression of all transcripts within a transcriptome, which reflects the functional elements of the genome and its dynamic fluctuations under variable conditions and environments. The rapidly expanding field of functional genomics has initiated several new research fields and in conjunction with the increase in genomic pathogen data, has paved the way forward to new opportunities for drug discovery, which laid the foundation for modern biomedical research (Le Roch *et al.*, 2012). For instance, the above mentioned techniques have recently been applied in eight drug discovery projects, across four disciplines (oncology, virology, neuroscience, metabolic disease) and confirmed its success as valuable tools for drug discovery, by detecting the biological effects of compounds across disease areas, targets and scaffolds (Verbist *et al.*, 2015). The application of functional genomics has also been invaluable in anti-bacterial drug discovery (*i.e. Mycobacterium tuberculosis*), by improving knowledge regarding gene function, bacterial metabolism and physiology as well as drug target and mode-of-action identification (Freiberg and Brotz-Oesterhelt, 2005, Boshoff *et al.*, 2004). *Trypanosoma* and *Leishmania* related research has also incorporated functional genomics and data mining to identify potential drug targets and therapeutic strategies (Cowman and Crabb, 2003). Functional genomics and genome-wide analysis have also been applied in malaria research to better understand gene functions and

metabolic pathways as well as to assist in the identification of parasite-specific genes and several candidate genes and/or loci as potential vaccine or drug targets (Mu *et al.*, 2010, Birkholtz *et al.*, 2008). It has become an indispensable tool in anti-malarial drug discovery and has been used to investigate therapeutic effects at an integrated cellular level (Ohlstein *et al.*, 2000). A few examples of functional genomics applied in anti-malarial drug discovery include, the identification of thiolactomycin (Waller *et al.*, 2003) and fosmidomycin (Lell *et al.*, 2003) as inhibitors of *in vitro* parasitic growth; the identification of novel antifolate compounds as potential inhibitors of the *P. falciparum* folate pathway as well as identifying several proteases as potential drug targets among *P. falciparum* and *Plasmodium yoelii* (Cowman and Crabb, 2003). Oligonucleotide microarrays have successfully been used to investigate choline analogue treated *P. falciparum* parasites to determine the parasitic response to treatment (Birkholtz *et al.*, 2006).

Technologies of major importance for transcriptome studies are represented by DNA microarrays and next-generation RNA-sequencing (RNA-Seq) (Di Girolamo *et al.*, 2005). However, DNA-microarrays remain essential tools to address gene and protein expression profiles in response to genetic or environmental changes, in order to identify and validate new drug targets (Wang *et al.*, 2004).

Microarray experimental design forms a pivotal part of the experiment and should take into account biological (variation linked to all living organisms) and technical (variation introduced in the laboratory) replication, the degree of which is required to ensure statistical confidence in the data (Simon *et al.*, 2003). An additional factor to consider is the application of either direct or indirect technical comparisons (comparisons within or between slides) (Slonim and Yanai, 2009). Several microarray expression platforms are established (Affymetrix, Agilent, Amersham, NimbleGen, Febit and CodeLink Bioarray) based on either full-length cDNA's, pre-synthesized cDNA's or *in situ* synthesized oligonucleotides used as probes. The particular platform selected

for use depends on the nature of the experiment - in this study we applied an Agilent platform. Agilent Technologies manufacture a variety of proprietary and custom oligonucleotide microarrays (Wolber *et al.*, 2006) and are based on the *in situ* synthesis of probes on the microarray slide, using inkjet printing and phosphoramidite chemistry (Hardiman, 2004). The standard Agilent oligonucleotide arrays are designed based on a 60-mer probe design and can be produced in different formats, ranging from 1x 244, 000 to 8x 15, 000 probes per slide and employ a two-color labelling strategy (Wolber *et al.*, 2006).

In a typical two-color microarray experiment, purified RNA samples are reverse transcribed into cDNA, labelled with either Cy3 (green, G) or Cy5 (red, R) cyanine fluorescent dyes, mixed in equal portions and competitively hybridized to the probe DNA sequences on the glass slide. The glass slides are subsequently imaged, based on the relative fluorescent measurements associated with each dye, at each spot (feature), present on the array. Following hybridization and image processing, microarray data is normalized and differentially expressed genes (DEG's) identified (Hardiman, 2004). Data normalization is required to ensure accurate data comparisons, either within or between arrays (Irizarry *et al.*, 2003) and is generally applied to the log-ratios of gene expression (Equation 4.1) as well as the overall brightness and log-intensity of spots (Equation 4.2) (Smyth and Speed, 2003).

$$M = \log_2 R - \log_2 G \quad \text{(Equation 4.1)}$$

$$A = (\log_2 R + \log_2 G) / 2 \quad \text{(Equation 4.2)}$$

* *M* (minus) represents \log_2 ratio values and *A* (addition) represents \log_2 intensity values for each array.

* *R* and *G* represent the background corrected red and green fluorescent intensities associated with each spot (feature).

Pearson correlation coefficient (r) is a measure of similarity which measures the strength between two variables and range between -1 (anti-correlation) and 1 (perfect correlation) and is frequently used in gene expression profiling analyses to establish the similarities between samples (Bozdech *et al.*, 2003, Llinas *et al.*, 2006, Dahl *et al.*, 2006). Several software packages are available for microarray data analysis and for establishing differential transcript expression profiles - the linear model for microarray data analysis (LIMMA), available in the R-statistical environment is routinely used (Smyth, 2004). As mentioned, two-color microarray experiments simultaneously quantify relative gene expression levels between samples for a vast amount of probes. The observed pixel intensities for either Cy3 or Cy5 images, represent the amount of hybridization that occurred between the RNA-samples and immobilized probe sequences. Background correction is subsequently required to remove any non-specific binding effects and is followed by data normalization within and between arrays (Quackenbush, 2002, Ritchie *et al.*, 2007). Within-array normalization requires the calculation of a best-fit slope, using linear regression techniques such as the locally weighted scatterplot smoothing analysis (LOWESS). Between-array normalization of A -values requires a quantile normalization strategy to correct for the individual green (G-quantile) and red (R-quantile) channels. Normalization by LOWESS removes intensity-dependant dye biases, which can be visualized by MA -plots (M refers to the \log_2 ratio of signal intensities and A refers to the average \log_2 intensities) (Smyth *et al.*, 2005).

MIAME (minimum information about a microarray experiment) dictates accurate guidelines and a standard for recording and analysing microarray gene expression data. The MIAME guidelines stipulate the minimum information required to allow for accurate comparisons between different data sets and across different microarray platforms (Brazma *et al.*, 2001).

In this study, we present a comprehensive analysis of the transcriptome of *B. divergens* parasite, evaluated under different (treated vs. untreated) conditions, using a hybridization-

based technique (Agilent platform). This chapter will focus on classical DNA microarray analysis of A51B1C1_1 treated *B. divergens* parasites to quantify gene expression levels and identify DEG's amongst the treated parasites. Additionally, we set out to define key gene expression differences between galvastine-1 treated *A. thaliana* and two apicomplexan species treated with A51B1C1_1; identify conserved gene expression networks as well as identify candidate gene transcripts that may have contributed to the parasite's response to treatment and the drug mode-of-action.

4.2 Materials and Methods

4.2.1 Hybridization-based (microarray) transcriptomics

Chapter 2 provided a brief description of the materials and methods used for the hybridization-based transcriptomic evaluation of untreated (control) samples. This chapter is an extension to Chapter 2 and Chapter 3 and provides a more comprehensive description of the materials and methods applied to both A51B1C1_1 treated and untreated (control) samples.

Sample collection and drug treatment for transcriptomic investigation

Asynchronous *B. divergens* cultures were maintained as described in Chapter 2. Both treated and untreated cultures were monitored microscopically using Giemsa-stained smears, where after samples were collected for the transcriptomic time-course evaluation.

Three biological replicate samples (5% hematocrit, 12% parasitaemia, 10 ml) were collected from both treated (2x IC₅₀ A51B1C1_1) and untreated cultures, at four time-points (0, 4, 9 and 16 hours) from newly initiated cultures (Figure 4.1). Infected erythrocytes were washed three times with 15 ml 1xPBS and centrifugation at room temperature (2500g) for 5 minutes. The

supernatant was aspirated and the infected erythrocyte pellet washed three times with 15 ml 1xPBS. The washed infected erythrocyte pellets of both treated and untreated samples were snap-cooled in liquid nitrogen and stored at -70°C for RNA-isolation.

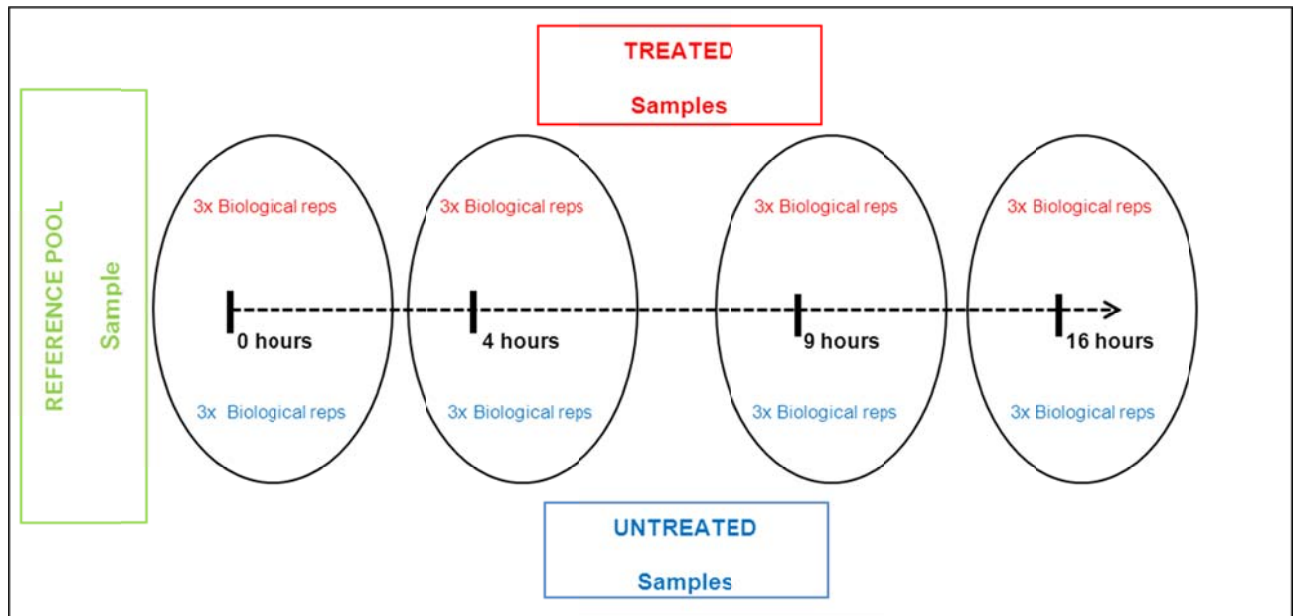


Figure 4.1 Hybridization-based (microarray) experimental design and layout.

A common reference pool design strategy was used for *B. divergens* transcriptome investigation for both treated and untreated samples. The reference sample was stained with Cy3 (green) and all other samples, collected over the 16-hour time period were stained with Cy5 (red). A total of 24 hybridizations were performed, consisting of three biological replicates (reps) collected per time-point, for both treated and untreated samples.

Microarray probe design from *B. bovis* sequences

The base composition probe design strategy is regarded as the standard design methodology for gene expression probes, as it creates probes of equal length and is suitable for most Agilent protocols on eukaryotes. As described in Chapter 2, the custom designed *B. bovis* microarray slides were synthesized with unique descriptors, printed onto microarray slides and directly ordered from Agilent Technologies (<https://earray.chem.agilent.com/earray/>).

RNA isolation and quality assessment

Total RNA was isolated from the 24 samples (12 treated and 12 untreated in triplicate; four time-points). Samples were isolated under RNase-free conditions based on acid guanidium thiocyanate-phenol-chloroform extraction (Chomczynski and Sacchi, 2006). The combination of TRI-Reagent (Sigma, USA) and the Rneasy Protect Mini kit (Qiagen, Germany) ensured the quality and purity of the RNA to be of high standard.

Briefly, lysis buffer (600 μ l, Rneasy Kit) was added to the 10 ml thawed parasite pellet, mixed by vortexing and passed through two QIA-Shredder™ columns (Qiagen) to allow physical cell rupture. Tri-reagent (600 μ l) was added, mixed by vortexing vigorously and incubated at room temperature for 5 minutes. After the addition of chloroform (400 μ l), each sample was vortexed vigorously, incubated at room temperature for 10 minutes and centrifuged for 15 minutes at 15700g. The homogenate was subsequently separated into an aqueous and organic phase where after the upper aqueous phase containing the RNA was transferred to new microfuge tubes. Ethanol (700 μ l, 70% (v/v)) was added to each sample to allow RNA precipitation to the Rneasy column (Qiagen). The samples were mixed, loaded onto the column and centrifuged for 15 seconds at 8000g and flow-through subsequently discarded. Manufacturer's recommendations were followed for the Rneasy kit, which involved washing of RNA several times with two different buffers as well as on column treatment with 27 units DNase 1 mixture (Qiagen) for 15 minutes. A final volume of RNase-free water (30 μ l) was used to elute RNA from each sample.

Isolated RNA concentrations were determined using the NanoDrop® ND-1000 spectrophotometer, based on the absorbance measured at 260 nm. RNA purity was based on the $A_{260}:A_{280}$ ratio. RNA integrity and quality was further analyzed using the highly sensitive Experion® automated electrophoresis system (Bio-Rad, USA) by Mr. Nicky Olivier at the ACGT

Microarray Facility (University of Pretoria). RNA samples were prepared as per manufacturer's instructions. The RNA integrity was established based on capillary electrophoresis and a fluorescent RNA-binding dye. Results were subsequently expressed as RNA quality indicator (RQI) values along with color-codes RQI classification. These values were obtained from mapping RNA samples to a standardized set of degraded RNA samples.

cDNA synthesis, clean-up and labeling

A reference pool design strategy was followed for gene expression profiling. The representative RNA reference pool consisted of equal RNA quantities (4 µg), prepared from all biological replicates and collected over the 16-hour time period, from both treated and untreated samples (Figure 4.1).

First-strand cDNA synthesis, clean-up and sample labelling were performed for both treated and untreated samples. Labelling efficiency, the extent of dye incorporation and sample concentration was determined using the microarray settings on the NanoDrop® ND-1000 system. The measure represents a value of labelled nucleotides to unlabeled nucleotides, and should be at least 10 sufficiently labelled nucleotides out of 1000 nucleotides (10:1000) to be considered acceptable for hybridization. Labelling efficiency was calculated for each sample based on Equation 4.3.

$$\text{Labeling efficiency} = \frac{\text{pmol dye} \times 324.5 \text{ pg/mol}}{\text{ng DNA}} \quad (\text{Equation 4.3})$$

(* Average mass of a dNTP)

Microarray hybridization, washing and scanning

To ensure successful hybridization, 20 pmol of each Cy3 (reference pool) and Cy5 (target) – cDNA samples were combined in 0.2 µl tubes, with several buffers, including a 10x blocking buffer, 25x fragmentation buffer, 2x GE hybridization buffer and Wash Buffers 1 and 2 supplied by Agilent Technologies (Proprietary, Agilent Technologies). To each labelled cDNA sample mixture, 5 µl 10x blocking buffer, 1 µl 25x fragmentation buffer, RNase-free water was added (to adjust the final reaction volume to 25 µl) and incubated for 30 minutes at 60°C (in a PE2400 thermal cycler, Applied Biosystems).

Following incubation, 25 µl 2x GE hybridization buffer was carefully added to each sample and placed on ice ($\pm 4^{\circ}\text{C}$). The 8-array gasket slide (Agilent Technologies) was placed in the hybridization assembly chamber (Agilent Technologies) and 40 µl of each individually labelled cDNA sample slowly pipetted onto the separate gasket slide chambers, taking care so as to not introduce bubbles. The printed Agilent microarray slide was carefully placed onto the loaded gasket slide which was firmly closed, sealed and placed in the pre-heated Agilent Hybridization Oven (G2545A, Agilent Technologies) for overnight hybridization at 65°C (rotation speed of 10). Following hybridization, slides were removed and washed twice (by submerging) with Wash Buffer 1 for one minute, followed by wash with Wash Buffer 2 for one minute. The slide was dried by centrifugation in a Slide Spinner centrifuge (C1303, Labnet International, Inc.) for one minute, prior to slide scanning with the Axon GenePix 4000B scanner (Molecular Devices, USA), by Mr. Nicky Olivier at the ACGT Microarray Facility (University of Pretoria).

Differential transcript abundance data analysis and functional annotation

Once the images were acquired (after slide scanning), the signal intensity of each spot (feature) was measured, recorded and analyzed with the Axon GenePix Pro 6.0 software (Molecular Devices), as discussed in Chapter 2.

The functional annotation of transcripts was firstly conducted using dCAS, which incorporates a workflow concept which integrates several steps including sequence processing, analysis and the Basic local alignment search tool (BLAST) searches to identify previously annotated protein and nucleotide sequences (Guo *et al.*, 2009). Large-scale BLAST searches were conducted using the software's default settings between transcripts and several databases, including gene ontology protein sequence database (GO), eukaryotic orthologous group database (COG), mitochondrial and plastid database (Mit-Pla), non-redundant (NR), protein family sequence database (Pfam), rRNA subset database (RRNA) and the simple modular architecture research tool (SMART) (<http://exon.niaid.nih.gov>). The data output generated by dCAS was provided in a tab-delimited text-file. Manual inspection of each transcript followed, based on similarities observed between two or more of the above mentioned databases and their corresponding *E-values* (cut-off of less than 1×10^{-4}).

Functional annotation and transcript descriptions were subsequently verified by Uniprot (<http://www.uniprot.org/uniprot/>) and the B2G functional annotation computer software and organized into various functional groups (Conesa *et al.*, 2005). The B2G software incorporates specific transcript identifiers and accession numbers to identify GO-annotations and their corresponding enzyme commission (EC) numbers, which were subsequently compared to the NCBI's non-redundant (NR) database using a BLASTx search strategy with an *E-value* cut-off of 1×10^{-4} . Transcripts were subsequently annotated for function and assigned GO-terms, describing their molecular functions, biological processes and cellular compartments.

Metabolic pathway identification, enrichment analysis and mapping followed, which was based on the Kyoto Encyclopedia of Genes and Genomes database (KEGG) using the KEGG Automatic Annotation Server (KAAS) web server and the bi-directional best hit (BBH) information method (Moriya *et al.*, 2007). All the DEG's were mapped to terms in the KEGG-database and further analyzed for significantly enriched KEGG-terms, based on comparisons to the available reference pathways associated with the *B. bovis* genome.

The Gene Set Enrichment Analysis (GSEA) computer software was used to further evaluate and refine our microarray data set (Subramanian *et al.*, 2005). Differential gene expression analysis was based on analyzing groups of genes (gene-sets) that shared common biological functions which correlated to specific phenotypic distinctions. The GSEA software determined the level to which DEG's were overrepresented at either the top or bottom of the predefined list of ranked genes (top-table). As mentioned, the predefined list of ranked genes was constructed using LIMMA and its linear models of empirical Bayes methods to evaluate differential gene expression. The GSEA software calculated an enrichment score (ES) to reflect enrichment of a gene-set, either at the top (positive ES-value) or bottom (negative ES-value) of the ranked gene list. In addition, GSEA calculated a normalized enrichment score (NES) which allowed for comparisons across different gene sets including treated and untreated phenotypes. A FDR was used to evaluate the significance of enrichment, associated with each NES and a P -value ≤ 0.05 , was regarded as significant.

4.2.2 Comparative transcriptomic evaluation between species in response to A51B1C1_1 treatment

Comparative analyses

The orthology study generated genome-wide orthologue groups based on BLASTP searches; an *E-value* cut-off of 1×10^{-4} ; the reciprocal best hit approach as well as the Markov Clustering algorithm to improve sensitivity and specificity using the OrthoMCL database (<http://www.orthomcl.org/orthomcl/>) (Li *et al.*, 2003). The OrthoMCL procedure was conducted on three selected species including *A. thaliana* (<http://www.arabidopsis.org/index.jsp>), *B. bovis* (Brayton *et al.*, 2007); <http://piroplasmadb.org/piro/>) and *P. falciparum* (Gardner *et al.*, 2002); <http://plasmodb.org/plasmo/>), to identify a preliminary list of orthologue groups between them. The orthologue groups identified were merged within the R-statistical environment (<http://cran.r-project.org/>) and manually curated to identify shared groups between the species. The shared groups were subsequently combined into two orthologue group-matrices described as the *B. bovis* - *P. falciparum* orthologue group matrix and the *B. bovis* - *A. thaliana* orthologue group matrix. These matrices were used for further transcriptome comparisons.

Comparative transcriptome expression analyses

A comparative method was designed to compare expression data sets based on the above mentioned orthologue group-matrices. Comparisons were performed between the differential transcriptomic data sets of A51B1C1_1 treated *B. divergens* and *P. falciparum* parasites as well as between A51B1C1_1 treated *B. divergens* parasites and galvastine-1 treated *A. thaliana* plants.

The differential transcriptomic data set associated with the treated *P. falciparum* parasites was provided by Mrs. J. Reader (University of Pretoria) (Snyman, 2011). Data was based on parasitic treatment at 2x IC₅₀ (447 ±16 nM), transcript abundance (> 1.7-fold) and *P*-values (< 0.05) associated with each differentially expressed transcript. The differential transcriptomic data set of galvestine-1 treated *A. thaliana* was obtained from previously published work (Botte *et al.*, 2011). Data was collected from the complete array data of an Affymetrix ATH1 GeneChip, hybridized with RNA collected from *A. thaliana* leaves, treated for three days with galvestine-1 (100 µM) with a *P*-value threshold ≤ 1x10⁻³. Only DEG's in A51B1C1_1 and galvestine-1 treated data sets were used for the comparative transcriptomic analysis. Comparisons were visualized using the online, integrative tool VENNY (<http://bioinfogp.cnb.csic.es/tools/venny/>) to generate Venn Diagrams (Oliveros, 2007).

4.3 Results and Discussion

4.3.1 Hybridization-based (microarray) transcriptomics

RNA-isolation and analysis

To allow for statistical analysis, biological replicates were collected in triplicate at four time-points for both treated and untreated samples. By using a reference design strategy we allowed for simultaneous analysis and comparison between all samples.

The integrity and purity of all 24 RNA samples were evaluated by the Experion[®] automated electrophoresis system (Bio-Rad). Virtual gel images and electropherograms shows defined, dark bands between ~1600 bp and ~3000 bp (indicating 18S and 28S rRNA units, respectively) with low smearing associated with the RNA samples, indicating high quality RNA (Figure 4.2 A).

Both gel and electropherogram images indicated no DNA contamination and that all 24 RNA samples could be used for subsequent microarray analysis (Figure 4.2 B).

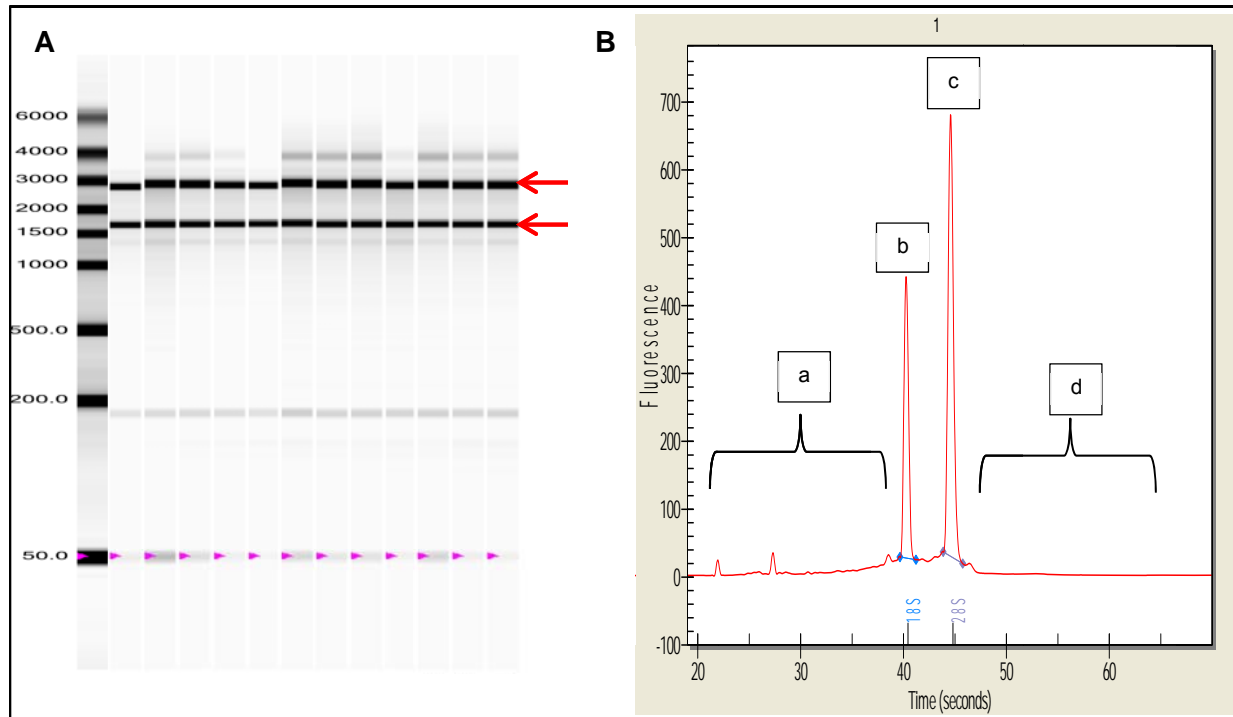


Figure 4.2 RNA purity and quality assessment by Experion[®] for use in the microarray experiment.

Typical results for RNA purity and quality assessment represented by (A) Virtual gel image with arrows indicating 18S and 28S ribosomal subunits (rRNA) between ~1600 and ~3000 bp. The band observed at 50 bp is the standard (supplied by manufacturer) and included in the sample buffer. (B) Depicts the electropherogram indicating sample purity based on peak regions a, b, c and d. Peaks or smears observed in regions a and d, indicate sample degradation or genomic contamination, respectively. Peaks b and c, indicate the positions of the 18S and 28S rRNA subunits, respectively.

The RNA integrity of each sample was further evaluated and expressed as a RQI-value along with color-codes RQI classification. The RQI-values generally range between 1.0 (completely degraded RNA) and 10.0 (intact RNA), with values between 7.0 and 10.0 considered as good quality RNA. The RQI color-codes classification generally range between red ($1 \leq \text{RQI} \leq 4$), yellow ($4 < \text{RQI} \leq 7$) and green ($7 < \text{RQI} \leq 10$) (Denisov *et al.*, 2008). These values all ranged between 9.6 and 10.0, with green RQI color-codes indicating high quality RNA for each of the

24 sample. In addition, high RNA yields were observed for all samples (between 475.51 – 1699.51 ng/μl) (Appendix 4.1).

Sample preparations and quality control checkpoints for microarray analysis

Based on the experimental design, a total of 24 hybridizations (12 treated and 12 untreated) were performed. It was determined that ~4.5 μg starting material was required for each test sample to synthesize sufficient cDNA quantities. The cDNA was labelled and re-purified to conduct the 24 hybridizations. Labelling efficiencies ranged between 10.82 and 33.02 for all samples and conform to the recommended efficiency of 10 (Smit, 2010). For the hybridizations, 20 pmol Cy3 and Cy5 labelled samples were hybridized per array. As results for all 24 samples adhere to the above mentioned requirements, only the first eight samples and one reference sample is presented in Table 4.2.

Table 4.2 RNA yield, cDNA synthesis and labeling efficiency of eight representative samples.

Sample Name	RNA (ng/μl)	A260/A280	cDNA (ng/μl)	Labelled cDNA (ng/μl)	Cy-Dye	pmol dye/μl	Labelling efficiency
1	1026.66	2.18	148.5	47.6	Cy5	1.8	12.27
2	473.51	2.16	129.6	57.9	Cy5	1.9	10.82
3	802.16	2.16	115.1	49.4	Cy5	2.9	19.05
4	1452.24	2.18	140.3	58.1	Cy5	2.6	14.52
5	1699.51	2.18	147.6	33.4	Cy5	1.3	12.63
6	785.67	2.13	138.6	58	Cy5	2.5	13.99
7	976.35	2.17	155.6	53.9	Cy5	2.1	12.64
8	915.79	2.19	80.5	61.1	Cy5	2.1	11.15
Reference			109.1	59.4	Cy3	2.8	15.3

Hybridization quality was assessed by visual inspection of the scanned images, which contain various control spots (features). The corners of each individual array contain these control spots, and can be identified as either bright (positive control) or dark (negative control) corners. As the data are not normalized at this point, it is merely for illustration purposes (Figure 4.3).

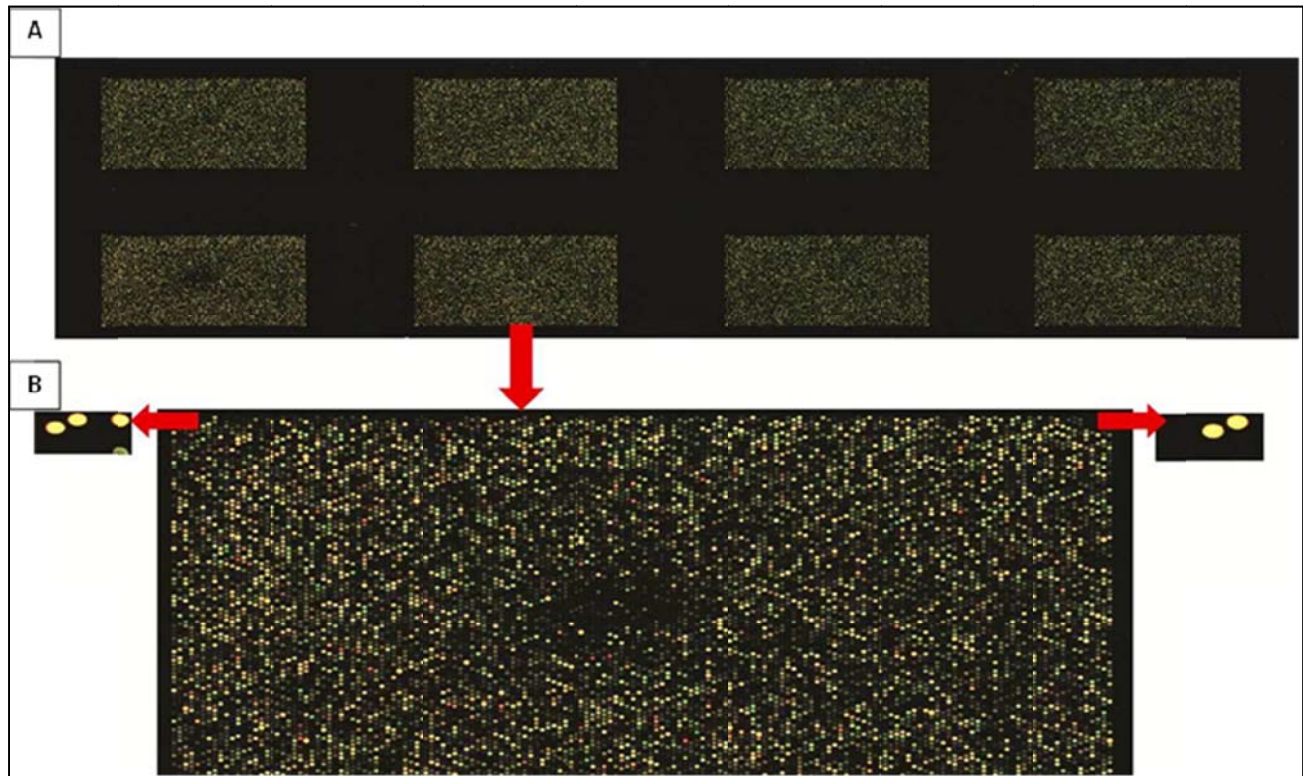


Figure 4.3 Example of the scanned custom designed 8x 15K Agilent arrays.

(A) Scanned image following hybridization with Cy3 (reference pool sample) and Cy5 (test sample) labeled cDNA on a typical 8x 15K microarray slide, consisting of 8 arrays each with 15000 features (B) Agilent includes control features on their slides - positive controls are indicated by the bright features (left arrow) and negative controls indicated by dark features in each corner of the array (right arrows). The bright corners should always be hybridized, compared to the dark corners which should remain dark, indicating no signal after hybridization.

Data analysis

Normalization of data

To allow for correction of variation between the biological replicates data normalization, correction and background subtraction were conducted to ensure accurate DNA microarray analyses. Box plots indicate the scattered *M*-value (\log_2 ratio) and *A*-value (intensity) distributions observed for all 24 arrays prior to normalization (Figure 4.4 A; C). These box plots illustrate the need for within and between array normalization. After global LOWESS normalization, the median *M*-values (of all 24 arrays) were centered around zero (Figure 4.4 B; D) (Smyth, 2004). Insufficient normalization was, however observed for several arrays (array 19 representing an outlier). Intensity values (*A*-values) were successfully transformed after normalization and evenly distributed.

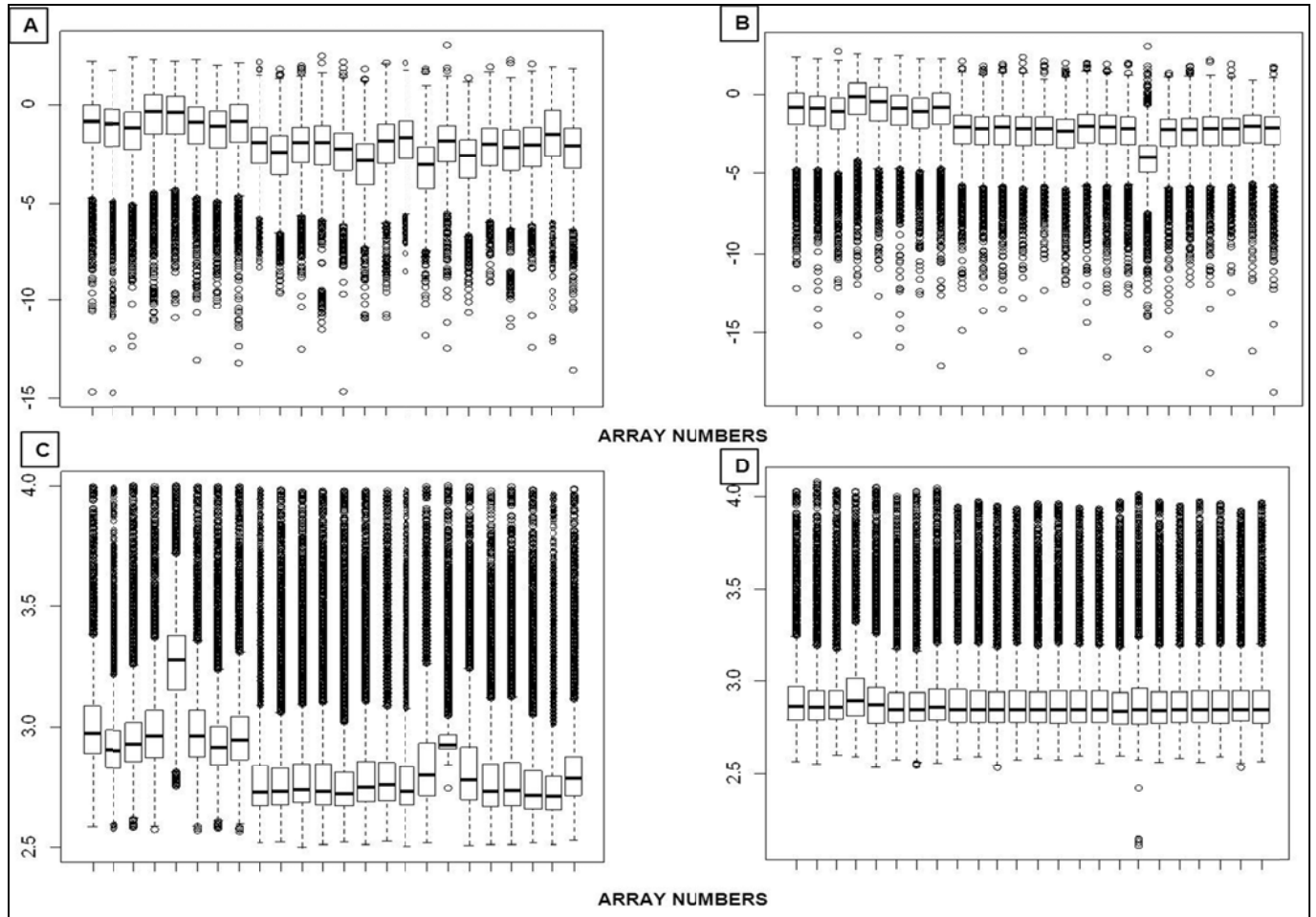


Figure 4.4 Box plots of all M -values (\log_2 ratio) and A -values (intensity) for all 24 arrays, before and after normalization.

(A; C) The scattered M -value and A -value distributions observed across all 24 arrays in the pre-normalized boxplots, illustrated the need for within and between -array normalization. (B; D) After global LOWESS and Q quintile normalizations, the median M -values and A -values were centered around 0 and 3, respectively.

The MA -scatterplots were evaluated to further assess microarray data quality (generated from each array) as well as to confirm that data normalization achieved the desired effect. The MA -plots should ideally represent \log_2 ratios (M -values) evenly distributed around zero, independent of feature intensity (A -value). Following normalization a clear improvement with regard to gene distribution about the median axes can be observed (Figure 4.5 A). Total signal intensities of the red and green channels in the two-color microarray experiment were not perfectly balanced and

subsequently required normalization (Figure 4.5 B). The red-green (Cy5/Cy3) density plots were used to visualize dye biases observed between-arrays. Prior to normalization, the density plot indicated a dye bias towards the green channel for several arrays (Figure 4.5 C). Gquintile normalization of intensities (*A*-values) between arrays ensured an even distribution of \log_2 ratios (*M*-values) across all arrays and revealed a single, representative density curve for the green channel, against which all the arrays were subsequently normalized against (Figure 4.5 D).

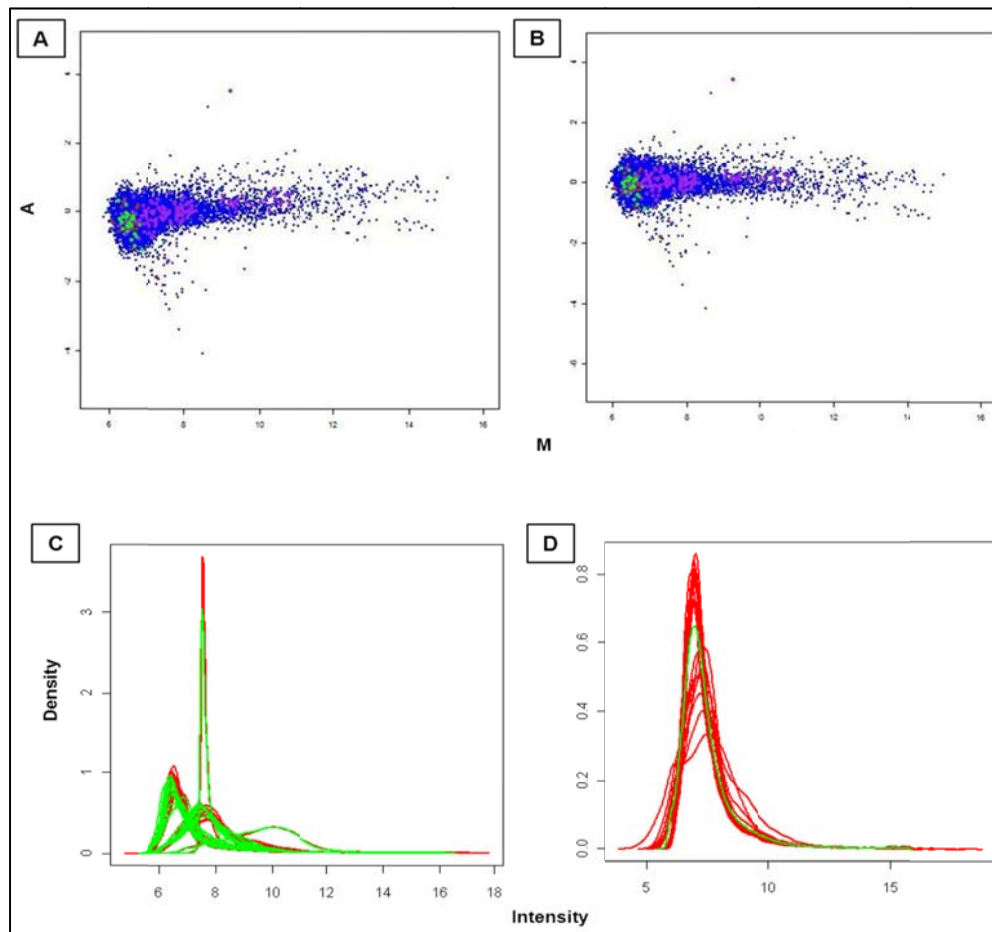


Figure 4.5 Representative MA-plot before and after data normalization as well as Red-Green (RG) density plots of all three microarray slides before and after normalization.

(A) A representative MA-plot before and (B) after data normalization illustrates the relationship between the dye bias and spot-intensity in the two-color microarray experiment. The log-ratio of both red and green color channels is plotted against the overall intensity of each feature (spot). The log-ratio is presented by *M*-values and the overall intensity by *A*-values. Red-Green (RG) density plots indicate the intensity distributions for Cy5 (red) and Cy3 (green) channels, measured across all three microarray slides, before (C) and after (D) data normalization.

Differential transcript abundance analysis using LIMMA software

After obtaining the normalized intensity values within and between arrays, differential transcript abundance was evaluated using LIMMA and presented in the predefined list of ranked genes (top-tables). The \log_2 -ratios of each transcript's fold change (\log_2FC) between treated and untreated samples were evaluated to identify gene transcripts with similar expression levels and to determine the change in expression levels of a specific gene at a specific point in time. Over the 16-hour collection period, 801 transcripts were differentially expressed (1.7 fold change; $0.75 \leq \log_2 \text{ ratio} \leq -0.75$; $P\text{-value} < 0.05$). Of these transcripts, 238 were up-regulated (increase in abundance) and 563 down-regulated (decrease in abundance). Most of the DEG's were identified between time-points 0 and 4 hours post treatment. Based on the \log_2FC and adjusted P -values, a summary of transcripts with the highest differential abundance levels observed between 0 - 16 hours post treatment is provided in Table 4.3.

Table 4.3 Differential transcript abundance analyses using the LIMMA software package.

The top 20 transcripts with highest increase and decrease in abundance (post treatment) are presented, respectively.

Transcript ID (PiroplasmaDB)	Product description	E-value	log2FC ^a	Adj. P-value ^b
Increase				
BBOV_III009450	RNase L inhibitor, ABC superfamily	5.00E-60	2.06466	0.02543
BBOV_III008390	Valyl-tRNA synthetase	5.00E-59	1.6594	0.0324
BBOV_III000960	RNA polymerase III, second largest subunit	1.00E-58	1.90272	0.03433
BBOV_IV011160	mRNA splicing factor ATP-dependent RNA helicase	1.00E-47	2.1605	0.02404
BBOV_IV005830	F0F1-type ATP synthase, beta subunit	2.00E-47	2.64057	0.00511
BBOV_II007250	Translation initiation factor 5B	9.00E-38	1.87807	0.03065
BBOV_IV005840	Glycine/serine hydroxymethyltransferase	3.00E-31	1.92183	0.01258
BBOV_III011840	Glutamyl-tRNA synthetase	2.00E-29	3.86336	0.00067
BBOV_III000930	Glycerol-3-phosphate dehydrogenase	2.00E-24	2.22355	0.03082
BBOV_III004900	Mitochondrial Fe/S cluster exporter, ABC superfamily	4.00E-22	2.35207	0.01213
BBOV_IV009600	RNA polymerase I, large subunit	5.00E-22	2.43159	0.02931
BBOV_IV007190	Dihydrolipoamide dehydrogenase	9.00E-21	2.01192	0.00994
BBOV_II003080	Notchless-like WD40 repeat-containing protein	1.00E-20	2.18445	0.0369
BBOV_I002740	Translation initiation factor 3, subunit a (eIF-3a)	2.00E-20	1.89248	0.04917
BBOV_I003140	Endonuclease III	6.00E-20	1.35332	0.03433
BBOV_III002280	Metallopeptidase	1.00E-19	2.49333	0.01246
BBOV_IV011550	Aminopeptidase I zinc metalloprotease (M18)	2.00E-19	1.68013	0.03709
BBOV_II005900	DNA replication licensing factor, MCM2 component	4.00E-19	1.91443	0.02406
BBOV_IV010920	GTPase Ran/TC4/GSP1	1.00E-18	1.02142	0.04851
BBOV_III007090	20S proteasome, regulatory subunit beta	3.00E-18	1.13578	0.03136
Decrease				
BBOV_I000740	Serine/threonine specific protein phosphatase	3.00E-29	-1.62609	0.0187
BBOV_I003460	GTP-binding protein DRG2	3.00E-28	-2.09826	0.04542
BBOV_III010890	Deoxyhypusine synthase	3.00E-25	-1.6361	0.03171
BBOV_II002230	5'-3' exonuclease HKE1/RAT1	1.00E-24	-2.7564	0.00865
BBOV_I004920	RNA helicase	1.00E-24	-1.53465	0.02056
BBOV_III009710	Chromatin remodeling protein HARP/SMARCAL1, DEAD-box superfamily	9.00E-23	-1.28666	0.04202
BBOV_III009080	DNA polymerase epsilon, catalytic subunit A	4.00E-20	-1.81516	0.01983
BBOV_IV005130	Sof1-like rRNA processing protein (contains WD40 repeats)	4.00E-18	-2.8313	0.03118
BBOV_II006920	Citrate synthase	8.00E-17	-2.40353	0.01238
BBOV_III006690	Vesicle coat complex AP-1/AP-2/AP-4, beta subunit	1.00E-16	-2.16468	0.02776
BBOV_III002500	Long-chain acyl-CoA synthetases	1.00E-16	-2.01321	0.02667
BBOV_II007190	Dihydroorotate dehydrogenase	3.00E-16	-2.10267	0.04851
BBOV_IV008880	Predicted RNA-binding protein Pno1p	9.00E-16	-3.37942	0.002
BBOV_IV009520	Phosphatidylinositol 4-kinase	2.00E-15	-1.65373	0.03065

BBOV_II002690	Global transcriptional regulator	2.00E-15	-2.22212	0.01262
BBOV_IV004470	U4/U6-associated splicing factor PRP4	3.00E-15	-1.76411	0.01348
BBOV_IV011410	Mitochondrial RNA helicase SUV3, DEAD-box superfamily	6.00E-15	-1.76475	0.02776
BBOV_III001380	AAA+-type ATPase	8.00E-15	-2.15609	0.01567
BBOV_III011550	Translation initiation factor 1A (eIF-1A)	2.00E-14	-1.10255	0.04865
BBOV_I001740	S-adenosylhomocysteine hydrolase	2.00E-14	-1.89833	0.01964

*a \log_2FC cut-off values; *b Adjusted P-value (indication of transcript significance statistically determined by LIMMA, $P < 0.05$)

Pearson correlation coefficients (r) of the mRNA abundance levels of *B. divergens* parasites were subsequently calculated within the R-statistical environment to identify expression similarities as well as differences in development between untreated (UT) and treated (T) samples, collected over a 16-hour period. This allowed for subsequent, direct comparisons between the parasites. Due to the high number of DEG's identified between time-points 0 (UT0) and 4 (T4) hours post treatment, particular emphasis was given to the associated comparison and correlation values observed at this time-point (UT0 vs. T4; $r=0.0056$). As described in Chapter 2, high levels of DEG's were also observed between the initiate culture and the parasites 4 hours after inoculation, with correlation data indicating low correlation between these parasites (C0 vs. C4; $r=0.0358$). We ascribed this to general life cycle, growth variations, development and culture adaptations during the parasite's IDC. To eliminate these variables as possible reasons for the current high differential transcript abundance levels observed between treated and untreated parasites (UT0 vs. T4), subsequent comparative analysis and manual curation of transcripts was conducted. Comparisons between the top 20 transcripts with highest increase and decrease in abundance between 0 and 4 hours post treatment and the subset of transcripts associated with differential abundance upon culture adaptation (Table 2.1), identified mostly unique transcripts for each data set (C0 vs. C4 and UT0 vs. T4). Interestingly, within the treated data set, transcripts associated with the ABC transporter superfamily (BBOV_III009450; BBOV_III004900) were identified. It therefore appears as though transmembrane movement of the drug takes place during the first four hours post treatment. In addition, the lipid metabolism

was influenced by treatment as transcripts associated with glycerol-3-phosphate dehydrogenase (BBOV_III000930) and long-chain acyl-CoA synthetases (BBOV_III002500) were differentially expressed within the first four hours post treatment.

Functional annotation and transcript description using the dCAS platform

Appendix 4.2 represents the entire repertoire of DEG's which were functionally annotated using the integrative dCAS platform. Here we present only the COG data and the DEG's which were functionally annotated based on their corresponding COG classification (*E-value* cut-off $\leq 1 \times 10^{-4}$). From the 238 up-regulated transcripts, only 78 (33%) were annotatable, compared to the 563 down-regulated transcripts of which only 306 (30%) were annotatable using COG.

Functional annotation and transcript description using BLAST2GO software

Several functional groups associated with the differentially expressed transcripts were identified using the B2G annotation programme. Gene sequences were first searched using BLASTx against the non-redundant (NR) NCBI database. Sequences were subsequently run through B2G annotation and mapping steps, to identify the three major GO-assignments including biological process, molecular function and cellular component (for all up-regulated and down-regulated sequences). Figure 4.6 (A – C) represent the three major GO-assignments associated with all the up and down -regulated transcripts identified in our data set.

Interestingly, the largest clusters of affected transcripts with either an increase or decrease in abundance were mostly the same and included the response to stimuli and metabolic processes (biological processes), binding and catalytic activities (molecular functions) and organelle and cell (cellular compartments). Additionally, the membrane enclosed lumen, transporter and

electron carrier activity was only affected in transcripts with an increase in abundance compared to the symplast only affected in transcripts with a decrease in abundance (Figure 4.6).

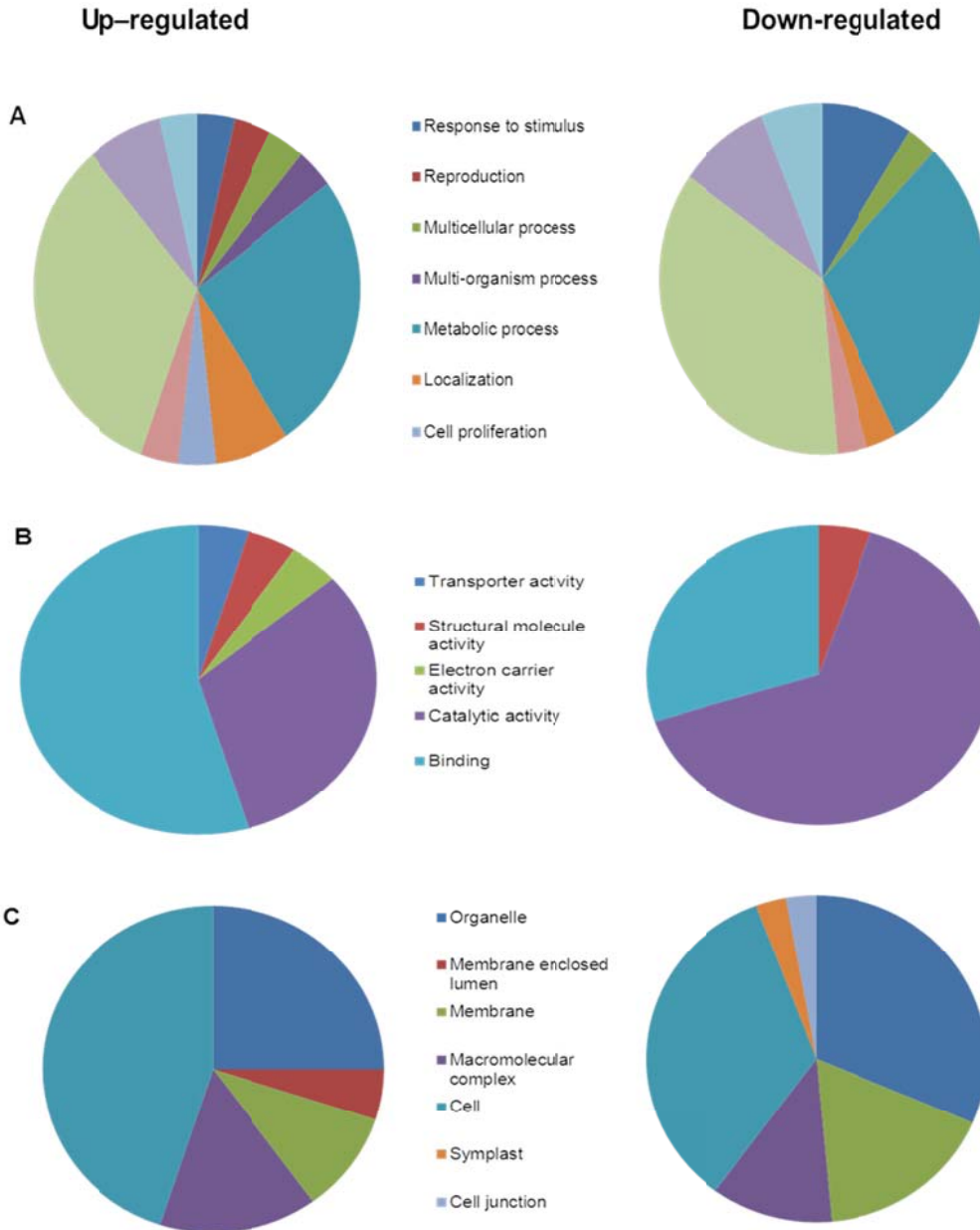


Figure 4.6 GO-annotation and functional grouping of transcripts of increased (up-regulated) and decreased (down-regulated) abundance after treatment.

Transcripts were assigned to various groups based on the three major GO-assignments (biological process, molecular function and cellular component) and functional annotations. (A) Biological processes (B) Molecular functions and (C) Cellular components mostly affected for both up and down-regulated transcripts are shown.

Metabolic pathway identification, enrichment and mapping using the KAAS-KEGG database

KEGG pathway analysis is an alternative approach to categorize gene functions with emphasis on biochemical pathways. Upon further enrichment of the GO-annotations, the annotated gene sequences were searched for genes involved in COG classification. To identify the biological pathways activated, approximately 166 annotated sequences (1×10^{-4} *E-value*) were mapped to the reference pathways of *B. bovis* using the KAAS-KEGG computer programme (<http://www.genome.jp/tools/kaas/>). The pathways were analysed based on the highest results related to the COG classification system (*E-value* of 1×10^{-4}). Data is presented for the gene transcripts and pathways with the highest increase and decrease in abundance, respectively (Table 4.4).

Table 4.4 Functional annotations of gene transcripts with the highest increase and decrease in abundance according to COG (E -values 1×10^{-4}), together with the number of genes involved in each pathway.

Functional annotation	*No. genes
Increase in abundance (in treated samples)	
Aminoacyl-tRNA biosynthesis	5
Spliceosome	4
Biosynthesis of secondary metabolites	3
Purine metabolism	3
Oxidative phosphorylation	2
Glycine, serine and threonine metabolism	2
RNA polymerase	2
Pyruvate metabolism	2
Pyrimidine metabolism	2
Decrease in abundance (in treated samples)	
Biosynthesis of secondary metabolites	4
RNA transport	4
Purine metabolism	4
mRNA surveillance pathway	3
RNA degradation	3
Spliceosome	3
Ubiquitin mediated proteolysis	3
Pyrimidine metabolism	3
Ribosome	3

* No. genes represent the number of genes associated with each pathway that were either up or down –regulated

Besides GO-analysis, KEGG pathway analysis was also carried out for all DEG's, including all transcripts that either increased or decreased in abundance. The pathways and enzymes identified for all transcripts that either increase or decrease in abundance are summarized in Appendix 4.3. KEGG pathways were constructed for the top five pathways involved in differential gene expression (Table 4.5) and include the purine metabolism, aminoacyl-tRNA biosynthesis, spliceosome, RNA transport as well as the pyrimidine metabolism. The entire repertoire of KEGG pathways and enzymes involved in differential gene expression is presented in Appendix 4.4.

Table 4.5 The top five KEGG pathways involved in differential gene expression.

KEGG entry	Definition	Genetic information processing	Enzymes	Direction (Up / Down)
Purine Metabolism				
k00948	Ribose-phosphate pyrophosphokinase	Nucleotide metabolism	Transferase	Down
k03040	DNA-directed RNA polymerase subunit alpha	Nucleotide metabolism	Transferase	Down
k02335	DNA polymerase I	Nucleotide metabolism	Transferase	Down
k01951	GMP synthase (glutamine-hydrolyzing)	Nucleotide metabolism	Transferase	Up
k01939	Adenylosuccinate synthase	Nucleotide metabolism	Transferase	Down
Aminoacyl-tRNA biosynthesis				
k01885	Glutamyl-tRNA synthetase	Translation	Ligase	Up
k02433	Aspartyl-tRNA / glutamyl-tRNA (Gln) amidotransferase subunit A	Translation	Ligase	Down
k01874	Methionyl-tRNA synthetase	Translation	Ligase	Down
k01873	Valyl-tRNA synthetase	Translation	Ligase	Up
k01870	Isoleucyl-tRNA synthetase	Translation	Ligase	Up
k04566	Lysyl-tRNA synthetase, class I	Translation	Ligase	Up
k01889	Phenylalanyl-tRNA synthetase alpha chain	Translation	Ligase	Up
Spliceosome				
k12811	ATP-dependent RNA helicase PRP5	Transcription	Hydrolase	Down
k12813	pre-mRNA splicing factor ATP dependent RNA helicase	Transcription	Hydrolase	Up
k12828	Splicing factor 3B subunit 1	Transcription	Hydrolase	Up
k12872	pre-mRNA splicing factor RBM22	Transcription	Hydrolase	Up
k12848	Tri-snRNP component SNU23	Transcription	Hydrolase	Up
k12877	Protein mago nashi	Transcription	Hydrolase	Down
RNA-transport and Pyrimidine metabolism				
k07936	GTP-binding nuclear protein Ran	Translation	-	Down
k03245	Translation initiation factor 3 subunit J	Translation	-	Down
k12877	Protein mago nashi	Translation	-	Down
k13126	Polyadenylate-binding protein	Translation	-	Down
k00226	Dihydroorotate dehydrogenase (fumarate)	Nucleotide metabolism	Oxidoreductases	Down
k03040	DNA-directed RNA polymerase subunit alpha	Nucleotide metabolism	Transferases	Down
k02335	DNA polymerase I	Nucleotide metabolism	Transferases	Down

Functional annotation using GSEA computer software

Unlike traditional GO-term analysis, GSEA used a ranked ordered list of genes as input, rather than individual genes. Results obtained may potentially be more biologically meaningful as it considers entire data set and functionally related gene annotations, as opposed to individual terms. For the GSEA analysis (conducted across the entire temporal evaluation spectra), a total of 24 gene-sets were selected according to certain filters (*i.e.* gene-set size) and used for subsequent analysis. The rank ordered gene list for all features within the data set is presented in Figure 4.7. The data set used for GSEA analysis contained approximately 2705 features (genes), of which 1284 genes were classified as untreated with a correlation area of 46.3%, compared to the 1421 treated genes with a 53.7% correlation area (Figure 4.7). Nine out of the total of 24 gene-sets were up-regulated among untreated samples, with one gene-set (transcription) significantly enriched at nominal $P < 0.05$. This was fully understandable and could be ascribed to general life-cycle, growth and development and culture adaptations during the parasite's IDC. Among the treated samples, 15 gene-sets were up-regulated with one (cytoskeleton) significantly enriched at nominal $P < 0.05$. Interestingly, the transcription gene-set (significantly enriched among untreated samples) was not one of the 15 gene-sets enriched among the treated samples (Table 4.6).

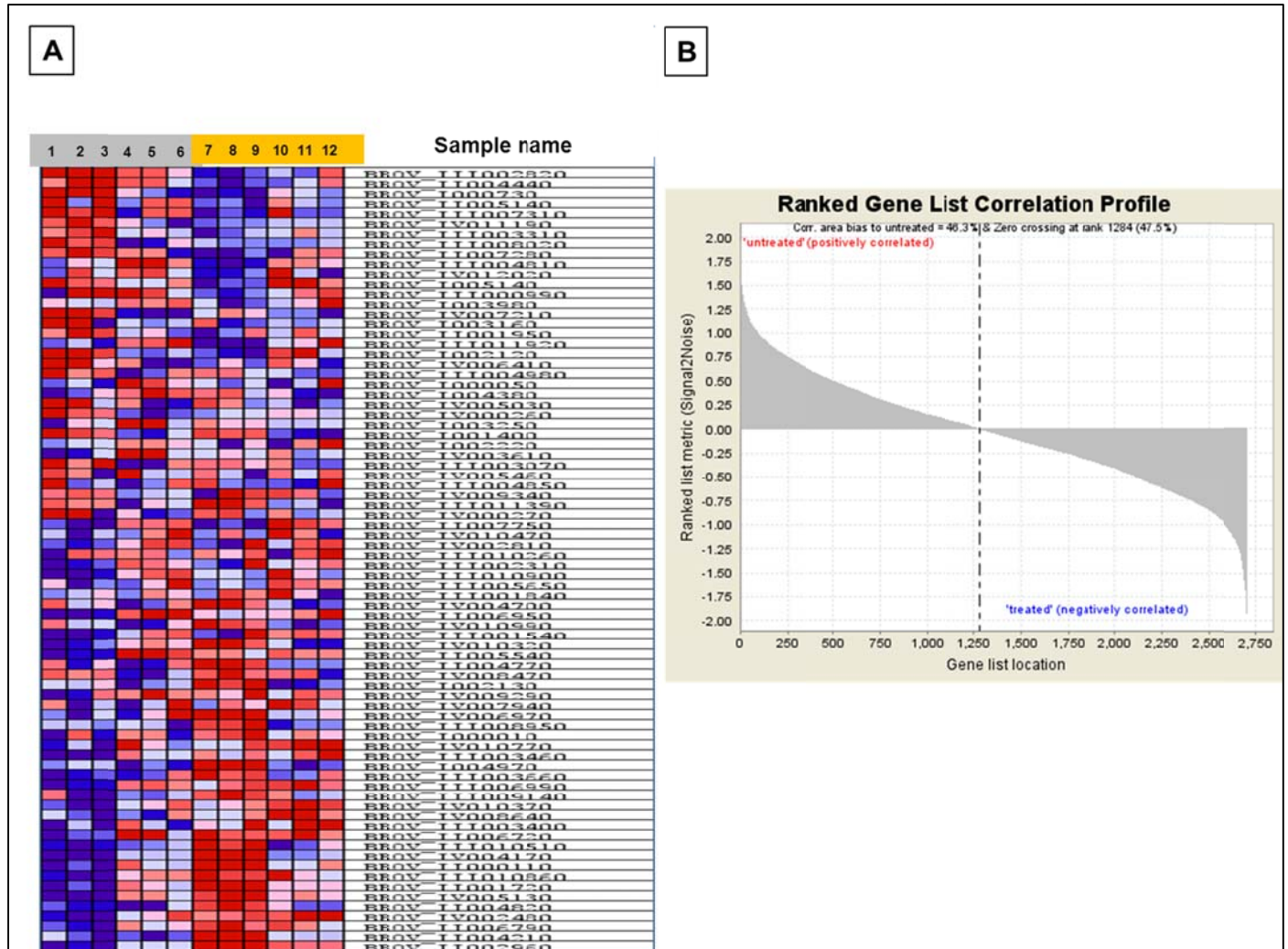


Figure 4.7 Heatmap and correlation plot of the top 50 features associated with each phenotype (untreated or treated) in association with the ranked list of genes.

(A) Heatmap of the top 50 genes found within the data set that differed significantly between the untreated and treated phenotypes. These genes are shown and labelled (top left) according to the original sampled time categories (1) 0-4 hrs; (2) 0-9 hrs; (3) 0-16 hrs; (4) 4-9 hrs; (5) 4-16 hrs and (6) 9-16 hrs for untreated (grey) phenotypes and (7) 0-4 hrs; (8) 0-9 hrs; (9) 0-16 hrs; (10) 4-9 hrs; (11) 4-16 hrs and (12) 9-16 hrs for treated (yellow) phenotypes. The range of color bars indicate the range of expression values as follows red (high), pink (moderate), light blue (low) and dark blue (lowest). (B) Correlation plot indicating the sorted expression data set's correlation to a particular phenotype (*i.e.* untreated or treated). The ranking metric measures the correlation between genes (identified from the expression data set) and either untreated or treated phenotypes. A positive value indicates correlation to the untreated phenotype, while a negative value indicates correlation to the treated phenotype.

Table 4.6 Gene-sets enriched among untreated and treated phenotypes (with highest associated significance levels) observed across all time-points.

Enriched gene-sets associated with untreated samples	ES ^a	NES ^b	NOM P-value ^c
Transcription	0.24958	1.26010	0.02244
Energy production and conversion	0.26416	1.27887	0.07128
RNA processing and modification	0.20779	1.08328	0.25933
Extracellular structures	0.25603	0.95539	0.54960
Translation, ribosomal structure and biogenesis	0.17291	0.90482	0.72564
Carbohydrate transport and metabolism	0.20069	0.86413	0.72727
Lipid transport and metabolism	0.18295	0.81292	0.85192
Inorganic ion transport and metabolism	0.16061	0.77193	0.96108
Cell cycle control, cell division, chromosome partitioning	0.15203	0.70559	0.96463
Enriched gene-sets associated with treated samples	ES ^a	NES ^b	NOM P-value ^c
Cytoskeleton	-0.3571	-1.43756	0.01402
Cell wall/membrane/envelope biogenesis	-0.3280	-1.30792	0.07171
Coenzyme transport and metabolism	-0.3909	-1.18278	0.30434
Nucleotide transport and metabolism	-0.3120	-1.12872	0.27027
Signal transduction mechanisms	-0.2018	-1.06898	0.26946
Amino-acid transport and metabolism	-0.2436	-1.05200	0.34291
Post-translational modification, protein turnover, chaperones	-0.2002	-1.05077	0.35892
Secondary metabolites biosynthesis, transport and catabolism	-0.3076	-1.01931	0.44874
Function unknown	-0.1883	-0.93740	0.66267
Intracellular trafficking, secretion, and vesicular transport	-0.1768	-0.91661	0.70833
Defence mechanisms	-0.2829	-0.90624	0.61660
Nuclear structure	-0.2532	-0.89239	0.65753
General function prediction	-0.1694	-0.86380	0.81800
Chromatin structure and dynamics	-0.1858	-0.81715	0.80838
Replication, recombination and repair	-0.1444	-0.74443	0.96687

**a Enrichment score (ES) for the associated gene-set represents the degree to which the gene-set is over-represented at the top of bottom of the ranked list of genes in the expression data set; *b Normalized enrichment score (NES) represents the enrichment score for the gene-set after normalization across the analyzed gene-sets; *c Nominal p-value (NOM P-value) represents the statistical significance of a gene-set ($P < 0.05$).*

The top 50 genes enriched within the data set that differed significantly ($P < 0.05$) between the untreated and treated phenotypes are illustrated in Figure 4.7 (A), where the range of gene expression is indicated by a range of colors. The primary result obtained from the GSEA analysis was the enrichment score (ES), which represented the degree to which a gene-set was overrepresented at either the top or bottom of the ranked list of genes. The distribution pattern

of gene-sets significantly enriched at nominal $P < 0.05$ (for both untreated and treated phenotypes) are illustrated in Figure 4.8, with their respective ES values between 0.26 and -0.35.

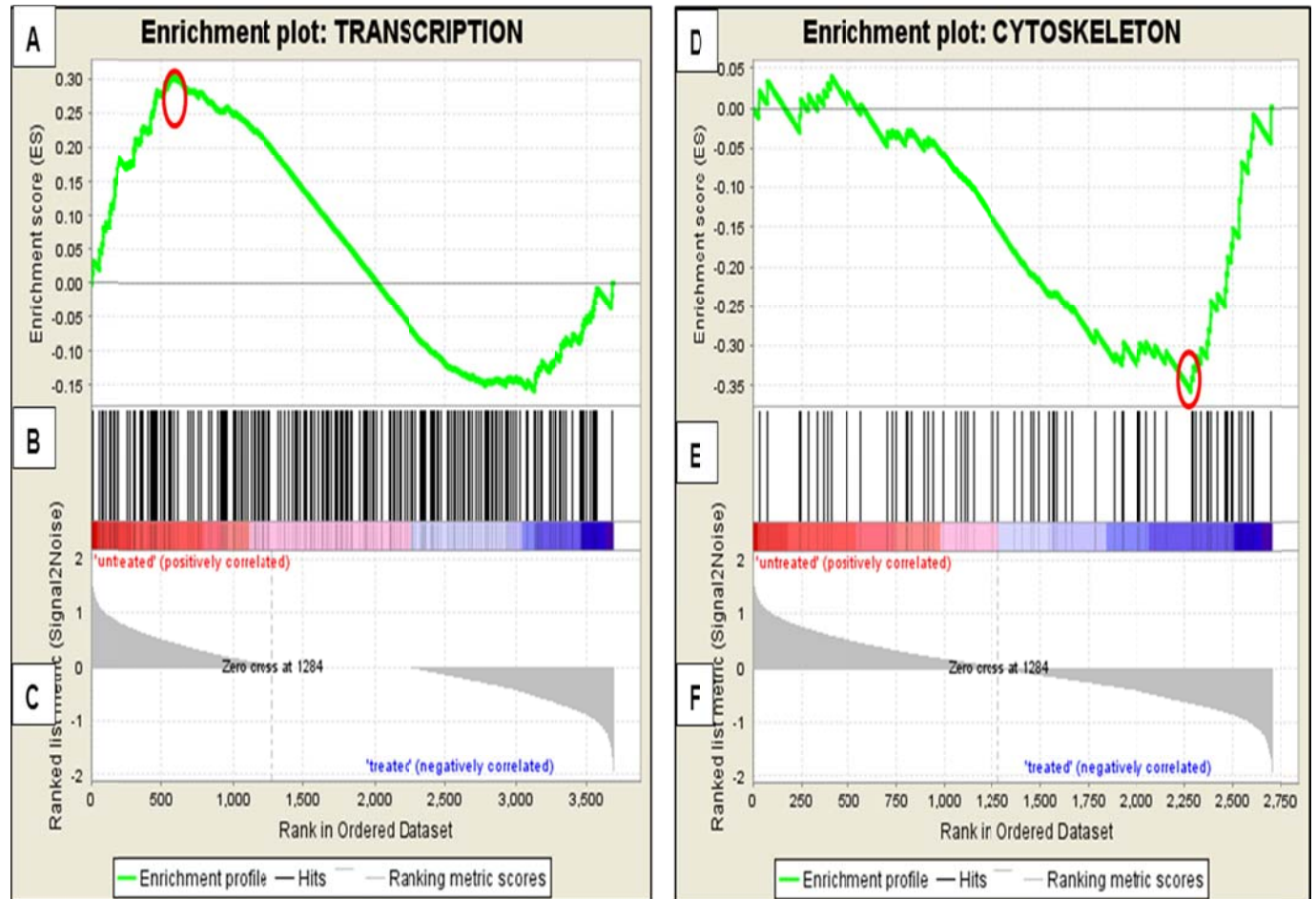


Figure 4.8 Graphical representation (enrichment plots) for the two most significantly enriched gene-sets associated with untreated (transcription; left plot) and treated (cytoskeleton; right plot) phenotypes.

The areas indicated by A and D represents the level of enrichment (ES) for most significantly enriched untreated (transcription) and treated (cytoskeleton) gene-sets, respectively. The scores furthest from 0.0 (marked with red circles) are regarded as the ES for the particular gene-sets (0.26 and -0.35, respectively). The plot areas indicated by B and E represents the location of the maximum ES scores of the particular gene-sets, within the ranked gene list. The ranking metric (C and F) measures the correlation between genes (identified from the expression data set) and either untreated or treated phenotypes. A positive value indicates correlation to the untreated phenotype, while a negative value indicates correlation to the treated phenotype.

Metabolic profiling of differential transcriptional responses

Based on *in silico* methods previously developed for other apicomplexans such as *P. falciparum*, *B. bovis* and *Theileria* species, we were able to link gene annotations for treated *B. divergens* parasites (over a 16-hour period) into a metabolic response. A series of metabolic pathways for the treated pathogen were predicted *in silico* and reconstructed based on the *B. bovis* metabolic profile and automated functional annotations with subsequent manual curation.

The predicted metabolic profile of *B. bovis* is more closely related to that of *Theileria* than that of *P. falciparum* (Brayton *et al.*, 2007). Upon invasion, *Babesia* parasites rapidly escape their parasitophorous vacuole and freely proliferate within the cytoplasm of erythrocytes and lymphocytes, consequently gaining more direct access to hosts' nutrients (Seeber *et al.*, 2008). This nutrient abundance is reflected in the absence of several major metabolic pathways including purine salvage, folate biosynthesis, polyamine biosynthesis, urea cycle, *de novo* purine biosynthesis, gluconeogenesis, haem biosynthesis, type II fatty-acid biosynthesis and the shikimic acid pathway (Brayton *et al.*, 2007).

The mitochondria and apicoplast of apicomplexans are physically closely associated, which may complicate separate biochemical analysis of these organelles. Glucose is the major carbon and energy source for *B. bovis* parasites, however based on the absence of pyruvate dehydrogenase, no classical link between glycolysis and the tricarboxylic acid cycle (TCA-cycle) is known (Brayton *et al.*, 2007). In treated parasites, a decrease in glyceraldehyde-3-phosphate dehydrogenase; long-chain acyl-CoA synthetases (AMP-forming) and citrate synthase, associated with the TCA-cycle was observed (Table 4.3 and Figure 4.9). Within the mitochondria carbon fuels are oxidized to generate cellular energy *via* oxidative phosphorylation. We hypothesize that the decreased TCA-cycle substrates and cycle activity was balanced by the observed increase in oxidative phosphorylation levels (F-type H⁺-

transporting ATPase; cytochrome c oxidase) within the mitochondria (Table 4.4 and Appendix 4.3).

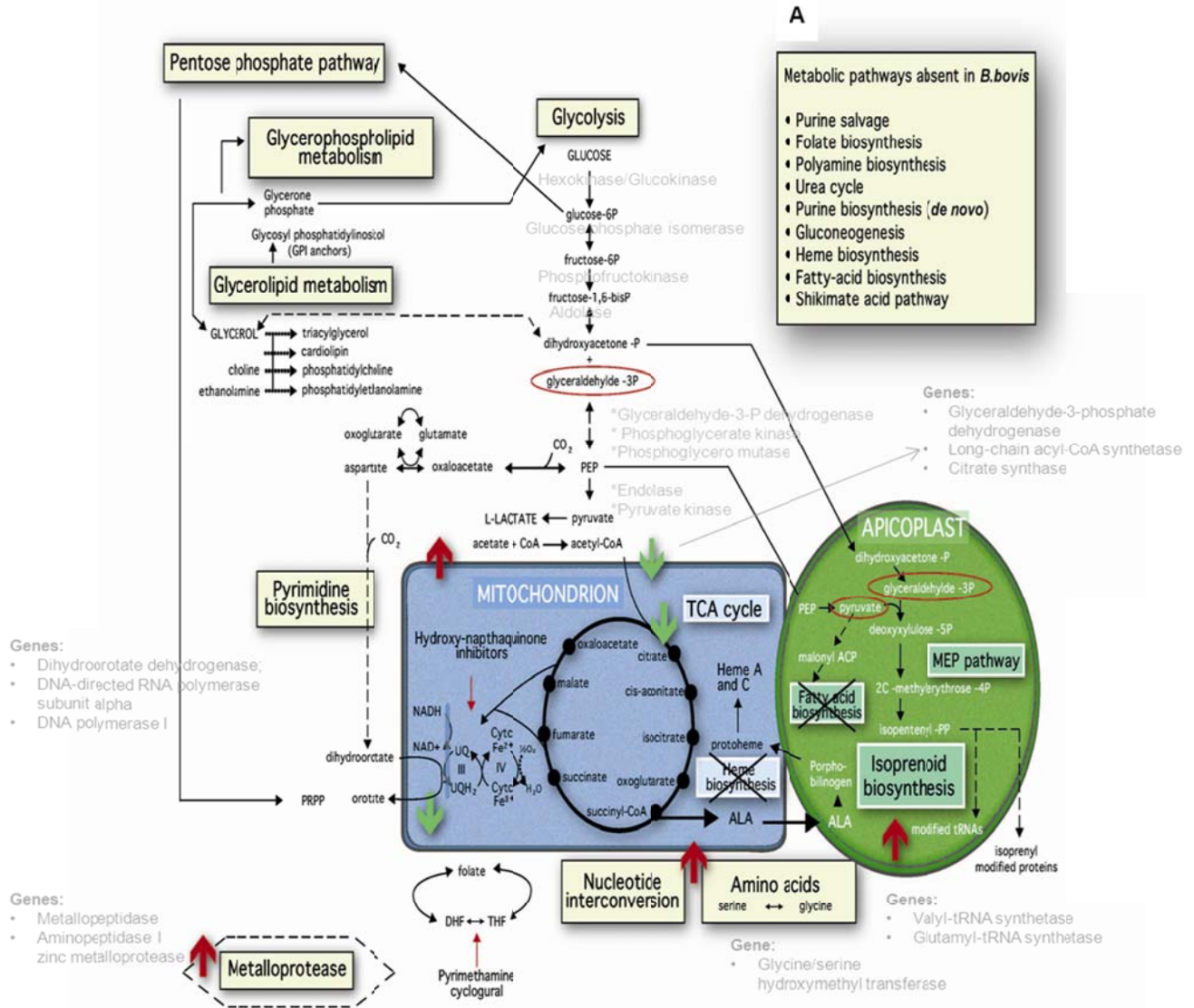


Figure 4.9 Major metabolic pathways of *B. divergens* affected by treatment.

Non-functional pathways in *B. bovis* are indicated by box A. Red and green arrows indicate pathways or substrates affected by treatment as well as the degree of activity (either increase [red] or decrease [green]). Solid black arrows indicate single step enzymatic reactions and dotted arrows indicate multiple-step reactions. Red encircled substrates indicate molecules affected by treatment.

A glycine-cleavage system, comprising of four enzymes that convert glycine into N5, N10-methylenetetrahydrofolate (a known precursor for pyrimidine biosynthesis) was also detected. In addition the cleavage system allows serine catalysis *via* serine hydroxymethyltransferase (Seeber *et al.*, 2008). The pyrimidine biosynthesis pathway was influenced by treatment, as a reduction in pyrimidine precursors was observed (dihydroorotate dehydrogenase (fumerate); DNA-directed RNA polymerase subunit alpha; DNA polymerase I) (Table 4.4 and Table 4.5). We hypothesize that the observed increased amino acid inter-conversion activity between serine and glycine aimed to balance the reduced pyrimidine precursor levels (Figure 4.9).

The apicoplast houses several metabolic pathways essential for the synthesis of fatty acids (FA II), isoprenoids and iron-sulphur (Fe-S) clusters, only two of which are shared among all apicomplexans - the non-mevalonate pathway (also known as the DOXP pathway [1-deoxy-D-xylose-5-phosphate] or MEP pathway [2C-methyl-D-erythritol-4-phosphate]) and the partial iron-sulphur cluster assembly (Fe-S) pathway (Fleige *et al.*, 2010). To ensure functionality of these pathways and their products, the apicoplast must import certain compounds such as phosphoenolpyruvate (PEP), dihydroxyacetone-phosphate and aminolevulinic acid (ALA) (van Dooren and Striepen, 2013) (Figure 4.9). Isopentenyl pyrophosphate (IPP) forms the basic building blocks and universal precursor of isoprenoids, synthesized *via* the DOXP/MEP pathway (van Dooren and Striepen, 2013), which form key components in several biological systems including protein modification, tRNA modification and cell membrane maintenance (Hunter, 2011). Increased pyruvate metabolism activity (glycerol-3-phosphate dehydrogenase) was observed after treatment (Table 4.3), which subsequently increased glyceraldehyde-3-phosphate (G3P) levels within the cell. As both are precursors for the DOXP/MEP pathway, an increase in the isoprenoid biosynthesis pathway can be expected. An increase in modified tRNA production was subsequently observed (valyl-tRNA synthetase; glutamyl-tRNA synthetase) (Table 4.3; Table 4.4; Table 4.5). In contrast to elevated tRNA levels, proteolytic activity was

reduced (predicted RNA-binding protein Pno1p) which suggests that either no protein is being degraded and/or no new proteins are being synthesized (Table 4.3 and Table 4.4). The proteolytic machinery was originally thought to be primarily involved in protein recognition and elimination, studies have however uncovered additional proteolytic functions in several important biological processes such as the modulation of the cellular micro-environment by metalloproteases (Chang and Werb, 2001). We suggest that in order to counter balance the observed reduction in proteolytic activity, metalloprotease production (metallopeptidase; aminopeptidase I zinc metalloprotease (M18)) was subsequently increased (Table 4.3).

RNA helicase; chromatin remodeling protein HARP/SMARCAL1, DNA polymerase epsilon catalytic subunit A; Sof1-like rRNA processing protein; global transcriptional regulator, cell division control protein and U4/U6-associated splicing factor PRP4 were affected, suggests that the traditional flow of transcription within *B. divergens* cells was altered upon treatment (Table 4.3).

The observed decrease in ribosomal activity (protein phosphatase 2; protein mago nashi; polyadenylate-binding protein) (Table 4.4 and Appendix 4.3) was overcome by the elevated RNA pol I (RNA polymerase I, large subunit) and RNA pol III production (RNA polymerase III, second largest subunit) (Table 4.3 and Figure 4.10 A₁-A₂). The increased RNA pol I and III levels subsequently allowed for increased tRNA production (valyl-tRNA synthetase; glutamyl-tRNA synthetase) (Table 4.3 and Figure 4.10 D₁). In general, RNA polymerase II (Pol II) mediated mRNA synthesis (pre-mRNA) is capped at the 5' end, spliced, cleaved at the 3' end and polyadenylated (Köhler and Hurt, 2007). RNA Pol II biogenesis and activity was not affected by treatment.

The spliceosome is a dynamic, ribonucleoprotein complex responsible for the catalysis of nuclear pre-mRNA splicing (Will and Lührmann, 2011). Increased spliceosomal activity was

observed after treatment (ATP-dependent RNA helicase PRP5; pre-mRNA splicing factor ATP dependent RNA helicase; pre-mRNA splicing factor RBM22; splicing factor 3B subunit 1; tri-snRNP component SNU23) (Table 4.4; Table 4.5; Figure 4.10 B; Appendix 4.4), we hypothesized that the increased spliceosomal activity subsequently increased nuclear pre-mRNA production which inundated the nucleus and decreased mRNA transport to the cytoplasm (Figure 4.10 C). The transport/export of mRNA molecules from the nucleus to the cytoplasm is essential for successful gene expression (Köhler and Hurt, 2007). A decrease in mRNA transport from the nucleus to the cytoplasm was observed after treatment (GTP-binding nuclear protein Ran; translation initiation factor 3 subunit J; protein mago nashi; polyadenylate-binding protein), thereby hindering protein synthesis and gene expression (Table 4.4; Table 4.5; Figure 4.10 C).

The observed decrease in RNA degradation (ATP-dependent DNA helicase; chaperonin GroEL; 5'-3' exoribonuclease 2; polyadenylate-binding protein) and mRNA surveillance pathway (protein phosphatase 2; protein mago nashi; polyadenylate-binding protein) activity within the cytoplasm implies that the cell stores processed mRNA already present within the cytoplasm for translation to take place at a later stage (Table 4.4 and Appendix 4.3). It ultimately appeared as if protein production was hindered (Figure 4.10 D₂). As no proteins were synthesized, the cell was in a “protein-stand-by-mode”, preparing for protein production at a later stage, with tRNA and ribosomes available.

The dynamic fibrous cytoskeleton network is located within the cytoplasm of the cell and has the ability to be remodeled in order to meet cellular requirements in response to environmental changes. In addition, it is a signaling platform modulating cellular and molecular events and provides structural scaffolding to the cell (Fletcher and Mullins, 2010). Apicomplexans are characterized by their unique cytoskeleton. The polar-ring complex is a specialized microtubule-organizing center present at the apical end of the organism which assists in motility and

invasion processes (Gordon and Sibley, 2005). Recent evidence suggests that the cytoskeleton is additionally involved in the spatial organization and regulation of translation in such a manner that is essential for cell growth and function referred to as the cytoskeleton-associated protein synthesis machinery (Kim and Coulombe, 2010). The physical link between the cytoskeleton and translation components assists in global and local protein synthesis and therefore allows aminoacyl-tRNA's and their metabolites to be transferred by cytoskeleton-bound components associated with the protein synthesis apparatus including aminoacyl-tRNA synthetase; glutamyl-tRNA synthetase; aspartyl-tRNA/glutamyl-tRNA amidotransferase subunit A; aspartyl-tRNA/glutamyl-tRNA amidotransferase subunit A; methionyl-tRNA synthetase; valyl-tRNA synthetase; isoleucyl-tRNA synthetase; lysyl-tRNA synthetase, class I; phenylalanyl-tRNA synthetase alpha chain and eukaryotic elongation factors (translation initiation factor 1A) (Table 4.3). Free tRNA's are charged as aminoacyl-tRNA's and subsequently used as building blocks for the elongation of protein chains (Kim and Coulombe, 2010). The enriched cytoskeletal gene-set associated with the treated sample phenotype links to results of Table 4.3 and Table 4.4, where we observed increased aminoacyl-tRNA biosynthesis levels.

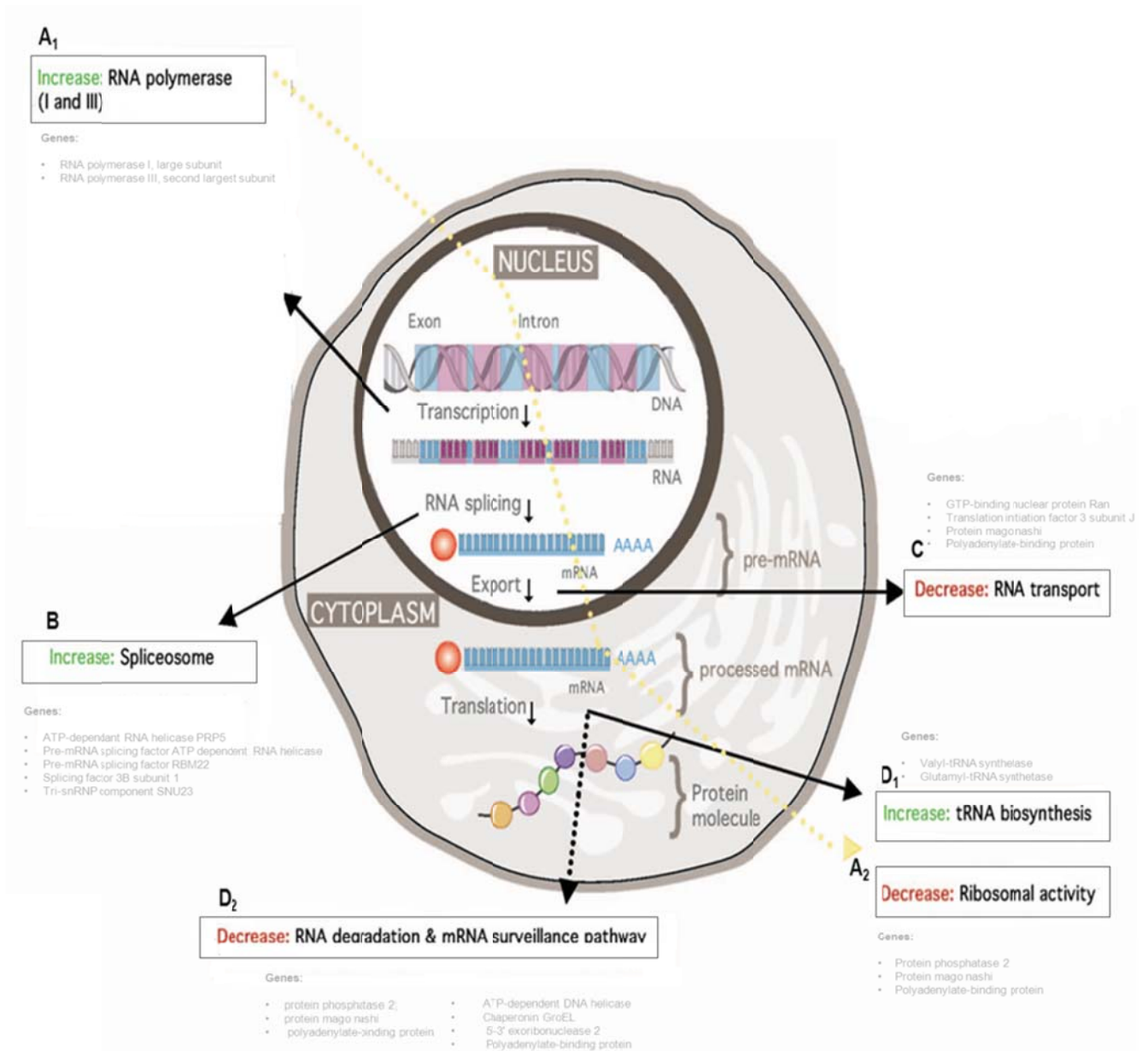


Figure 4.10 Overview of flow of information in treated *B. divergens* parasites, from DNA to protein.

(A₁) Within the nucleus, transcription was altered by an increase in RNA pol I and RNA pol III production (A₂) which was linked to the decrease in ribosomal activity in the cytoplasm (B) RNA-splicing was affected by the increase in spliceosomal activity (C) A decrease in RNA transport/export from the nucleus to the cytoplasm (D₁) Within the cytoplasm an increase in tRNA biosynthesis (D₂) along with a decrease in RNA degradation and mRNA surveillance pathways were observed. Black arrows indicate the altered cellular activity and its position within the cell. Yellow dotted arrow links altered activity within the nucleus to altered activity within the cytoplasm.

In a parallel study within our research group, the hybridization-based (DNA-microarray) assessment of A51B1C1_1 treated *B. divergens* parasites was compared to a next-generation sequencing-based (RNA-Sequencing) assessment of the parasites *in vitro*. Results revealed several shared differentially expressed transcripts under drug (A51B1C1_1) treatment.

4.3.2 Comparative transcriptome analyses between species

***B. divergens* and *P. falciparum* response to A51B1C1_1 treatment**

For the orthologue group comparisons to be accurate, comparable data sets between different species, under similar conditions were used. The transcriptional effects of galvestine-1 and one of its derivatives (A51B1C1_1) was previously evaluated as monogalactosyldiacylglycerol (MGDG) inhibitors in *A. thaliana* (Botte *et al.*, 2011) as well as for their anti-malarial properties against *P. falciparum* (Snyman, 2011). As previously described, both compounds have similar chemical structures and are derivatives of the scaffold compound.

During clustering, the OrthoMCL database determined the global pattern of sequence similarity between provisionally grouped sequences (Chen *et al.*, 2005). The orthologue clustering of transcripts associated with *B. bovis* and *P. falciparum* were constructed, and presented as an orthologue group-matrix. Using a combination of orthologue group identification and manual curation strategies, we matched 317 differentially expressed *B. divergens* transcripts (based on their corresponding *B. bovis* gene names) to orthologue groups within the *B. bovis* - *P. falciparum* orthologue group-matrix (Appendix 4.5). In addition, 520 differentially expressed *P. falciparum* transcripts were matched to orthologue groups within the *B. bovis* - *P. falciparum* orthologue group-matrix (Appendix 4.6). The transcripts differentially expressed in both A51B1C1_1 treated data sets were used for subsequent comparative analyses.

In total we identified 90 shared orthologue groups, distributed throughout 34 domains (including the hypothetical protein domain) between the differentially expressed *P. falciparum* and *B. divergens* A51B1C1_1 treated transcriptome data sets. Genes associated with each of these groups can therefore be regarded as orthologues between the two apicomplexan species based on the *P*-value (< 0.05) generated using the *phyper* function within the R-statistical environment (Figure 4.11). An important application of orthologue group identification and grouping is the ability to functionally characterize proteins (Li *et al.*, 2003). The 90 orthologue groups with corresponding functional annotations, domains and biological processes shared between the differentially expressed transcripts of treated *P. falciparum* and *B. divergens* cultures, are summarized in Table 4.7. The differential transcript abundance (based on the \log_2 -ratios of each gene's fold change) for each gene, associated with either *P. falciparum* or *B. divergens* is additionally provided, indicating either an increase or decrease in gene expression levels. Among the differentially expressed transcripts, a total of 224 *B. divergens* specific (unique) orthologue groups were observed compared to the 418 *P. falciparum* specific (unique) orthologue groups (Appendix 4.7; Figure 4.11). These unique transcripts represent good candidates for understanding species-specific differences and transcriptomic response to treatment, while the 90 shared orthologue groups guide the way to potential targets for therapeutic use.

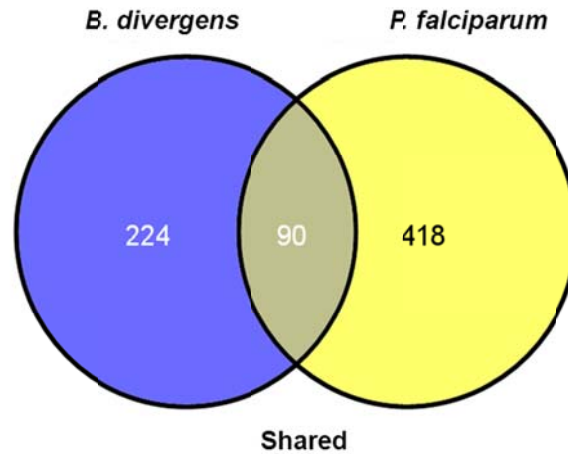


Figure 4.11 Unique and shared orthologue groups between the A51B1C1_1 treated transcriptome data sets from *B. divergens* and *P. falciparum*.

A total of 90 orthologue groups were shared between the differentially expressed transcripts. A total of 224 *B. divergens* and 418 *P. falciparum* specific orthologue groups were observed among the differentially expressed transcripts of each data set.

Table 4.7 Orthologue clustering and functional grouping of transcripts present in *P. falciparum* and *B. divergens* data sets post A51B1C1_1 treatment.

Orthologue group name	<i>P. falciparum</i> DEG's	<i>B. bovis</i> gene name (<i>B. divergens</i> DEG's)	Functional annotation and Domain	Associated biological process	^a <i>P. falciparum</i> (Up/Down)	^b <i>B. divergens</i> (Up/Down)
OG5_126579	PFE0070w	BBOV_IV003650	NA	-	-	-
OG5_126620	PF11_0296	BBOV_IV002290	ParA/MinD ATPase like	Binding	Up	Up
OG5_126678	PFE0960w	BBOV_II002750	Ribosomal protein	Translation	Down	Up
OG5_126684	PF13_0179	BBOV_II005760	tRNA synthetases class I	Translation	Down	Up
OG5_126730	PF13_0143	BBOV_IV008060	Phosphoribosyl transferase domain	Nucleoside metabolism	Up	Down
OG5_126733	PF14_0455	BBOV_III011170	ABC transporter transmembrane region	Transport	Up	Up
OG5_126885	PF14_0075	BBOV_III003510	Eukaryotic aspartyl protease	Protein degradation	Up	Down
OG5_126886	PFA0555c	BBOV_II007680	Adenylate kinase	Signaling	Down	Down
OG5_126969	PF10_0193	BBOV_III005950	Microtubule associated protein 1A/1B	Mitochondrial associated activity	Down	Up
OG5_127127	PF11_0447	BBOV_III011550	Translation initiation factor	Translation	Up	Down
OG5_127148	PFA0520c	BBOV_IV001160	WD domain	Signaling	Up	Up
OG5_127152	PF10_0123	BBOV_IV009110	GMP synthase C terminal domain	Binding	Up	Up
OG5_127153	PF08_0085	BBOV_II004660	Ubiquitin-conjugating enzyme	Protein degradation	Up	Up
OG5_127206	PF13_0213	BBOV_II000880	Ribosomal protein	Translation	Up	Up
OG5_127256	PF11_0461	BBOV_III004450	Ras family	Signaling	Down	Down
OG5_127273	PF13_0049	BBOV_III003570	Ribosomal protein	Translation	Up	Up
OG5_127312	PFF0345w	BBOV_II007250	Elongation factor Tu domain 2	Translation	Up	Up
OG5_127313	PF10_0066	BBOV_IV006740	Thioredoxin	Signaling	Up	Down
OG5_127333	PF14_0241	BBOV_III010510	NAC domain	Transcription	Up	Down
OG5_127366	PF08_0099	BBOV_IV000490	Acyl CoA binding protein	Fatty acid biosynthesis	Up	Down
OG5_127402	PF07_0057	BBOV_I002910	Transcription factor S-II central domain	Transcription	Up	Down
OG5_127464	PF14_0661	BBOV_IV008880	KH domain	Binding	Up	Down
OG5_127465	PFB0895c	BBOV_III002070	ATPase family	Transport	Down	Down
OG5_127498	PFL0660w	BBOV_IV005110	Dynein light chain type 1	Transport	Up	Up
OG5_127529	PFL2120w	BBOV_IV011250		NA		

OG5_127557	PF08_0094	BBOV_III006880	Cullin family protein domain	Translation	Down	Down
OG5_127574	PF14_0373	BBOV_III009930	Ubiquinol cytochrome reductase transmembrane region	Oxidation-reduction	Down	Down
OG5_127581	PFL0180w	BBOV_III011500	Cytochrome c/c1 haem lyase	Mitochondrial associated activity	Up	Up
OG5_127594	PF11_0477	BBOV_I000180	Histone-like transcription	Transcription	Down	Up
OG5_127669	PFF1335c	BBOV_I002290	DJ-1/Pfpl family	Transcription	Up	Up
OG5_127670	MAL7P1.130	BBOV_II007370	Methyltransferase domain	Transcription	Up	Up
OG5_127764	PF14_0177	BBOV_II005900	MCM2/3/5 family	DNA replication	Down	Up
OG5_127773	MAL7P1.147	BBOV_IV001730	Ubiquitin carboxyl-terminal hydrolase domain	Protein degradation	Down	Down
OG5_127784	PFB0860c	BBOV_I004200	DEAD/DEAH box helicase	RNA metabolism	Up	Up
OG5_127854	PF08_0109	BBOV_II002240	Proteasome	Protein degradation	Down	Down
OG5_127874	PFC0340w	BBOV_III004800	DNA polymerase alpha/epsilon subunit B	DNA replication	Up	Up
OG5_127881	PFD0930w	BBOV_II003960	Got1-like family	Transport	Down	Down
OG5_127936	PFL0665c	BBOV_IV005100	RNA polymerase	Transcription	Up	Down
OG5_127942	PFF1470c	BBOV_III009080	DNA polymerase	DNA replication	Down	Down
OG5_128020	PF11570c	BBOV_IV011550	Aminopeptidase I zinc metalloprotease	Protein degradation	Up	Up
OG5_128047	PF14_0429	BBOV_IV001200	DEAD/DEAH box helicase	RNA metabolism	Down	Down
OG5_128098	MAL13P1.36	BBOV_III004170		NA		
OG5_128133	PF11_0311	BBOV_III000660	Phosphoglucomutase C-terminal domain	Glucose metabolism	Up	Down
OG5_128165	PF14_0584	BBOV_IV002230	Ribosomal protein	Translation	Up	Up
OG5_128182	PFF1030w	BBOV_II007100	CPL (NUC119) domain	Binding	Down	Down
OG5_128219	PFL2195w	BBOV_I002870	ENTH domain	Cytoskeletal machinery	Down	Up
OG5_128225	PF11_0259	BBOV_IV008270	Ribosome biogenesis regulatory protein	Translation	Up	Up
OG5_128226	MAL13P1.294	BBOV_I003460	GTPase of unknown function	Various functions	Up	Down
OG5_128266	PF14_0328	BBOV_IV008220	Tim17/Tim22/Tim23 family	Mitochondrial associated activity	Up	Down
OG5_128295	PF13_0308	BBOV_III009710	SNF2 family N-terminal domain	Binding	Down	Down
OG5_128435	PF13_0234	BBOV_I003550	Phosphoenolpyruvate carboxykinase	Glucose metabolism	Up	Down
OG5_128486	PFF1140c	BBOV_IV011410	Helicase conserved C-terminal domain	Binding	Up	Down
OG5_128660	PF07_0091	BBOV_III002180	Cwf15/Cwc15 cell cycle control	Splicing	Down	Down

OG5_128667	PF13_0050	BBOV_II002160	HORMA domain	Chromatin associated activity	Down	Down
OG5_128678	PFI0335w	BBOV_IV005610	CAP-Gly domain	Cytoskeletal machinery	Up	Down
OG5_128839	PFL0430w	BBOV_IV008900	Tim10/DDP family zinc finger	Mitochondrial associated activity	Up	Up
OG5_128881	PF13_0164	BBOV_III003430		NA		
OG5_129173	PF14_0288	BBOV_IV010440	Cytochrome C oxidase subunit II, periplasmic domain	Transport	Down	Up
OG5_129228	PF14_0580	BBOV_III010690		NA		
OG5_129313	PFD0700c	BBOV_III008620	RNA recognition motif domain	Binding	Down	Down
OG5_129533	PF14_0679	BBOV_II006030	Sulfate transporter family	Transport	Down	Up
OG5_129939	PFC0850c	BBOV_II004670	Endonuclease family	Signaling	Up	Down
OG5_129958	MAL7P1.209	BBOV_III001380	ATPase family associated with various cellular activities	Transport	Up	Down
OG5_130863	PF10_0188	BBOV_III004710		NA		
OG5_133546	PF14_0281	BBOV_IV007890	Eukaryotic aspartyl protease	Protein degradation	Down	Down
OG5_135175	PFL1545c	BBOV_IV007010	TCP-1/cpn60 chaperonin family	Binding	Down	Up
OG5_136181	MAL7P1.13	BBOV_III009490		NA		
OG5_137217	PF07_0070	BBOV_III009010		NA		
OG5_138116	PF07_0017	BBOV_II006980	WD domain	Signaling	Down	Down
OG5_139037	PFB0435c	BBOV_IV002780	Sodium neurotransmitter symporter family	Transport	Down	Down
OG5_141266	PF14_0530	BBOV_II003690	C2 domain	Binding	Down	Down
OG5_141671	PF14_0383	BBOV_II001140		NA		
OG5_141728	PFI0845w	BBOV_I004350		NA		
OG5_141731	MAL13P1.308	BBOV_IV000700		NA		
OG5_142870	PF14_0495	BBOV_I001630		NA		
OG5_143209	PFD0910w	BBOV_IV004240	Domain of unknown function			
OG5_143212	MAL7P1.88	BBOV_IV007040	Thioredoxin	Signaling	Up	Down
OG5_144402	PFL1895w	BBOV_IV011820	Ribosomal protein	Translation	Up	Down
OG5_144710	PF10_0039	BBOV_II004030		NA		
OG5_145099	MAL8P1.25	BBOV_II000830		NA		
OG5_146858	PFE0670w	BBOV_IV003470		NA		

OG5_147414	PF10_0236	BBOV_IV003000		NA		
OG5_149676	PF11_0382	BBOV_III000770	Ribosomal protein	Translation	Up	Down
OG5_150527	MAL13P1.43	BBOV_I002960		NA		
OG5_150553	PFE1435c	BBOV_II004980	GTPase	Various functions	Up	Up
OG5_150565	PFC0911c	BBOV_IV006590		NA		
OG5_153060	MAL13P1.180	BBOV_I002860		NA		
OG5_153341	PFF0780w	BBOV_I003190		NA		
OG5_156796	PFE0770w	BBOV_II002720		NA		
OG5_160480	PF14_0166	BBOV_II001160	tRNA synthetases class II	Translation	Up	Up

**NA refers to non-annotatable in both species; a refers to P. falciparum transcripts that either increase (up) or decrease in abundance after treatment; b refers to B. divergens transcripts that either increase (up) or decrease in abundance after treatment*

Among the 90 shared orthologue groups, several biological processes including translation, transcription, transport, signalling, protein degradation, binding, glucose metabolism, fatty acid metabolism, nucleoside metabolism, spliceosomal activity, oxidation-reduction activity, cytoskeletal machinery and mitochondrial associated activities, were identified and associated with each group and transcript. Based on the expression levels of the associated transcript, translation, transcription, signalling and the mitochondrial associated pathways were predominantly up-regulated, while transport and binding activities mostly down-regulated among *P. falciparum*. Comparatively, translation and mitochondrial associated activities were mostly up-regulated, while binding and signalling activities predominantly down-regulated among *B. divergens* transcripts.

The “incompleteness” of several apicomplexan species’ genome sequence data poses a challenge for eukaryotic orthologue group identification, for example, within the apicomplexan lineage, *P. falciparum* is the only species with complete genome sequences available. Several true orthologues may therefore be missing and incorrect matches may be made (Li *et al.*, 2003). An additional challenge to consider in comparative gene expression studies is the dynamic nature of gene-expression, which is why we considered comparing orthologue groups, instead of gene expression values. The orthologue group comparison strategy takes into account the similarities and differences in the relative positions of the orthologue genes within their respective expression networks (Stuart *et al.*, 2003, Tirosh and Barkai, 2005).

***B. divergens* and *A. thaliana* response to treatment (A51B1C1_1 and galvestine-1)**

Orthologue clustering of transcripts associated with *B. bovis* and *A. thaliana* were constructed and presented as an orthologue group-matrix. Using a combination of orthologue group identification and manual curation strategies, we matched 237 differentially expressed *B. divergens* transcripts (based on their corresponding *B. bovis* gene names) to

orthologue groups within the *B. bovis* – *A. thaliana* orthologue group-matrix (Appendix 4.8). In addition, 101 differentially expressed *A. thaliana* transcripts (P -value < 0.05) were matched to orthologue groups within the *B. bovis* – *A. thaliana* orthologue group-matrix (Appendix 4.9). The transcripts differentially expressed between the A51B1C1_1 treated data set and the galvestine-1 treated data set were used for further comparative transcriptomic analyses.

In total we identified ten shared orthologue groups between the differentially expressed *A. thaliana* and *B. divergens* data sets. The minor differences in compound structures (Chapter 1) may result in differences related to compound effects. Genes associated with each of these groups can therefore be regarded as orthologues, based on the P -value (< 0.05) generated within the R-statistical environment (Figure 4.12). The ten shared orthologue groups with corresponding functional annotations and domains are summarized in Table 4.8. Among the differentially expressed transcripts a total of 223 *B. divergens* specific (unique) orthologue groups were observed, compared to the 51 *A. thaliana* specific (unique) orthologue groups (Appendix 4.10; Figure 4.12).

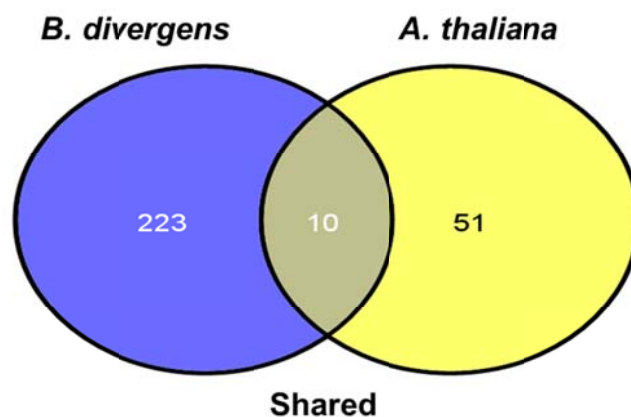


Figure 4.12 Unique and shared orthologue groups between the treated transcriptome data sets associated with *B. divergens* and *A. thaliana*.

A total of ten orthologue groups were shared between the differentially expressed transcripts. A total of 223 *B. divergens* and 51 *A. thaliana* specific orthologue groups were observed among the differentially expressed transcripts of each data set.

Table 4.8 Orthologue clustering and functional annotations associated transcripts within the *B. divergens* and *A. thaliana* data sets, after A51B1C1_1 and galvestine-1 treatment, respectively.

Orthologue group name	<i>A. thaliana</i> gene name	<i>B. bovis</i> gene name (<i>B. divergens</i> DEG's)	Functional annotation and domain	Associated biological process
OG5_127453	NP_567388	BBOV_I002210	SEC1B; protein transporter (<i>A. thaliana</i>); syntaxin binding protein (<i>B. bovis</i>)	Transport
OG5_127669	NP_188117	BBOV_I002290	DJ-1/Pfpl family	Transcription
OG5_128435	NP_195500	BBOV_I003550	Phosphoenolpyruvate carboxykinase	Glucose biosynthesis
OG5_128059	NP_564785	BBOV_I004950	glucose-6-phosphate/phosphate translocator (<i>A. thaliana</i>); triose or hexose phosphate/phosphate translocator (<i>B. bovis</i>)	Glucose biosynthesis
OG5_133088	NP_001032108	BBOV_II004880	DNA binding / SUMO ligase (<i>A. thaliana</i>); MIZ zinc finger domain containing protein (<i>B. bovis</i>)	Binding
OG5_126773	NP_179646	BBOV_II006560	DNAJ heat shock protein	Protein degradation
OG5_129958	NP_195376	BBOV_III001380	ATPase family associated with various cellular activities	Transport
OG5_126561	NP_188762	BBOV_III005820	ABC transporter family protein	Transport
OG5_126969	NP_849298	BBOV_III005950	microtubule binding (<i>A. thaliana</i>); hypothetical protein (<i>B. bovis</i>)	Mitochondria associated
OG5_128001	NP_567236	BBOV_IV001710	ATP binding or mismatched DNA binding (<i>A. thaliana</i>); DNA mismatch repair protein (<i>B. bovis</i>)	Binding

Among the ten shared orthologue groups, several biological processes including transcription, transport, binding, glucose metabolism protein degradation and mitochondrial associated activities were identified and associated with each group and transcript. These results link to the findings previously presented here, as well as to the comparative transcriptome analyses conducted between *B. divergens* and *P. falciparum* in response A51B1C1_1 treatment.

In this study we assembled and compared expression data sets (based on sequence data) and subsequently identified one “core” or conserved orthologue group (OG5_127669; indicated in blue in Table 4.7 and Table 4.8), which forms part of the DJ-1 protein family domain. The DJ-1 protein family is a redox-dependent chaperone, associated with Parkinson’s disease (Silva *et al.*, 2013). The DJ-1 protein family has several reported functions including cellular transformation (Nagakubo *et al.*, 1997), transcriptional effects (Takahashi *et al.*, 2001), mRNA stability control (Hod *et al.*, 1999) and oxidative stress (Mitsumoto *et al.*, 2001). The closest grouping to the eukaryotic DJ-1 orthologue is the

bacterial ThiJ family of 4-methyl-5(b-hydroxyethyl)-thiazole monophosphate biosynthesis enzymes, suggesting evolution of the DJ-1 protein family from thiamine synthesis genes, found throughout eukaryotes. The enzymatic reactions of ThiJ genes are not yet fully described, however what is known is its catalytic functions (Bandyopadhyay and Cookson, 2004). The *A. thaliana* gene transcript associated with this orthologue group (NP_188117) is described as a homologue of the animal DJ-1 superfamily protein, involved in the positive regulation of cellular response to oxidative stress and is located in the chloroplast, cytosol or nucleus of the cell (<http://www.arabidopsis.org/index.jsp>).

Both *Babesia* (BBOV_I002290) and *Plasmodium* (PFF1335c) transcripts associated with the conserved orthologue group are described as 4-methyl-5(b-hydroxyethyl)-thiazole monophosphate biosynthesis enzymes (<http://piroplasmadb.org/piro/>; <http://plasmodb.org/plasmo/>) and were up-regulated after treatment. The apicoplast is a plastid-like organelle of cyanobacterial origin, homologues to the chloroplast of plants, without photosynthetic characteristics (McFadden, 2014). Comparative apicomplexan studies revealed unique differences with regards to apicoplast functionality and confirmed its heterogeneous nature depending on the particular niche and lifestyle the parasite occupies (Fleige *et al.*, 2010). *Plasmodium* species for example, harbour processes analogous to those present in plant plastids, such as the fatty acid (FA II) pathway (Marechal and Cesbron-Delauw, 2001). Little has been described concerning the fatty acid composition and metabolism in *B. bovis* (Brayton *et al.*, 2007). The *B. bovis* pathogen may have lost some of the important components as it adapted and evolved into its asexual, intra-erythrocytic niche (Caballero *et al.*, 2012).

Botte (2011) and Saidani (2014) characterized new piperidinyl-benzimidazolone analogues which triggered MGDG synthase inhibition in *A. thaliana* with a subsequent decrease in chloroplast size, chloroplast membrane expansion and genes involved in galactolipid synthesis (Botte *et al.*, 2011, Saidani *et al.*, 2014). MGDG and DGDG are the predominant lipids found within photosynthetic plant membranes and are synthesized by MGD and DGD

galactosyltransferases. Important functions of these galactolipids include photosynthetic membrane biogenesis as well as a polyunsaturated fatty acid source to the entire cell (Botte *et al.*, 2011). Transcriptome effects of A51B1C1_1 treatment on *P. falciparum* identified several transcripts involved in fatty acid biosynthesis (Snyman, 2011). Our findings differ from the above mentioned results due to the absence of a complete fatty acid (FA II) biosynthesis pathway in *Babesia* species. As one would ideally prefer one drug compound to be effective and treat numerous apicomplexan parasites based on a single, commonly shared target (Marechal and Cesbron-Delauw, 2001) the conserved “core” orthologue group identified throughout all three transcriptome data sets, with its associated gene transcripts in *Arabidopsis*, *Plasmodium* and *Babesia* species, may provide such a possibility.

If we, however, include the functional, expression data, more transcripts and pathways can be considered as potential drug targets, compared to the one conserved orthologue group and its associated transcripts (identified based on sequencing data), between all three species. In addition to sequence based analysis, manual curation of the treated transcriptomic data set under investigation identified the ABC transporter, ATPase transport (transport) and phosphoenolpyruvate carboxykinase (glucose metabolism) as products and processes to be considered in future as new and/or alternative drug targets.

4.4 Conclusion

In the post-genomic era, bioinformatics along with several computational strategies have become invaluable for drug discovery as well as drug target identification and validation. The identification of new drug targets is urgently required for treatment of zoonotic parasites of socio-economic importance. Ideally one would prefer one drug compound to be effective against numerous pathogens based on a single, commonly shared target feature (Marechal and Cesbron-Delauw, 2001). In this chapter we aimed to contribute and improve current

anti-babesiocidal control strategies by unravelling the *Babesia* transcriptome using several post-genomic tools and bioinformatic programs.

Data revealed that most DEG's were observed between 0 and 4 hours post-treatment, with several cellular compartments, metabolic functions and biological processes affected by treatment. Specific reference to essential pathways associated with the mitochondria and apicoplast, including the oxidative phosphorylation and isoprenoid biosynthesis pathways as well as lipid metabolism were affected by treatment. It appeared as though protein production/turnover was hindered by treatment, placing the cell in a "protein stand-by mode", preparing for protein production to take place at a later stage. Based on these findings we were able to define key gene expression transcripts and identify conserved gene expression networks between *P. falciparum* and *B. divergens* parasites treated with the same herbicide derivative (A51B1C1_1). These results ultimately contributed to the identification of an apicomplexan parasitic response to treatment as well as established the drug mode-of-action. This study substantiates the hypothesis regarding the conservation of gene transcripts between two apicomplexan parasites and paves the way for further comparative analysis for the identification of one drug target, applicable to different apicomplexan species. The one conserved orthologue group identified may for instance, provide an alternative target for the herbicide-derived A51B1C1_1, which can be explored in future anti-apicomplexan drug design and evaluation studies.

The vast amount of *Babesia* expression data generated throughout this study (under a variety of conditions and time-points), provides a valuable resource for future comparative gene expression studies across apicomplexan species, to potentially identify conserved expression profiles of functional importance.

To further improve the scaffold of compound A51B1C1_1 used in this study, we suggest the incorporation of next-generation sequence based technologies in conjunction with manual curation of transcripts. Based on the strategy employed in this study, we were able to

produce additional pathways and transcripts (as opposed to the one orthologue group identified with orthologue group clustering only) to be considered as potential drug targets.

4.5 References

- ALTENHOFF, A. M., GIL, M., GONNET, G. H. & DESSIMOZ, C. 2013. Inferring hierarchical orthologous groups from orthologous gene pairs. *PLoS One*, 8, e53786.
- BANDYOPADHYAY, S. & COOKSON, M. R. 2004. Evolutionary and functional relationships within the DJ1 superfamily. *BMC Evol Biol*, 4, 6.
- BECK, J. R., FUNG, C., STRAUB, K. W., COPPENS, I., VASHISHT, A. A., WOHLSCHLEGEL, J. A. & BRADLEY, P. J. 2013. A Toxoplasma palmitoyl acyl transferase and the palmitoylated armadillo repeat protein TgARO govern apical rhoptry tethering and reveal a critical role for the rhoptries in host cell invasion but not egress. *PLoS Pathog*, 9, e1003162.
- BIRKHOLTZ, L., VAN BRUMMELEN, A. C., CLARK, K., NIEMAND, J., MARECHAL, E., LLINAS, M. & LOUW, A. I. 2008. Exploring functional genomics for drug target and therapeutics discovery in Plasmodia. *Acta Trop*, 105, 113-23.
- BIRKHOLTZ, L. M., BASTIEN, O., WELLS, G., GRANDO, D., JOUBERT, F., KASAM, V., ZIMMERMANN, M., ORTET, P., JACQ, N., SAIDANI, N., ROY, S., HOFMANN-APITIUS, M., BRETON, V., LOUW, A. I. & MARECHAL, E. 2006. Integration and mining of malaria molecular, functional and pharmacological data: how far are we from a chemogenomic knowledge space? *Malar J*, 5, 110.
- BOSHOF, H. I., MYERS, T. G., COPP, B. R., MCNEIL, M. R., WILSON, M. A. & BARRY, C. E. 2004. The transcriptional responses of Mycobacterium tuberculosis to inhibitors of metabolism novel insights into drug mechanisms of action. *Journal of Biological Chemistry*, 279, 40174-40184.
- BOTTE, C. Y., DELIGNY, M., ROCCIA, A., BONNEAU, A. L., SAIDANI, N., HARDRE, H., ACI, S., YAMARYO-BOTTE, Y., JOUHET, J., DUBOTS, E., LOIZEAU, K., BASTIEN, O., BREHELIN, L., JOYARD, J., CINTRAT, J. C., FALCONET, D., BLOCK, M. A., ROUSSEAU, B., LOPEZ, R. & MARECHAL, E. 2011. Chemical inhibitors of monogalactosyldiacylglycerol synthases in Arabidopsis thaliana. *Nat Chem Biol*, 7, 834-42.
- BOZDECH, Z., LLINÁS, M., PULLIAM, B. L., WONG, E. D., ZHU, J. & DERISI, J. L. 2003. The transcriptome of the intraerythrocytic developmental cycle of Plasmodium falciparum. *PLoS biology*, 1, e5.
- BRAYTON, K. A., LAU, A. O., HERNDON, D. R., HANNICK, L., KAPPMAYER, L. S., BERENS, S. J., BIDWELL, S. L., BROWN, W. C., CRABTREE, J. & FADROSH, D. 2007. Genome sequence of Babesia bovis and comparative analysis of apicomplexan hemoprotozoa. *PLoS pathogens*, 3, e148.
- BRAZMA, A., HINGAMP, P., QUACKENBUSH, J., SHERLOCK, G., SPELLMAN, P., STOECKERT, C., AACH, J., ANSORGE, W., BALL, C. A. & CAUSTON, H. C. 2001. Minimum information about a microarray experiment (MIAME)—toward standards for microarray data. *Nature genetics*, 29, 365-371.
- CABALLERO, M. C., PEDRONI, M. J., PALMER, G. H., SUAREZ, C. E., DAVITT, C. & LAU, A. O. 2012. Characterization of acyl carrier protein and LytB in Babesia bovis apicoplast. *Mol Biochem Parasitol*, 181, 125-33.
- CHANG, C. & WERB, Z. 2001. The many faces of metalloproteases: cell growth, invasion, angiogenesis and metastasis. *Trends in cell biology*, 11, S37-S43.
- CHEN, F., MACKAY, A. J., VERMUNT, J. K. & ROOS, D. S. 2007. Assessing performance of orthology detection strategies applied to eukaryotic genomes. *PLoS One*, 2, e383.
- CHEN, X., ZHENG, J., FU, Z., NAN, P., ZHONG, Y., LONARDI, S. & JIANG, T. 2005. Assignment of orthologous genes via genome rearrangement. *IEEE/ACM Trans Comput Biol Bioinform*, 2, 302-15.
- CHOMCZYNSKI, P. & SACCHI, N. 2006. The single-step method of RNA isolation by acid guanidinium thiocyanate-phenol-chloroform extraction: twenty-something years on. *Nat Protoc*, 1, 581-5.
- CONESA, A., GÖTZ, S., GARCÍA-GÓMEZ, J. M., TEROL, J., TALÓN, M. & ROBLES, M. 2005. Blast2GO: a universal tool for annotation, visualization and analysis in functional genomics research. *Bioinformatics*, 21, 3674-3676.

- COWMAN, A. F. & CRABB, B. S. 2003. Functional genomics: identifying drug targets for parasitic diseases. *Trends Parasitol*, 19, 538-43.
- DAHL, E. L., SHOCK, J. L., SHENAI, B. R., GUT, J., DERISI, J. L. & ROSENTHAL, P. J. 2006. Tetracyclines specifically target the apicoplast of the malaria parasite Plasmodium falciparum. *Antimicrob Agents Chemother*, 50, 3124-31.
- DEBARRY, J. D. & KISSINGER, J. C. 2011. Jumbled genomes: missing Apicomplexan synteny. *Molecular biology and evolution*, 28, 2855-2871.
- DENISOV, V., STRONG, W., WALDER, M., GINGRICH, J. & WINTZ, H. 2008. Development and validation of RQI: an RNA quality indicator for the Experion automated electrophoresis system. *Bio-Rad Bulletin*, 5761.
- DI GIROLAMO, F., RAGGI, C., BULTRINI, E., LANFRANCOTTI, A., SILVESTRINI, F., SARGIACOMO, M., BIRAGO, C., PIZZI, E., ALANO, P. & PONZI, M. 2005. Functional genomics, new tools in malaria research. *Ann Ist Super Sanita*, 41, 469-77.
- FLEIGE, T., LIMENITAKIS, J. & SOLDATI-FAVRE, D. 2010. Apicoplast: keep it or leave it. *Microbes Infect*, 12, 253-62.
- FLETCHER, D. A. & MULLINS, R. D. 2010. Cell mechanics and the cytoskeleton. *Nature*, 463, 485-492.
- FREIBERG, C. & BROTZ-OESTERHELT, H. 2005. Functional genomics in antibacterial drug discovery. *Drug Discov Today*, 10, 927-35.
- GARDNER, M. J., HALL, N., FUNG, E., WHITE, O., BERRIMAN, M., HYMAN, R. W., CARLTON, J. M., PAIN, A., NELSON, K. E., BOWMAN, S., PAULSEN, I. T., JAMES, K., EISEN, J. A., RUTHERFORD, K., SALZBERG, S. L., CRAIG, A., KYES, S., CHAN, M. S., NENE, V., SHALLOM, S. J., SUH, B., PETERSON, J., ANGIUOLI, S., PERTEA, M., ALLEN, J., SELENGUT, J., HAFT, D., MATHER, M. W., VAIDYA, A. B., MARTIN, D. M., FAIRLAMB, A. H., FRAUNHOLZ, M. J., ROOS, D. S., RALPH, S. A., MCFADDEN, G. I., CUMMINGS, L. M., SUBRAMANIAN, G. M., MUNGALL, C., VENTER, J. C., CARUCCI, D. J., HOFFMAN, S. L., NEWBOLD, C., DAVIS, R. W., FRASER, C. M. & BARRELL, B. 2002. Genome sequence of the human malaria parasite Plasmodium falciparum. *Nature*, 419, 498-511.
- GORDON, J. L. & SIBLEY, L. D. 2005. Comparative genome analysis reveals a conserved family of actin-like proteins in apicomplexan parasites. *BMC genomics*, 6, 179.
- GUO, Y., RIBEIRO, J. M., ANDERSON, J. M. & BOUR, S. 2009. dCAS: a desktop application for cDNA sequence annotation. *Bioinformatics*, 25, 1195-1196.
- HARDIMAN, G. 2004. Microarray platforms-comparisons and contrasts. *Pharmacogenomics*, 5, 487-502.
- HIETER, P. & BOGUSKI, M. 1997. Functional genomics: it's all how you read it. *Science*, 278, 601-2.
- HOD, Y., PENTYALA, S. N., WHYARD, T. C. & EL-MAGHRABI, M. R. 1999. Identification and characterization of a novel protein that regulates RNA-protein interaction. *J Cell Biochem*, 72, 435-44.
- HUNTER, W. N. 2011. Isoprenoid precursor biosynthesis offers potential targets for drug discovery against diseases caused by apicomplexan parasites. *Curr Top Med Chem*, 11, 2048-59.
- IRIZARRY, R. A., HOBBS, B., COLLIN, F., BEAZER-BARCLAY, Y. D., ANTONELLIS, K. J., SCHERF, U. & SPEED, T. P. 2003. Exploration, normalization, and summaries of high density oligonucleotide array probe level data. *Biostatistics*, 4, 249-264.
- KIM, S. & COULOMBE, P. A. 2010. Emerging role for the cytoskeleton as an organizer and regulator of translation. *Nature reviews Molecular cell biology*, 11, 75-81.
- KÖHLER, A. & HURT, E. 2007. Exporting RNA from the nucleus to the cytoplasm. *Nature reviews Molecular cell biology*, 8, 761-773.
- LAU, A. 2009a. An overview of the Babesia, Plasmodium and Theileria genomes: a comparative perspective. *Molecular and biochemical parasitology*, 164, 1.
- LAU, A. O. 2009b. An overview of the Babesia, Plasmodium and Theileria genomes: a comparative perspective. *Mol Biochem Parasitol*, 164, 1-8.

- LAU, A. O., MCELWAIN, T. F., BRAYTON, K. A., KNOWLES, D. P. & ROALSON, E. H. 2009. Babesia bovis: a comprehensive phylogenetic analysis of plastid-encoded genes supports green algal origin of apicoplasts. *Experimental parasitology*, 123, 236-243.
- LE ROCH, K. G., CHUNG, D. W. & PONTS, N. 2012. Genomics and integrated systems biology in Plasmodium falciparum: a path to malaria control and eradication. *Parasite Immunol*, 34, 50-60.
- LELL, B., RUANGWEERAYUT, R., WIESNER, J., MISSINOU, M. A., SCHINDLER, A., BARANEK, T., HINTZ, M., HUTCHINSON, D., JOMAA, H. & KREMSNER, P. G. 2003. Fosmidomycin, a novel chemotherapeutic agent for malaria. *Antimicrobial agents and chemotherapy*, 47, 735-738.
- LI, L., STOECKERT, C. J. & ROOS, D. S. 2003. OrthoMCL: identification of ortholog groups for eukaryotic genomes. *Genome research*, 13, 2178-2189.
- LLINAS, M., BOZDECH, Z., WONG, E. D., ADAI, A. T. & DERISI, J. L. 2006. Comparative whole genome transcriptome analysis of three Plasmodium falciparum strains. *Nucleic Acids Res*, 34, 1166-73.
- MARECHAL, E. & CESBRON-DELAUW, M. F. 2001. The apicoplast: a new member of the plastid family. *Trends Plant Sci*, 6, 200-5.
- MCFADDEN, G. I. 2014. Apicoplast. *Curr Biol*, 24, R262-3.
- MITSUMOTO, A., NAKAGAWA, Y., TAKEUCHI, A., OKAWA, K., IWAMATSU, A. & TAKANEZAWA, Y. 2001. Oxidized forms of peroxiredoxins and DJ-1 on two-dimensional gels increased in response to sublethal levels of paraquat. *Free Radic Res*, 35, 301-10.
- MORIYA, Y., ITOH, M., OKUDA, S., YOSHIZAWA, A. C. & KANEHISA, M. 2007. KAAS: an automatic genome annotation and pathway reconstruction server. *Nucleic acids research*, 35, W182-W185.
- MU, J., SEYDEL, K. B., BATES, A. & SU, X. Z. 2010. Recent Progress in Functional Genomic Research in Plasmodium falciparum. *Curr Genomics*, 11, 279-86.
- NAGAKUBO, D., TAIRA, T., KITAURA, H., IKEDA, M., TAMAI, K., IGUCHI-ARIGA, S. M. & ARIGA, H. 1997. DJ-1, a novel oncogene which transforms mouse NIH3T3 cells in cooperation with ras. *Biochem Biophys Res Commun*, 231, 509-13.
- OHLSTEIN, E. H., RUFFOLO, R. R., JR. & ELLIOTT, J. D. 2000. Drug discovery in the next millennium. *Annu Rev Pharmacol Toxicol*, 40, 177-91.
- OLIVEROS, J. C. 2007. VENNY. An interactive tool for comparing lists with Venn Diagrams.
- QUACKENBUSH, J. 2002. Microarray data normalization and transformation. *Nature genetics*, 32, 496-501.
- RITCHIE, M. E., SILVER, J., OSHLACK, A., HOLMES, M., DIYAGAMA, D., HOLLOWAY, A. & SMYTH, G. K. 2007. A comparison of background correction methods for two-color microarrays. *Bioinformatics*, 23, 2700-2707.
- SAIDANI, N., BOTTE, C. Y., DELIGNY, M., BONNEAU, A. L., READER, J., LASSELIN, R., MERER, G., NIEPCERON, A., BROSSIER, F., CINTRAT, J. C., ROUSSEAU, B., BIRKHOLTZ, L. M., CESBRON-DELAUW, M. F., DUBREMETZ, J. F., MERCIER, C., VIAL, H., LOPEZ, R. & MARECHAL, E. 2014. Discovery of compounds blocking the proliferation of Toxoplasma gondii and Plasmodium falciparum in a chemical space based on piperidinyl-benzimidazolone analogs. *Antimicrob Agents Chemother*, 58, 2586-97.
- SEEBER, F., LIMENITAKIS, J. & SOLDATI-FAVRE, D. 2008. Apicomplexan mitochondrial metabolism: a story of gains, losses and retentions. *Trends in parasitology*, 24, 468-478.
- SILVA, B. A., BREYDO, L., FINK, A. L. & UVERSKY, V. N. 2013. Agrochemicals, alpha-synuclein, and Parkinson's disease. *Mol Neurobiol*, 47, 598-612.
- SIMON, R., RADMACHER, M. D., DOBBIN, K. & MCSHANE, L. M. 2003. Pitfalls in the use of DNA microarray data for diagnostic and prognostic classification. *Journal of the National Cancer Institute*, 95, 14-18.
- SLONIM, D. K. & YANAI, I. 2009. Getting started in gene expression microarray analysis. *PLoS Comput Biol*, 5, e1000543.

- SMIT, S. 2010. *Functional consequences of the inhibition of Malaria S-adenosylmethionine decarboxylase as a key regulator of polyamine and methionine metabolism*. Department of Biochemistry, University of Pretoria.
- SMYTH, G. K. 2004. Linear models and empirical bayes methods for assessing differential expression in microarray experiments. *Statistical applications in genetics and molecular biology*, 3, 1-25.
- SMYTH, G. K., MICHAUD, J. & SCOTT, H. S. 2005. Use of within-array replicate spots for assessing differential expression in microarray experiments. *Bioinformatics*, 21, 2067-2075.
- SMYTH, G. K. & SPEED, T. 2003. Normalization of cDNA microarray data. *Methods*, 31, 265-273.
- SNYMAN, J. 2011. *The effect of herbicides as novel antimalarial drugs on the transcriptome and proteome of Plasmodium falciparum*. *Magister Scientiae*, University of Pretoria.
- STUART, J. M., SEGAL, E., KOLLER, D. & KIM, S. K. 2003. A gene-coexpression network for global discovery of conserved genetic modules. *science*, 302, 249-255.
- SUBRAMANIAN, A., TAMAYO, P., MOOTHA, V. K., MUKHERJEE, S., EBERT, B. L., GILLETTE, M. A., PAULOVICH, A., POMEROY, S. L., GOLUB, T. R. & LANDER, E. S. 2005. Gene set enrichment analysis: a knowledge-based approach for interpreting genome-wide expression profiles. *Proceedings of the National Academy of Sciences of the United States of America*, 102, 15545-15550.
- TAKAHASHI, K., TAIRA, T., NIKI, T., SEINO, C., IGUCHI-ARIGA, S. M. & ARIGA, H. 2001. DJ-1 positively regulates the androgen receptor by impairing the binding of PIAS α to the receptor. *J Biol Chem*, 276, 37556-63.
- TIROSH, I. & BARKAI, N. 2005. Computational verification of protein-protein interactions by orthologous co-expression. *BMC Bioinformatics*, 6, 40.
- VAN DOOREN, G. G. & STRIEPEN, B. 2013. The algal past and parasite present of the apicoplast. *Annu Rev Microbiol*, 67, 271-89.
- VEMURI, G. N. & ARISTIDOU, A. A. 2005. Metabolic engineering in the -omics era: elucidating and modulating regulatory networks. *Microbiol Mol Biol Rev*, 69, 197-216.
- VERBIST, B., KLAMBAUER, G., VERVOORT, L., TALLOEN, W., SHKEDY, Z., THAS, O., BENDER, A., GOHLMANN, H. W. & HOCHREITER, S. 2015. Using transcriptomics to guide lead optimization in drug discovery projects. *Drug Discov Today*.
- WALLER, R. F., RALPH, S. A., REED, M. B., SU, V., DOUGLAS, J. D., MINNIKIN, D. E., COWMAN, A. F., BESRA, G. S. & MCFADDEN, G. I. 2003. A type II pathway for fatty acid biosynthesis presents drug targets in *Plasmodium falciparum*. *Antimicrobial agents and chemotherapy*, 47, 297-301.
- WANG, S., SIM, T. B., KIM, Y. S. & CHANG, Y. T. 2004. Tools for target identification and validation. *Curr Opin Chem Biol*, 8, 371-7.
- WILL, C. L. & LÜHRMANN, R. 2011. Spliceosome structure and function. *Cold Spring Harbor perspectives in biology*, 3, a003707.
- WOLBER, P. K., COLLINS, P. J., LUCAS, A. B., DE WITTE, A. & SHANNON, K. W. 2006. The Agilent in situ-synthesized microarray platform. *Methods Enzymol*, 410, 28-57.

Chapter 5

Concluding Discussion

5.1 Problem statement

The large, diverse *Apicomplexa* phylum with its wide environmental distribution contains several infamous pathogens of considerable medical, veterinary and economic importance (Fleige *et al.*, 2010, van Dooren and Striepen, 2013). Human babesiosis (caused mainly by *B. microti* or *B. divergens*) is recognized as an emerging infectious disease and public health threat (Lobo *et al.*, 2013). A pressing need for new treatment strategies against these vector-borne parasitic diseases are therefore crucial. The search for new and effective drug compounds, with low toxicity, high specificity and strong resistance characteristics is an ongoing process towards decreasing morbidity and mortality levels associated with apicomplexan parasitic infections. Ideally one would prefer one drug compound to be effective and treat numerous pathogens based on a single, commonly shared target feature within the cells, such as the apicoplast (Marechal and Cesbron-Delauw, 2001). Unfortunately, basic biological processes of *Babesia* parasites are poorly understood due to their neglected status. Additionally, recent reports of drug resistance against the current therapeutics applied to human babesiosis (atovaquone and azithromycin) have emerged (Krause *et al.*, 2000).

Transcriptome analyses of a MGDG synthase inhibitor (A51B1C1_1) in *A. thaliana* was recently evaluated for its anti-malarial properties against *P. falciparum*, which identified several differentially expressed transcripts involved in the fatty acid (FA II) biosynthesis pathway. We were interested in evaluating this compounds' effect on *B. divergens*, as some of the observed targets identified in *P. falciparum* are absent among *Babesia* species.

Additionally, current knowledge regarding the fatty acid composition and metabolism among *Babesia* species are lacking (Brayton *et al.*, 2007).

The primary objective of this study was to determine the anti-babesiocidal potential of this promising apicoplast specific, piperidinyl-benzimidazolone analogue (A51B1C1_1) using a functional genomics approach.

5.2 Experimental overview and findings

Current detection, diagnosis and evaluation of human babesiosis are predominantly cell-based and require visual inspection of the intra-erythrocytic parasites by Giemsa-staining of thin blood smears. Identification of the various parasitic stages is however time-consuming, subjective, labor intensive and inter-operator dependent. In this study, the incorporation of SYBR-Green I as fluorescent DNA stain provides an alternative approach to light microscopy, to detect and estimate parasitic burden and opens the possibility for fast, accurate, inexpensive, high-throughput strategies to evaluate *in vitro* cultivated *B. divergens*. We furthermore established a flow cytometry assay which allows the quantification of parasites in different developmental stages, based on their nuclear DNA content, previously unknown for *Babesia* parasites.

By applying sensitive cell biological and molecular functional genomics tools, we described the IDC of *B. divergens* parasites from immature, mono-nucleated ring forms to bi-nucleated paired piriforms and ultimately multi-nucleated tetrads. This was further correlated to nuclear content increases during intra-erythrocytic development progression, providing insight into the part of the life cycle that occurs during human infection. High-content temporal evaluation elucidated the contribution of the different stages to life cycle progression. Additionally, these tools (cell biological and advanced functional genomics) were applied to reveal the first descriptors of the parasite's transcriptome during its *in vitro* development cycle. This study described the first transcriptional analysis of *B. divergens* parasites,

observed over time, under variable conditions. Moreover, the molecular descriptors indicated that *B. divergens* parasites employ physiological adaptation to *in vitro* cultivation. Differential gene expression was observed as the parasite progressed during its life cycle, with the various developmental formations reaching equilibrium. This information is unique and does not only expand our knowledge on *Babesia* biology, but also provides information that can be exploited for future anti-babesiocidal drug discoveries - for example, stage-specific genes can be used as potential future markers.

This study additionally evaluated the anti-babesiocidal activity of an active MGDG synthase inhibitor (A51B1C1_1) against *B. divergens*. The investigation made use of DNA microarrays to evaluate the transcriptional response and inferred physiological characteristics of treated *B. divergens* parasites and so doing advanced our understanding of the expression profile of *B. divergens* upon treatment and insight into the drug mode-of-action. Since the rationale of this study was to interfere with a process occurring within the biomembranes, the relatively fast trans-membrane movement as observed during the first four hours post A51B1C1_1 treatment confirmed this speculation by influencing the lipid metabolism. Additionally we identified differentially regulated transcripts pertaining to specific metabolic pathways including purine metabolism, aminoacyl-tRNA biosynthesis, spliceosome, RNA transport and the pyrimidine metabolism as well as essential pathways associated with the mitochondria and apicoplast such as the oxidative phosphorylation and isoprenoid biosynthesis pathways. Traditional flow of information (transcription, RNA splicing, mRNA export and translation) within *B. divergens* cells were altered upon treatment and it appeared as though the parasite was in a cellular stress situation. Protein production was subsequently interrupted and halted within the first four hours post treatment, thereby placing the cell in a “protein-stand-by mode”, preparing the production of translation machinery.

Comparative analyses between related apicomplexan members have escalated as advances in large-scale, sequencing technologies increased (Lau *et al.*, 2009). Knowledge gained from these comparable expression data sets is expected to improve existing disease

treatment strategies (Beck *et al.*, 2013). Based on this premise, our comparative analyses focused predominantly on the conserved features (orthologue groups) observed between treated *P. falciparum* and *B. divergens*, to ultimately identify shared functional elements and the compounds' mode-of-action. The 90 shared orthologue groups identified between the differentially expressed *P. falciparum* and *B. divergens* data sets represent the first 90 targets for the development of a potential treatment strategy targeting both *Babesia* and *Plasmodium* related infections. Several *B. divergens* and *P. falciparum* specific (unique) orthologue groups were also observed among the differentially expressed transcripts (Appendix 4.7), which represent good candidates for understanding species-specific differences. One conserved orthologue group (OG5_127669) was identified among all three investigated transcriptomic data sets and forms part of the DJ-1 protein family domain. This orthologue group with its associated gene transcripts in *A. thaliana*, *P. falciparum* and *B. divergens* can be used to further explore the chemical space and scaffolds of piperidinyl-benzimidazolone analogues of galvestine-1, to refine the novel compound A51B1C1_1 acting on the proliferation of *P. falciparum* and *B. divergens*.

5.3 Implications, limitations and future perspectives

Future avenues in *Babesia* related research to be explored should focus on the application of flow cytometry and the use of fluorescent based dyes to improve diagnostics, especially in *B. divergens* endemic regions, which will ultimately improve our understanding of this disease causing pathogen. The strong inhibitory effect achieved by the application of compound A51B1C1_1 on *in vitro* cultured *B. divergens*, encourages its application in future studies related to *in vivo* studies and the compounds' inhibitory effect against the rodent species *B. microti* associated with infected mice. *In vivo* related studies will consequently allow for the extension of results beyond its current human application (as conducted in this study) into the veterinary field and subsequently different *Babesia* species.

In future studies, the growth inhibitory effect/concentration of compound A51B1C1_1 against *B. divergens* should be re-evaluated using fluorescence based assays, as this assay was only established after our drug sensitivity assay was completed (Guswanto *et al.*, 2014). The lack of commercial availability of the compound additionally inhibited re-evaluation of *Babesia* growth inhibition with the newly published methods. One of the piperidinyl-benzimidazolone analogues (A87B1C1_1) (identified by Saidani (2014)) which had an equally efficient and potent anti-parasitic effect against both *P. falciparum* and *T. gondii* should be evaluated in future studies (using a similar functional genomics approach as applied in this study), to establish its anti-babesiacidal effect against *B. divergens* and additionally identify potential drug targets. Based on the newly described and optimized flow cytometry techniques (incorporating fluorescent based dyes such as SYBR-Green I), specific life cycle formations (*i.e.* stages) of *B. divergens* affected by A51B1C1_1 treatment can be identified in future *Babesia* related studies.

Several experimental constraints such as morphological, metabolic or nuclear changes that occur during the asynchronous *in vitro* *B. divergens* life cycle may have influenced the transcriptional response. *In vitro* synchronization of *P. falciparum* parasites on a weekly basis, allows for drug treatment strategies to be conducted against a specific parasitic developmental stage, unfortunately this is currently not a feasible reality for *Babesia* parasites, which may have influenced our results. Future research should focus on designing synchronization strategies related to *Babesia* parasites which will improve growth inhibitory studies and establishing drug-mode-of-action strategies.

Transcriptome profiling of A51B1C1_1 treated and untreated *B. divergens* parasites was performed using our custom designed, *B. bovis* specific Agilent microarray slides. The microarray slides and protocol described in this study provide a sensitive, easy-to-use, high-quality and cost-effective platform for gene expression analysis of various *Babesia* species, its application is therefore not limited to a particular *Babesia* parasite. The custom designed *B. bovis* slide may, however, also be regarded as a limitation in this study, as several *B.*

divergens transcripts may have been missed (not identified). Another challenge facing *Babesia* transcriptional response to drug treatment research is the lack of a known, standard, transcriptional profile to which comparisons can be made in order to recognize and identify variations and changes in parasitic gene expression. The completion of more apicomplexan genomes will be vital for future comparative genomic studies, which will ultimately contribute to the discovery of novel drug targets and improve our understanding of host-parasite interactions and immune evasion mechanisms. Realtime PCR should be used to further investigate and validate the transcriptomic results and *in vitro* effects of the piperidinyl-benzimidazolone analogue A51B1C1_1 on *B. divergens*. Validation of the 90 orthologue groups identified between *B. divergens* and *P. falciparum* both treated with the same compound (A51B1C1_1) will subsequently be possible.

More research is required to further investigate the transcriptional response (or lack thereof) of *in vitro* cultured, A51B1C1_1 treated *Babesia* parasites to extend our current knowledge as to whether challenges are compound or pathway specific. Next-generation sequencing (RNA-Seq) has been increasingly applied to transcriptome quantification and characterization in various studies and organisms with the ultimate goal to improve gene expression studies (Su *et al.*, 2011). In order to improve the current transcriptome repertoire of *B. divergens* and to provide an additional source of information for comparative transcriptomic studies regarding the evolution and dynamics of *Babesia* species and ultimately improve diagnosis and target specific treatment of disease infected patients, future *Babesia* studies should incorporate both DNA microarrays and RNA-Seq. To date, several studies have been performed comparing hybridization based (DNA microarrays) and sequencing based (RNA-Seq) technologies, which revealed high concordance between these technologies with regards to reproducibility, accuracy and dynamic abilities to quantify gene expression levels. Concordance between the two technologies have, however, not been established for dose-response experiments over a range of chemical treatment conditions (Wang *et al.*, 2014). Future investigations to improve our understanding of the

parasite's response to treatment should, therefore, incorporate both DNA microarrays and RNA-Seq. In order to eliminate any discrepancies between these techniques, *B. divergens* sample collection for both (future) experiments should take place concurrently, under the same conditions.

Similar to what has been reported in the malaria field with *P. falciparum*'s ability to develop resistance against anti-malarial compounds (such as artemisinin) (Miotto *et al.*, 2013), recent reports of drug resistance related to the current therapeutics against human babesiosis (atovaquone with azithromycin or quinine plus clindamycin) have also been noted (Wormser *et al.*, 2010, Krause *et al.*, 2000). The need to develop alternative treatment strategies is therefore evident. Based on recent findings regarding *P. falciparum* and artemisinin-resistance in western Cambodia (Miotto *et al.*, 2013), future *Babesia* research should include both DNA microarray and RNA-Seq technologies to assist in the identification of a population genetic framework to further investigate the biological origins and evolutionary adaptation of resistance and in so doing, identify molecular markers to ultimately assist in its elimination

The "One Health" concept provides an opportunity to maximize tick-borne disease control, reduce morbidity and mortality rates associated with ticks and tick-borne diseases and ultimately improve the health of people, animals and the environment. This concept emphasizes the need for a collaborative, integrative, interdisciplinary effort by unifying medical and veterinary disciplines. With the emergence of babesiosis as a global zoonotic disease, the "One Health" principle should be regarded as a vital approach in future studies to improve the current tick and tick-borne disease management strategies as well as enhance the current limited resources and knowledge available in the field.

5.4 References

- ABOULAILA, M., MUNKHJARGAL, T., SIVAKUMAR, T., UENO, A., NAKANO, Y., YOKOYAMA, M., YOSHINARI, T., NAGANO, D., KATAYAMA, K., EL-BAHY, N., YOKOYAMA, N. & IGARASHI, I. 2012. Apicoplast-targeting antibacterials inhibit the growth of Babesia parasites. *Antimicrob Agents Chemother*, 56, 3196-206.
- ABOULAILA, M., NAKAMURA, K., GOVIND, Y., YOKOYAMA, N. & IGARASHI, I. 2010a. Evaluation of the in vitro growth-inhibitory effect of epoxomicin on Babesia parasites. *Vet Parasitol*, 167, 19-27.
- ABOULAILA, M., SIVAKUMAR, T., YOKOYAMA, N. & IGARASHI, I. 2010b. Inhibitory effect of terpene nerolidol on the growth of Babesia parasites. *Parasitol Int*, 59, 278-82.
- ABOULAILA, M., YOKOYAMA, N. & IGARASHI, I. 2010c. Inhibitory effects of (-)-epigallocatechin-3-gallate from green tea on the growth of Babesia parasites. *Parasitology*, 137, 785-91.
- ALTENHOFF, A. M., GIL, M., GONNET, G. H. & DESSIMOZ, C. 2013. Inferring hierarchical orthologous groups from orthologous gene pairs. *PLoS One*, 8, e53786.
- ARNOT, D. E., RONANDER, E. & BENGTSSON, D. C. 2011. The progression of the intra-erythrocytic cell cycle of *Plasmodium falciparum* and the role of the centriolar plaques in asynchronous mitotic division during schizogony. *International journal for parasitology*, 41, 71-80.
- BANDYOPADHYAY, S. & COOKSON, M. R. 2004. Evolutionary and functional relationships within the DJ1 superfamily. *BMC Evol Biol*, 4, 6.
- BECK, J. R., FUNG, C., STRAUB, K. W., COPPENS, I., VASHISHT, A. A., WOHLSCHEGEL, J. A. & BRADLEY, P. J. 2013. A Toxoplasma palmitoyl acyl transferase and the palmitoylated armadillo repeat protein TgARO govern apical rhoptry tethering and reveal a critical role for the rhoptries in host cell invasion but not egress. *PLoS Pathog*, 9, e1003162.
- BECKER, C. A., BOUJU-ALBERT, A., JOUGLIN, M., CHAUVIN, A. & MALANDRIN, L. 2009. Natural transmission of Zoonotic Babesia spp. by Ixodes ricinus ticks. *Emerg Infect Dis*, 15, 320-2.
- BECKER, C. A., MALANDRIN, L., DEPOIX, D., LARCHER, T., DAVID, P. H., CHAUVIN, A., BISCHOFF, E. & BONNET, S. 2010. Identification of three CCp genes in Babesia divergens: novel markers for sexual stages parasites. *Mol Biochem Parasitol*, 174, 36-43.
- BECKER, C. A., MALANDRIN, L., LARCHER, T., CHAUVIN, A., BISCHOFF, E. & BONNET, S. I. 2013. Validation of BdCCp2 as a marker for Babesia divergens sexual stages in ticks. *Exp Parasitol*, 133, 51-6.
- BECKER, K. 2011. *Apicomplexan Parasites. Molecular approaches toward targeted drug development*, Wiley-Blackwell.
- BENNETT, T. N., PAGUIO, M., GLIGORIJEVIC, B., SEUDIEU, C., KOSAR, A. D., DAVIDSON, E. & ROEPE, P. D. 2004. Novel, rapid, and inexpensive cell-based quantification of antimalarial drug efficacy. *Antimicrobial agents and chemotherapy*, 48, 1807-1810.
- BIRKHOLTZ, L., VAN BRUMMELEN, A. C., CLARK, K., NIEMAND, J., MARECHAL, E., LLINAS, M. & LOUW, A. I. 2008. Exploring functional genomics for drug target and therapeutics discovery in Plasmodia. *Acta Trop*, 105, 113-23.
- BIRKHOLTZ, L. M., BASTIEN, O., WELLS, G., GRANDO, D., JOUBERT, F., KASAM, V., ZIMMERMANN, M., ORTET, P., JACQ, N., SAIDANI, N., ROY, S., HOFMANN-APITIUS, M., BRETON, V., LOUW, A. I. & MARECHAL, E. 2006. Integration and mining of malaria molecular, functional and pharmacological data: how far are we from a chemogenomic knowledge space? *Malar J*, 5, 110.
- BOCK, R., JACKSON, L., DE VOS, A. & JORGENSEN, W. 2004. Babesiosis of cattle. *Parasitology*, 129, S247-S269.
- BORK, S., DAS, S., OKUBO, K., YOKOYAMA, N. & IGARASHI, I. 2006. Effects of protein kinase inhibitors on the in vitro growth of Babesia bovis. *Parasitology*, 132, 775-9.

- BORK, S., YOKOYAMA, N., IKEHARA, Y., KUMAR, S., SUGIMOTO, C. & IGARASHI, I. 2004. Growth-inhibitory effect of heparin on Babesia parasites. *Antimicrobial agents and chemotherapy*, 48, 236-241.
- BORK, S., YOKOYAMA, N., MATSUO, T., CLAVERIA, F. G., FUJISAKI, K. & IGARASHI, I. 2003. Growth inhibitory effect of triclosan on equine and bovine Babesia parasites. *The American journal of tropical medicine and hygiene*, 68, 334-340.
- BOSHOF, H. I., MYERS, T. G., COPP, B. R., MCNEIL, M. R., WILSON, M. A. & BARRY, C. E. 2004. The transcriptional responses of Mycobacterium tuberculosis to inhibitors of metabolism novel insights into drug mechanisms of action. *Journal of Biological Chemistry*, 279, 40174-40184.
- BOTTE, C. Y., DELIGNY, M., ROCCIA, A., BONNEAU, A. L., SAIDANI, N., HARDRE, H., ACI, S., YAMARYO-BOTTE, Y., JOUHET, J., DUBOTS, E., LOIZEAU, K., BASTIEN, O., BREHELIN, L., JOYARD, J., CINTRAT, J. C., FALCONET, D., BLOCK, M. A., ROUSSEAU, B., LOPEZ, R. & MARECHAL, E. 2011. Chemical inhibitors of monogalactosyldiacylglycerol synthases in Arabidopsis thaliana. *Nat Chem Biol*, 7, 834-42.
- BOTTE, C. Y., DUBAR, F., MCFADDEN, G. I., MARECHAL, E. & BIOT, C. 2012. Plasmodium falciparum apicoplast drugs: targets or off-targets? *Chem Rev*, 112, 1269-83.
- BOUDIERE, L., BOTTE, C. Y., SAIDANI, N., LAJOIE, M., MARION, J., BREHELIN, L., YAMARYO-BOTTE, Y., SATIAT-JEUNEMAITRE, B., BRETON, C., GIRARD-EGROT, A., BASTIEN, O., JOUHET, J., FALCONET, D., BLOCK, M. A. & MARECHAL, E. 2012. Galvestine-1, a novel chemical probe for the study of the glycerolipid homeostasis system in plant cells. *Mol Biosyst*, 8, 2023-35, 2014.
- BOZDECH, Z., LLINÁS, M., PULLIAM, B. L., WONG, E. D., ZHU, J. & DERISI, J. L. 2003. The transcriptome of the intraerythrocytic developmental cycle of Plasmodium falciparum. *PLoS biology*, 1, e5.
- BRASSEUR, P., LECOUBLET, S., KAPEL, N., FAVENNEC, L. & BALLE, J. J. 1998. In Vitro Evaluation of Drug Susceptibilities of Babesia divergens Isolates. *Antimicrobial agents and chemotherapy*, 42, 818-820.
- BRAYTON, K. A., LAU, A. O., HERNDON, D. R., HANNICK, L., KAPPEMEYER, L. S., BERENS, S. J., BIDWELL, S. L., BROWN, W. C., CRABTREE, J. & FADROSH, D. 2007. Genome sequence of Babesia bovis and comparative analysis of apicomplexan hemoprotozoa. *PLoS pathogens*, 3, e148.
- BRAZMA, A., HINGAMP, P., QUACKENBUSH, J., SHERLOCK, G., SPELLMAN, P., STOECKERT, C., AACH, J., ANSORGE, W., BALL, C. A. & CAUSTON, H. C. 2001. Minimum information about a microarray experiment (MIAME)—toward standards for microarray data. *Nature genetics*, 29, 365-371.
- BURROWS, J. N., HOOFT VAN HUIJSDUIJNEN, R., MÖHRLE, J. J., OEUVRAY, C. & WELLS, T. 2013. Designing the next generation of medicines for malaria control and eradication. *Malar J*, 12, 187.
- BUSH, J. B., ISAACSON, M., MOHAMED, A. S., POTGIETER, F. T. & DE WAAL, D. T. 1990. Human babesiosis—a preliminary report of 2 suspected cases in South Africa. *S Afr Med J*, 78, 699.
- CABALLERO, M. C., PEDRONI, M. J., PALMER, G. H., SUAREZ, C. E., DAVITT, C. & LAU, A. O. 2012. Characterization of acyl carrier protein and LytB in Babesia bovis apicoplast. *Mol Biochem Parasitol*, 181, 125-33.
- CHANG, C. & WERB, Z. 2001. The many faces of metalloproteases: cell growth, invasion, angiogenesis and metastasis. *Trends in cell biology*, 11, S37-S43.
- CHAUVIN, A., MOREAU, E., BONNET, S., PLANTARD, O. & MALANDRIN, L. 2009. Babesia and its hosts: adaptation to long-lasting interactions as a way to achieve efficient transmission. *Veterinary research*, 40, 1-18.
- CHEN, F., MACKAY, A. J., VERMUNT, J. K. & ROOS, D. S. 2007. Assessing performance of orthology detection strategies applied to eukaryotic genomes. *PLoS One*, 2, e383.

- CHEN, X., ZHENG, J., FU, Z., NAN, P., ZHONG, Y., LONARDI, S. & JIANG, T. 2005. Assignment of orthologous genes via genome rearrangement. *IEEE/ACM Trans Comput Biol Bioinform*, 2, 302-15.
- CHOMCZYNSKI, P. & SACCHI, N. 2006. The single-step method of RNA isolation by acid guanidinium thiocyanate-phenol-chloroform extraction: twenty-something years on. *Nat Protoc*, 1, 581-5.
- COLWELL, D. D., DANTAS-TORRES, F. & OTRANTO, D. 2011. Vector-borne parasitic zoonoses: emerging scenarios and new perspectives. *Veterinary parasitology*, 182, 14-21.
- CONESA, A., GÖTZ, S., GARCÍA-GÓMEZ, J. M., TEROL, J., TALÓN, M. & ROBLES, M. 2005. Blast2GO: a universal tool for annotation, visualization and analysis in functional genomics research. *Bioinformatics*, 21, 3674-3676.
- COWMAN, A. F. & CRABB, B. S. 2003. Functional genomics: identifying drug targets for parasitic diseases. *Trends Parasitol*, 19, 538-43.
- CRANMER, S. L., MAGOWAN, C., LIANG, J., COPPEL, R. L. & COOKE, B. M. 1997. An alternative to serum for cultivation of *Plasmodium falciparum* in vitro. *Trans R Soc Trop Med Hyg*, 91, 363-5.
- CUESTA, I., GONZALEZ, L. M., ESTRADA, K., GRANDE, R., ZABALLOS, A., LOBO, C. A., BARRERA, J., SANCHEZ-FLORES, A. & MONTERO, E. 2014. High-Quality Draft Genome Sequence of *Babesia divergens*, the Etiological Agent of Cattle and Human Babesiosis. *Genome Announc*, 2.
- DAHL, E. L., SHOCK, J. L., SHENAI, B. R., GUT, J., DERISI, J. L. & ROSENTHAL, P. J. 2006. Tetracyclines specifically target the apicoplast of the malaria parasite *Plasmodium falciparum*. *Antimicrob Agents Chemother*, 50, 3124-31.
- DANTAS-TORRES, F., CHOMEL, B. B. & OTRANTO, D. 2012. Ticks and tick-borne diseases: a One Health perspective. *Trends in parasitology*, 28, 437-446.
- DE CASTRO, J. J. 1997. Sustainable tick and tickborne disease control in livestock improvement in developing countries. *Vet Parasitol*, 71, 77-97.
- DE LA FUENTE, J., NARANJO, V., RUIZ-FONS, F., VICENTE, J., ESTRADA-PEÑA, A., ALMAZÁN, C., KOCAN, K. M., MARTÍN, M. P. & GORTÁZAR, C. 2004. Prevalence of tick-borne pathogens in ixodid ticks (Acari: Ixodidae) collected from European wild boar (*Sus scrofa*) and Iberian red deer (*Cervus elaphus hispanicus*) in central Spain. *European Journal of Wildlife Research*, 50, 187-196.
- DEBARRY, J. D. & KISSINGER, J. C. 2011. Jumbled genomes: missing Apicomplexan synteny. *Molecular biology and evolution*, 28, 2855-2871.
- DECHAMPS, S., SHASTRI, S., WENDELNIK, K. & VIAL, H. J. 2010. Glycerophospholipid acquisition in *Plasmodium* - a puzzling assembly of biosynthetic pathways. *Int J Parasitol*, 40, 1347-65.
- DELLIBOVI-RAGHEB, T. A., GISSELBERG, J. E. & PRIGGE, S. T. 2013. Parasites FeS up: iron-sulfur cluster biogenesis in eukaryotic pathogens. *PLoS Pathog*, 9, e1003227.
- DENISOV, V., STRONG, W., WALDER, M., GINGRICH, J. & WINTZ, H. 2008. Development and validation of RQI: an RNA quality indicator for the Experion automated electrophoresis system. *Bio-Rad Bulletin*, 5761.
- DERBYSHIRE, E. T., FRANSEN, F. J., DE VRIES, E., MORIN, C., WOODROW, C. J., KRISHNA, S. & STAINES, H. M. 2008. Identification, expression and characterisation of a *Babesia bovis* hexose transporter. *Mol Biochem Parasitol*, 161, 124-9.
- DI GIROLAMO, F., RAGGI, C., BULTRINI, E., LANFRANCOTTI, A., SILVESTRINI, F., SARGIACOMO, M., BIRAGO, C., PIZZI, E., ALANO, P. & PONZI, M. 2005. Functional genomics, new tools in malaria research. *Ann Ist Super Sanita*, 41, 469-77.
- DUBOTS, E., AUDRY, M., YAMARYO, Y., BASTIEN, O., OHTA, H., BRETON, C., MARECHAL, E. & BLOCK, M. A. 2010. Activation of the chloroplast monogalactosyldiacylglycerol synthase MGD1 by phosphatidic acid and phosphatidylglycerol. *J Biol Chem*, 285, 6003-11.
- EISEN, M. B., SPELLMAN, P. T., BROWN, P. O. & BOTSTEIN, D. 1998. Cluster analysis and display of genome-wide expression patterns. *Proceedings of the National Academy of Sciences*, 95, 14863-14868.

- EISENREICH, W., BACHER, A., ARIGONI, D. & ROHDICH, F. 2004. Biosynthesis of isoprenoids via the non-mevalonate pathway. *Cell Mol Life Sci*, 61, 1401-26.
- ERP, E. E., GRAVELY, S. M., SMITH, R. D., RISTIC, M., OSORNO, B. M. & CARSON, C. A. 1978. Growth of *Babesia bovis* in bovine erythrocyte cultures. *Am J Trop Med Hyg*, 27, 1061-4.
- FILBIN, M. R., MYLONAKIS, E. E., CALLEGARI, L. & LEGOME, E. 2001. Babesiosis. *The Journal of emergency medicine*, 20, 21-24.
- FLEIGE, T., LIMENITAKIS, J. & SOLDATI-FAVRE, D. 2010. Apicoplast: keep it or leave it. *Microbes Infect*, 12, 253-62.
- FLETCHER, D. A. & MULLINS, R. D. 2010. Cell mechanics and the cytoskeleton. *Nature*, 463, 485-492.
- FLORES, M. V., BERGER-EISZELE, S. M. & STEWART, T. S. 1997. Long-term cultivation of *Plasmodium falciparum* in media with commercial non-serum supplements. *Parasitol Res*, 83, 734-6.
- FLORIN-CHRISTENSEN, M., SCHNITTGER, L., DOMINGUEZ, M., MESPLET, M., RODRIGUEZ, A., FERRERI, L., ASENZO, G., WILKOWSKY, S., FARBER, M., ECHAIDE, I. & SUAREZ, C. 2007. Search for *Babesia bovis* vaccine candidates. *Parassitologia*, 49 Suppl 1, 9-12.
- FOTH, B. J. & MCFADDEN, G. I. 2003. The apicoplast: a plastid in *Plasmodium falciparum* and other Apicomplexan parasites. *Int Rev Cytol*, 224, 57-110.
- FREIBERG, C. & BROTZ-OESTERHELT, H. 2005. Functional genomics in antibacterial drug discovery. *Drug Discov Today*, 10, 927-35.
- FRIEDMAN, A. & YAKUBU, A. A. 2014. A Bovine Babesiosis model with dispersion. *Bull Math Biol*, 76, 98-135.
- FRITZ, C. L. 2009. Emerging tick-borne diseases. *Veterinary Clinics of North America: Small Animal Practice*, 39, 265-278.
- GARDNER, M. J., HALL, N., FUNG, E., WHITE, O., BERRIMAN, M., HYMAN, R. W., CARLTON, J. M., PAIN, A., NELSON, K. E., BOWMAN, S., PAULSEN, I. T., JAMES, K., EISEN, J. A., RUTHERFORD, K., SALZBERG, S. L., CRAIG, A., KYES, S., CHAN, M. S., NENE, V., SHALLOM, S. J., SUH, B., PETERSON, J., ANGIUOLI, S., PERTEA, M., ALLEN, J., SELENGUT, J., HAFT, D., MATHER, M. W., VAIDYA, A. B., MARTIN, D. M., FAIRLAMB, A. H., FRAUNHOLZ, M. J., ROOS, D. S., RALPH, S. A., MCFADDEN, G. I., CUMMINGS, L. M., SUBRAMANIAN, G. M., MUNGALL, C., VENTER, J. C., CARUCCI, D. J., HOFFMAN, S. L., NEWBOLD, C., DAVIS, R. W., FRASER, C. M. & BARRELL, B. 2002. Genome sequence of the human malaria parasite *Plasmodium falciparum*. *Nature*, 419, 498-511.
- GOES, T. S., GOES, V. S., RIBEIRO, M. F. & GONTIJO, C. M. 2007. Bovine babesiosis: anti-erythrocyte antibodies purification from the sera of naturally infected cattle. *Vet Immunol Immunopathol*, 116, 215-8.
- GOHIL, S., HERRMANN, S., GUNTHER, S. & COOKE, B. M. 2013. Bovine babesiosis in the 21st century: advances in biology and functional genomics. *Int J Parasitol*, 43, 125-32.
- GOHIL, S., KATS, L. M., STURM, A. & COOKE, B. M. 2010. Recent insights into alteration of red blood cells by *Babesia bovis*: moovin' forward. *Trends Parasitol*, 26, 591-9.
- GORDON, J. L. & SIBLEY, L. D. 2005. Comparative genome analysis reveals a conserved family of actin-like proteins in apicomplexan parasites. *BMC genomics*, 6, 179.
- GORENFLOT, A., BRASSEUR, P., PRECIGOUT, E., L'HOSTIS, M., MARCHAND, A. & SCHREVEL, J. 1991. Cytological and immunological responses to *Babesia divergens* in different hosts: Ox, gerbil, man. *Parasitology research*, 77, 3-12.
- GRANDE, N., PRECIGOUT, E., ANCELIN, M., MOUBRI, K., CARCY, B., LEMESRE, J., VIAL, H. & GORENFLOT, A. 1997. Continuous in vitro culture of *Babesia divergens* in a serum-free medium. *Parasitology*, 115, 81-89.
- GRAY, J., ZINTL, A., HILDEBRANDT, A., HUNFELD, K.-P. & WEISS, L. 2010. Zoonotic babesiosis: overview of the disease and novel aspects of pathogen identity. *Ticks and tick-borne diseases*, 1, 3-10.
- GRAY, J. S. 2006. Identity of the causal agents of human babesiosis in Europe. *Int J Med Microbiol*, 296 Suppl 40, 131-6.

- GRELLIER, P., VALENTIN, A., MILLERIOUX, V., SCHREVEL, J. & RIGOMIER, D. 1994. 3-Hydroxy-3-methylglutaryl coenzyme A reductase inhibitors lovastatin and simvastatin inhibit in vitro development of Plasmodium falciparum and Babesia divergens in human erythrocytes. *Antimicrob Agents Chemother*, 38, 1144-8.
- GRIMBERG, B. T., ERICKSON, J. J., SRAMKOSKI, R. M., JACOBBERGER, J. W. & ZIMMERMAN, P. A. 2008. Monitoring Plasmodium falciparum growth and development by UV flow cytometry using an optimized Hoechst-thiazole orange staining strategy. *Cytometry Part A*, 73, 546-554.
- GUGLIELMONE, A. A., ROBBINS, R. G., APANASKEVICH, D. A., PETNEY, T. N., ESTRADA-PENA, A., HORAK, I. G., SHAO, R. & BARKER, S. C. 2010. The Argasidae, Ixodidae and Nuttalliellidae (Acari: Ixodida) of the world: a list of valid species names.
- GUO, Y., RIBEIRO, J. M., ANDERSON, J. M. & BOUR, S. 2009. dCAS: a desktop application for cDNA sequence annotation. *Bioinformatics*, 25, 1195-1196.
- GUSWANTO, A., SIVAKUMAR, T., RIZK, M. A., ELSAYED, S. A. E., YOUSSEF, M. A., ELSAID, E. E. S., YOKOYAMA, N. & IGARASHI, I. 2014. Evaluation of a fluorescence-based method for antibabesial drug screening. *Antimicrobial agents and chemotherapy*, 58, 4713-4717.
- HARDIMAN, G. 2004. Microarray platforms-comparisons and contrasts. *Pharmacogenomics*, 5, 487-502.
- HEMMER, R. M., FERRICK, D. A. & CONRAD, P. A. 2000. Role of T cells and cytokines in fatal and resolving experimental babesiosis: protection in TNFRp55^{-/-} mice infected with the human Babesia WA1 parasite. *J Parasitol*, 86, 736-42.
- HIETER, P. & BOGUSKI, M. 1997. Functional genomics: it's all how you read it. *Science*, 278, 601-2.
- HILDEBRANDT, A., GRAY, J. & HUNFELD, K.-P. 2013. Human Babesiosis in Europe: what clinicians need to know. *Infection*, 41, 1057-1072.
- HOD, Y., PENTYALA, S. N., WHYARD, T. C. & EL-MAGHRABI, M. R. 1999. Identification and characterization of a novel protein that regulates RNA-protein interaction. *J Cell Biochem*, 72, 435-44.
- HOLLINGDALE, M. R. 1992. Is culture of the entire plasmodium cycle, in vitro, now a reality? *Parasitol Today*, 8, 223.
- HOLMAN, P. J., CHIEVES, L., FRERICHS, W. M., OLSON, D. & WAGNER, G. G. 1994. Babesia equi erythrocytic stage continuously cultured in an enriched medium. *J Parasitol*, 80, 232-6.
- HOLMAN, P. J., WALDRUP, K. A. & WAGNER, G. G. 1988. In vitro cultivation of a Babesia isolated from a white-tailed deer (Odocoileus virginianus). *J Parasitol*, 74, 111-5.
- HOMER, M. J., AGUILAR-DELFIN, I., TELFORD, S. R., KRAUSE, P. J. & PERSING, D. H. 2000. Babesiosis. *Clinical microbiology reviews*, 13, 451-469.
- HORAK, I. G., CAMICAS, J.-L. & KEIRANS, J. E. 2002. The Argasidae, Ixodidae and Nuttalliellidae (Acari: Ixodida): a world list of valid tick names. *Experimental & applied acarology*, 28, 27-54.
- HUNFELD, K.-P., HILDEBRANDT, A. & GRAY, J. 2008. Babesiosis: recent insights into an ancient disease. *International Journal for Parasitology*, 38, 1219-1237.
- HUNFELD, K. P. & BRADE, V. 2004. Zoonotic Babesia: possibly emerging pathogens to be considered for tick-infested humans in Central Europe. *Int J Med Microbiol*, 293 Suppl 37, 93-103.
- HUNTER, W. N. 2011. Isoprenoid precursor biosynthesis offers potential targets for drug discovery against diseases caused by apicomplexan parasites. *Curr Top Med Chem*, 11, 2048-59.
- IGARASHI, I., SUZUKI, R., WAKI, S., TAGAWA, Y., SENG, S., TUM, S., OMATA, Y., SAITO, A., NAGASAWA, H., IWAKURA, Y., SUZUKI, N., MIKAMI, T. & TOYODA, Y. 1999. Roles of CD4(+) T cells and gamma interferon in protective immunity against Babesia microti infection in mice. *Infect Immun*, 67, 4143-8.
- IGARASHI, S., MINEGISHI, T., NAKAMURA, K., NAKAMURA, M., TANO, M., MIYAMOTO, K. & IBUKI, Y. 1994. Functional expression of recombinant human luteinizing hormone/human chorionic gonadotropin receptor. *Biochem Biophys Res Commun*, 201, 248-56.

- IRIZARRY, R. A., HOBBS, B., COLLIN, F., BEAZER-BARCLAY, Y. D., ANTONELLIS, K. J., SCHERF, U. & SPEED, T. P. 2003. Exploration, normalization, and summaries of high density oligonucleotide array probe level data. *Biostatistics*, 4, 249-264.
- IZUMIYAMA, S., OMURA, M., TAKASAKI, T., OHMAE, H. & ASAHI, H. 2009. *Plasmodium falciparum*: Development and validation of a measure of intraerythrocytic growth using SYBR Green I in a flow cytometer. *Experimental parasitology*, 121, 144-150.
- JACKSON, A. P., OTTO, T. D., DARBY, A., RAMAPRASAD, A., XIA, D., ECHAIDE, I. E., FARBER, M., GAHLOT, S., GAMBLE, J., GUPTA, D., GUPTA, Y., JACKSON, L., MALANDRIN, L., MALAS, T. B., MOUSSA, E., NAIR, M., REID, A. J., SANDERS, M., SHARMA, J., TRACEY, A., QUAIL, M. A., WEIR, W., WASTLING, J. M., HALL, N., WILLADSEN, P., LINGELBACH, K., SHIELS, B., TAIT, A., BERRIMAN, M., ALLRED, D. R. & PAIN, A. 2014. The evolutionary dynamics of variant antigen genes in *Babesia* reveal a history of genomic innovation underlying host-parasite interaction. *Nucleic Acids Res*, 42, 7113-31.
- JASMER, D. P. & GOFF, W. L. 1989. In vitro killing of *Babesia bovis* by the ornithine analog alpha-monofluoromethyldehydroornithine methyl ester. *J Protozool*, 36, 493-7.
- JONGEJAN, F. & UILENBERG, G. 2004. The global importance of ticks. *Parasitology*, 129, S3-S14.
- JOUHET, J., MARECHAL, E. & BLOCK, M. A. 2007. Glycerolipid transfer for the building of membranes in plant cells. *Prog Lipid Res*, 46, 37-55.
- KAHN, L. H. 2006. Confronting zoonoses, linking human and veterinary medicine. *Emerging infectious diseases*, 12, 556.
- KAVANAUGH, M. J. & DECKER, C. F. 2012. Babesiosis. *Dis Mon*, 58, 355-60.
- KIM, S. & COULOMBE, P. A. 2010. Emerging role for the cytoskeleton as an organizer and regulator of translation. *Nature reviews Molecular cell biology*, 11, 75-81.
- KJEMTRUP, A. & CONRAD, P. 2000. Human babesiosis: an emerging tick-borne disease. *International journal for parasitology*, 30, 1323-1337.
- KÖHLER, A. & HURT, E. 2007. Exporting RNA from the nucleus to the cytoplasm. *Nature reviews Molecular cell biology*, 8, 761-773.
- KRAUSE, P. J., LEPORE, T., SIKAND, V. K., GADBAW JR, J., BURKE, G., TELFORD, S. R., BRASSARD, P., PEARL, D., AZLANZADEH, J. & CHRISTIANSON, D. 2000. Atovaquone and azithromycin for the treatment of babesiosis. *New England Journal of Medicine*, 343, 1454-1458.
- LAMBROS, C. & VANDERBERG, J. P. 1979. Synchronization of *Plasmodium falciparum* erythrocytic stages in culture. *The Journal of parasitology*, 418-420.
- LAU, A. 2009a. An overview of the *Babesia*, *Plasmodium* and *Theileria* genomes: a comparative perspective. *Molecular and biochemical parasitology*, 164, 1.
- LAU, A. O. 2009b. An overview of the *Babesia*, *Plasmodium* and *Theileria* genomes: a comparative perspective. *Mol Biochem Parasitol*, 164, 1-8.
- LAU, A. O. 2009c. An overview of the *Babesia*, *Plasmodium* and *Theileria* genomes: A comparative perspective. *Molecular and biochemical parasitology*, 164, 1-8.
- LAU, A. O., MCELWAIN, T. F., BRAYTON, K. A., KNOWLES, D. P. & ROALSON, E. H. 2009. *Babesia bovis*: a comprehensive phylogenetic analysis of plastid-encoded genes supports green algal origin of apicoplasts. *Experimental parasitology*, 123, 236-243.
- LE ROCH, K. G., CHUNG, D. W. & PONTIS, N. 2012. Genomics and integrated systems biology in *Plasmodium falciparum*: a path to malaria control and eradication. *Parasite Immunol*, 34, 50-60.
- LELL, B., RUANGWEERAYUT, R., WIESNER, J., MISSINOU, M. A., SCHINDLER, A., BARANEK, T., HINTZ, M., HUTCHINSON, D., JOMAA, H. & KREMSNER, P. G. 2003. Fosmidomycin, a novel chemotherapeutic agent for malaria. *Antimicrobial agents and chemotherapy*, 47, 735-738.
- LEROY, D., CAMPO, B., DING, X. C., BURROWS, J. N. & CHERBUIN, S. 2014. Defining the biology component of the drug discovery strategy for malaria eradication. *Trends in parasitology*, 30, 478-490.

- LEVY, M. G. & RISTIC, M. 1980. Babesia bovis: continuous cultivation in a microaerophilous stationary phase culture. *Science*, 207, 1218-20.
- LI, L., STOECKERT, C. J. & ROOS, D. S. 2003. OrthoMCL: identification of ortholog groups for eukaryotic genomes. *Genome research*, 13, 2178-2189.
- LIM, L. & MCFADDEN, G. I. 2010. The evolution, metabolism and functions of the apicoplast. *Philos Trans R Soc Lond B Biol Sci*, 365, 749-63.
- LINGNAU, A., MARGOS, G., MAIER, W. A. & SEITZ, H. M. 1993. Serum-free cultivation of Plasmodium falciparum gametocytes in vitro. *Parasitol Res*, 79, 378-84.
- LLINAS, M., BOZDECH, Z., WONG, E. D., ADAI, A. T. & DERISI, J. L. 2006. Comparative whole genome transcriptome analysis of three Plasmodium falciparum strains. *Nucleic Acids Res*, 34, 1166-73.
- LOBO, C. A., CURSINO-SANTOS, J. R., ALHASSAN, A. & RODRIGUES, M. 2013. Babesia: an emerging infectious threat in transfusion medicine. *PLoS pathogens*, 9, e1003387.
- MACKENSTEDT, U., GAUER, M., MEHLHORN, H., SCHEIN, E. & HAUSCHILD, S. 1990. Sexual cycle of Babesia divergens confirmed by DNA measurements. *Parasitology research*, 76, 199-206.
- MARATHE, A., TRIPATHI, J., HANDA, V. & DATE, V. 2005. Human babesiosis--a case report. *Indian J Med Microbiol*, 23, 267-9.
- MARECHAL, E. & CESBRON-DELAUW, M. F. 2001. The apicoplast: a new member of the plastid family. *Trends Plant Sci*, 6, 200-5.
- MCDANIEL, C. J., CARDWELL, D. M., MOELLER, R. B. & GRAY, G. C. 2014. Humans and cattle: a review of bovine zoonoses. *Vector-Borne and Zoonotic Diseases*, 14, 1-19.
- MCFADDEN, G. I. 2014. Apicoplast. *Curr Biol*, 24, R262-3.
- MEBIUS, R. E. & KRAAL, G. 2005. Structure and function of the spleen. *Nat Rev Immunol*, 5, 606-16.
- MEDLOCK, J. M., HANSFORD, K. M., BORMANE, A., DERDAKOVA, M., ESTRADA-PENA, A., GEORGE, J. C., GOLOVLJOVA, I., JAENSON, T. G., JENSEN, J. K., JENSEN, P. M., KAZIMIROVA, M., OTEO, J. A., PAPA, A., PFISTER, K., PLANTARD, O., RANDOLPH, S. E., RIZZOLI, A., SANTOS-SILVA, M. M., SPRONG, H., VIAL, L., HENDRICKX, G., ZELLER, H. & VAN BORTEL, W. 2013. Driving forces for changes in geographical distribution of Ixodes ricinus ticks in Europe. *Parasit Vectors*, 6, 1.
- MILLS, J. N., GAGE, K. L. & KHAN, A. S. 2010. Potential influence of climate change on vector-borne and zoonotic diseases: a review and proposed research plan. *Environ Health Perspect*, 118, 1507-14.
- MIOTTO, O., ALMAGRO-GARCIA, J., MANSKE, M., MACINNIS, B., CAMPINO, S., ROCKETT, K. A., AMARATUNGA, C., LIM, P., SUON, S., SRENG, S., ANDERSON, J. M., DUONG, S., NGUON, C., CHUOR, C. M., SAUNDERS, D., SE, Y., LON, C., FUKUDA, M. M., AMENGA-ETEGO, L., HODGSON, A. V., ASOALA, V., IMWONG, M., TAKALA-HARRISON, S., NOSTEN, F., SU, X. Z., RINGWALD, P., ARIEY, F., DOLECEK, C., HIEN, T. T., BONI, M. F., THAI, C. Q., AMAMBUANGWA, A., CONWAY, D. J., DJIMDE, A. A., DOUMBO, O. K., ZONGO, I., OUEDRAOGO, J. B., ALCOCK, D., DRURY, E., AUBURN, S., KOCH, O., SANDERS, M., HUBBART, C., MASLEN, G., RUANO-RUBIO, V., JYOTHI, D., MILES, A., O'BRIEN, J., GAMBLE, C., OYOLA, S. O., RAYNER, J. C., NEWBOLD, C. I., BERRIMAN, M., SPENCER, C. C., MCVEAN, G., DAY, N. P., WHITE, N. J., BETHELL, D., DONDORP, A. M., PLOWE, C. V., FAIRHURST, R. M. & KWIATKOWSKI, D. P. 2013. Multiple populations of artemisinin-resistant Plasmodium falciparum in Cambodia. *Nat Genet*, 45, 648-55.
- MITSUMOTO, A., NAKAGAWA, Y., TAKEUCHI, A., OKAWA, K., IWAMATSU, A. & TAKANEZAWA, Y. 2001. Oxidized forms of peroxiredoxins and DJ-1 on two-dimensional gels increased in response to sublethal levels of paraquat. *Free Radic Res*, 35, 301-10.
- MORIYA, Y., ITOH, M., OKUDA, S., YOSHIZAWA, A. C. & KANEHISA, M. 2007. KAAS: an automatic genome annotation and pathway reconstruction server. *Nucleic acids research*, 35, W182-W185.
- MOSQUEDA, J., OLVERA-RAMIREZ, A., AGUILAR-TIPACAMÚ, G. & CANTO, G. 2012. Current advances in detection and treatment of babesiosis. *Current medicinal chemistry*, 19, 1504.

- MU, J., SEYDEL, K. B., BATES, A. & SU, X. Z. 2010. Recent Progress in Functional Genomic Research in *Plasmodium falciparum*. *Curr Genomics*, 11, 279-86.
- MULLER, J. & HEMPHILL, A. 2013. In vitro culture systems for the study of apicomplexan parasites in farm animals. *Int J Parasitol*, 43, 115-24.
- MUNKHJARGAL, T., ABOULAILA, M., TERKAWI, M. A., SIVAKUMAR, T., ICHIKAWA, M., DAVAASUREN, B., NYAMJARGAL, T., YOKOYAMA, N. & IGARASHI, I. 2012. Inhibitory effects of pepstatin A and mefloquine on the growth of *Babesia* parasites. *The American journal of tropical medicine and hygiene*, 87, 681-688.
- NAGAI, A., YOKOYAMA, N., MATSUO, T., BORK, S., HIRATA, H., XUAN, X., ZHU, Y., CLAVERIA, F. G., FUJISAKI, K. & IGARASHI, I. 2003. Growth-inhibitory effects of artesunate, pyrimethamine, and pamaquine against *Babesia equi* and *Babesia caballi* in in vitro cultures. *Antimicrob Agents Chemother*, 47, 800-3.
- NAGAKUBO, D., TAIRA, T., KITaura, H., IKEDA, M., TAMAI, K., IGUCHI-ARIGA, S. M. & ARIGA, H. 1997. DJ-1, a novel oncogene which transforms mouse NIH3T3 cells in cooperation with ras. *Biochem Biophys Res Commun*, 231, 509-13.
- NEHRBASS-STUEDLI, A., BOYKIN, D., TIDWELL, R. R. & BRUN, R. 2011. Novel diamidines with activity against *Babesia divergens* in vitro and *Babesia microti* in vivo. *Antimicrob Agents Chemother*, 55, 3439-45.
- OHLSTEIN, E. H., RUFFOLO, R. R., JR. & ELLIOTT, J. D. 2000. Drug discovery in the next millennium. *Annu Rev Pharmacol Toxicol*, 40, 177-91.
- OLIVEROS, J. C. 2007. VENNY. An interactive tool for comparing lists with Venn Diagrams.
- OZ, H. S. & WESTLUND, K. H. 2012. "Human babesiosis": an emerging transfusion dilemma. *Int J Hepatol*, 2012, 431761.
- PUDNEY, M. & GRAY, J. S. 1997. Therapeutic efficacy of atovaquone against the bovine intraerythrocytic parasite, *Babesia divergens*. *J Parasitol*, 83, 307-10.
- QUACKENBUSH, J. 2002. Microarray data normalization and transformation. *Nature genetics*, 32, 496-501.
- RALPH, S. A., VAN DOOREN, G. G., WALLER, R. F., CRAWFORD, M. J., FRAUNHOLZ, M. J., FOTH, B. J., TONKIN, C. J., ROOS, D. S. & MCFADDEN, G. I. 2004. Tropical infectious diseases: metabolic maps and functions of the *Plasmodium falciparum* apicoplast. *Nat Rev Microbiol*, 2, 203-16.
- REGASSA, A., PENZHORN, B. L. & BRYSON, N. R. 2003. Attainment of endemic stability to *Babesia bigemina* in cattle on a South African ranch where non-intensive tick control was applied. *Vet Parasitol*, 116, 267-74.
- RIBEIRO, J. M., ALARCON-CHAIDEZ, F., FRANCISCETTI, I. M., MANS, B. J., MATHER, T. N., VALENZUELA, J. G. & WIKEL, S. K. 2006. An annotated catalog of salivary gland transcripts from *Ixodes scapularis* ticks. *Insect Biochem Mol Biol*, 36, 111-29.
- RICHER, E., BIAGINI, G. A., WEIN, S., BOUDOU, F., BRAY, P. G., WARD, S. A., PRECIGOUT, E., CALAS, M., DUBREMETZ, J. F. & VIAL, H. J. 2006. Potent antihematozoan activity of novel bithiazolium drug T16: evidence for inhibition of phosphatidylcholine metabolism in erythrocytes infected with *Babesia* and *Plasmodium* spp. *Antimicrob Agents Chemother*, 50, 3381-8.
- RITCHIE, M. E., SILVER, J., OSHLACK, A., HOLMES, M., DIYAGAMA, D., HOLLOWAY, A. & SMYTH, G. K. 2007. A comparison of background correction methods for two-colour microarrays. *Bioinformatics*, 23, 2700-2707.
- RUDZINSKA, M. A., TRAGER, W., LEWENGRUB, S. J. & GUBERT, E. 1976. An electron microscopic study of *Babesia microti* invading erythrocytes. *Cell and tissue research*, 169, 323-334.
- RUIZ-FONS, F., FERNANDEZ-DE-MERA, I. G., ACEVEDO, P., GORTAZAR, C. & DE LA FUENTE, J. 2012. Factors driving the abundance of *Ixodes ricinus* ticks and the prevalence of zoonotic *I. ricinus*-borne pathogens in natural foci. *Appl Environ Microbiol*, 78, 2669-76.
- SAIDANI, N., BOTTE, C. Y., DELIGNY, M., BONNEAU, A. L., READER, J., LASSELIN, R., MERER, G., NIEPCERON, A., BROSSIER, F., CINTRAT, J. C., ROUSSEAU, B., BIRKHOLTZ, L. M., CESBRON-

- DELAUW, M. F., DUBREMETZ, J. F., MERCIER, C., VIAL, H., LOPEZ, R. & MARECHAL, E. 2014. Discovery of compounds blocking the proliferation of *Toxoplasma gondii* and *Plasmodium falciparum* in a chemical space based on piperidinyl-benzimidazolone analogs. *Antimicrob Agents Chemother*, 58, 2586-97.
- SALAMA, A. A., ABOULAILA, M., MOUSSA, A. A., NAYEL, M. A., EL-SIFY, A., TERKAWI, M. A., HASSAN, H. Y., YOKOYAMA, N. & IGARASHI, I. 2013. Evaluation of in vitro and in vivo inhibitory effects of fusidic acid on *Babesia* and *Theileria* parasites. *Vet Parasitol*, 191, 1-10.
- SAMISH, M., GINSBERG, H. & GLAZER, I. 2008. 20• Anti-tick biological control agents: assessment and future perspectives. *Biology, Disease and Control*, 447.
- SCHNITTGER, L., RODRIGUEZ, A., FLORIN-CHRISTENSEN, M. & MORRISON, D. 2012. *Babesia*: a world emerging. *Infection, genetics and evolution: journal of molecular epidemiology and evolutionary genetics in infectious diseases*, 12, 1788-1809.
- SCHUSTER, F. L. 2002a. Cultivation of *Babesia* and *Babesia*-like blood parasites: agents of an emerging zoonotic disease. *Clin Microbiol Rev*, 15, 365-73.
- SCHUSTER, F. L. 2002b. Cultivation of *Babesia* and *Babesia*-like blood parasites: agents of an emerging zoonotic disease. *Clinical microbiology reviews*, 15, 365-373.
- SEEBER, F. 2003. Biosynthetic pathways of plastid-derived organelles as potential drug targets against parasitic apicomplexa. *Curr Drug Targets Immune Endocr Metabol Disord*, 3, 99-109.
- SEEBER, F., LIMENITAKIS, J. & SOLDATI-FAVRE, D. 2008. Apicomplexan mitochondrial metabolism: a story of gains, losses and retentions. *Trends in parasitology*, 24, 468-478.
- SHIKANO, S., NAKADA, K., HASHIGUCHI, R., SHIMADA, T. & ONO, K. 1995. A short term in vitro cultivation of *Babesia rodhaini* and *Babesia microti*. *J Vet Med Sci*, 57, 955-7.
- SILVA, B. A., BREYDO, L., FINK, A. L. & UVERSKY, V. N. 2013. Agrochemicals, alpha-synuclein, and Parkinson's disease. *Mol Neurobiol*, 47, 598-612.
- SIMON, R., RADMACHER, M. D., DOBBIN, K. & MCSHANE, L. M. 2003. Pitfalls in the use of DNA microarray data for diagnostic and prognostic classification. *Journal of the National Cancer Institute*, 95, 14-18.
- SINGH-BEHL, D., LA ROSA, S. & TOMECKI, K. 2003. Tick-borne infections. *Dermatologic clinics*, 21, 237.
- SIVAKUMAR, T., ABOULAILA, M., KHUKHUU, A., ISEKI, H., ALHASSAN, A., YOKOYAMA, N., IGARASHI, I., 横山直明 & 五十嵐郁男 2008. In vitro inhibitory effect of fosmidomycin on the asexual growth of *Babesia bovis* and *Babesia bigemina*.
- SLONIM, D. K. & YANAI, I. 2009. Getting started in gene expression microarray analysis. *PLoS Comput Biol*, 5, e1000543.
- SMILKSTEIN, M., SRIWILAJAROEN, N., KELLY, J. X., WILAIRAT, P. & RISCOE, M. 2004. Simple and inexpensive fluorescence-based technique for high-throughput antimalarial drug screening. *Antimicrobial Agents and Chemotherapy*, 48, 1803-1806.
- SMIT, S. 2010. *Functional consequences of the inhibition of Malaria S-adenosylmethionine decarboxylase as a key regulator of polyamine and methionine metabolism*. Department of Biochemistry, University of Pretoria.
- SMYTH, G. K. 2004. Linear models and empirical bayes methods for assessing differential expression in microarray experiments. *Statistical applications in genetics and molecular biology*, 3, 1-25.
- SMYTH, G. K., MICHAUD, J. & SCOTT, H. S. 2005. Use of within-array replicate spots for assessing differential expression in microarray experiments. *Bioinformatics*, 21, 2067-2075.
- SMYTH, G. K. & SPEED, T. 2003. Normalization of cDNA microarray data. *Methods*, 31, 265-273.
- SNYMAN, J. 2011. *The effect of herbicides as novel antimalarial drugs on the transcriptome and proteome of Plasmodium falciparum*. *Magister Scientiae*, University of Pretoria.
- STUART, J. M., SEGAL, E., KOLLER, D. & KIM, S. K. 2003. A gene-coexpression network for global discovery of conserved genetic modules. *science*, 302, 249-255.
- SU, Z., LI, Z., CHEN, T., LI, Q. Z., FANG, H., DING, D., GE, W., NING, B., HONG, H., PERKINS, R. G., TONG, W. & SHI, L. 2011. Comparing next-generation sequencing and microarray

- technologies in a toxicological study of the effects of aristolochic acid on rat kidneys. *Chem Res Toxicol*, 24, 1486-93.
- SUAREZ, C. E. & NOH, S. 2011. Emerging perspectives in the research of bovine babesiosis and anaplasmosis. *Vet Parasitol*, 180, 109-25.
- SUAREZ, C. E., NORIMINE, J., LACY, P. & MCELWAIN, T. F. 2006. Characterization and gene expression of *Babesia bovis* elongation factor-1 α . *International journal for parasitology*, 36, 965-973.
- SUBRAMANIAN, A., TAMAYO, P., MOOTHA, V. K., MUKHERJEE, S., EBERT, B. L., GILLETTE, M. A., PAULOVICH, A., POMEROY, S. L., GOLUB, T. R. & LANDER, E. S. 2005. Gene set enrichment analysis: a knowledge-based approach for interpreting genome-wide expression profiles. *Proceedings of the National Academy of Sciences of the United States of America*, 102, 15545-15550.
- SUN, Y., MOREAU, E., CHAUVIN, A. & MALANDRIN, L. 2011. The invasion process of bovine erythrocyte by *Babesia divergens*: knowledge from an in vitro assay. *Vet Res*, 42, 62.
- TAKAHASHI, K., TAIRA, T., NIKI, T., SEINO, C., IGUCHI-ARIGA, S. M. & ARIGA, H. 2001. DJ-1 positively regulates the androgen receptor by impairing the binding of PIAS α to the receptor. *J Biol Chem*, 276, 37556-63.
- THOMFORD, J. W., CONRAD, P. A., TELFORD, S. R., 3RD, MATHIESEN, D., BOWMAN, B. H., SPIELMAN, A., EBERHARD, M. L., HERWALDT, B. L., QUICK, R. E. & PERSING, D. H. 1994. Cultivation and phylogenetic characterization of a newly recognized human pathogenic protozoan. *J Infect Dis*, 169, 1050-6.
- TIROSH, I. & BARKAI, N. 2005. Computational verification of protein-protein interactions by orthologous co-expression. *BMC Bioinformatics*, 6, 40.
- TRAGER, W. 1994. Digestion and indigestion in malaria parasites. *J Clin Invest*, 93, 1353.
- TRAGER, W. & JENSEN, J. B. 1976. Human malaria parasites in continuous culture. *Science*, 193, 673-675.
- UENO, A., TERKAWI, M. A., YOKOYAMA, M., CAO, S., ABOGE, G., ABOULAILA, M., NISHIKAWA, Y., XUAN, X., YOKOYAMA, N. & IGARASHI, I. 2013. Farnesyl pyrophosphate synthase is a potential molecular drug target of rispedronate in *Babesia bovis*. *Parasitol Int*, 62, 189-92.
- VALENTIN, A., RIGOMIER, D., PRÉCIGOUT, É., CARCY, B., GORENFLOT, A. & SCHRÉVEL, J. 1991. Lipid trafficking between high density lipoproteins and *Babesia divergens*-infected human erythrocytes. *Biology of the Cell*, 73, 63-70.
- VAN BRUMMELEN, A. C., OLSZEWSKI, K. L., WILINSKI, D., LLINÁS, M., LOUW, A. I. & BIRKHOLTZ, L.-M. 2009. Co-inhibition of Plasmodium falciparum S-adenosylmethionine decarboxylase/ornithine decarboxylase reveals perturbation-specific compensatory mechanisms by transcriptome, proteome, and metabolome analyses. *Journal of Biological Chemistry*, 284, 4635-4646.
- VAN DOOREN, G. G. & STRIEPEN, B. 2013. The algal past and parasite present of the apicoplast. *Annu Rev Microbiol*, 67, 271-89.
- VANNIER, E., BORGGRAEFE, I., TELFORD, S. R., 3RD, MENON, S., BRAUNS, T., SPIELMAN, A., GELFAND, J. A. & WORTIS, H. H. 2004. Age-associated decline in resistance to *Babesia microti* is genetically determined. *J Infect Dis*, 189, 1721-8.
- VANNIER, E. & KRAUSE, P. J. 2009. Update on babesiosis. *Interdisciplinary perspectives on infectious diseases*, 2009.
- VANNIER, E. & KRAUSE, P. J. 2012. Human babesiosis. *New England Journal of Medicine*, 366, 2397-2407.
- VAYRYNEN, R. & TUOMI, J. 1982. Continuous in vitro cultivation of *Babesia divergens*. *Acta Vet Scand*, 23, 471-2.
- VEMURI, G. N. & ARISTIDOU, A. A. 2005. Metabolic engineering in the -omics era: elucidating and modulating regulatory networks. *Microbiol Mol Biol Rev*, 69, 197-216.

- VERBIST, B., KLAMBAUER, G., VERVOORT, L., TALLOEN, W., SHKEDY, Z., THAS, O., BENDER, A., GOHLMANN, H. W. & HOCHREITER, S. 2015. Using transcriptomics to guide lead optimization in drug discovery projects. *Drug Discov Today*.
- VERLINDEN, B. K., NIEMAND, J., SNYMAN, J., SHARMA, S. K., BEATTIE, R. J., WOSTER, P. M. & BIRKHOLTZ, L.-M. 2011. Discovery of novel alkylated (bis) urea and (bis) thiourea polyamine analogues with potent antimalarial activities. *Journal of medicinal chemistry*, 54, 6624-6633.
- VIAL, H. J. & GORENFLOT, A. 2006. Chemotherapy against babesiosis. *Veterinary parasitology*, 138, 147-160.
- VYAS, J. M., TELFORD, S. R. & ROBBINS, G. K. 2007. Treatment of refractory Babesia microti infection with atovaquone-proguanil in an HIV-infected patient: case report. *Clinical infectious diseases*, 45, 1588-1560.
- WALKER, A. R. 2011. Eradication and control of livestock ticks: biological, economic and social perspectives. *Parasitology*, 138, 945-959.
- WALLER, R. F. & MCFADDEN, G. I. 2005. The apicoplast: a review of the derived plastid of apicomplexan parasites. *Curr Issues Mol Biol*, 7, 57-79.
- WALLER, R. F., RALPH, S. A., REED, M. B., SU, V., DOUGLAS, J. D., MINNIKIN, D. E., COWMAN, A. F., BESRA, G. S. & MCFADDEN, G. I. 2003. A type II pathway for fatty acid biosynthesis presents drug targets in Plasmodium falciparum. *Antimicrobial agents and chemotherapy*, 47, 297-301.
- WANG, C., GONG, B., BUSHEL, P. R., THIERRY-MIEG, J., THIERRY-MIEG, D., XU, J., FANG, H., HONG, H., SHEN, J., SU, Z., MEEHAN, J., LI, X., YANG, L., LI, H., LABAJ, P. P., KREIL, D. P., MEGHERBI, D., GAJ, S., CAIMENT, F., VAN DELFT, J., KLEINJANS, J., SCHERER, A., DEVANARAYAN, V., WANG, J., YANG, Y., QIAN, H. R., LANCASHIRE, L. J., BESSARABOVA, M., NIKOLSKY, Y. & FURLANELLO, C. 2014. The concordance between RNA-seq and microarray data depends on chemical treatment and transcript abundance. 32, 926-32.
- WANG, S., SIM, T. B., KIM, Y. S. & CHANG, Y. T. 2004. Tools for target identification and validation. *Curr Opin Chem Biol*, 8, 371-7.
- WILL, C. L. & LÜHRMANN, R. 2011. Spliceosome structure and function. *Cold Spring Harbor perspectives in biology*, 3, a003707.
- WILLADSEN, P. 2006. Tick control: thoughts on a research agenda. *Vet Parasitol*, 138, 161-8.
- WILLADSEN, P. 2008. Antigen cocktails: valid hypothesis or unsubstantiated hope? *Trends in parasitology*, 24, 164-167.
- WOLBER, P. K., COLLINS, P. J., LUCAS, A. B., DE WITTE, A. & SHANNON, K. W. 2006. The Agilent in situ-synthesized microarray platform. *Methods Enzymol*, 410, 28-57.
- WORMSER, G. P., PRASAD, A., NEUHAUS, E., JOSHI, S., NOWAKOWSKI, J., NELSON, J., MITTLEMAN, A., AGUERO-ROSENFELD, M., TOPAL, J. & KRAUSE, P. J. 2010. Emergence of resistance to azithromycin-atovaquone in immunocompromised patients with Babesia microti infection. *Clinical infectious diseases*, 50, 381-386.
- YABSLEY, M. J. & SHOCK, B. C. 2013. Natural history of Zoonotic Babesia: Role of wildlife reservoirs. *Int J Parasitol Parasites Wildl*, 2, 18-31.
- ZINTL, A., MULCAHY, G., SKERRETT, H. E., TAYLOR, S. M. & GRAY, J. S. 2003. Babesia divergens, a bovine blood parasite of veterinary and zoonotic importance. *Clinical microbiology reviews*, 16, 622-636.
- ZWEYGARTH, E. & LOPEZ-REBOLLAR, L. M. 2000. Continuous in vitro cultivation of Babesia gibsoni. *Parasitol Res*, 86, 905-7.
- ZWEYGARTH, E., VAN NIEKERK, C. J. & DE WAAL, D. T. 1999. Continuous in vitro cultivation of Babesia caballi in serum-free medium. *Parasitol Res*, 85, 413-6.

APPENDIX 1.1 Summary of tick vectors and the associated diseases affecting animals (Compiled from de la Fuente *et al.*, 2007)

Pathogen	Tick vector	Host (s)	Geographic distribution	Disease
Protozoa: genus <i>Babesia</i>				
<i>B. beliceri</i>	<i>Hyalomma</i> spp.	Cattle	Russia	Not named
<i>B. bigemina</i>	<i>Boophilus</i> spp., <i>Rhipicephalus</i> spp.	Cattle, buffalo	Africa, America, Asia, Australia	Cattle babesiosis
<i>B. bovis</i>	<i>Boophilus</i> spp.	Cattle, buffalo	Africa, America, Asia, Australia	Cattle babesiosis
<i>B. major</i>	<i>Haemaphysalis</i> spp.	Cattle	Europe	Cattle babesiosis
<i>B. ovate</i>	<i>Haemaphysalis</i> spp.	Cattle	Asia	Not named
<i>B. occultans</i>	<i>Hyalomma</i> spp.	Cattle	Africa	Not named
<i>B. divergens</i>	<i>Ixodes</i> spp.	Cattle	Europe	Cattle babesiosis
<i>B. microti</i>	<i>Ixodes scapularis</i>	Rodents	USA, Canada	Babesiosis
<i>B. canis</i>	<i>Rhipicephalus sanguineus</i> , <i>Dermacentor reticulatus</i> , <i>Dermacentor marginatus</i>	Dogs	Tropical and semitropical regions worldwide	Dog babesiosis
<i>B. vogeli</i>	<i>R. sanguineus</i>	Dogs	Tropical and semitropical regions worldwide	Dog babesiosis
<i>B. rossi</i>	<i>Haemaphysalis leachi</i>	Dogs	Southern Africa	Dog babesiosis
<i>B. gibsoni</i>	<i>Haemaphysalis bispinosa</i> , <i>Haemaphysalis longicornis</i> , <i>R. sanguineus</i>	Dogs	Africa, Asia, USA, southern Europe	Dog babesiosis
<i>B. ovis</i>	<i>Rhipicephalus bursa</i> , <i>Rhipicephalus turanicus</i>	Sheep	Africa, Asia, Europe	Sheep babesiosis
<i>B. motasi</i>	<i>Haemaphysalis</i> spp.	Sheep	Africa, Asia, Europe	Sheep babesiosis
<i>B. caballi</i>	<i>Dermacentor</i> spp., <i>Rhipicephalus evertsi evertsi</i>	Horses, mules, donkeys	Africa, America, Asia, Europe	Horse babesiosis
<i>B. felis</i>	Unknown	Cats	Africa	Not named
<i>B. bicornis</i>	Unknown	Black rhinoceros	Southern Africa	Not named
<i>B. odocoilei</i>	<i>I. scapularis</i>	Cervidae and wild Bovidae	America	Not named
Protozoa: genus <i>Theileria</i>				
<i>T. annulata</i>	<i>Hyalomma</i> spp.	Cattle, Camels	Eurasia, Africa, Central Asia	Tropical theileriosis
<i>T. orientalis</i>	<i>Haemaphysalis</i> spp.	Cattle, Asian buffalo	Asia	Not named
<i>T. parva</i>	<i>Rhipicephalus appendiculatus</i>	Cattle	Africa	East Coast Fever

<i>T. lawrencei</i>	<i>Rhipicephalus zambeziensis</i>	Cattle	Africa	Corridor disease
<i>T. velifera</i>	<i>Amblyomma</i> spp.	Cattle, African buffalo	Africa	Apathogenic
<i>T. buffeli</i>	<i>Haemaphysalis</i> spp.	Cattle, Asian buffalo	Asia	Apathogenic
<i>T. mutans</i>	<i>Amblyomma hebraeum</i> , <i>Amblyomma lepidum</i> , <i>Amblyomma variegatum</i> , <i>Amblyomma cohaerens</i>	Cattle	Africa	Benign Theileriosis
<i>T. taurotragi</i>	<i>R. appendiculatus</i> , <i>Rhipicephalus pulchellus</i> , <i>R. zambeziensis</i>	Cattle	Africa	Benign Theileriosis
<i>T. ovis</i>	<i>Hyalomma</i> spp., <i>R. bursa</i>	Sheep	Africa, Asia	Sheep theileriosis
<i>T. lestoquardi</i>	<i>Hyalomma</i> spp.	Sheep, goats	Mediterranean, Asia, Middle East, India	Sheep theileriosis
<i>T. separate</i>	<i>R. evertsi</i>	Sheep, goats	Africa	Non-pathogenic
<i>T. bicornis</i>	Unknown	Black rhinoceros	southern Africa	Not named
<i>T. equi</i>	<i>Dermacentor</i> spp., <i>Rhipicephalus</i> spp., <i>Hyalomma</i> spp., <i>Boophilus</i> spp.	Horses, mules, donkeys	southern Europe, Africa, Asia	Equine biliary fever
<i>T. cervi</i>	<i>Amblyomma americanum</i>	White-tailed deer	Nearctic	Non-pathogenic
Protozoa: genus Hepatozoan				
<i>H. canis</i>	<i>R. sanguineus</i> , <i>H. longicornis</i>	Dogs	Southern Europe, Middle East, Africa	Hepatozoonosis
<i>H. americanum</i>	<i>Amblyomma maculatum</i>	Dogs	Southern USA	Hepatozoonosis
Protozoa: genus Cytauxzoon				
<i>C. felis</i>	<i>Dermacentor variabilis</i>	Domestic cats and wild felids	USA, Brazil	Cytauxzoonosis
Bacteria: genus Aegyptianella				
<i>A. pullorum</i>	<i>Argas walkerae</i> , <i>Argas persicus</i> , <i>Argas reflexus</i>	Domestic poultry	Africa, southern Europe, Middle Asia	Aegyptianellosis
Bacteria: genus Rickettsia				
<i>R. rickettsia</i>	<i>Dermacentor andersoni</i> , <i>D. variabilis</i> , <i>Amblyomma cajennense</i> , <i>Amblyomma aureolatum</i> , <i>R. sanguineus</i>	Dog	Americas	Rocky Mountain spotted fever
<i>R. conorii conorii</i>	<i>R. sanguineus</i>	Dog	Europe, Africa, Asia	Mediterranean spotted fever
Bacteria: genus Ehrlichia				
<i>E. chaffeensis</i>	<i>A. americanum</i> , <i>D. variabilis</i>	Various mammals	USA	Human monocytic ehrlichiosis
<i>E. ruminantium</i>	<i>A. hebraeum</i> , <i>Amblyomma astrion</i> , <i>A. cohaerens</i> , <i>Amblyomma gemma</i> ,	Mainly cattle	Africa, Caribbean	Heartwater

	<i>Amblyomma marmoreum</i> , <i>A. lepidum</i> , <i>Amblyomma pomposum</i> , <i>A. variegatum</i> , <i>A. mericanum</i>			
<i>E. canis</i>	<i>R. sanguineus</i>	Dogs	Southern USA, southern Europe, Africa, Middle East, eastern Asia	Canine ehrlichiosis
Bacteria: genus				
<i>Anaplasma</i>, <i>Francisella</i>, <i>Coxiella</i>				
<i>A. phagocytophilum</i>	<i>I. scapularis</i> , <i>I. pacificus</i> , <i>Ixodes ricinus</i> , <i>Ixodes hexagonus</i>	Various mammals	USA, Europe	Human granulocytic anaplasmosis
<i>A. marginale</i>	Various	Cattle	Worldwide	Bovine Anaplasmosis
<i>A. central</i>	Various	Cattle	Worldwide	Bovine Anaplasmosis
<i>A. ovis</i>	Various	Sheep	Worldwide	Ovine Anaplasmosis
<i>A. platys</i>	<i>R. sanguineus</i>	Dog	Not named	Canine ehrlichiosis
<i>F. tularensis</i>	Various	Various mammals	Eurasia	Tularemia
<i>C. burnetii</i>	Various	Various mammals	Worldwide	Q fever
Bacteria: genus <i>Borrelia</i>				
<i>B. theileri</i>	<i>Boophilus spp.</i> , <i>R. evertsi</i>	Cattle	Africa, Central and South America, Australia	Bovine borreliosis
<i>B. turcica</i>	<i>Hyalomma aegyptium</i>	Not named	Parts of Turkey	Not named
<i>B. miyamotoi</i>	<i>I. persulcatus</i>	Not named	Asia	Not named
<i>B. anserine</i>	<i>Argas spp.</i>	Birds	Worldwide	Avian borreliosis
<i>B. coraciae</i>	<i>Ornithodoros coriaceus</i>	Cattle	USA	Bovine epizootic abortion
Bacteria: genus <i>Dermatophilus</i>				
<i>D. congolensis</i>	<i>A. variegatum</i>	Ruminants	Africa	Dermatophilosis
Virus				
<i>Bunyaviridae</i> , <i>Nairovirus</i>	<i>R. appendiculatus</i> , <i>R. pulchelus</i> , <i>A. variegatum</i>	Sheep, goat	Kenya, Uganda, Rwanda, Tanzania, Somalia	Nairobi Sheep Disease
<i>Bunyaviridae</i> ungrouped	<i>Argas vespertilionis</i> , <i>A. pusillus</i> , <i>Ixodes vespertilionis</i>	Bats	Tadzhikistan, Kyrgyzstan, Turkmenistan	Issyk-Kul fever virus
<i>Orthomyxoviridae</i> <i>Thogotovirus</i>	<i>Amblyomma spp.</i> , <i>Boophilus spp.</i> , <i>Hyalomma</i> <i>spp.</i> , <i>Rhipicephalus spp.</i>	Sheep	USA	Thogotovirus
<i>Flaviviridae</i> , <i>Flavivirus</i>	<i>Ixodes granulatus</i> , <i>Haemaphysalis papuana</i>	Wild rodents	Europe, Asia	Langat virus
<i>Flaviviridae</i> , <i>Flavivirus</i>	<i>I. ricinus</i>	Sheep	Malaysia	Louping ill
<i>Flaviviridae</i> , <i>Flavivirus</i>	<i>Ixodes cookie</i> , <i>Ixodes marxi</i> , <i>I. scapularis</i> , <i>D. andersoni</i> ,	Rodents	United Kingdom	Powassan Encephalitis

<i>Flaviviridae, Flavivirus</i>	<i>Haemaphysalis spp.</i>	Monkeys	Canada, USA, Russia	Kyasanur Forest
<i>Asfaviridae, Asfavis</i>	<i>Ornithodoros moubata, Ornithodoros erraticus, O. turicata, O. coriaceus, Ornithodoros puertoricensis</i>	Domestic pigs	Africa, southern Europe, Caribbean	African Swine Fever
Nematoda: genus <i>Acanthocheilonema</i>				
<i>A. viteae</i>	<i>Ornithodoros tartakovskyi</i>	Rodents	Asia	Not named
<i>A. dracunculoides</i>	<i>R. sanguineus</i>	Dogs	Not named	Not named

APPENDIX 1.2 Summary of tick vectors and the associated diseases affecting humans (Compiled from de la Fuente *et al.*, 2007)

Pathogen	Tick vector	Geographic distribution	Disease
Protozoa: genus <i>Babesia</i>			
<i>B. divergens</i>	<i>Ixodes spp.</i>	Europe	Babesiosis
<i>B. divergens-like</i>	Unknown	USA	Babesiosis
<i>B. microti</i>	<i>I. scapularis</i>	USA, Canada	Babesiosis
<i>B. microti-like</i>	<i>I. ovatus</i>	Japan, Taiwan	Babesiosis
<i>B. venatorum</i>	<i>Ixodes spp.</i>	Austria, Italy, Germany, Belgium	Babesiosis
<i>B. duncani</i>	Unknown	USA	Babesiosis
<i>B. species (CA1, CA3, C4)</i>	Unknown	USA	Babesiosis
<i>B. species KO-1 (ovine)</i>	Unknown	South Korea	Babesiosis
<i>R. rickettsia</i>	<i>D. andersoni</i> , <i>D. variabilis</i> , <i>A. cajennense</i> , <i>A. aureolatum</i> , <i>R. sanguineus</i>	Americas	Rocky Mountain spotted fever
<i>R. amblyommii</i>	<i>A. americanum</i> , <i>Amblyomma neumanni</i> , <i>A. cajennense</i> , <i>A. coelebs</i>	Americas	Spotted fever rickettsiae
<i>R. conorii conorii</i>	<i>R. sanguineus</i>	Europe, Africa, Asia	Mediterranean spotted fever
<i>R. conorii israelensis</i>	<i>R. sanguineus</i>	Israel	Israeli spotted fever
<i>R. conorii caspia</i>	<i>R. sanguineus</i> , <i>Rhipicephalus pumilio</i>	Africa, Asia	Astrakhan fever
<i>R. conorii indica</i>	<i>R. sanguineus</i>	India	Indian tick typhus
<i>R. sibirica sibirica</i>	<i>Dermacentor nuttalli</i> , <i>D. marginatus</i> , <i>Dermacentor</i> <i>silvarum</i> , <i>Dermacentor sinicus</i> , <i>Haemaphysalis concinna</i>	Asia	Siberian or North Asian tick typhus
<i>R. sibiricamongolotimonae</i>	<i>Hyalomma asiaticum</i> , <i>Hyalomma truncatum</i> , <i>Hyalomma anatolicum excavatum</i>	Africa, China, France	Unnamed
<i>R. australis</i>	<i>Ixodes holocyclus</i> , <i>I. tasmani</i>	Australia	Queensland tick typhus
<i>R. japonica</i>	<i>I. ovatus</i> , <i>Dermacentor taiwanensis</i> , <i>H. longicornis</i> , <i>Haemaphysalis flava</i>	Japan	Oriental or Japanese spotted fever
<i>R. africae</i>	<i>A. hebraeum</i> , <i>A. variegatum</i>	Africa, Reunion Island, West Indies	African tick-bite fever
<i>R. honei</i>	<i>Bothriocroton hydrosauri</i> , <i>A. cajennense</i> , <i>I. granulatus</i>	Australia, USA, Thailand	Flinders island spotted fever
<i>R. slovacica T</i>	<i>D. marginatus</i> , <i>D. reticulatus</i>	Europe, Asia	Ibola, Debonel
<i>R. helvetica</i>	<i>I. ricinus</i>	Europe	Pathogenicity suspected
<i>R. heilongjiangensis</i>	<i>D. silvarum</i>	China	Unnamed
<i>R. aeschlimannii</i>	<i>H. marginatum marginatum</i> , <i>H. m. rufipes</i> , <i>R. appendiculatus</i>	Europe, Africa	Unnamed

<i>R. parkeri</i>	<i>A. maculatum</i> , <i>Amblyomma triste</i> , <i>Amblyomma dubitatum</i>	USA, Uruguay, Brazil	Unnamed
<i>R. massiliae</i>	<i>R. sanguineus</i> , <i>R. turanicus</i> , <i>R. muhsamae</i> , <i>R. lunulatus</i> , <i>R. sulcatus</i>	Europe, Asia, Argentina, USA	Unnamed
<i>R. marmionii</i>	<i>Haemaphysalis novaeguineae</i> , <i>Ixodes holocyclus</i>	Australia	Australian spotted fever
<i>R. monacensis</i>	<i>I. ricinus</i>	Europe	Unnamed
Bacteria: genus Ehrlichia			
<i>E. chaffeensis</i>	<i>A. americanum</i> , <i>D. variabilis</i>	USA	Human monocytic ehrlichiosis
<i>E. ewingii</i>	<i>A. americanum</i>	USA	Human ehrlichiosis
Bacteria: genus Anaplasma, Francisella, Coxiella			
<i>A. phagocytophilum</i>	<i>I. scapularis</i> , <i>I. pacificus</i> , <i>I. ricinus</i> , <i>I. hexagonus</i>	USA, Europe	Human granulocytic anaplasmosis
<i>F. tularensis</i>	Various	Eurasia	Tularemia
<i>C. burnetii</i>	Various	Worldwide	Q fever
Bacteria: genus Borrelia			
<i>B. burgdorferi</i>	<i>I. pacificus</i> , <i>I. persulcatus</i> , <i>I. ricinus</i> , <i>I. scapularis</i>	USA, Canada, Europe, Asia, Africa	Lyme disease
<i>B. garinii</i>	<i>I. persulcatus</i> , <i>I. ricinus</i>	Europe, Asia, Africa	Lyme disease
<i>B. afzelii</i>	<i>I. persulcatus</i> , <i>I. ricinus</i>	Europe, Asia, Africa	Lyme disease
<i>B. valaisiana</i>	<i>I. ricinus</i>	Europe, Asia	Lyme disease
<i>B. lusitaniae</i>	<i>I. ricinus</i>	Europe	Unnamed
<i>B. spielmani</i>	<i>I. ricinus</i>	Europe	Lyme disease
<i>B. japonica</i>	<i>I. ovatus</i>	Japan	Lyme disease
<i>B. lonestari</i>	<i>A. americanum</i>	USA	Unnamed
<i>B. turcica</i>	<i>H. aegyptium</i>	Parts of Turkey	Unnamed
<i>B. miyamotoi</i>	<i>I. persulcatus</i>	Asia	Unnamed
<i>B. hermsii</i>	<i>Ornithodoros hermsi</i>	USA, Canada	New World tick-borne relapsing fever
<i>B. turicatae</i>	<i>O. turicata</i>	USA, Mexico	New World tick-borne relapsing fever
<i>B. parkeri</i>	<i>Ornithodoros parkeri</i>	USA	New World tick-borne relapsing fever
<i>B. mazzottii</i>	<i>Ornithodoros talaje</i>	USA, Mexico	New World tick-borne relapsing fever
<i>B. venezuelensis</i>	<i>Ornithodoros rudis</i>	Central and South America	New World tick-borne relapsing fever

<i>B. duttonii</i>	<i>O. moubata</i>	Africa	Old World tick-borne relapsing fever
<i>B. crocidurae</i>	<i>Ornithodoros erraticus</i>	Europe, Africa	Old World tick-borne relapsing fever
<i>B. persica</i>	<i>Ornithodoros tholozani</i>	Asia	Persian relapsing fever
<i>B. hispanica</i>	<i>O. erraticus</i>	Spain, Portugal	Old World tick-borne relapsing fever
<i>B. latyschevii</i>	<i>O. tartakovskyi</i>	Iran, Central Asia	Old World tick-borne relapsing fever
<i>B. caucasica</i>	<i>Ornithodoros asperses</i>	Asia	Old World tick-borne relapsing
<i>B. graingeri</i>	<i>Ornithodoros graingeri</i>	Africa	Unnamed
<i>B. tillae</i>	<i>Ornithodoros zumpti</i>	Africa	Unnamed
<i>B. parkeri</i>	<i>O. parkeri</i>	USA	Unnamed
Virus			
<i>Bunyaviridae, Nairovirus</i>	<i>H. marginatum, A. variegatum, Haemaphysalis punctata, I. ricinus, Dermacentor spp., Rhipicephalus spp.</i>	Africa, Asia, Europe	Crimean-Congo Hemorrhagic Fever
<i>Bunyaviridae, Nairovirus</i>	<i>Ornithodoros maritimus, O. capensis, Ornithodoros denmarki</i>	Trinidad, Hawaii, Seychelles, Ethiopia, South Africa, Morocco, France, United Kingdom	Soldado virus
<i>Bunyaviridae ungrouped</i>	<i>Argas vespertilionis, A. pusillus, Ixodes vespertilionis</i>	Tadzhikistan, Kyrgyzstan, Turkmenistan	Issyk-Kul fever virus
<i>Reoviridae, Orbivirus</i>	<i>I. ricinus, I. ventraloi</i>	Europe	Eyach virus
<i>Reoviridae, Orbivirus</i>	<i>D. andersoni, D. occidentalis, D. albipictus</i>	Nearctic	Colorado tick fever
<i>Reoviridae, Orbivirus</i>	<i>Argas monolakensis, A. cooleyi</i>	Unnamed	Mono Lake virus
<i>Orthomyxoviridae Thogotovirus</i>	<i>Amblyomma spp., Boophilus spp., Hyalomma spp., Rhipicephalus spp.</i>	USA	Thogotovirus
<i>Flaviviridae, Flavivirus</i>	<i>D. reticulatus</i>	Central and East Africa, southern Europe	Omsk Hemorrhagic fever
<i>Flaviviridae, Flavivirus</i>	<i>I. ricinus, I. persulcatus, Haemaphysalis concinna, H. punctata</i>	Omsk and Novosibirsk	Tick Borne Encephalitis
<i>Flaviviridae, Flavivirus</i>	<i>I. cookie, I. marxi, I. scapularis, D. andersoni</i>	United Kingdom	Powassan Encephalitis
<i>Flaviviridae, Flavivirus</i>	<i>Haemaphysalis spp.</i>	Canada, USA, Russia	Kyasanur Forest disease

APPENDIX 4.1 RNA yield and quality assessment conducted with the Experion[®] automated electrophoresis system for all 24 RNA samples to be used for microarray analysis.

Sample Name	RNA Concentration (ng/μl)	RQI ^a	RQI Classification ^b
1	1026.66	9.9	Green
2	473.51	9.6	Green
3	802.16	9.9	Green
4	1452.24	9.9	Green
5	1699.51	9.9	Green
6	785.67	9.7	Green
7	976.35	9.8	Green
8	915.79	9.8	Green
9	1344.04	9.7	Green
10	526.78	9.9	Green
11	1247.4	9.9	Green
12	1396.56	9.9	Green
13	1033.44	9.8	Green
14	742.94	9.8	Green
15	1357.73	9.9	Green
16	1225.57	9.9	Green
17	875.99	9.9	Green
18	1226.17	9.9	Green
19	1218.16	9.8	Green
20	874.02	9.8	Green
21	1266.15	10	Green
22	1128.37	9.9	Green
23	1427.38	9.9	Green
24	857.54	9.9	Green

**a RNA Quality Index values range between 1.0 (completely degraded RNA) and 10.0 (intact RNA); *b RQI colour-codes classification range between red ($1 \leq RQI \leq 4$), yellow ($4 < RQI \leq 7$) and green ($7 < RQI \leq 10$).*

APPENDIX 4.2 Summary of all functionally annotated DEG transcripts with descriptions based on dCAS and BLAST2GO –platforms, respectively.

**See Excel document on CD*

APPENDIX 4.3 KEGG pathways and enzymes identified for all up and down -regulated gene transcripts

KEGG pathways identified	Enzymes identified within each KEGG pathway
Metabolic pathways	
	dihydroorotate dehydrogenase (fumarate)
	dihydrolipoamide dehydrogenase
	glycine hydroxymethyltransferase
	phosphatidylinositol 4-kinase
	ribose-phosphate pyrophosphokinase
	citrate synthase
	glutamyl-tRNA synthetase
	long-chain acyl-CoA synthetase
	adenylosuccinate synthase
	GMP synthase (glutamine-hydrolysing)
	F-type H ⁺ -transporting ATPase subunit beta
	cytochrome c oxidase subunit 2
	DNA polymerase epsilon subunit 1
	aspartyl-tRNA(Asn)/glutamyl-tRNA (Gln) amidotransferase subunit A
	DNA-directed RNA polymerase I subunit RPA1
	DNA-directed RNA polymerases I, II, and III subunit RPABC3
	DNA-directed RNA polymerase III subunit RPC2
	N-acetylglucosaminylphosphatidylinositol deacetylase
	2-oxoisovalerate dehydrogenase E2 component (dihydrolipoyl transacylase)
Purine metabolism	
	ribose-phosphate pyrophosphokinase
	adenylosuccinate synthase
	GMP synthase (glutamine-hydrolysing)
	DNA polymerase epsilon subunit 1
	DNA-directed RNA polymerase I subunit RPA1
	DNA-directed RNA polymerases I, II, and III subunit RPABC3
	DNA-directed RNA polymerase III subunit RPC2
Aminoacyl tRNA biosynthesis	
	isoleucyl-tRNA synthetase
	valyl-tRNA synthetase
	methionyl-tRNA synthetase
	glutamyl-tRNA synthetase
	phenylalanyl-tRNA synthetase alpha chain
	aspartyl-tRNA(Asn)/glutamyl-tRNA (Gln) amidotransferase subunit A
	lysyl-tRNA synthetase, class II
Biosynthesis of secondary metabolites	

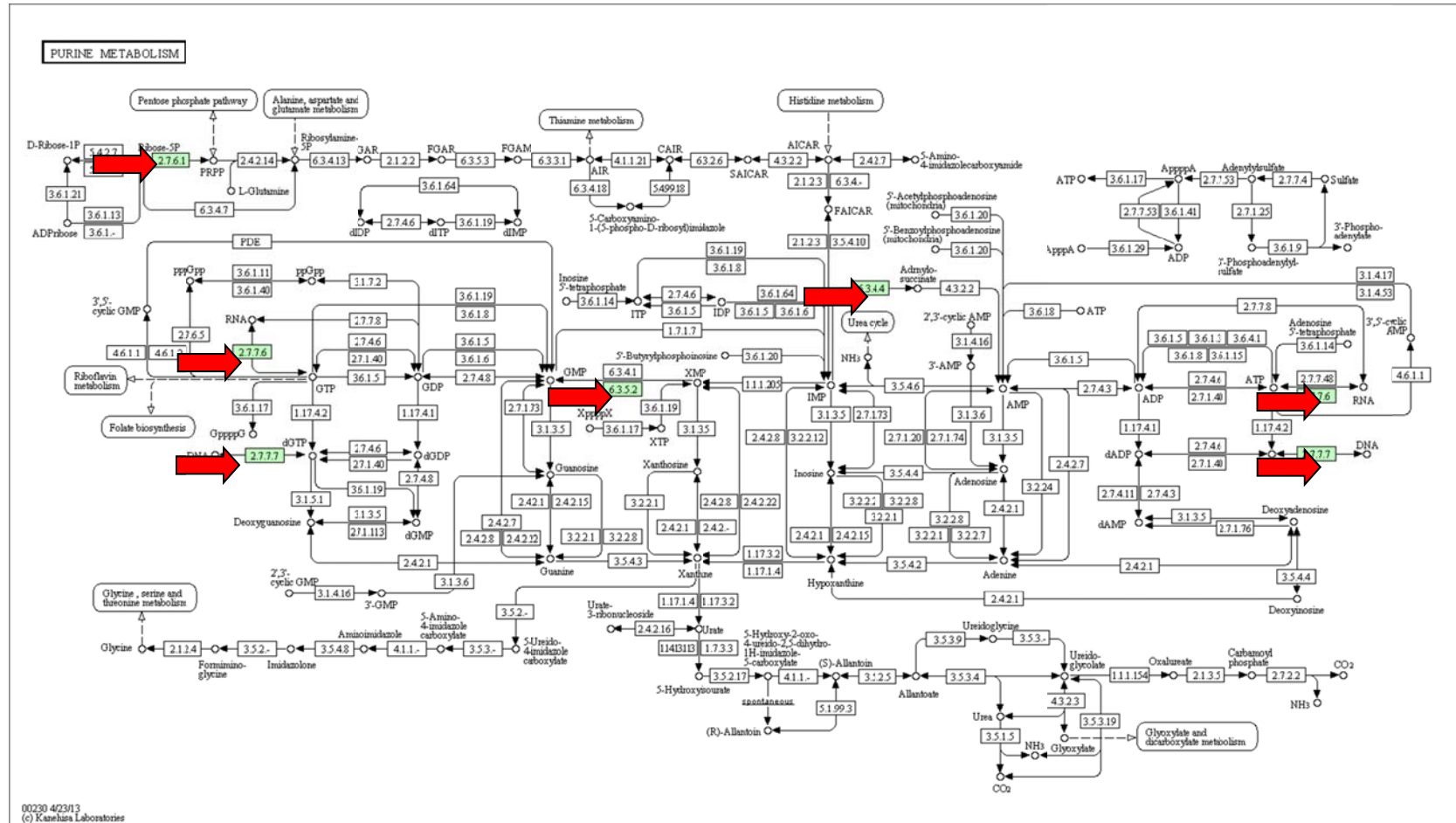
	dihydrolipoamide dehydrogenase
	glycine hydroxymethyltransferase
	ribose-phosphate pyrophosphokinase
	citrate synthase
	phosphoacetylglucosamine mutase
	glutamyl-tRNA synthetase
	2-oxoisovalerate dehydrogenase E2 component (dihydrolipoyl transacylase)
Sliceosome	
	ATP-dependent RNA helicase DDX46/PRP5
	pre-mRNA-splicing factor ATP-dependent RNA helicase DHX16
	PHD finger-like domain-containing protein 5A
	U4/U6.U5 tri-snRNP component SNU23
	pre-mRNA-splicing factor RBM22/SLT11
	protein mago nashi
RNA transport	
	translation initiation factor 1A
	translation initiation factor 3 subunit B
	GTP-binding nuclear protein Ran
	protein mago nashi
	polyadenylate-binding protein
Pyrimidine metabolism	
	dihydroorotate dehydrogenase (fumarate)
	DNA polymerase epsilon subunit 1
	DNA-directed RNA polymerase I subunit RPA1
	DNA-directed RNA polymerases I, II, and III subunit RPABC3
	DNA-directed RNA polymerase III subunit RPC2
Ubiquitin mediated proteolysis	
	S-phase kinase-associated protein 1
	ubiquitin-conjugating enzyme E2 A
	ubiquitin-conjugating enzyme E2 B
	ubiquitin-protein ligase E3 C
RNA degradation	
	ATP-dependent DNA helicase RecQ
	chaperonin GroEL
	5'-3' exoribonuclease 2
	polyadenylate-binding protein
RNA polymerase	
	DNA-directed RNA polymerase I subunit RPA1
	DNA-directed RNA polymerases I, II, and III subunit RPABC3
	DNA-directed RNA polymerase III subunit RPC2

Base excision repair	
	DNA polymerase epsilon subunit 1
	N-glycosylase/DNA lyase
	endonuclease III
Proteasome	
	20S proteasome subunit beta 3
	26S proteasome regulatory subunit N10
	26S proteasome regulatory subunit N6
mRNA surveillance pathway	
	protein phosphatase 2 (formerly 2A), catalytic subunit
	protein mago nashi
	polyadenylate-binding protein
DNA replication	
	DNA polymerase epsilon subunit 1
	DNA replication licensing factor MCM2
	replication factor C subunit 1
Biosynthesis of amino-acids	
	glycine hydroxymethyltransferase
	ribose-phosphate pyrophosphokinase
	citrate synthase
Ribosomes	
	large subunit ribosomal protein L24e
	small subunit ribosomal protein S15Ae
	small subunit ribosomal protein S18e
Valine, leucine and isoleucine degradation	
	dihydrolipoamide dehydrogenase
	2-oxoisovalerate dehydrogenase E2 component (dihydrolipoyl transacylase)
Endocytosis	
	AP-2 complex subunit alpha
	ADP-ribosylation factor GTPase-activating protein 1
Synaptic vesicle cycle	
	AP-2 complex subunit alpha
	syntaxin-binding protein 1
Citrate cycle	
	dihydrolipoamide dehydrogenase
	citrate synthase
TGF-beta signaling pathway	
	S-phase kinase-associated protein 1
	protein phosphatase 2 (formerly 2A), catalytic subunit
Mismatch repair	

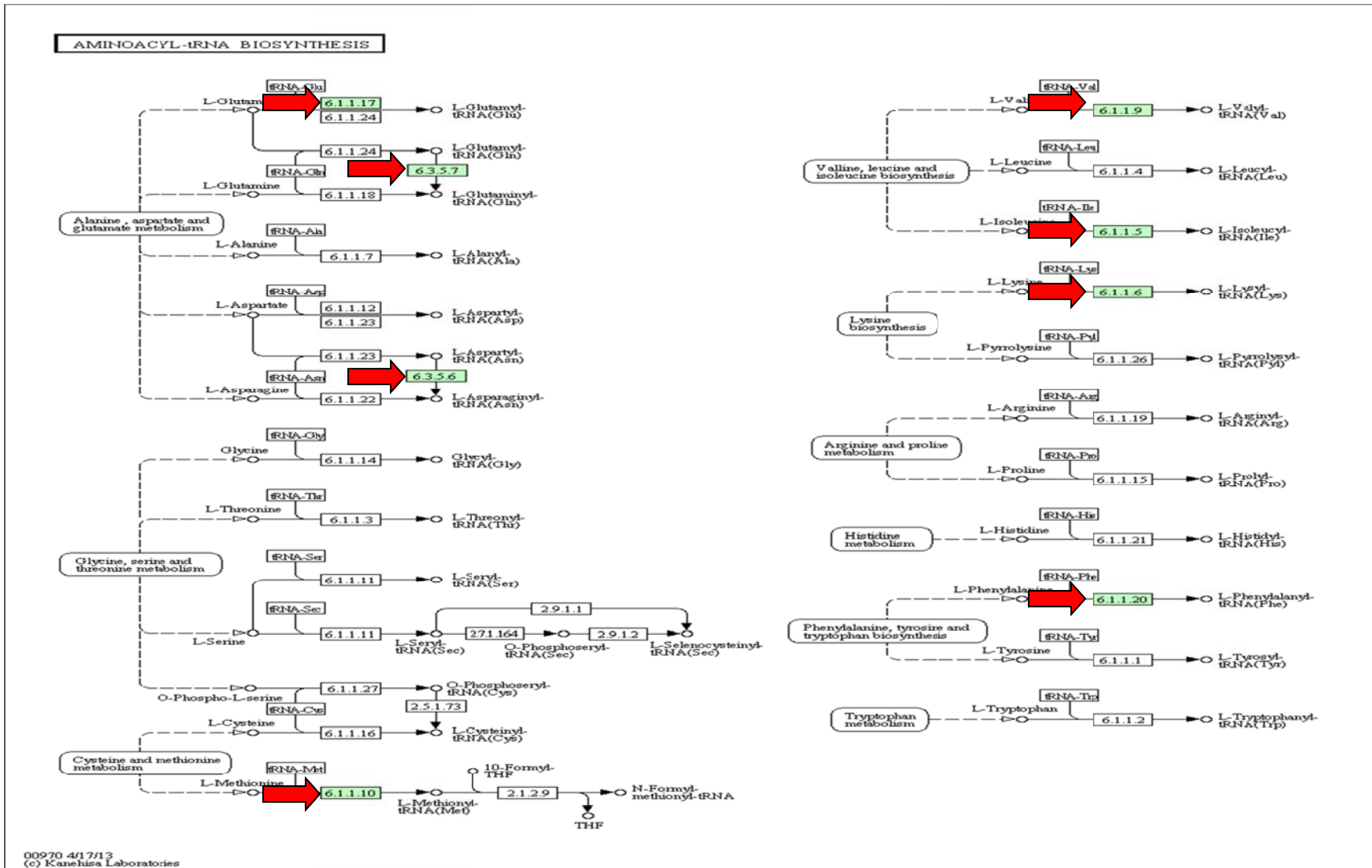
	replication factor C subunit 1
	DNA mismatch repair protein PMS2
Protein processing in endoplasmic reticulum	
	S-phase kinase-associated protein 1
	E3 ubiquitin-protein ligase RNF5
Oxidative phosphorylation	
	F-type H ⁺ -transporting ATPase subunit beta
	cytochrome c oxidase subunit 2
Glycine, serine and threonine metabolism	
	dihydroliipoamide dehydrogenase
	glycine hydroxymethyltransferase
Nucleotide excision repair	
	DNA polymerase epsilon subunit 1
	replication factor C subunit 1
Pyruvate metabolism	
	dihydroliipoamide dehydrogenase
	hydroxyacylglutathione hydrolase
Glyoxlate and dicarboxylate metabolism	
	glycine hydroxymethyltransferase
	citrate synthase
Cytosolic DNA-sensing pathway	
	DNA-directed RNA polymerases I, II, and III subunit RPABC3
	DNA-directed RNA polymerase III subunit RPC2
Cell cycle	
	DNA replication licensing factor MCM2
	S-phase kinase-associated protein 1
One carbon pool folate	
	glycine hydroxymethyltransferase
Tight junction	
	protein phosphatase 2 (formerly 2A), catalytic subunit
Endocrine and other factor-regulated calcium reabsorption	
	AP-2 complex subunit alpha
Drug metabolism - other enzymes	
	GMP synthase (glutamine-hydrolysing)
Inositol phosphate metabolism	
	phosphatidylinositol 4-kinase
Glycolysis/Gluconeogenesis	
	dihydroliipoamide dehydrogenase
Lysosome	
	AP-1 complex subunit gamma-1

Homologous recombination	double-strand break repair protein MRE11
Phosphatidylinositol signaling system	phosphatidylinositol 4-kinase
SNARE interactions in vesicular transport	synaptobrevin homolog YKT6
Non-homologous end-joining	double-strand break repair protein MRE11
Methane metabolism	glycine hydroxymethyltransferase
Porphyrin and chlorophyll metabolism	glutamyl-tRNA synthetase
Pentose phosphate pathway	ribose-phosphate pyrophosphokinase
Glycosylphosphatidylinositol (GPI-anchor biosynthesis)	N-acetylglucosaminylphosphatidylinositol deacetylase
Fatty-acid metabolism	long-chain acyl-CoA synthetase
Alanine, aspartate and glutamate metabolism	adenylosuccinate synthase
Peroxisome	long-chain acyl-CoA synthetase
Adipocytokine signaling pathway	long-chain acyl-CoA synthetase
2-Oxocarboxylic acid metabolism	citrate synthase
Phagosome	dynein heavy chain 1, cytosolic
Amino sugar and nucleotide sugar metabolism	phosphoacetylglucosamine mutase
Cyanoamino metabolism	glycine hydroxymethyltransferase
Selenocompound metabolism	methionyl-tRNA synthetase
Wnt signalling pathway	S-phase kinase-associated protein 1
Glycerophospholipid metabolism	glycerol-3-phosphate dehydrogenase
PPAR signaling pathway	long-chain acyl-CoA synthetase

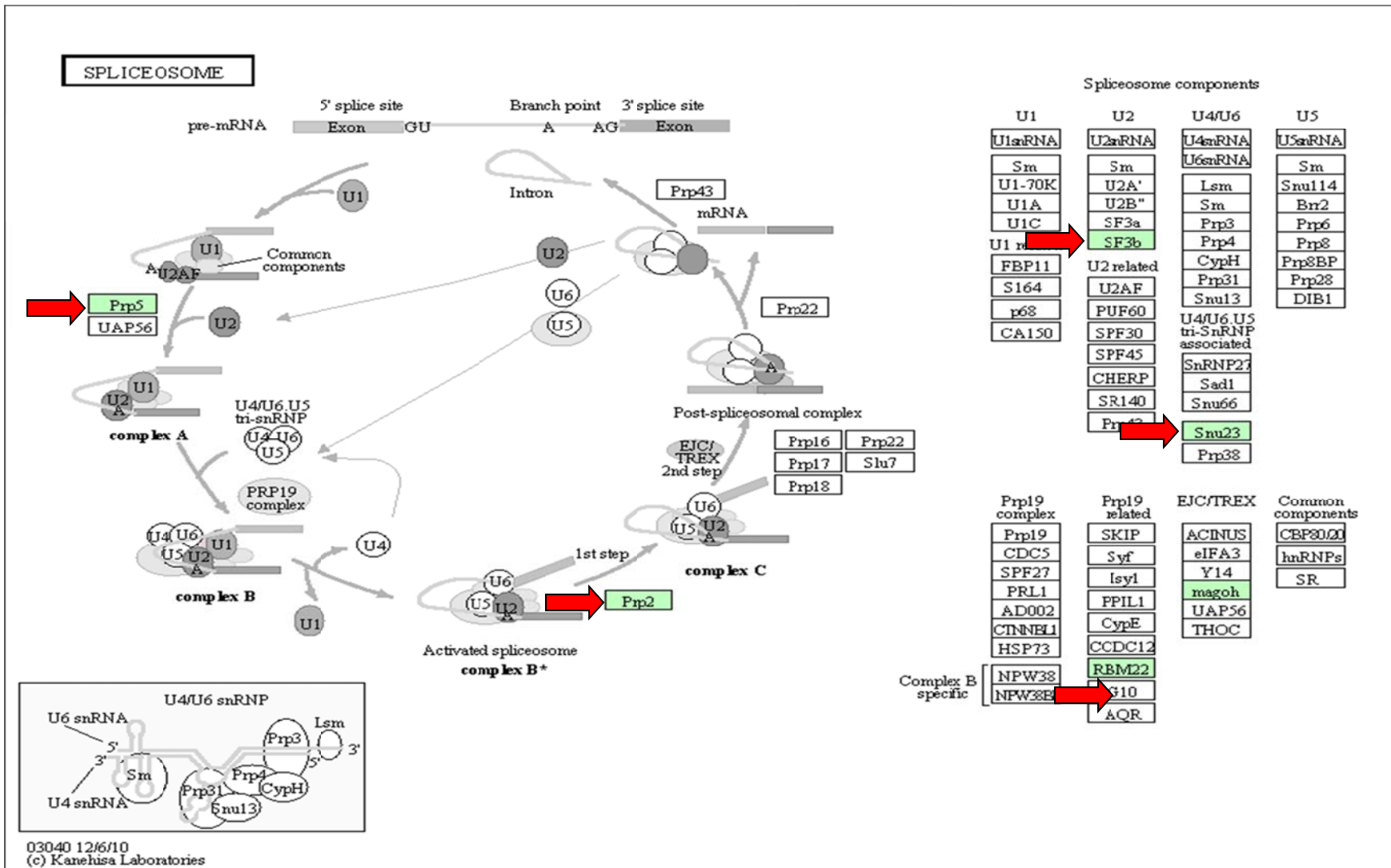
APPENDIX 4.4 KEGG pathways constructed for the top five pathways involved in differential gene expression (including purine metabolism, aminoacyl-tRNA biosynthesis, spliceosome, RNA transport and pyrimidine metabolism) identified with DNA microarrays



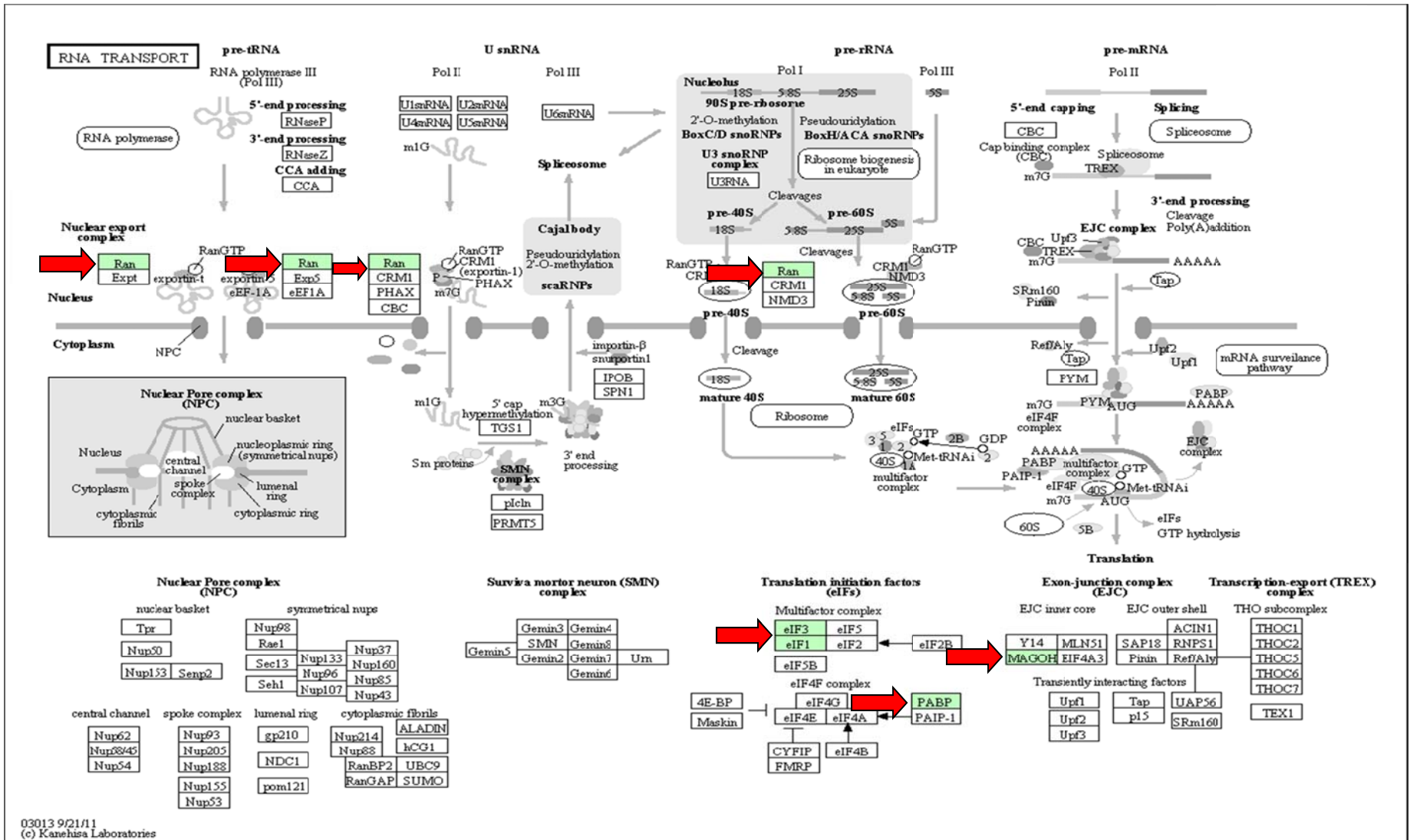
* KEGG map representation of the Purine biosynthetic pathway. Arrows indicate enzymes identified within this pathway for all up-and-down regulated genes.



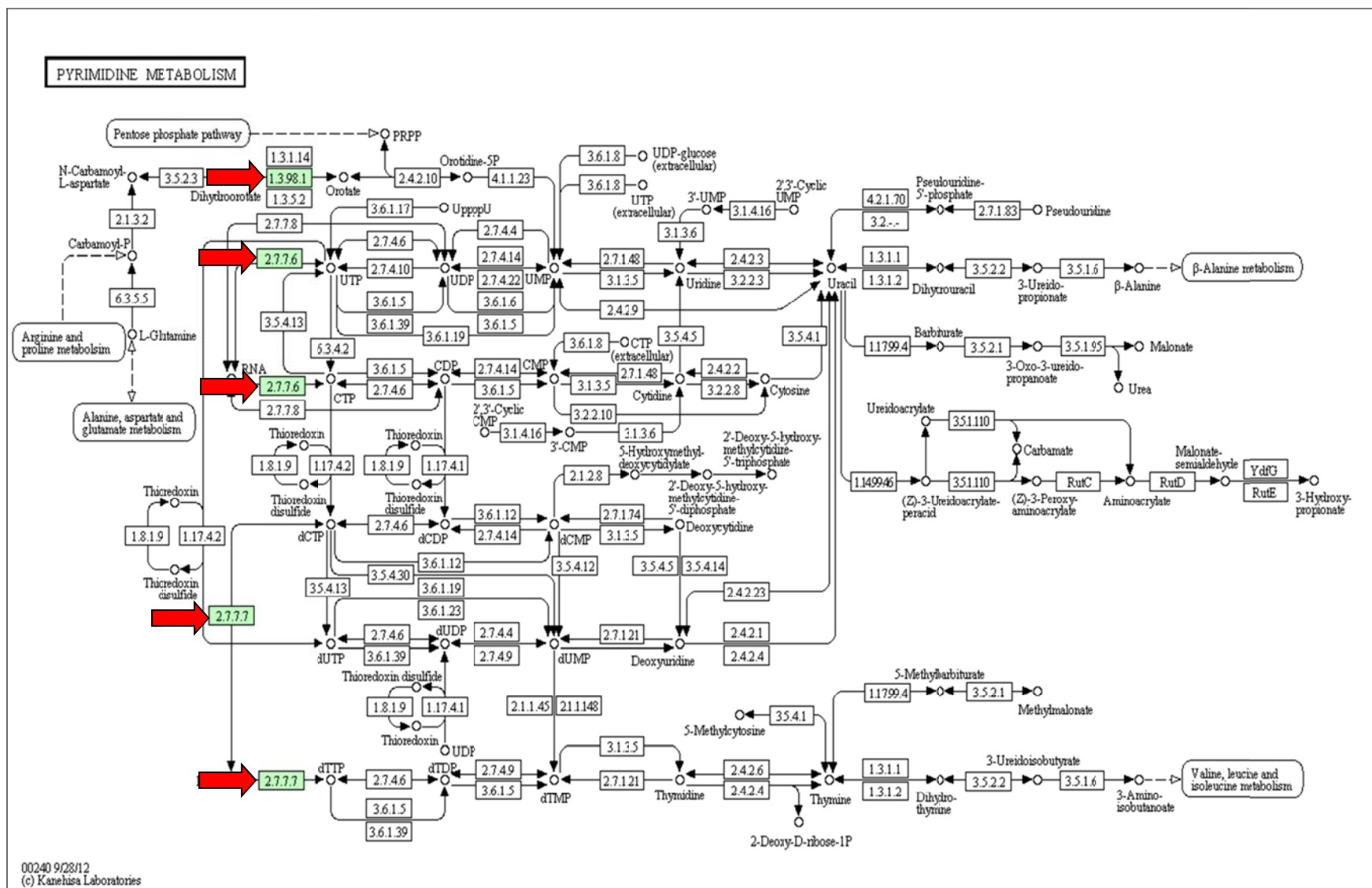
* KEGG map representation of the Aminoacyl tRNA biosynthetic pathway. Arrows indicate enzymes identified within this pathway for all up-and-down regulated genes.



* KEGG map representation of the Spliceosome biosynthetic pathway. Arrows indicate enzymes identified within this pathway for all up-and-down regulated genes.



* KEGG map representation of the RNA transport. Arrows indicate enzymes identified within this pathway for all up-and-down regulated genes.



* KEGG map representation of the Pyrimidine metabolism. Arrows indicate enzymes identified within this pathway for all up and down -regulated genes.

OG5_126854	BBOV_I002740
OG5_126854	BBOV_I002740
OG5_126854	BBOV_I002740
OG5_126854	BBOV_I002740
OG5_126854	BBOV_I002740
OG5_126854	BBOV_I002740
OG5_126854	BBOV_I002740
OG5_126854	BBOV_I002740
OG5_126854	BBOV_I002740
OG5_126854	BBOV_I002740
OG5_126854	BBOV_I002740
OG5_126854	BBOV_I002740
OG5_126854	BBOV_I002740
OG5_126854	BBOV_I002740
OG5_126854	BBOV_I002740
OG5_153060	BBOV_I002860
OG5_128219	BBOV_I002870
OG5_127402	BBOV_I002910
OG5_150527	BBOV_I002960
OG5_152614	BBOV_I003040
OG5_126913	BBOV_I003140
OG5_153341	BBOV_I003190
OG5_128226	BBOV_I003460
OG5_128435	BBOV_I003550
OG5_152413	BBOV_I003630
OG5_136182	BBOV_I003650
OG5_153536	BBOV_I003730
OG5_153070	BBOV_I004100
OG5_127784	BBOV_I004200
OG5_127994	BBOV_I004290
OG5_141728	BBOV_I004350
OG5_126936	BBOV_I004650
OG5_128255	BBOV_I004760
OG5_127962	BBOV_I004920
OG5_128059	BBOV_I004950
OG5_128059	BBOV_I004970
OG5_128059	BBOV_I004970
OG5_139383	BBOV_I005070
OG5_139383	BBOV_I005070
OG5_144638	BBOV_I005100
OG5_144638	BBOV_I005100
OG5_156790	BBOV_II000430
OG5_150395	BBOV_II000650
OG5_126644	BBOV_II000810

OG5_126644	BBOV_II000810
OG5_145099	BBOV_II000830
OG5_145099	BBOV_II000830
OG5_127206	BBOV_II000880
OG5_156791	BBOV_II000970
OG5_141671	BBOV_II001140
OG5_160480	BBOV_II001160
OG5_128117	BBOV_II001300
OG5_129047	BBOV_II002070
OG5_128457	BBOV_II002140
OG5_128667	BBOV_II002160
OG5_126774	BBOV_II002230
OG5_126774	BBOV_II002230
OG5_126774	BBOV_II002230
OG5_126774	BBOV_II002230
OG5_127854	BBOV_II002240
OG5_128816	BBOV_II002560
OG5_128055	BBOV_II002690
OG5_156796	BBOV_II002720
OG5_126678	BBOV_II002750
OG5_126678	BBOV_II002750
OG5_127496	BBOV_II002810
OG5_127608	BBOV_II002960
OG5_130456	BBOV_II002970
OG5_127223	BBOV_II003080
OG5_141740	BBOV_II003200
OG5_140539	BBOV_II003240
OG5_128215	BBOV_II003250
OG5_127934	BBOV_II003360
OG5_128058	BBOV_II003390
OG5_128469	BBOV_II003490
OG5_128469	BBOV_II003490
OG5_128599	BBOV_II003510
OG5_128495	BBOV_II003590
OG5_139182	BBOV_II003660
OG5_127319	BBOV_II003680
OG5_141266	BBOV_II003690
OG5_127173	BBOV_II003780
OG5_127173	BBOV_II003780
OG5_127173	BBOV_II003780
OG5_128487	BBOV_II003830
OG5_127881	BBOV_II003960
OG5_126956	BBOV_II004010

OG5_144710	BBOV_II004030
OG5_156799	BBOV_II004280
OG5_156800	BBOV_II004310
OG5_127153	BBOV_II004660
OG5_127153	BBOV_II004660
OG5_129939	BBOV_II004670
OG5_155120	BBOV_II004720
OG5_133088	BBOV_II004880
OG5_127011	BBOV_II004950
OG5_150553	BBOV_II004980
OG5_127512	BBOV_II005020
OG5_153559	BBOV_II005410
OG5_147429	BBOV_II005500
OG5_126684	BBOV_II005760
OG5_127764	BBOV_II005900
OG5_141745	BBOV_II005960
OG5_141745	BBOV_II005960
OG5_141746	BBOV_II006000
OG5_129533	BBOV_II006030
OG5_153324	BBOV_II006390
OG5_150555	BBOV_II006520
OG5_126773	BBOV_II006560
OG5_126773	BBOV_II006560
OG5_126773	BBOV_II006560
OG5_141466	BBOV_II006720
OG5_127570	BBOV_II006920
OG5_131688	BBOV_II006940
OG5_126904	BBOV_II006950
OG5_138116	BBOV_II006980
OG5_128182	BBOV_II007100
OG5_128182	BBOV_II007100
OG5_127289	BBOV_II007190
OG5_127312	BBOV_II007250
OG5_127633	BBOV_II007360
OG5_127670	BBOV_II007370
OG5_156807	BBOV_II007490
OG5_127535	BBOV_II007550
OG5_126886	BBOV_II007680
OG5_126665	BBOV_II007740
OG5_150576	BBOV_III000150
OG5_152508	BBOV_III000240
OG5_141545	BBOV_III000300
OG5_127654	BBOV_III000560

OG5_131701	BBOV_III000620
OG5_128133	BBOV_III000660
OG5_153594	BBOV_III000730
OG5_131401	BBOV_III000740
OG5_149676	BBOV_III000770
OG5_127215	BBOV_III000930
OG5_126694	BBOV_III000960
OG5_126694	BBOV_III000960
OG5_127906	BBOV_III001050
OG5_126867	BBOV_III001350
OG5_129958	BBOV_III001380
OG5_156825	BBOV_III001390
OG5_127465	BBOV_III002070
OG5_127269	BBOV_III002090
OG5_128660	BBOV_III002180
OG5_127231	BBOV_III002280
OG5_156829	BBOV_III002450
OG5_126601	BBOV_III002500
OG5_127624	BBOV_III002670
OG5_126745	BBOV_III002690
OG5_126745	BBOV_III002690
OG5_150584	BBOV_III003240
OG5_134232	BBOV_III003260
OG5_147462	BBOV_III003320
OG5_127153	BBOV_III003380
OG5_127153	BBOV_III003380
OG5_128881	BBOV_III003430
OG5_128884	BBOV_III003480
OG5_128884	BBOV_III003480
OG5_126885	BBOV_III003510
OG5_126885	BBOV_III003510
OG5_126885	BBOV_III003510
OG5_126885	BBOV_III003510
OG5_127711	BBOV_III003540
OG5_127273	BBOV_III003570
OG5_128366	BBOV_III003580
OG5_127572	BBOV_III003940
OG5_147466	BBOV_III003960
OG5_127797	BBOV_III004100
OG5_127408	BBOV_III004110
OG5_127408	BBOV_III004110
OG5_128098	BBOV_III004170
OG5_127256	BBOV_III004450

OG5_150588	BBOV_III004600
OG5_127481	BBOV_III004670
OG5_130863	BBOV_III004710
OG5_127874	BBOV_III004800
OG5_126733	BBOV_III004900
OG5_127732	BBOV_III005130
OG5_127604	BBOV_III005690
OG5_127604	BBOV_III005690
OG5_126969	BBOV_III005950
OG5_137714	BBOV_III006240
OG5_150591	BBOV_III006310
OG5_127900	BBOV_III006340
OG5_130661	BBOV_III006370
OG5_127081	BBOV_III006690
OG5_143221	BBOV_III006770
OG5_127557	BBOV_III006880
OG5_158546	BBOV_III006980
OG5_128077	BBOV_III007080
OG5_127761	BBOV_III007090
OG5_127036	BBOV_III007240
OG5_127969	BBOV_III007250
OG5_127107	BBOV_III007370
OG5_143222	BBOV_III007550
OG5_159765	BBOV_III007620
OG5_127017	BBOV_III007880
OG5_127017	BBOV_III007880
OG5_127017	BBOV_III007880
OG5_127641	BBOV_III008010
OG5_127641	BBOV_III008010
OG5_147475	BBOV_III008270
OG5_126723	BBOV_III008390
OG5_127922	BBOV_III008580
OG5_127922	BBOV_III008580
OG5_129313	BBOV_III008620
OG5_132300	BBOV_III008840
OG5_132300	BBOV_III008840
OG5_128066	BBOV_III008890
OG5_130216	BBOV_III008900
OG5_127553	BBOV_III008970
OG5_137217	BBOV_III009010
OG5_137217	BBOV_III009010
OG5_137217	BBOV_III009010
OG5_127942	BBOV_III009080

OG5_128354	BBOV_III009290
OG5_128354	BBOV_III009290
OG5_127677	BBOV_III009410
OG5_127149	BBOV_III009450
OG5_127149	BBOV_III009450
OG5_136181	BBOV_III009490
OG5_130129	BBOV_III009670
OG5_128295	BBOV_III009710
OG5_127466	BBOV_III009760
OG5_128528	BBOV_III009770
OG5_127574	BBOV_III009930
OG5_153619	BBOV_III010230
OG5_127333	BBOV_III010510
OG5_129228	BBOV_III010690
OG5_126878	BBOV_III010810
OG5_127351	BBOV_III010890
OG5_128449	BBOV_III011080
OG5_130916	BBOV_III011150
OG5_127127	BBOV_III011550
OG5_126865	BBOV_III011610
OG5_128638	BBOV_III011840
OG5_126579	BBOV_IV000140
OG5_153539	BBOV_IV000290
OG5_150530	BBOV_IV000420
OG5_127366	BBOV_IV000490
OG5_127366	BBOV_IV000490
OG5_127366	BBOV_IV000490
OG5_141731	BBOV_IV000700
OG5_127297	BBOV_IV000740
OG5_128587	BBOV_IV000850
OG5_127751	BBOV_IV000970
OG5_127751	BBOV_IV000980
OG5_127751	BBOV_IV000980
OG5_142443	BBOV_IV001080
OG5_127148	BBOV_IV001160
OG5_127148	BBOV_IV001160
OG5_127148	BBOV_IV001160
OG5_128047	BBOV_IV001200
OG5_141599	BBOV_IV001240
OG5_128121	BBOV_IV001360
OG5_128001	BBOV_IV001710
OG5_127773	BBOV_IV001730
OG5_127480	BBOV_IV001820

OG5_126740	BBOV_IV001910
OG5_126740	BBOV_IV001910
OG5_128799	BBOV_IV002190
OG5_128165	BBOV_IV002230
OG5_126620	BBOV_IV002290
OG5_126620	BBOV_IV002290
OG5_130299	BBOV_IV002400
OG5_139037	BBOV_IV002780
OG5_130616	BBOV_IV002810
OG5_140537	BBOV_IV002820
OG5_131402	BBOV_IV002890
OG5_147414	BBOV_IV003000
OG5_147414	BBOV_IV003000
OG5_127610	BBOV_IV003160
OG5_149560	BBOV_IV003360
OG5_149560	BBOV_IV003360
OG5_146858	BBOV_IV003470
OG5_141736	BBOV_IV003520
OG5_130659	BBOV_IV003570
OG5_129568	BBOV_IV003640
OG5_127038	BBOV_IV003820
OG5_150558	BBOV_IV003830
OG5_152974	BBOV_IV003990
OG5_152974	BBOV_IV003990
OG5_152974	BBOV_IV003990
OG5_147437	BBOV_IV004040
OG5_129285	BBOV_IV004150
OG5_143209	BBOV_IV004240
OG5_128795	BBOV_IV004470
OG5_127448	BBOV_IV004550
OG5_127291	BBOV_IV004560
OG5_127291	BBOV_IV004560
OG5_145108	BBOV_IV004890
OG5_153566	BBOV_IV004900
OG5_127936	BBOV_IV005100
OG5_127498	BBOV_IV005110
OG5_127890	BBOV_IV005130
OG5_150559	BBOV_IV005140
OG5_147442	BBOV_IV005430
OG5_126668	BBOV_IV005450
OG5_127311	BBOV_IV005540
OG5_128136	BBOV_IV005570
OG5_128678	BBOV_IV005610

OG5_128863	BBOV_IV005710
OG5_139980	BBOV_IV005730
OG5_127099	BBOV_IV005830
OG5_126679	BBOV_IV005840
OG5_130370	BBOV_IV005880
OG5_150563	BBOV_IV006060
OG5_144050	BBOV_IV006080
OG5_142685	BBOV_IV006170
OG5_150565	BBOV_IV006590
OG5_150565	BBOV_IV006590
OG5_128332	BBOV_IV006710
OG5_127313	BBOV_IV006740
OG5_127313	BBOV_IV006740
OG5_150567	BBOV_IV006800
OG5_127430	BBOV_IV006860
OG5_127497	BBOV_IV006880
OG5_135175	BBOV_IV007010
OG5_143212	BBOV_IV007040
OG5_126968	BBOV_IV007190
OG5_126641	BBOV_IV007450
OG5_126641	BBOV_IV007450
OG5_126641	BBOV_IV007450
OG5_126641	BBOV_IV007450
OG5_143151	BBOV_IV007520
OG5_156814	BBOV_IV007820
OG5_133546	BBOV_IV007890
OG5_133546	BBOV_IV007890
OG5_126730	BBOV_IV008060
OG5_128266	BBOV_IV008220
OG5_127814	BBOV_IV008240
OG5_147448	BBOV_IV008250
OG5_128225	BBOV_IV008270
OG5_126795	BBOV_IV008280
OG5_153577	BBOV_IV008330
OG5_156816	BBOV_IV008610
OG5_127464	BBOV_IV008880
OG5_127581	BBOV_IV008890
OG5_127581	BBOV_IV008890
OG5_128839	BBOV_IV008900
OG5_127152	BBOV_IV009110
OG5_141155	BBOV_IV009120
OG5_126558	BBOV_IV009380
OG5_126558	BBOV_IV009380

OG5_126558	BBOV_IV009380
OG5_126558	BBOV_IV009380
OG5_156817	BBOV_IV009390
OG5_127682	BBOV_IV009520
OG5_127813	BBOV_IV009590
OG5_127924	BBOV_IV009600
OG5_145118	BBOV_IV009660
OG5_146494	BBOV_IV009980
OG5_129173	BBOV_IV010440
OG5_128429	BBOV_IV010580
OG5_150574	BBOV_IV010800
OG5_127514	BBOV_IV010920
OG5_126599	BBOV_IV011160
OG5_126599	BBOV_IV011160
OG5_126599	BBOV_IV011160
OG5_152980	BBOV_IV011210
OG5_127529	BBOV_IV011250
OG5_128401	BBOV_IV011380
OG5_128486	BBOV_IV011410
OG5_153588	BBOV_IV011440
OG5_141514	BBOV_IV011500
OG5_128020	BBOV_IV011550
OG5_144402	BBOV_IV011820
OG5_144402	BBOV_IV011820
OG5_178105	BBOV_V000400
OG5_168705	BBOV_V000420

* Differentially expressed *B. divergens* gene transcript names correspond to *B. bovis* transcript names

APPENDIX 4.6 *P. falciparum* differentially expressed transcriptomic data with corresponding orthologue groups identified from the *B. bovis* - *P. falciparum* orthologue group matrix

Orthologue group name	<i>P. falciparum</i> DEG's
OG5_130344	MAL13P1.118
OG5_128830	MAL13P1.122
OG5_140542	MAL13P1.130
OG5_143145	MAL13P1.150
OG5_140345	MAL13P1.153
OG5_126954	MAL13P1.164
OG5_126954	MAL13P1.164
OG5_127926	MAL13P1.169
OG5_153060	MAL13P1.180
OG5_128475	MAL13P1.184
OG5_142982	MAL13P1.188
OG5_127236	MAL13P1.209
OG5_127359	MAL13P1.218
OG5_127375	MAL13P1.22
OG5_127375	MAL13P1.22
OG5_128535	MAL13P1.221
OG5_153563	MAL13P1.237
OG5_141744	MAL13P1.241
OG5_128224	MAL13P1.253
OG5_130478	MAL13P1.255
OG5_128549	MAL13P1.257
OG5_139161	MAL13P1.260
OG5_127832	MAL13P1.283
OG5_128226	MAL13P1.294
OG5_145093	MAL13P1.297
OG5_141731	MAL13P1.308
OG5_128932	MAL13P1.310
OG5_126648	MAL13P1.324
OG5_127990	MAL13P1.341
OG5_136346	MAL13P1.347
OG5_128098	MAL13P1.36
OG5_156847	MAL13P1.37
OG5_150527	MAL13P1.43
OG5_128656	MAL13P1.45
OG5_128247	MAL13P1.52
OG5_129603	MAL13P1.53
OG5_135283	MAL13P1.63
OG5_141625	MAL13P1.79
OG5_153558	MAL13P1.89
OG5_145102	MAL13P1.94

OG5_127360	MAL13P1.96
OG5_126970	MAL7P1.110
OG5_143207	MAL7P1.114
OG5_141752	MAL7P1.125
OG5_136181	MAL7P1.13
OG5_127670	MAL7P1.130
OG5_127670	MAL7P1.130
OG5_127773	MAL7P1.147
OG5_130786	MAL7P1.158
OG5_153589	MAL7P1.201
OG5_129958	MAL7P1.209
OG5_129027	MAL7P1.21
OG5_126588	MAL7P1.228
OG5_126588	MAL7P1.228
OG5_133154	MAL7P1.27
OG5_160579	MAL7P1.33
OG5_129865	MAL7P1.75
OG5_129167	MAL7P1.76
OG5_152312	MAL7P1.78
OG5_127718	MAL7P1.81
OG5_146589	MAL7P1.83
OG5_143212	MAL7P1.88
OG5_150068	MAL7P1.91
OG5_130342	MAL7P1.93
OG5_128417	MAL8P1.10
OG5_131254	MAL8P1.108
OG5_133046	MAL8P1.126
OG5_130898	MAL8P1.13
OG5_130898	MAL8P1.13
OG5_137859	MAL8P1.134
OG5_131282	MAL8P1.135
OG5_127562	MAL8P1.142
OG5_136021	MAL8P1.146
OG5_140107	MAL8P1.150
OG5_140107	MAL8P1.150
OG5_127555	MAL8P1.156
OG5_128298	MAL8P1.19
OG5_127551	MAL8P1.23
OG5_145099	MAL8P1.25
OG5_146254	MAL8P1.33
OG5_156804	MAL8P1.45
OG5_128490	MAL8P1.48
OG5_145117	MAL8P1.50

OG5_145117	MAL8P1.50
OG5_153587	MAL8P1.73
OG5_191856	MAL8P1.97
OG5_127434	PF07_0015
OG5_138116	PF07_0017
OG5_129560	PF07_0030
OG5_127363	PF07_0034
OG5_127295	PF07_0036
OG5_127255	PF07_0046
OG5_128467	PF07_0047
OG5_143032	PF07_0052
OG5_127402	PF07_0057
OG5_153576	PF07_0063
OG5_138354	PF07_0066
OG5_137217	PF07_0070
OG5_126784	PF07_0085
OG5_127064	PF07_0088
OG5_128660	PF07_0091
OG5_152184	PF07_0099
OG5_128317	PF07_0102
OG5_150545	PF07_0106
OG5_128978	PF07_0110
OG5_127754	PF07_0121
OG5_127903	PF07_0122
OG5_129618	PF07_0123
OG5_141730	PF07_0127
OG5_160575	PF08_0015
OG5_127126	PF08_0018
OG5_127126	PF08_0018
OG5_128694	PF08_0020
OG5_145103	PF08_0029
OG5_127781	PF08_0034
OG5_127203	PF08_0036
OG5_128346	PF08_0049
OG5_128348	PF08_0065
OG5_150585	PF08_0082
OG5_156188	PF08_0083
OG5_127153	PF08_0085
OG5_127153	PF08_0085
OG5_126761	PF08_0087
OG5_127557	PF08_0094
OG5_126849	PF08_0096
OG5_127366	PF08_0099

OG5_133546	PF08_0108
OG5_127854	PF08_0109
OG5_129014	PF08_0121
OG5_129462	PF08_0124
OG5_127652	PF08_0125
OG5_128106	PF08_0130
OG5_126593	PF08_0131
OG5_126593	PF08_0131
OG5_130284	PF08_0132
OG5_127366	PF10_0016
OG5_147399	PF10_0029
OG5_144710	PF10_0039
OG5_126957	PF10_0043
OG5_150566	PF10_0051
OG5_128175	PF10_0054
OG5_150524	PF10_0060
OG5_150523	PF10_0061
OG5_160572	PF10_0064
OG5_127313	PF10_0066
OG5_127313	PF10_0066
OG5_127824	PF10_0069
OG5_130776	PF10_0071
OG5_140457	PF10_0072
OG5_128265	PF10_0077
OG5_127592	PF10_0085
OG5_128975	PF10_0097
OG5_128456	PF10_0099
OG5_147127	PF10_0105
OG5_127152	PF10_0123
OG5_141009	PF10_0141
OG5_127420	PF10_0143
OG5_127420	PF10_0143
OG5_126721	PF10_0150
OG5_126721	PF10_0150
OG5_128508	PF10_0152
OG5_126788	PF10_0153
OG5_160582	PF10_0166
OG5_127005	PF10_0187
OG5_130863	PF10_0188
OG5_126969	PF10_0193
OG5_126696	PF10_0203
OG5_144058	PF10_0216
OG5_126793	PF10_0225

OG5_126793	PF10_0225
OG5_128209	PF10_0232
OG5_147414	PF10_0236
OG5_147416	PF10_0241
OG5_153509	PF10_0259
OG5_127014	PF10_0264
OG5_127887	PF10_0268
OG5_127981	PF10_0269
OG5_126830	PF10_0273
OG5_126830	PF10_0273
OG5_126830	PF10_0273
OG5_127909	PF10_0278
OG5_127245	PF10_0289
OG5_143206	PF10_0295
OG5_143206	PF10_0295
OG5_127891	PF10_0298
OG5_128972	PF10_0306
OG5_160617	PF10_0315
OG5_147422	PF10_0321
OG5_127435	PF10_0325
OG5_126927	PF10_0334
OG5_144357	PF10_0363
OG5_126841	PF10_0366
OG5_126660	PF10_0368
OG5_126660	PF10_0368
OG5_127208	PF10_0369
OG5_128127	PF11_0049
OG5_143223	PF11_0069
OG5_153611	PF11_0077
OG5_150031	PF11_0083
OG5_150031	PF11_0083
OG5_126834	PF11_0087
OG5_128236	PF11_0105
OG5_141753	PF11_0114
OG5_141223	PF11_0124
OG5_127044	PF11_0141
OG5_141754	PF11_0158
OG5_140130	PF11_0171
OG5_130898	PF11_0172
OG5_127413	PF11_0181
OG5_129844	PF11_0188
OG5_130105	PF11_0197
OG5_127450	PF11_0200

OG5_126616	PF11_0203
OG5_126616	PF11_0203
OG5_126616	PF11_0203
OG5_150531	PF11_0228
OG5_127225	PF11_0245
OG5_128760	PF11_0255
OG5_127649	PF11_0257
OG5_127649	PF11_0257
OG5_126978	PF11_0258
OG5_128225	PF11_0259
OG5_127975	PF11_0264
OG5_128571	PF11_0265
OG5_126764	PF11_0270
OG5_128064	PF11_0280
OG5_127590	PF11_0295
OG5_126620	PF11_0296
OG5_126620	PF11_0296
OG5_128053	PF11_0298
OG5_150520	PF11_0300
OG5_126796	PF11_0305
OG5_126796	PF11_0305
OG5_128133	PF11_0311
OG5_127163	PF11_0329
OG5_127998	PF11_0331
OG5_147077	PF11_0343
OG5_147452	PF11_0344
OG5_127767	PF11_0370
OG5_129463	PF11_0371
OG5_129463	PF11_0371
OG5_129463	PF11_0371
OG5_141756	PF11_0379
OG5_149676	PF11_0382
OG5_150581	PF11_0383
OG5_128383	PF11_0393
OG5_133188	PF11_0395
OG5_146556	PF11_0419
OG5_147473	PF11_0423
OG5_147473	PF11_0423
OG5_147482	PF11_0429
OG5_127072	PF11_0438
OG5_129798	PF11_0439
OG5_127819	PF11_0445
OG5_127127	PF11_0447

OG5_128466	PF11_0452
OG5_127484	PF11_0454
OG5_127256	PF11_0461
OG5_126660	PF11_0465
OG5_126660	PF11_0465
OG5_127594	PF11_0477
OG5_129463	PF11_0479
OG5_129463	PF11_0479
OG5_129463	PF11_0479
OG5_127404	PF11_0485
OG5_136226	PF11_0487
OG5_127368	PF13_0014
OG5_153553	PF13_0015
OG5_126935	PF13_0021
OG5_127688	PF13_0023
OG5_127008	PF13_0045
OG5_127273	PF13_0049
OG5_128667	PF13_0050
OG5_153573	PF13_0058
OG5_156840	PF13_0077
OG5_150597	PF13_0078
OG5_143224	PF13_0079
OG5_153568	PF13_0086
OG5_129463	PF13_0097
OG5_129463	PF13_0097
OG5_129463	PF13_0097
OG5_127349	PF13_0109
OG5_127362	PF13_0121
OG5_156786	PF13_0126
OG5_128708	PF13_0138
OG5_128262	PF13_0142
OG5_126730	PF13_0143
OG5_126637	PF13_0150
OG5_126637	PF13_0150
OG5_126637	PF13_0150
OG5_160594	PF13_0161
OG5_128881	PF13_0164
OG5_126678	PF13_0171
OG5_126678	PF13_0171
OG5_139591	PF13_0173
OG5_129467	PF13_0176
OG5_126684	PF13_0179
OG5_126684	PF13_0179

OG5_126769	PF13_0180
OG5_126769	PF13_0180
OG5_146901	PF13_0182
OG5_140089	PF13_0190
OG5_128369	PF13_0204
OG5_127096	PF13_0205
OG5_126600	PF13_0211
OG5_126600	PF13_0211
OG5_127206	PF13_0213
OG5_128259	PF13_0222
OG5_126691	PF13_0229
OG5_126672	PF13_0233
OG5_126672	PF13_0233
OG5_128435	PF13_0234
OG5_141734	PF13_0263
OG5_126900	PF13_0268
OG5_127759	PF13_0282
OG5_126871	PF13_0286
OG5_126871	PF13_0286
OG5_127960	PF13_0291
OG5_128826	PF13_0301
OG5_140270	PF13_0303
OG5_128295	PF13_0308
OG5_127089	PF13_0316
OG5_127676	PF13_0322
OG5_150534	PF13_0329
OG5_128002	PF13_0330
OG5_128172	PF13_0335
OG5_126882	PF13_0340
OG5_127455	PF13_0341
OG5_126966	PF13_0344
OG5_126708	PF13_0349
OG5_126932	PF13_0350
OG5_129185	PF13_0358
OG5_130756	PF14_0026
OG5_127221	PF14_0027
OG5_129457	PF14_0028
OG5_126838	PF14_0034
OG5_127365	PF14_0038
OG5_127264	PF14_0052
OG5_128313	PF14_0055
OG5_128178	PF14_0056
OG5_129496	PF14_0057

OG5_133657	PF14_0063
OG5_143227	PF14_0065
OG5_126885	PF14_0075
OG5_126885	PF14_0077
OG5_128104	PF14_0090
OG5_143228	PF14_0092
OG5_153618	PF14_0095
OG5_127441	PF14_0097
OG5_127367	PF14_0107
OG5_126595	PF14_0124
OG5_141156	PF14_0126
OG5_126821	PF14_0142
OG5_126973	PF14_0143
OG5_127816	PF14_0145
OG5_128997	PF14_0159
OG5_141737	PF14_0160
OG5_160480	PF14_0166
OG5_128303	PF14_0167
OG5_141204	PF14_0173
OG5_127764	PF14_0177
OG5_127577	PF14_0178
OG5_126914	PF14_0200
OG5_128080	PF14_0215
OG5_134377	PF14_0224
OG5_127333	PF14_0241
OG5_127234	PF14_0256
OG5_128510	PF14_0257
OG5_130906	PF14_0262
OG5_129547	PF14_0274
OG5_127198	PF14_0276
OG5_127198	PF14_0276
OG5_127619	PF14_0277
OG5_133546	PF14_0281
OG5_133546	PF14_0281
OG5_126857	PF14_0286
OG5_129173	PF14_0288
OG5_128701	PF14_0307
OG5_127148	PF14_0314
OG5_127148	PF14_0314
OG5_150579	PF14_0325
OG5_128266	PF14_0328
OG5_129822	PF14_0329
OG5_156828	PF14_0332

OG5_126980	PF14_0341
OG5_144531	PF14_0350
OG5_126839	PF14_0352
OG5_129184	PF14_0365
OG5_139232	PF14_0369
OG5_127574	PF14_0373
OG5_128092	PF14_0374
OG5_141671	PF14_0383
OG5_127114	PF14_0391
OG5_137359	PF14_0392
OG5_128047	PF14_0429
OG5_153136	PF14_0433
OG5_138807	PF14_0443
OG5_126733	PF14_0455
OG5_126733	PF14_0455
OG5_153620	PF14_0461
OG5_145098	PF14_0472
OG5_152986	PF14_0480
OG5_142870	PF14_0495
OG5_135576	PF14_0496
OG5_127121	PF14_0511
OG5_127189	PF14_0517
OG5_153550	PF14_0527
OG5_141266	PF14_0530
OG5_150546	PF14_0535
OG5_150547	PF14_0540
OG5_128338	PF14_0564
OG5_129362	PF14_0571
OG5_129228	PF14_0580
OG5_128165	PF14_0584
OG5_128039	PF14_0587
OG5_141738	PF14_0607
OG5_139221	PF14_0608
OG5_140039	PF14_0610
OG5_127160	PF14_0632
OG5_127869	PF14_0635
OG5_128936	PF14_0640
OG5_141603	PF14_0649
OG5_141231	PF14_0652
OG5_127464	PF14_0661
OG5_146934	PF14_0665
OG5_150606	PF14_0673
OG5_129533	PF14_0679

OG5_143205	PF14_0691
OG5_137697	PF14_0694
OG5_147370	PF14_0695
OG5_156780	PF14_0696
OG5_128430	PF14_0713
OG5_127884	PF14_0716
OG5_127952	PF14_0784
OG5_127770	PFA0260c
OG5_150528	PFA0270c
OG5_156826	PFA0350c
OG5_128243	PFA0505c
OG5_127148	PFA0520c
OG5_127148	PFA0520c
OG5_126886	PFA0555c
OG5_128004	PFB0175c
OG5_127855	PFB0370c
OG5_139037	PFB0435c
OG5_156492	PFB0467w
OG5_128444	PFB0515w
OG5_126884	PFB0545c
OG5_126884	PFB0545c
OG5_127250	PFB0550w
OG5_156591	PFB0575c
OG5_150556	PFB0600c
OG5_127506	PFB0640c
OG5_127268	PFB0645c
OG5_127784	PFB0860c
OG5_127784	PFB0860c
OG5_127465	PFB0895c
OG5_127665	PFC0140c
OG5_136403	PFC0185w
OG5_160574	PFC0221c
OG5_145107	PFC0262c
OG5_147456	PFC0280c
OG5_127874	PFC0340w
OG5_150568	PFC0370w
OG5_153604	PFC0506w
OG5_156784	PFC0590c
OG5_150596	PFC0701w
OG5_155210	PFC0760c
OG5_130170	PFC0825c
OG5_129939	PFC0850c
OG5_150565	PFC0911c

OG5_127804	PFC0915w
OG5_128200	PFC0995c
OG5_128090	PFD0180c
OG5_130816	PFD0190w
OG5_139451	PFD0275w
OG5_145112	PFD0325w
OG5_145112	PFD0325w
OG5_141743	PFD0380c
OG5_129313	PFD0700c
OG5_143115	PFD0720w
OG5_128198	PFD0835c
OG5_143209	PFD0910w
OG5_127881	PFD0930w
OG5_127881	PFD0930w
OG5_156846	PFD0945c
OG5_127684	PFD0975w
OG5_156239	PFD0985w
OG5_127927	PFD1070w
OG5_141755	PFD1110w
OG5_126579	PFE0070w
OG5_142490	PFE0275w
OG5_126912	PFE0305w
OG5_141542	PFE0400w
OG5_128131	PFE0605c
OG5_143215	PFE0650c
OG5_127209	PFE0665c
OG5_127209	PFE0665c
OG5_127209	PFE0665c
OG5_146858	PFE0670w
OG5_127414	PFE0730c
OG5_156796	PFE0770w
OG5_127876	PFE0820c
OG5_132466	PFE0895c
OG5_127834	PFE0915c
OG5_126678	PFE0960w
OG5_126678	PFE0960w
OG5_126983	PFE1005w
OG5_146323	PFE1285w
OG5_128443	PFE1405c
OG5_126830	PFE1415w
OG5_126830	PFE1415w
OG5_126830	PFE1415w
OG5_150553	PFE1435c

OG5_149875	PFE1510c
OG5_140540	PFF0185c
OG5_127312	PFF0345w
OG5_127428	PFF0430w
OG5_126830	PFF0485c
OG5_126830	PFF0485c
OG5_126830	PFF0485c
OG5_153341	PFF0780w
OG5_140027	PFF0825c
OG5_126569	PFF0865w
OG5_126569	PFF0865w
OG5_126569	PFF0865w
OG5_127016	PFF0885w
OG5_126926	PFF0940c
OG5_126926	PFF0940c
OG5_128182	PFF1030w
OG5_153614	PFF1080w
OG5_128486	PFF1140c
OG5_126908	PFF1150w
OG5_147396	PFF1160w
OG5_126621	PFF1265w
OG5_127669	PFF1335c
OG5_140247	PFF1370w
OG5_127942	PFF1470c
OG5_143217	PFI0205w
OG5_150560	PFI0285w
OG5_145111	PFI0295c
OG5_128678	PFI0335w
OG5_128385	PFI0490c
OG5_147312	PFI0655c
OG5_153565	PFI0670w
OG5_141728	PFI0845w
OG5_136347	PFI0970c
OG5_128253	PFI1070c
OG5_126776	PFI1105w
OG5_127639	PFI1360c
OG5_128020	PFI1570c
OG5_126806	PFI1645c
OG5_126806	PFI1645c
OG5_150518	PFI1665w
OG5_126748	PFI1685w
OG5_127563	PFL0075w
OG5_127220	PFL0110c

OG5_127581	PFL0180w
OG5_127581	PFL0180w
OG5_128148	PFL0355c
OG5_128839	PFL0430w
OG5_147441	PFL0640w
OG5_127498	PFL0660w
OG5_127936	PFL0665c
OG5_136815	PFL1005c
OG5_147428	PFL1090w
OG5_147430	PFL1195w
OG5_138778	PFL1270w
OG5_141163	PFL1275c
OG5_127483	PFL1425w
OG5_126796	PFL1475w
OG5_126796	PFL1475w
OG5_135175	PFL1545c
OG5_128558	PFL1680w
OG5_130096	PFL1715w
OG5_144402	PFL1895w
OG5_150535	PFL1985c
OG5_147457	PFL2045w
OG5_127529	PFL2120w
OG5_128219	PFL2195w
OG5_141757	PFL2225w
OG5_153529	PFL2260w
OG5_152418	PFL2410w

APPENDIX 4.7 Unique and shared orthologue groups among the differentially expressed transcripts of *B. divergens* and *P. falciparum* both treated with piperidinyl-benzimidazolone analog (A51B1C1_1).

Unique orthologue groups among <i>B. divergens</i> DEG's	Shared orthologue groups	Unique orthologue groups among <i>P. falciparum</i> DEG's
OG5_127833	OG5_127594	OG5_130344
OG5_153528	OG5_142870	OG5_128830
OG5_127472	OG5_127669	OG5_140542
OG5_127692	OG5_153060	OG5_143145
OG5_128702	OG5_128219	OG5_140345
OG5_127141	OG5_127402	OG5_126954
OG5_143196	OG5_150527	OG5_127926
OG5_153530	OG5_153341	OG5_128475
OG5_147397	OG5_128226	OG5_142982
OG5_150522	OG5_128435	OG5_127236
OG5_127233	OG5_127784	OG5_127359
OG5_135486	OG5_141728	OG5_127375
OG5_127468	OG5_145099	OG5_128535
OG5_127453	OG5_127206	OG5_153563
OG5_131748	OG5_141671	OG5_141744
OG5_135732	OG5_160480	OG5_128224
OG5_131400	OG5_128667	OG5_130478
OG5_126854	OG5_127854	OG5_128549
OG5_152614	OG5_156796	OG5_139161
OG5_126913	OG5_126678	OG5_127832
OG5_152413	OG5_141266	OG5_145093
OG5_136182	OG5_127881	OG5_128932
OG5_153536	OG5_144710	OG5_126648
OG5_153070	OG5_127153	OG5_127990
OG5_127994	OG5_129939	OG5_136346
OG5_126936	OG5_150553	OG5_156847
OG5_128255	OG5_126684	OG5_128656
OG5_127962	OG5_127764	OG5_128247
OG5_128059	OG5_129533	OG5_129603
OG5_139383	OG5_138116	OG5_135283
OG5_144638	OG5_128182	OG5_141625
OG5_156790	OG5_127312	OG5_153558
OG5_150395	OG5_127670	OG5_145102
OG5_126644	OG5_126886	OG5_127360
OG5_156791	OG5_128133	OG5_126970
OG5_128117	OG5_149676	OG5_143207
OG5_129047	OG5_129958	OG5_141752
OG5_128457	OG5_127465	OG5_130786

OG5_126774	OG5_128660	OG5_153589
OG5_128816	OG5_128881	OG5_129027
OG5_128055	OG5_126885	OG5_126588
OG5_127496	OG5_127273	OG5_133154
OG5_127608	OG5_128098	OG5_160579
OG5_130456	OG5_127256	OG5_129865
OG5_127223	OG5_130863	OG5_129167
OG5_141740	OG5_127874	OG5_152312
OG5_140539	OG5_126733	OG5_127718
OG5_128215	OG5_126969	OG5_146589
OG5_127934	OG5_127557	OG5_150068
OG5_128058	OG5_129313	OG5_130342
OG5_128469	OG5_137217	OG5_128417
OG5_128599	OG5_127942	OG5_131254
OG5_128495	OG5_136181	OG5_133046
OG5_139182	OG5_128295	OG5_130898
OG5_127319	OG5_127574	OG5_137859
OG5_127173	OG5_127333	OG5_131282
OG5_128487	OG5_129228	OG5_127562
OG5_126956	OG5_127127	OG5_136021
OG5_156799	OG5_126579	OG5_140107
OG5_156800	OG5_127366	OG5_127555
OG5_155120	OG5_141731	OG5_128298
OG5_133088	OG5_127148	OG5_127551
OG5_127011	OG5_128047	OG5_146254
OG5_127512	OG5_127773	OG5_156804
OG5_153559	OG5_128165	OG5_128490
OG5_147429	OG5_126620	OG5_145117
OG5_141745	OG5_139037	OG5_153587
OG5_141746	OG5_147414	OG5_191856
OG5_153324	OG5_146858	OG5_127434
OG5_150555	OG5_143209	OG5_129560
OG5_126773	OG5_127936	OG5_127363
OG5_141466	OG5_127498	OG5_127295
OG5_127570	OG5_128678	OG5_127255
OG5_131688	OG5_150565	OG5_128467
OG5_126904	OG5_127313	OG5_143032
OG5_127289	OG5_135175	OG5_153576
OG5_127633	OG5_143212	OG5_138354
OG5_156807	OG5_133546	OG5_126784
OG5_127535	OG5_126730	OG5_127064
OG5_126665	OG5_128266	OG5_152184
OG5_150576	OG5_128225	OG5_128317

OG5_152508	OG5_127464	OG5_150545
OG5_141545	OG5_127581	OG5_128978
OG5_127654	OG5_128839	OG5_127754
OG5_131701	OG5_127152	OG5_127903
OG5_153594	OG5_129173	OG5_129618
OG5_131401	OG5_127529	OG5_141730
OG5_127215	OG5_128486	OG5_160575
OG5_126694	OG5_128020	OG5_127126
OG5_127906	OG5_144402	OG5_128694
Unique orthologue groups		
OG5_126867		OG5_145103
OG5_156825		OG5_127781
OG5_127269		OG5_127203
OG5_127231		OG5_128346
OG5_156829		OG5_128348
OG5_126601		OG5_150585
OG5_127624		OG5_156188
OG5_126745		OG5_126761
OG5_150584		OG5_126849
OG5_134232		OG5_129014
OG5_147462		OG5_129462
OG5_128884		OG5_127652
OG5_127711		OG5_128106
OG5_128366		OG5_126593
OG5_127572		OG5_130284
OG5_147466		OG5_147399
OG5_127797		OG5_126957
OG5_127408		OG5_150566
OG5_150588		OG5_128175
OG5_127481		OG5_150524
OG5_127732		OG5_150523
OG5_127604		OG5_160572
OG5_137714		OG5_127824
OG5_150591		OG5_130776
OG5_127900		OG5_140457
OG5_130661		OG5_128265
OG5_127081		OG5_127592
OG5_143221		OG5_128975
OG5_158546		OG5_128456
OG5_128077		OG5_147127
OG5_127761		OG5_141009
OG5_127036		OG5_127420

OG5_127969	OG5_126721
OG5_127107	OG5_128508
OG5_143222	OG5_126788
OG5_159765	OG5_160582
OG5_127017	OG5_127005
OG5_127641	OG5_126696
OG5_147475	OG5_144058
OG5_126723	OG5_126793
OG5_127922	OG5_128209
OG5_132300	OG5_147416
OG5_128066	OG5_153509
OG5_130216	OG5_127014
OG5_127553	OG5_127887
OG5_128354	OG5_127981
OG5_127677	OG5_126830
OG5_127149	OG5_127909
OG5_130129	OG5_127245
OG5_127466	OG5_143206
OG5_128528	OG5_127891
OG5_153619	OG5_128972
OG5_126878	OG5_160617
OG5_127351	OG5_147422
OG5_128449	OG5_127435
OG5_130916	OG5_126927
OG5_126865	OG5_144357
OG5_128638	OG5_126841
OG5_153539	OG5_126660
OG5_150530	OG5_127208
OG5_127297	OG5_128127
OG5_128587	OG5_143223
OG5_127751	OG5_153611
OG5_142443	OG5_150031
OG5_141599	OG5_126834
OG5_128121	OG5_128236
OG5_128001	OG5_141753
OG5_127480	OG5_141223
OG5_126740	OG5_127044
OG5_128799	OG5_141754
OG5_130299	OG5_140130
OG5_130616	OG5_127413
OG5_140537	OG5_129844
OG5_131402	OG5_130105
OG5_127610	OG5_127450

OG5_149560	OG5_126616
OG5_141736	OG5_150531
OG5_130659	OG5_127225
OG5_129568	OG5_128760
OG5_127038	OG5_127649
OG5_150558	OG5_126978
OG5_152974	OG5_127975
OG5_147437	OG5_128571
OG5_129285	OG5_126764
OG5_128795	OG5_128064
OG5_127448	OG5_127590
OG5_127291	OG5_128053
OG5_145108	OG5_150520
OG5_153566	OG5_126796
OG5_127890	OG5_127163
OG5_150559	OG5_127998
OG5_147442	OG5_147077
OG5_126668	OG5_147452
OG5_127311	OG5_127767
OG5_128136	OG5_129463
OG5_128863	OG5_141756
OG5_139980	OG5_150581
OG5_127099	OG5_128383
OG5_126679	OG5_133188
OG5_130370	OG5_146556
OG5_150563	OG5_147473
OG5_144050	OG5_147482
OG5_142685	OG5_127072
OG5_128332	OG5_129798
OG5_150567	OG5_127819
OG5_127430	OG5_128466
OG5_127497	OG5_127484
OG5_126968	OG5_127404
OG5_126641	OG5_136226
OG5_143151	OG5_127368
OG5_156814	OG5_153553
OG5_127814	OG5_126935
OG5_147448	OG5_127688
OG5_126795	OG5_127008
OG5_153577	OG5_153573
OG5_156816	OG5_156840
OG5_141155	OG5_150597
OG5_126558	OG5_143224

OG5_156817	OG5_153568
OG5_127682	OG5_127349
OG5_127813	OG5_127362
OG5_127924	OG5_156786
OG5_145118	OG5_128708
OG5_146494	OG5_128262
OG5_128429	OG5_126637
OG5_150574	OG5_160594
OG5_127514	OG5_139591
OG5_126599	OG5_129467
OG5_152980	OG5_126769
OG5_128401	OG5_146901
OG5_153588	OG5_140089
OG5_141514	OG5_128369
OG5_178105	OG5_127096
OG5_168705	OG5_126600
	OG5_128259
	OG5_126691
	OG5_126672
	OG5_141734
	OG5_126900
	OG5_127759
	OG5_126871
	OG5_127960
	OG5_128826
	OG5_140270
	OG5_127089
	OG5_127676
	OG5_150534
	OG5_128002
	OG5_128172
	OG5_126882
	OG5_127455
	OG5_126966
	OG5_126708
	OG5_126932
	OG5_129185
	OG5_130756
	OG5_127221
	OG5_129457
	OG5_126838
	OG5_127365
	OG5_127264

OG5_128313
OG5_128178
OG5_129496
OG5_133657
OG5_143227
OG5_128104
OG5_143228
OG5_153618
OG5_127441
OG5_127367
OG5_126595
OG5_141156
OG5_126821
OG5_126973
OG5_127816
OG5_128997
OG5_141737
OG5_128303
OG5_141204
OG5_127577
OG5_126914
OG5_128080
OG5_134377
OG5_127234
OG5_128510
OG5_130906
OG5_129547
OG5_127198
OG5_127619
OG5_126857
OG5_128701
OG5_150579
OG5_129822
OG5_156828
OG5_126980
OG5_144531
OG5_126839
OG5_129184
OG5_139232
OG5_128092
OG5_127114
OG5_137359
OG5_153136

OG5_138807
OG5_153620
OG5_145098
OG5_152986
OG5_135576
OG5_127121
OG5_127189
OG5_153550
OG5_150546
OG5_150547
OG5_128338
OG5_129362
OG5_128039
OG5_141738
OG5_139221
OG5_140039
OG5_127160
OG5_127869
OG5_128936
OG5_141603
OG5_141231
OG5_146934
OG5_150606
OG5_143205
OG5_137697
OG5_147370
OG5_156780
OG5_128430
OG5_127884
OG5_127952
OG5_127770
OG5_150528
OG5_156826
OG5_128243
OG5_128004
OG5_127855
OG5_156492
OG5_128444
OG5_126884
OG5_127250
OG5_156591
OG5_150556
OG5_127506

OG5_127268
OG5_127665
OG5_136403
OG5_160574
OG5_145107
OG5_147456
OG5_150568
OG5_153604
OG5_156784
OG5_150596
OG5_155210
OG5_130170
OG5_127804
OG5_128200
OG5_128090
OG5_130816
OG5_139451
OG5_145112
OG5_141743
OG5_143115
OG5_128198
OG5_156846
OG5_127684
OG5_156239
OG5_127927
OG5_141755
OG5_142490
OG5_126912
OG5_141542
OG5_128131
OG5_143215
OG5_127209
OG5_127414
OG5_127876
OG5_132466
OG5_127834
OG5_126983
OG5_146323
OG5_128443
OG5_149875
OG5_140540
OG5_127428
OG5_140027

OG5_126569
OG5_127016
OG5_126926
OG5_153614
OG5_126908
OG5_147396
OG5_126621
OG5_140247
OG5_143217
OG5_150560
OG5_145111
OG5_128385
OG5_147312
OG5_153565
OG5_136347
OG5_128253
OG5_126776
OG5_127639
OG5_126806
OG5_150518
OG5_126748
OG5_127563
OG5_127220
OG5_128148
OG5_147441
OG5_136815
OG5_147428
OG5_147430
OG5_138778
OG5_141163
OG5_127483
OG5_128558
OG5_130096
OG5_150535
OG5_147457
OG5_141757
OG5_153529
OG5_152418

APPENDIX 4.8 *B. divergens* differentially expressed transcriptomic data with corresponding orthologue groups identified from the *B. bovis* – *A. thaliana* orthologue group matrix.

Orthologue group name	* <i>B. divergens</i> DEG's
OG5_127833	BBOV_I000130
OG5_127833	BBOV_I000130
OG5_127833	BBOV_I000130
OG5_127594	BBOV_I000180
OG5_127594	BBOV_I000180
OG5_127594	BBOV_I000180
OG5_127594	BBOV_I000180
OG5_127594	BBOV_I000180
OG5_127594	BBOV_I000180
OG5_127594	BBOV_I000180
OG5_127594	BBOV_I000180
OG5_127594	BBOV_I000180
OG5_127594	BBOV_I000180
OG5_127594	BBOV_I000180
OG5_127594	BBOV_I000180
OG5_127594	BBOV_I000180
OG5_127594	BBOV_I000180
OG5_127594	BBOV_I000180
OG5_127594	BBOV_I000180
OG5_127594	BBOV_I000180
OG5_127594	BBOV_I000180
OG5_127594	BBOV_I000180
OG5_127472	BBOV_I000370
OG5_127472	BBOV_I000370
OG5_127692	BBOV_I000460
OG5_127692	BBOV_I000460
OG5_127692	BBOV_I000460
OG5_129396	BBOV_I000530
OG5_129396	BBOV_I000530
OG5_129396	BBOV_I000530
OG5_128702	BBOV_I000560
OG5_128702	BBOV_I000560
OG5_128702	BBOV_I000560
OG5_128702	BBOV_I000560
OG5_127141	BBOV_I000740
OG5_127141	BBOV_I000740
OG5_127141	BBOV_I000740
OG5_127141	BBOV_I000740
OG5_127141	BBOV_I000740
OG5_130042	BBOV_I000780
OG5_127233	BBOV_I001740
OG5_127233	BBOV_I001740
OG5_127233	BBOV_I001740
OG5_127233	BBOV_I001740
OG5_127910	BBOV_I001880
OG5_127910	BBOV_I001880

OG5_127910	BBOV_I001880
OG5_127910	BBOV_I001880
OG5_127468	BBOV_I001970
OG5_127468	BBOV_I001970
OG5_127453	BBOV_I002210
OG5_127453	BBOV_I002210
OG5_127453	BBOV_I002210
OG5_131748	BBOV_I002280
OG5_127669	BBOV_I002290
OG5_127669	BBOV_I002290
OG5_127669	BBOV_I002290
OG5_127669	BBOV_I002290
OG5_135732	BBOV_I002370
OG5_131400	BBOV_I002510
OG5_126854	BBOV_I002740
OG5_128219	BBOV_I002870
OG5_128219	BBOV_I002870
OG5_128219	BBOV_I002870
OG5_128219	BBOV_I002870
OG5_128219	BBOV_I002870
OG5_128219	BBOV_I002870
OG5_128219	BBOV_I002870
OG5_127402	BBOV_I002910
OG5_126913	BBOV_I003140
OG5_126913	BBOV_I003140
OG5_126913	BBOV_I003140
OG5_126913	BBOV_I003140
OG5_128226	BBOV_I003460
OG5_128226	BBOV_I003460
OG5_128226	BBOV_I003460
OG5_128226	BBOV_I003460
OG5_128226	BBOV_I003460
OG5_128226	BBOV_I003460
OG5_128435	BBOV_I003550
OG5_128435	BBOV_I003550
OG5_127784	BBOV_I004200
OG5_127994	BBOV_I004290
OG5_128517	BBOV_I004440
OG5_128517	BBOV_I004440
OG5_126936	BBOV_I004650
OG5_126936	BBOV_I004650
OG5_126936	BBOV_I004650
OG5_126936	BBOV_I004650
OG5_126936	BBOV_I004650
OG5_126936	BBOV_I004650

OG5_126936	BBOV_I004650
OG5_126936	BBOV_I004650
OG5_128255	BBOV_I004760
OG5_127962	BBOV_I004920
OG5_127962	BBOV_I004920
OG5_127962	BBOV_I004920
OG5_128059	BBOV_I004950
OG5_128059	BBOV_I004950
OG5_128059	BBOV_I004950
OG5_128059	BBOV_I004950
OG5_128059	BBOV_I004950
OG5_128059	BBOV_I004950
OG5_128059	BBOV_I004950
OG5_128059	BBOV_I004950
OG5_128059	BBOV_I004970
OG5_128059	BBOV_I004970
OG5_128059	BBOV_I004970
OG5_128059	BBOV_I004970
OG5_128059	BBOV_I004970
OG5_128059	BBOV_I004970
OG5_128059	BBOV_I004970
OG5_128059	BBOV_I004970
OG5_128059	BBOV_I004970
OG5_128059	BBOV_I004970
OG5_128059	BBOV_I004970
OG5_128059	BBOV_I004970
OG5_128059	BBOV_I004970
OG5_126644	BBOV_I1000810
OG5_126644	BBOV_I1000810
OG5_126644	BBOV_I1000810
OG5_126644	BBOV_I1000810
OG5_126644	BBOV_I1000810
OG5_126644	BBOV_I1000810
OG5_126644	BBOV_I1000810
OG5_126644	BBOV_I1000810
OG5_127206	BBOV_I1000880
OG5_127206	BBOV_I1000880
OG5_127206	BBOV_I1000880
OG5_141671	BBOV_I1001140
OG5_128455	BBOV_I1001290
OG5_128455	BBOV_I1001290
OG5_128117	BBOV_I1001300
OG5_128117	BBOV_I1001300
OG5_129047	BBOV_I1002070
OG5_129047	BBOV_I1002070
OG5_128457	BBOV_I1002140
OG5_128457	BBOV_I1002140

OG5_128667	BBOV_II002160
OG5_128012	BBOV_II002190
OG5_126774	BBOV_II002230
OG5_126774	BBOV_II002230
OG5_126774	BBOV_II002230
OG5_126774	BBOV_II002230
OG5_126774	BBOV_II002230
OG5_126774	BBOV_II002230
OG5_126774	BBOV_II002230
OG5_127854	BBOV_II002240
OG5_128816	BBOV_II002560
OG5_128055	BBOV_II002690
OG5_126678	BBOV_II002750
OG5_126678	BBOV_II002750
OG5_126678	BBOV_II002750
OG5_126678	BBOV_II002750
OG5_126678	BBOV_II002750
OG5_127496	BBOV_II002810
OG5_127496	BBOV_II002810
OG5_127496	BBOV_II002810
OG5_127496	BBOV_II002810
OG5_127496	BBOV_II002810
OG5_127608	BBOV_II002960
OG5_130456	BBOV_II002970
OG5_127223	BBOV_II003080
OG5_128215	BBOV_II003250
OG5_128215	BBOV_II003250
OG5_128215	BBOV_II003250
OG5_127934	BBOV_II003360
OG5_128058	BBOV_II003390
OG5_128469	BBOV_II003490
OG5_128469	BBOV_II003490
OG5_128469	BBOV_II003490
OG5_128469	BBOV_II003490
OG5_128599	BBOV_II003510
OG5_128599	BBOV_II003510
OG5_128495	BBOV_II003590
OG5_127319	BBOV_II003680
OG5_127319	BBOV_II003680
OG5_127319	BBOV_II003680
OG5_127173	BBOV_II003780
OG5_127173	BBOV_II003780
OG5_127173	BBOV_II003780
OG5_127173	BBOV_II003780

OG5_128487	BBOV_II003830
OG5_127881	BBOV_II003960
OG5_127881	BBOV_II003960
OG5_127881	BBOV_II003960
OG5_127881	BBOV_II003960
OG5_127881	BBOV_II003960
OG5_126956	BBOV_II004010
OG5_128727	BBOV_II004340
OG5_128727	BBOV_II004340
OG5_128727	BBOV_II004340
OG5_128727	BBOV_II004340
OG5_128727	BBOV_II004340
OG5_128727	BBOV_II004340
OG5_127153	BBOV_II004660
OG5_127153	BBOV_II004660
OG5_127153	BBOV_II004660
OG5_127153	BBOV_II004660
OG5_133088	BBOV_II004880
OG5_133088	BBOV_II004880
OG5_133088	BBOV_II004880
OG5_133088	BBOV_II004880
OG5_133088	BBOV_II004880
OG5_127011	BBOV_II004950
OG5_127512	BBOV_II005020
OG5_126850	BBOV_II005420
OG5_126850	BBOV_II005420
OG5_126850	BBOV_II005420
OG5_126850	BBOV_II005420
OG5_126850	BBOV_II005420
OG5_126850	BBOV_II005420
OG5_126850	BBOV_II005420
OG5_126850	BBOV_II005420
OG5_126850	BBOV_II005420
OG5_126850	BBOV_II005420
OG5_126850	BBOV_II005420
OG5_126850	BBOV_II005420
OG5_126850	BBOV_II005420
OG5_126684	BBOV_II005760
OG5_126684	BBOV_II005760
OG5_126684	BBOV_II005760
OG5_127764	BBOV_II005900
OG5_128733	BBOV_II006350
OG5_128038	BBOV_II006420
OG5_128038	BBOV_II006420

OG5_126773	BBOV_II006560
OG5_126773	BBOV_II006560
OG5_126773	BBOV_II006560
OG5_126773	BBOV_II006560
OG5_126773	BBOV_II006560
OG5_126773	BBOV_II006560
OG5_126773	BBOV_II006560
OG5_134639	BBOV_II006690
OG5_127570	BBOV_II006920
OG5_127570	BBOV_II006920
OG5_127570	BBOV_II006920
OG5_126904	BBOV_II006950
OG5_128182	BBOV_II007100
OG5_128182	BBOV_II007100
OG5_127289	BBOV_II007190
OG5_127312	BBOV_II007250
OG5_127312	BBOV_II007250
OG5_127312	BBOV_II007250
OG5_127312	BBOV_II007250
OG5_127312	BBOV_II007250
OG5_127312	BBOV_II007250
OG5_127312	BBOV_II007250
OG5_127633	BBOV_II007360
OG5_127670	BBOV_II007370
OG5_127535	BBOV_II007550
OG5_126886	BBOV_II007680
OG5_126886	BBOV_II007680
OG5_126886	BBOV_II007680
OG5_126886	BBOV_II007680
OG5_126886	BBOV_II007680
OG5_126665	BBOV_II007740
OG5_126665	BBOV_II007740
OG5_128494	BBOV_III000460
OG5_128494	BBOV_III000460
OG5_127654	BBOV_III000560
OG5_127654	BBOV_III000560
OG5_127654	BBOV_III000560
OG5_127654	BBOV_III000560
OG5_131701	BBOV_III000620
OG5_128133	BBOV_III000660
OG5_131401	BBOV_III000740
OG5_127215	BBOV_III000930
OG5_126694	BBOV_III000960
OG5_126694	BBOV_III000960

OG5_126694	BBOV_III000960
OG5_126694	BBOV_III000960
OG5_127906	BBOV_III001050
OG5_127906	BBOV_III001050
OG5_127906	BBOV_III001050
OG5_126867	BBOV_III001350
OG5_126867	BBOV_III001350
OG5_126867	BBOV_III001350
OG5_126867	BBOV_III001350
OG5_126867	BBOV_III001350
OG5_126867	BBOV_III001350
OG5_126867	BBOV_III001350
OG5_126867	BBOV_III001350
OG5_126867	BBOV_III001350
OG5_129958	BBOV_III001380
OG5_129958	BBOV_III001380
OG5_129958	BBOV_III001380
OG5_129958	BBOV_III001380
OG5_129246	BBOV_III002040
OG5_127465	BBOV_III002070
OG5_127269	BBOV_III002090
OG5_127269	BBOV_III002090
OG5_127269	BBOV_III002090
OG5_128057	BBOV_III002150
OG5_128660	BBOV_III002180
OG5_127231	BBOV_III002280
OG5_127231	BBOV_III002280
OG5_127231	BBOV_III002280
OG5_127231	BBOV_III002280
OG5_126601	BBOV_III002500
OG5_126601	BBOV_III002500
OG5_126601	BBOV_III002500
OG5_126601	BBOV_III002500
OG5_126601	BBOV_III002500
OG5_126601	BBOV_III002500
OG5_126601	BBOV_III002500
OG5_126601	BBOV_III002500
OG5_126601	BBOV_III002500
OG5_126601	BBOV_III002500
OG5_126601	BBOV_III002500
OG5_126601	BBOV_III002500
OG5_126601	BBOV_III002500
OG5_126601	BBOV_III002500
OG5_126601	BBOV_III002500
OG5_126601	BBOV_III002500
OG5_126601	BBOV_III002500
OG5_126601	BBOV_III002500
OG5_126601	BBOV_III002500
OG5_127624	BBOV_III002670
OG5_127624	BBOV_III002670
OG5_127624	BBOV_III002670
OG5_127624	BBOV_III002670

OG5_127624	BBOV_III002670
OG5_127624	BBOV_III002670
OG5_127624	BBOV_III002670
OG5_127624	BBOV_III002670
OG5_127624	BBOV_III002670
OG5_127624	BBOV_III002670
OG5_127624	BBOV_III002670
OG5_126745	BBOV_III002690
OG5_126745	BBOV_III002690
OG5_126745	BBOV_III002690
OG5_126745	BBOV_III002690
OG5_126745	BBOV_III002690
OG5_128980	BBOV_III002720
OG5_134232	BBOV_III003260
OG5_127153	BBOV_III003380
OG5_127153	BBOV_III003380
OG5_127153	BBOV_III003380
OG5_127153	BBOV_III003380
OG5_128881	BBOV_III003430
OG5_128881	BBOV_III003430
OG5_128884	BBOV_III003480
OG5_128884	BBOV_III003480
OG5_126885	BBOV_III003510
OG5_126885	BBOV_III003510
OG5_126885	BBOV_III003510
OG5_126885	BBOV_III003510
OG5_127711	BBOV_III003540
OG5_127711	BBOV_III003540
OG5_127711	BBOV_III003540
OG5_127273	BBOV_III003570
OG5_127273	BBOV_III003570
OG5_128366	BBOV_III003580
OG5_131249	BBOV_III003660
OG5_127572	BBOV_III003940
OG5_127572	BBOV_III003940
OG5_127572	BBOV_III003940
OG5_127797	BBOV_III004100
OG5_127408	BBOV_III004110
OG5_127408	BBOV_III004110
OG5_127408	BBOV_III004110
OG5_128098	BBOV_III004170
OG5_128098	BBOV_III004170
OG5_128098	BBOV_III004170
OG5_127256	BBOV_III004450

OG5_127256	BBOV_III004450
OG5_127256	BBOV_III004450
OG5_127256	BBOV_III004450
OG5_127481	BBOV_III004670
OG5_127481	BBOV_III004670
OG5_127481	BBOV_III004670
OG5_127481	BBOV_III004670
OG5_127874	BBOV_III004800
OG5_127874	BBOV_III004800
OG5_126733	BBOV_III004900
OG5_126733	BBOV_III004900
OG5_126733	BBOV_III004900
OG5_127732	BBOV_III005130
OG5_127732	BBOV_III005130
OG5_127732	BBOV_III005130
OG5_127604	BBOV_III005690
OG5_127604	BBOV_III005690
OG5_127604	BBOV_III005690
OG5_127604	BBOV_III005690
OG5_127604	BBOV_III005690
OG5_127604	BBOV_III005690
OG5_126561	BBOV_III005820
OG5_126561	BBOV_III005820
OG5_126561	BBOV_III005820
OG5_126561	BBOV_III005820
OG5_126561	BBOV_III005820
OG5_126561	BBOV_III005820
OG5_126561	BBOV_III005820
OG5_126561	BBOV_III005820
OG5_126561	BBOV_III005820
OG5_126561	BBOV_III005820
OG5_126561	BBOV_III005820
OG5_126561	BBOV_III005820
OG5_126561	BBOV_III005820
OG5_126561	BBOV_III005820
OG5_126561	BBOV_III005820
OG5_126561	BBOV_III005820
OG5_126561	BBOV_III005820
OG5_126561	BBOV_III005820
OG5_126561	BBOV_III005820
OG5_126561	BBOV_III005820
OG5_126561	BBOV_III005820
OG5_126561	BBOV_III005820
OG5_126561	BBOV_III005820
OG5_126561	BBOV_III005820
OG5_126561	BBOV_III005820
OG5_126561	BBOV_III005820
OG5_126561	BBOV_III005820
OG5_126561	BBOV_III005820
OG5_126561	BBOV_III005820
OG5_126561	BBOV_III005820
OG5_126561	BBOV_III005820
OG5_129385	BBOV_III005940
OG5_129385	BBOV_III005940
OG5_129385	BBOV_III005940

OG5_126969	BBOV_III005950
OG5_126969	BBOV_III005950
OG5_126969	BBOV_III005950
OG5_126969	BBOV_III005950
OG5_126969	BBOV_III005950
OG5_126969	BBOV_III005950
OG5_126969	BBOV_III005950
OG5_126969	BBOV_III005950
OG5_126969	BBOV_III005950
OG5_126969	BBOV_III005950
OG5_126969	BBOV_III005950
OG5_126969	BBOV_III005950
OG5_126969	BBOV_III005950
OG5_126969	BBOV_III005950
OG5_137714	BBOV_III006240
OG5_127900	BBOV_III006340
OG5_127900	BBOV_III006340
OG5_127900	BBOV_III006340
OG5_127900	BBOV_III006340
OG5_127900	BBOV_III006340
OG5_130661	BBOV_III006370
OG5_130661	BBOV_III006370
OG5_127081	BBOV_III006690
OG5_127081	BBOV_III006690
OG5_127557	BBOV_III006880
OG5_127557	BBOV_III006880
OG5_127557	BBOV_III006880
OG5_127557	BBOV_III006880
OG5_127557	BBOV_III006880
OG5_127557	BBOV_III006880
OG5_128935	BBOV_III006960
OG5_128077	BBOV_III007080
OG5_128077	BBOV_III007080
OG5_128077	BBOV_III007080
OG5_128077	BBOV_III007080
OG5_128077	BBOV_III007080
OG5_128077	BBOV_III007080
OG5_128077	BBOV_III007080
OG5_127761	BBOV_III007090
OG5_127761	BBOV_III007090
OG5_127761	BBOV_III007090
OG5_127036	BBOV_III007240
OG5_127969	BBOV_III007250
OG5_127107	BBOV_III007370
OG5_127107	BBOV_III007370
OG5_127107	BBOV_III007370
OG5_127107	BBOV_III007370
OG5_127107	BBOV_III007370

OG5_127107	BBOV_III007370
OG5_127107	BBOV_III007370
OG5_127017	BBOV_III007880
OG5_127017	BBOV_III007880
OG5_127017	BBOV_III007880
OG5_127017	BBOV_III007880
OG5_127017	BBOV_III007880
OG5_127017	BBOV_III007880
OG5_127017	BBOV_III007880
OG5_127017	BBOV_III007880
OG5_127017	BBOV_III007880
OG5_127017	BBOV_III007880
OG5_127017	BBOV_III007880
OG5_127017	BBOV_III007880
OG5_127017	BBOV_III007880
OG5_127017	BBOV_III007880
OG5_127641	BBOV_III008010
OG5_127641	BBOV_III008010
OG5_127641	BBOV_III008010
OG5_127641	BBOV_III008010
OG5_127641	BBOV_III008010
OG5_127641	BBOV_III008010
OG5_127641	BBOV_III008010
OG5_131103	BBOV_III008040
OG5_126723	BBOV_III008390
OG5_126723	BBOV_III008390
OG5_127922	BBOV_III008580
OG5_127922	BBOV_III008580
OG5_129313	BBOV_III008620
OG5_129313	BBOV_III008620
OG5_129313	BBOV_III008620
OG5_129313	BBOV_III008620
OG5_129313	BBOV_III008620
OG5_129313	BBOV_III008620
OG5_129313	BBOV_III008620
OG5_129313	BBOV_III008620
OG5_129313	BBOV_III008620
OG5_132300	BBOV_III008840
OG5_132300	BBOV_III008840
OG5_132300	BBOV_III008840
OG5_132300	BBOV_III008840
OG5_128066	BBOV_III008890
OG5_128066	BBOV_III008890
OG5_130216	BBOV_III008900
OG5_130216	BBOV_III008900
OG5_127553	BBOV_III008970
OG5_127553	BBOV_III008970

OG5_127553	BBOV_III008970
OG5_127942	BBOV_III009080
OG5_127942	BBOV_III009080
OG5_127942	BBOV_III009080
OG5_128354	BBOV_III009290
OG5_128354	BBOV_III009290
OG5_128354	BBOV_III009290
OG5_128354	BBOV_III009290
OG5_127677	BBOV_III009410
OG5_127677	BBOV_III009410
OG5_127149	BBOV_III009450
OG5_127149	BBOV_III009450
OG5_127149	BBOV_III009450
OG5_127149	BBOV_III009450
OG5_130129	BBOV_III009670
OG5_128295	BBOV_III009710
OG5_127466	BBOV_III009760
OG5_128528	BBOV_III009770
OG5_128528	BBOV_III009770
OG5_128528	BBOV_III009770
OG5_128528	BBOV_III009770
OG5_127574	BBOV_III009930
OG5_127574	BBOV_III009930
OG5_127333	BBOV_III010510
OG5_127333	BBOV_III010510
OG5_129228	BBOV_III010690
OG5_129228	BBOV_III010690
OG5_126878	BBOV_III010810
OG5_126878	BBOV_III010810
OG5_126878	BBOV_III010810
OG5_126878	BBOV_III010810
OG5_126878	BBOV_III010810
OG5_127351	BBOV_III010890
OG5_127351	BBOV_III010890
OG5_128449	BBOV_III011080
OG5_127286	BBOV_III011100
OG5_127286	BBOV_III011100
OG5_127286	BBOV_III011100
OG5_127286	BBOV_III011100
OG5_138490	BBOV_III011400
OG5_138490	BBOV_III011400
OG5_138490	BBOV_III011400
OG5_127127	BBOV_III011550

OG5_127127	BBOV_III011550
OG5_127127	BBOV_III011550
OG5_126865	BBOV_III011610
OG5_126865	BBOV_III011610
OG5_126865	BBOV_III011610
OG5_128638	BBOV_III011840
OG5_126579	BBOV_IV000140
OG5_126579	BBOV_IV000140
OG5_129520	BBOV_IV000280
OG5_127366	BBOV_IV000490
OG5_127297	BBOV_IV000740
OG5_128587	BBOV_IV000850
OG5_127751	BBOV_IV000970
OG5_127751	BBOV_IV000970
OG5_127751	BBOV_IV000980
OG5_127751	BBOV_IV000980
OG5_127751	BBOV_IV000980
OG5_127751	BBOV_IV000980
OG5_127148	BBOV_IV001160
OG5_127148	BBOV_IV001160
OG5_127148	BBOV_IV001160
OG5_128047	BBOV_IV001200
OG5_128121	BBOV_IV001360
OG5_128001	BBOV_IV001710
OG5_127773	BBOV_IV001730
OG5_127773	BBOV_IV001730
OG5_127773	BBOV_IV001730
OG5_127773	BBOV_IV001730
OG5_127480	BBOV_IV001820
OG5_127480	BBOV_IV001820
OG5_126740	BBOV_IV001910
OG5_126740	BBOV_IV001910
OG5_126740	BBOV_IV001910
OG5_126740	BBOV_IV001910
OG5_126740	BBOV_IV001910
OG5_126740	BBOV_IV001910
OG5_126740	BBOV_IV001910
OG5_126740	BBOV_IV001910
OG5_126740	BBOV_IV001910
OG5_126740	BBOV_IV001910
OG5_126740	BBOV_IV001910
OG5_126740	BBOV_IV001910
OG5_128799	BBOV_IV002190
OG5_128799	BBOV_IV002190
OG5_128799	BBOV_IV002190
OG5_128165	BBOV_IV002230

OG5_126620	BBOV_IV002290
OG5_126620	BBOV_IV002290
OG5_126620	BBOV_IV002290
OG5_130616	BBOV_IV002810
OG5_130616	BBOV_IV002810
OG5_131402	BBOV_IV002890
OG5_127610	BBOV_IV003160
OG5_127610	BBOV_IV003160
OG5_127610	BBOV_IV003160
OG5_126683	BBOV_IV003180
OG5_126683	BBOV_IV003180
OG5_126683	BBOV_IV003180
OG5_126683	BBOV_IV003180
OG5_126683	BBOV_IV003180
OG5_126683	BBOV_IV003180
OG5_126683	BBOV_IV003180
OG5_126683	BBOV_IV003180
OG5_126683	BBOV_IV003180
OG5_126683	BBOV_IV003180
OG5_129568	BBOV_IV003640
OG5_128398	BBOV_IV003810
OG5_128398	BBOV_IV003810
OG5_128398	BBOV_IV003810
OG5_127038	BBOV_IV003820
OG5_127038	BBOV_IV003820
OG5_127038	BBOV_IV003820
OG5_127038	BBOV_IV003820
OG5_127038	BBOV_IV003820
OG5_127038	BBOV_IV003820
OG5_127038	BBOV_IV003820
OG5_127038	BBOV_IV003820
OG5_127038	BBOV_IV003820
OG5_127038	BBOV_IV003820
OG5_127038	BBOV_IV003820
OG5_127038	BBOV_IV003820
OG5_127038	BBOV_IV003820
OG5_140259	BBOV_IV003850
OG5_128309	BBOV_IV004010
OG5_129285	BBOV_IV004150
OG5_129285	BBOV_IV004150
OG5_129285	BBOV_IV004150
OG5_128795	BBOV_IV004470
OG5_128795	BBOV_IV004470
OG5_128795	BBOV_IV004470
OG5_128795	BBOV_IV004470
OG5_127448	BBOV_IV004550
OG5_127448	BBOV_IV004550
OG5_127291	BBOV_IV004560

OG5_127291	BBOV_IV004560
OG5_127291	BBOV_IV004560
OG5_127291	BBOV_IV004560
OG5_127291	BBOV_IV004560
OG5_127291	BBOV_IV004560
OG5_127291	BBOV_IV004560
OG5_127291	BBOV_IV004560
OG5_127291	BBOV_IV004560
OG5_127291	BBOV_IV004560
OG5_127291	BBOV_IV004560
OG5_127291	BBOV_IV004560
OG5_127291	BBOV_IV004560
OG5_127291	BBOV_IV004560
OG5_130517	BBOV_IV004600
OG5_127936	BBOV_IV005100
OG5_127936	BBOV_IV005100
OG5_127498	BBOV_IV005110
OG5_127890	BBOV_IV005130
OG5_126668	BBOV_IV005450
OG5_126668	BBOV_IV005450
OG5_126668	BBOV_IV005450
OG5_126668	BBOV_IV005450
OG5_126668	BBOV_IV005450
OG5_127311	BBOV_IV005540
OG5_127311	BBOV_IV005540
OG5_128136	BBOV_IV005570
OG5_128136	BBOV_IV005570
OG5_128678	BBOV_IV005610
OG5_128863	BBOV_IV005710
OG5_128777	BBOV_IV005820
OG5_127099	BBOV_IV005830
OG5_127099	BBOV_IV005830
OG5_127099	BBOV_IV005830
OG5_126679	BBOV_IV005840
OG5_126679	BBOV_IV005840
OG5_126679	BBOV_IV005840
OG5_126679	BBOV_IV005840
OG5_126679	BBOV_IV005840
OG5_126679	BBOV_IV005840
OG5_126679	BBOV_IV005840
OG5_126679	BBOV_IV005840
OG5_126679	BBOV_IV005840
OG5_126679	BBOV_IV005840
OG5_130370	BBOV_IV005880
OG5_127818	BBOV_IV006000
OG5_127818	BBOV_IV006000

OG5_127818	BBOV_IV006000
OG5_127818	BBOV_IV006000
OG5_127818	BBOV_IV006000
OG5_127818	BBOV_IV006000
OG5_127818	BBOV_IV006000
OG5_127818	BBOV_IV006000
OG5_127818	BBOV_IV006000
OG5_127818	BBOV_IV006000
OG5_128332	BBOV_IV006710
OG5_127313	BBOV_IV006740
OG5_127313	BBOV_IV006740
OG5_127313	BBOV_IV006740
OG5_127313	BBOV_IV006740
OG5_127430	BBOV_IV006860
OG5_127430	BBOV_IV006860
OG5_127430	BBOV_IV006860
OG5_127430	BBOV_IV006860
OG5_127430	BBOV_IV006860
OG5_127497	BBOV_IV006880
OG5_127497	BBOV_IV006880
OG5_135175	BBOV_IV007010
OG5_135175	BBOV_IV007010
OG5_126968	BBOV_IV007190
OG5_126968	BBOV_IV007190
OG5_126968	BBOV_IV007190
OG5_126968	BBOV_IV007190
OG5_126641	BBOV_IV007450
OG5_126641	BBOV_IV007450
OG5_126641	BBOV_IV007450
OG5_126641	BBOV_IV007450
OG5_126641	BBOV_IV007450
OG5_126641	BBOV_IV007450
OG5_126641	BBOV_IV007450
OG5_126641	BBOV_IV007450
OG5_126641	BBOV_IV007450
OG5_126641	BBOV_IV007450
OG5_126641	BBOV_IV007450
OG5_128003	BBOV_IV007690
OG5_128003	BBOV_IV007690
OG5_128003	BBOV_IV007690
OG5_128003	BBOV_IV007690
OG5_128003	BBOV_IV007690
OG5_126730	BBOV_IV008060
OG5_126730	BBOV_IV008060

OG5_126730	BBOV_IV008060
OG5_126730	BBOV_IV008060
OG5_126730	BBOV_IV008060
OG5_126730	BBOV_IV008060
OG5_128266	BBOV_IV008220
OG5_128266	BBOV_IV008220
OG5_128266	BBOV_IV008220
OG5_127814	BBOV_IV008240
OG5_127814	BBOV_IV008240
OG5_128225	BBOV_IV008270
OG5_126795	BBOV_IV008280
OG5_126795	BBOV_IV008280
OG5_126795	BBOV_IV008280
OG5_126795	BBOV_IV008280
OG5_126795	BBOV_IV008280
OG5_126795	BBOV_IV008280
OG5_127464	BBOV_IV008880
OG5_128839	BBOV_IV008900
OG5_128839	BBOV_IV008900
OG5_128839	BBOV_IV008900
OG5_127152	BBOV_IV009110
OG5_127152	BBOV_IV009110
OG5_127682	BBOV_IV009520
OG5_127682	BBOV_IV009520
OG5_127813	BBOV_IV009590
OG5_127813	BBOV_IV009590
OG5_127813	BBOV_IV009590
OG5_127813	BBOV_IV009590
OG5_127924	BBOV_IV009600
OG5_128776	BBOV_IV009810
OG5_169678	BBOV_IV010090
OG5_169678	BBOV_IV010090
OG5_130572	BBOV_IV010290
OG5_130572	BBOV_IV010290
OG5_128429	BBOV_IV010580
OG5_128429	BBOV_IV010580
OG5_127514	BBOV_IV010920
OG5_127514	BBOV_IV010920
OG5_127514	BBOV_IV010920
OG5_126599	BBOV_IV011160
OG5_126599	BBOV_IV011160
OG5_126599	BBOV_IV011160
OG5_126599	BBOV_IV011160
OG5_126599	BBOV_IV011160

OG5_126599	BBOV_IV011160
OG5_126599	BBOV_IV011160
OG5_127529	BBOV_IV011250
OG5_128401	BBOV_IV011380
OG5_128401	BBOV_IV011380
OG5_128401	BBOV_IV011380
OG5_128486	BBOV_IV011410
OG5_128486	BBOV_IV011410
OG5_128020	BBOV_IV011550
OG5_128020	BBOV_IV011550

** Differentially expressed B. divergens gene transcript names correspond to B. bovis transcript names*

APPENDIX 4.9 A. *thaliana* differentially expressed transcriptomic data with corresponding orthologue groups identified from the *B. bovis* – *A. thaliana* orthologue group matrix

Orthologue group name	* <i>A. thaliana</i> DEG's
OG5_126935	NP_172220
OG5_126588	NP_172382
OG5_126588	NP_173055
OG5_127506	NP_173317
OG5_128261	NP_173562
OG5_127279	NP_564326
OG5_126600	NP_174807
OG5_126613	NP_175128
OG5_129050	NP_175711
OG5_126935	NP_175759
OG5_128059	NP_564785
OG5_127912	NP_176564
OG5_126951	NP_564878
OG5_129033	NP_849852
OG5_129033	NP_564879
OG5_126613	NP_177146
OG5_126636	NP_565083
OG5_126843	NP_177875
OG5_126955	NP_177899
OG5_126969	NP_001154497
OG5_126969	NP_178631
OG5_126600	NP_565411
OG5_126773	NP_179646
OG5_128642	NP_565614
OG5_126935	NP_180511
OG5_127143	NP_181187
OG5_128822	NP_565854
OG5_126969	NP_850431
OG5_126969	NP_182042
OG5_129825	NP_566305
OG5_126973	NP_850536
OG5_126973	NP_566315
OG5_126877	NP_566331
OG5_130399	NP_566349
OG5_130399	NP_001154600
OG5_130399	NP_001078126
OG5_127933	NP_187736
OG5_126588	NP_187864
OG5_127172	NP_566435
OG5_127669	NP_188117

OG5_127669	NP_001030698
OG5_127669	NP_850588
OG5_129050	NP_566508
OG5_127550	NP_566666
OG5_126561	NP_188762
OG5_126610	NP_189189
OG5_126893	NP_001118718
OG5_126893	NP_189374
OG5_126935	NP_190209
OG5_126926	NP_190891
OG5_129200	NP_567044
OG5_128185	NP_001030918
OG5_128185	NP_567132
OG5_128001	NP_567236
OG5_126969	NP_849298
OG5_126969	NP_192371
OG5_126960	NP_567283
OG5_127365	NP_192742
OG5_127453	NP_567388
OG5_129413	NP_001031707
OG5_129413	NP_567701
OG5_126714	NP_567778
OG5_126841	NP_194568
OG5_127443	NP_194907
OG5_127443	NP_974655
OG5_129958	NP_195376
OG5_128435	NP_195500
OG5_128439	NP_195572
OG5_128439	NP_849567
OG5_126588	NP_195869
OG5_126703	NP_001031824
OG5_126703	NP_568112
OG5_126703	NP_851029
OG5_126610	NP_568146
OG5_126857	NP_001119183
OG5_126857	NP_001119184
OG5_126857	NP_196361
OG5_131121	NP_196581
OG5_126737	NP_196713
OG5_126841	NP_001031876
OG5_126841	NP_196853
OG5_126857	NP_197318
OG5_128555	NP_197348

OG5_126737	NP_197456
OG5_131493	NP_197591
OG5_127161	NP_568429
OG5_129362	NP_199523
OG5_126636	NP_568750
OG5_126623	NP_200076
OG5_126978	NP_200331
OG5_128426	NP_200420
OG5_126685	NP_200446
OG5_133088	NP_001032108
OG5_133088	NP_974969
OG5_133088	NP_001032109
OG5_133088	NP_200849
OG5_133088	NP_001119465
OG5_126864	NP_568962
OG5_126779	NP_201376
OG5_126927	NP_201477

* Differentially expressed *A. thaliana* gene transcript names correspond to *A. thaliana* transcript names in TAIR

APPENDIX 4.10 Unique and shared orthologue groups among the differentially expressed transcripts of *B. divergens* and *A. thaliana* treated with piperidinyl-benzimidazolone analog (A51B1C1_1) and galvastine-1, respectively

Unique orthologue groups among <i>B. divergens</i> DEG's		Unique orthologue groups among <i>A. thaliana</i> DEG's
Shared orthologue groups		
OG5_127833	OG5_127453	OG5_126935
OG5_127594	OG5_127669	OG5_126588
OG5_127472	OG5_128435	OG5_127506
OG5_127692	OG5_128059	OG5_128261
OG5_129396	OG5_133088	OG5_127279
OG5_128702	OG5_126773	OG5_126600
OG5_127141	OG5_129958	OG5_126613
OG5_130042	OG5_126561	OG5_129050
OG5_127233	OG5_126969	OG5_127912
OG5_127910	OG5_128001	OG5_126951
Unique orthologue groups		
OG5_127468		OG5_129033
OG5_131748		OG5_126636
OG5_135732		OG5_126843
OG5_131400		OG5_126955
OG5_126854		OG5_128642
OG5_128219		OG5_127143
OG5_127402		OG5_128822
OG5_126913		OG5_129825
OG5_128226		OG5_126973
OG5_127784		OG5_126877
OG5_127994		OG5_130399
OG5_128517		OG5_127933
OG5_126936		OG5_127172
OG5_128255		OG5_127550
OG5_127962		OG5_126610
OG5_126644		OG5_126893
OG5_127206		OG5_126926
OG5_141671		OG5_129200
OG5_128455		OG5_128185
OG5_128117		OG5_126960
OG5_129047		OG5_127365
OG5_128457		OG5_129413
OG5_128667		OG5_126714
OG5_128012		OG5_126841
OG5_126774		OG5_127443
OG5_127854		OG5_128439
OG5_128816		OG5_126703

OG5_128055	OG5_126857
OG5_126678	OG5_131121
OG5_127496	OG5_126737
OG5_127608	OG5_128555
OG5_130456	OG5_131493
OG5_127223	OG5_127161
OG5_128215	OG5_129362
OG5_127934	OG5_126623
OG5_128058	OG5_126978
OG5_128469	OG5_128426
OG5_128599	OG5_126685
OG5_128495	OG5_126864
OG5_127319	OG5_126779
OG5_127173	OG5_126927
OG5_128487	
OG5_127881	
OG5_126956	
OG5_128727	
OG5_127153	
OG5_127011	
OG5_127512	
OG5_126850	
OG5_126684	
OG5_127764	
OG5_128733	
OG5_128038	
OG5_134639	
OG5_127570	
OG5_126904	
OG5_128182	
OG5_127289	
OG5_127312	
OG5_127633	
OG5_127670	
OG5_127535	
OG5_126886	
OG5_126665	
OG5_128494	
OG5_127654	
OG5_131701	
OG5_128133	
OG5_131401	
OG5_127215	

OG5_126694
OG5_127906
OG5_126867
OG5_129246
OG5_127465
OG5_127269
OG5_128057
OG5_128660
OG5_127231
OG5_126601
OG5_127624
OG5_126745
OG5_128980
OG5_134232
OG5_128881
OG5_128884
OG5_126885
OG5_127711
OG5_127273
OG5_128366
OG5_131249
OG5_127572
OG5_127797
OG5_127408
OG5_128098
OG5_127256
OG5_127481
OG5_127874
OG5_126733
OG5_127732
OG5_127604
OG5_129385
OG5_137714
OG5_127900
OG5_130661
OG5_127081
OG5_127557
OG5_128935
OG5_128077
OG5_127761
OG5_127036
OG5_127969
OG5_127107

OG5_127017
OG5_127641
OG5_131103
OG5_126723
OG5_127922
OG5_129313
OG5_132300
OG5_128066
OG5_130216
OG5_127553
OG5_127942
OG5_128354
OG5_127677
OG5_127149
OG5_130129
OG5_128295
OG5_127466
OG5_128528
OG5_127574
OG5_127333
OG5_129228
OG5_126878
OG5_127351
OG5_128449
OG5_127286
OG5_138490
OG5_127127
OG5_126865
OG5_128638
OG5_126579
OG5_129520
OG5_127366
OG5_127297
OG5_128587
OG5_127751
OG5_127148
OG5_128047
OG5_128121
OG5_127773
OG5_127480
OG5_126740
OG5_128799
OG5_128165

OG5_126620
OG5_130616
OG5_131402
OG5_127610
OG5_126683
OG5_129568
OG5_128398
OG5_127038
OG5_140259
OG5_128309
OG5_129285
OG5_128795
OG5_127448
OG5_127291
OG5_130517
OG5_127936
OG5_127498
OG5_127890
OG5_126668
OG5_127311
OG5_128136
OG5_128678
OG5_128863
OG5_128777
OG5_127099
OG5_126679
OG5_130370
OG5_127818
OG5_128332
OG5_127313
OG5_127430
OG5_127497
OG5_135175
OG5_126968
OG5_126641
OG5_128003
OG5_126730
OG5_128266
OG5_127814
OG5_128225
OG5_126795
OG5_127464
OG5_128839

OG5_127152
OG5_127682
OG5_127813
OG5_127924
OG5_128776
OG5_169678
OG5_130572
OG5_128429
OG5_127514
OG5_126599
OG5_127529
OG5_128401
OG5_128486
OG5_128020